ABSTRACT

Title of dissertation: CARRYING CAPACITY
OF TWO-WAY COUPLED
EARTH–HUMAN SYSTEMS

Safa Motesharrei, Doctor of Philosophy, 2018

Dissertation directed by: Distinguished University Professor James A. Yorke

Department of Physics

Over the last two centuries, the impact of the Human System has grown dramatically, becoming strongly dominant within the Earth System in many different ways. Consumption, inequality, and population have increased extremely fast, especially since about 1950, threatening to overwhelm the many critical functions and ecosystems of the Earth System. Changes in the Earth System, in turn, have important feedback effects on the Human System, with costly and potentially serious consequences. However, current models do not incorporate these critical feedbacks. We argue that in order to understand the dynamics of either system, Earth System Models must be coupled with Human System Models through bidirectional couplings representing the positive, negative, and delayed feedbacks that exist in the real systems. In particular, key Human System variables, such as demographics, inequality, economic growth, and migration, are not coupled with the Earth

System but are instead driven by exogenous estimates, such as United Nations population projections. This makes current models likely to miss important feedbacks in the real Earth–Human system, especially those that may result in unexpected or counterintuitive outcomes, and thus requiring different policy interventions from current models. The importance and imminence of sustainability challenges, the dominant role of the Human System in the Earth System, and the essential roles the Earth System plays for the Human System, all call for collaboration of natural scientists, social scientists, and engineers in multidisciplinary research and modeling to develop coupled Earth–Human system models for devising effective science-based policies and measures to benefit current and future generations.

The official UMD Press Release for the Modeling Sustainability paper is available at:

https://umdrightnow.umd.edu/news/its-more-just-climate-change

Existing studies of freshwater systems generally focus on hydrological flows without considering impacts from human feedbacks on these natural flows. However, the human system has become the major driver of changes in freshwater systems. The Coupled Human–Climate–Water model (COWA) is a minimal dynamic model that aims to capture these bidirectional positive, negative, and delayed feedbacks. The results show remarkable differences between simulation outputs of two-way and one-way coupled models, showing that projecting both human and natural system variables without feedbacks over long periods of time yields unrealistic results. COWA shows that Carrying Capacity is not static but rather evolves in response to the dynamic interactions and feedbacks in a changing system of many human and natural factors. COWA allows to determine the Water Carrying Capacity (WCC) of a region, i.e., the level of population and water consumption that a region's natural hydrological regime can support over the long term. Additionally, it shows that implementing effective water management policies — such as recycling and conservation technologies — can expand WCC of a region. An unexpected result of including bidirectional coupling is that expanding reservoir size and water collection capacity produces short-term population growth without expanding WCC, but because groundwater stocks are depleted more rapidly, it leads to an earlier and steeper collapse of the water resources and population. Lack of a dynamic understanding of a system can lead to the opposite conclusion about its behavior. COWA shows the critical importance of long-term policies for sustaining water resources, especially when demand rises and when estimates of available groundwater or potential for contamination of freshwater sources are highly uncertain. Significant signals of potential collapse (or unsustainability) can be missed if we limit the horizon to short term and neglect bidirectional feedbacks.

Physical systems with time-varying internal couplings are abundant in nature. While the full governing equations of these systems are typically unknown due to insufficient understanding of their internal mechanisms, there is often interest in determining the leading element. Here, the leading element is defined as the sub-system with the largest coupling coefficient averaged over a selected time span. Previously, the Convergent Cross Mapping (CCM) method has been employed to determine causality and dominant component in weakly coupled systems with constant coupling coefficients. In this study, CCM is applied to a pair of coupled Lorenz systems with time-varying coupling coefficients, exhibiting switching between dominant sub-systems in different periods. Four sets of numerical experiments are carried out. The first three cases consist of different coupling coefficient schemes: I) Periodic–constant, II) Normal, and III) Mixed Normal/Non-normal. In case IV, numerical experiment of cases II and III are repeated with imposed temporal uncertainties as well as additive normal noise. Our results show that, through detecting directional interactions, CCM identifies the leading sub-system in all cases except when the average coupling coefficients are approximately equal, i.e., when the dominant sub-system is not well defined.

Wind and solar farms offer a major pathway to clean, renewable energies. However, these farms would significantly change land surface properties, and, if sufficiently large, the farms may lead to unintended climate consequences. In this study, we used a climate model with dynamic vegetation to show that large-scale installations of wind and solar farms covering the Sahara lead to a local temperature increase and more than a twofold precipitation increase, especially in the Sahel, through increased surface friction and reduced albedo. The resulting increase in vegetation further enhances precipitation, creating a positive albedo–precipitation–vegetation feedback that contributes ~80% of the precipitation increase for wind farms. This local enhancement is scale dependent and is particular to the Sahara, with small impacts in other deserts.

The official UMD Press Release for the Sahara paper is available at: https://umdrightnow.umd.edu/news/large-scale-wind-and-solar-farms-sahara-would-increase-rain-and-vegetation

CARRYING CAPACITY OF TWO-WAY COUPLED EARTH–HUMAN SYSTEMS

by

Safa Motesharrei

Dissertation submitted to the Faculty of the Graduate School of the
University of Maryland, College Park in partial fulfillment
of the requirements for the degree of
Doctor of Philosophy in Physics
2018

Dissertation Committee:
Distinguished University Professor James A. Yorke (Chair, Physics)
Professor Victor M. Yakovenko (Co-Advisor, Physics)
Distinguished University Professor Eugenia Kalnay (Atmospheric and Oceanic Science)
Professor William Dorland (Physics)
Professor Jelena Srebric (Mechanical Engineering, Dean's Representative)

Preface

I start this dissertation with a review of the key components of the Human System, the various impacts of the Human System on the Earth System, and the important feedbacks of the Earth System on the Human System. We discuss the current state of the models that project the future of the planet and humanity, and are used to inform policymakers nationally and internationally. We argue that due to lack of feedbacks that exist in reality, these current models are likely to miss important signals that could determine the fate of humanity and our planet. We propose a framework to couple the Earth and Human System models with bidirectional feedbacks. We argue that Dynamic Models would be the natural choice for developing the core of such models, and Input/Output Models could be coupled to the dynamic core of the models to provide detailed information about the economic system, especially trade and virtual trade. Finally, we propose to employ advances in Data Assimilation to estimate and constrain model parameters from observations and to quantify uncertainty for key variables and propagation of uncertainties through various components of the coupled system. This rather long discussion was published as an interdisciplinary review paper Motesharrei et al. [2016], which constitutes the first paper of my dissertation.

In the second paper of the dissertation, I present a partial implementation of our proposed framework for bidirectional coupling of the Earth and Human System models. The Coupled Human–Climate–Water model (COWA) includes bidirectional feedbacks between the Human and Freshwater Systems. An Earth System Model

(ESM) and a River Routing Module (RRM) provide the necessary precipitation, evaporation, and river flow time-series for COWA. The model is validated in the Phoenix Active Management Area (AMA) Watershed with the observations going back as far as 1900. The output from COWA is compared with the output from a similar model with only one-way couplings between the Human and Freshwater Systems. The comparison clearly demonstrates inherent incapability of one-way coupled models to capture non-trivial dynamics that exist in reality in the two-way coupled systems. Most importantly, COWA shows decisions that seem to be beneficial, and even essential, in the short term could seriously endanger the sustainability of the whole system in the long term. An analysis of various scenarios shows the key role that policies play in preventing catastrophes and reaching a sustainable state.

In the third paper of this dissertation, I present a method based on the theory of dynamical systems to detect the dominant driver in a coupled dynamical system. This work is based upon Sugihara et al. [2012], which introduced the Convergent Cross Mapping (CCM) method for identifying the dominant driver in a *weakly–coupled* dynamical system. We extend the work of Sugihara et al. [2012] by developing the CCM method further and applying it to *strongly–coupled* dynamical systems. This method would be useful for quantifying the uncertainties in modeled feedbacks between different sub-systems of a coupled system. An example would be the forcing between global temperature and atmospheric concentration of CO_2 [van Nes et al., 2015].

In the fourth paper of this dissertation, I discuss the climate and broader societal impacts of large-scale wind and solar farms in the African Sahara. Our two-way coupled climate–vegetation model simulations show that average rainfall increases on average by 150% in the Sahara, and up to 500 mm/year in the Sahel. This surprisingly strong increase are due to strong feedback mechanisms between climate and land surface. The first feedback mechanism is the land surface roughness–precipitation–vegetation feedback that was discovered by Y. C. Sud in 1985. The Sud feedback applies to wind farms. The second feedback mechanism is the Albedo–Precipitation–Vegetation feedback that was discovered by Jule Charney in 1975, and applies to both solar and wind farms. One more time, feedbacks lead to dynamics that are beyond perception of human mind. It again shows the importance of including key feedbacks between various physical or human systems when we create models. This paper was published in 2018 September 7 issue of the *Science* magazine [Li et al., 2018]

The work in this dissertation extends beyond a single discipline. Therefore, it is inevitable to introduce tools and methods from various areas of research: mathematics, physics, dynamical systems, atmospheric science, public policy, system dynamics, geography, demography, economics, dynamic modeling, etc. This is evident from the wide variety of expertise of my co-authors in Motesharrei et al. [2016] and Li et al. [2018]. We hope to show the interconnections between these methods and important problems that can only be addressed with such a toolset. Work presented in this dissertation is a new exploration in that direction. Naturally, it is just the beginning of a long road to understanding a wide range of global environmental and social problems, which will hopefully allow proposing and assessing a set of collective solutions to ensure sustainability of the environment and prosperity of humanity.

Full Publication List

Below is a complete list of my peer-reviewed publications during my PhD candidacy in the Physics Department at UMD (2014 August to 2018 December). Please note that only three of these papers are included in this dissertation.

9. Yan Li, Eugenia Kalnay, Safa Motesharrei, Jorge Rivas, Fred Kucharski, Daniel Kirk-Davidoff, Eviatar Bach, and Ning Zeng. Climate model shows large-scale wind and solar farms in the Sahara increase rain and vegetation. *Science*, 361(6406):1019–1022, September 2018. [Li et al., 2018]

   The "Sahara" paper was featured in over 250 news outlets including Reuters, NPR, BBC, Los Angeles Times, The Independent, New Scientist, Der Spiegel, Le Figaro, World Economic Forum, Financial Times, Japan Times, etc. It was downloaded more than 100,000 times within the first two weeks from its publication.

8. Yan Li, Damien Sulla-Menashe, Safa Motesharrei, Xiao-Peng Song, Eugenia Kalnay, Qing Ying, Shuangcheng Li, and Zongwen Ma. Inconsistent estimates of forest cover change in China between 2000 and 2013 from multiple datasets: differences in parameters, spatial resolution, and definitions. *Scientific Reports*, 7(1):8748, August 2017. [Li et al., 2017]

7. Alfredo Ruiz-Barradas, Eugenia Kalnay, Malaquías Peña, Amir E. BozorgMagham, and Safa Motesharrei. Finding the driver of local ocean–atmosphere coupling in reanalyses and CMIP5 climate models. *Climate Dynamics*, 48(7):2153–2172, April 2017. [Ruiz-Barradas et al., 2017]

6. Safa Motesharrei, Jorge Rivas, Eugenia Kalnay, Ghassem R. Asrar, Antonio J. Busalacchi, Robert F. Cahalan, Mark A. Cane, Rita R. Colwell, Kuishuang Feng, Rachel S. Franklin, Klaus Hubacek, Fernando Miralles-Wilhelm, Takemasa Miyoshi, Matthias Ruth, Roald Sagdeev, Adel Shirmohammadi, Jagadish Shukla, Jelena Srebric, Victor M. Yakovenko, and Ning Zeng. Modeling sustainability: population, inequality, consumption, and bidirectional coupling of the Earth and Human Systems. *National Science Review*, 3(4):470–494, December 2016. [Motesharrei et al., 2016]

   The "Modeling Sustainability" paper became the most downloaded paper of the Journal *National Science Review* soon after its publication, a position it still holds. Total downloads $\approx$ 40,000.

5. Yan Li, Maosheng Zhao, David J. Mildrexler, Safa Motesharrei, Qiaozhen Mu, Eugenia Kalnay, Fang Zhao, Shuangcheng Li, and Kaicun Wang. Potential and Actual impacts of deforestation and afforestation on land surface temperature. *Journal of Geophysical Research: Atmospheres*, 121(24):14,372–14,386, December 2016. [Li et al., 2016b]

   This paper became one of the most downloaded papers of the *Journal of Geophysical Research: Atmospheres.*

4. Yan Li, Nathalie De Noblet-Ducoudré, Edouard L. Davin, Safa Motesharrei, Ning Zeng, Shuangcheng Li, and Eugenia Kalnay. The role of spatial scale and background climate in the latitudinal temperature response to deforestation. *Earth System Dynamics*, 7(1):167–181, March 2016. [Li et al., 2016a]

3. Ya Liu, Yan Li, Shuangcheng Li, and Safa Motesharrei. Spatial and Temporal Patterns of Global NDVI Trends: Correlations with Climate and Human Factors. *Remote Sensing*, 7(10):13233–13250, October 2015. [Liu et al., 2015]

2. Amir E. BozorgMagham, Safa Motesharrei, Stephen G. Penny, and Eugenia Kalnay. Causality Analysis: Identifying the Leading Element in a Coupled Dynamical System. *PLoS ONE*, 10(6):e0131226, June 2015. [BozorgMagham et al., 2015]

1. Yan Li, Maosheng Zhao, Safa Motesharrei, Qiaozhen Mu, Eugenia Kalnay, and Shuangcheng Li. Local cooling and warming effects of forests based on satellite observations. *Nature Communications*, 6:6603, March 2015. [Li et al., 2015]

According to *Web of Science* (Clarivate Analytics), the "local climate impacts of deforestation" paper is among the **top 1%** cited papers in all fields of Geoscience.

One more time,

to my academic parents,

Eugenia Kalnay and Jim Yorke,

for their unwavering support during my graduate studies.

Acknowledgments

I have enormously benefited from interactions with a very large number of colleagues, advisors, collaborators, students, postdocs, referees, editors, and friends. To adequately acknowledge all the feedback I have received from my interactions with colleagues and friends would require a volume by itself. Here, I would briefly discuss some colleagues that provided key contributions to my research output over the past few years. I have only included a small part of this research output in this dissertation but I will mention the rest of the papers that I have published over the past four years.

First and foremost, I would like to thank the four key people without whom I could never produce this dissertation, as well as my other published research over the past four years: Eugenia Kalnay, Jorge Rivas, Yan Li, and Jim Yorke. Jim Yorke was my main motivation and inspiration to start doctoral studies in physics at UMD, and I am enormously grateful to him for his continued support over my explorations in various disciplines before eventually writing this dissertation. I learned a great deal from my daily interactions with Jim, and not just about academic research, but also about life, work, and many other interesting topics. The very same note also applies to Jorge and Eugenia, with whom I wrote the HANDY paper [Motesharrei et al., 2014], which constituted the core of my PhD dissertation in Applied Mathematics / Public Policy [Motesharrei, 2014]. Jorge and Eugenia were also my lead co-authors for the Modeling Sustainability paper [Motesharrei et al., 2016], COWA paper, and Eugenia and Yan were my lead co-authors for the Sahara paper [Li et al., 2018].

Majority of the ideas in both of my dissertations were developed and refined with Jorge and Eugenia over several years.

Next, I would like to thank my other dissertation committee members: Victor Yakovenko, Bill Dorland, and Jelena Srebric. I have benefited greatly from many discussions and insightful comments with my committee members. Victor and Jelena are also my co-authors on the Modeling Sustainability paper [Motesharrei et al., 2016], and have guided me on other projects and proposals.

I was very fortunate to work with Yan Li as my first PhD student (and later postdoc). Yan came to us from Peking University to conduct his doctoral research. We started a very fruitful collaboration that resulted in a series of groundbreaking papers focused on local climate impacts of deforestation [Li et al., 2015; Liu et al., 2015; Li et al., 2016a,b, 2017]. Yan is already an authority on this subject, and I can foresee that he will reach the highest levels of scientific distinction in the near future.

We were honored to be joined by a stellar, interdisciplinary team of co-authors for the Modeling Sustainability paper [Motesharrei et al., 2016], many of whom are members of the US National Academies and other international academies. This team of distinguished scientists includes Ghassem R. Asrar, Antonio J. Busalacchi, Robert F. Cahalan, Mark A. Cane, Rita R. Colwell, Kuishuang Feng, Rachel S. Franklin, Klaus Hubacek, Fernando Miralles-Wilhelm, Takemasa Miyoshi, Matthias Ruth, Roald Sagdeev, Adel Shirmohammadi, Jagadish Shukla, Jelena Srebric, Victor M. Yakovenko, and Ning Zeng. We learned very much from the deep knowledge and vision of our co-authors whose expertise spanned applied mathematics, physics,

systems science, dynamic modeling, political science, history, social science, data assimilation, human demography, remote sensing, geography, public policy, ecological economics, hydrology, engineering, water and energy sustainability, econophysics, and atmospheric, oceanic, land, agriculture, and climate sciences. Bridging together all these disciplines was an extremely challenging task through which we acquired various essential insights about solving the sustainability problems of the modern society. We believe that a successful endeavor toward sustainability must include the insights offered by these (and other) disciplines.

For the Modeling Sustainability paper, my co-authors and I additionally benefited from helpful discussions with many colleagues including Professors Mike Wallace, Jim Carton, Inez Fung, Deliang Chen, Ross Salawitch, Margaret Palmer, Russ Dickerson, Paolo D'Odorico, and Steve Penny. Ian Munoz and Philippe Marchand provided essential technical assistance for producing Fig. 2.1.

My work on Causality Analysis of strongly coupled systems with the Convergent Cross Mapping (CCM) method [BozorgMagham et al., 2015] was carried out together with Amir Bozorgmagham, Steve Penny, and Eugenia Kalnay.

I also learned much through the collaboration with Alfredo Ruiz-Barradas, Eugenia Kalnay, Malquías Peña, and Amir Bozorgmagham on the project for determining the dominant driver in the Ocean–Atmosphere coupling [Ruiz-Barradas et al., 2017].

I would like to thank my co-authors of the COWA paper [Motesharrei et al., 2019], Cortney Gustafson, Fang Zhao, Jorge Rivas, Eugenia Kalnay, Huan Wu, Fernando Miralles-Wilhelm, Ning Zeng, and Klaus Hubacek. My graduate student

Cortney Gustafson was essential in researching unique features of our case study region, Phoenix AMA watershed, and collecting large volumes of data that were necessary to validate COWA. She also tirelessly ran many scenarios of COWA after each update and produced appealing plots from the outputs of those simulations. Fang Zhao ran the Earth System Model and developed the River Routing Model under supervision of Eugenia Kalnay, Ning Zeng, and Huan Wu. My former graduate student intern, Warren Porter, wrote the documentation for the River Routing Model.

I thank my co-authors of the Sahara paper [Li et al., 2018], Yan Li, Eugenia Kalnay, Jorge Rivas, Fred Kucharski, Daniel Kirk-Davidoff, Eviatar Bach, and Ning Zeng. This paper was the result an ingenious idea by Professor Kalnay, and a great team effort by this "dream" team of brilliant colleagues. I am also grateful to our team for their work on the press coverage of our paper and media interviews following the publication of the paper: Reuters, NPR, BBC, Discover Magazine, The Independent, Los Angeles Times, New Scientist, World Economic Forum, The Financial Times, and dozens of other news outlets.

I appreciate the support I received from the staff at many departments and centers on and off campus: Physics, Mathematics, and AOSC Departments, Institute for Physical Science and Technology, SESYNC, School of Public Policy, ESSIC, JGCRI, and CSPAC.

I would like to acknowledge NASA, the University of Maryland Council on the Environment, ESSIC, SESYNC, and Dr. Genia Brin for providing funding for my research.

And finally, I would like to thank my family and friends for their continued interest in my research work.

Table of Contents

List of Tables

List of Figures

List of Abbreviations

AGCM	Atmospheric General Circulation Model
AMA	Active Management Area (Phoenix AMA Watershed)
AOSC	Department of Atmospheric and Oceanic Science (UMD)
CC	Carrying Capacity
CCM	Convergent Cross Mapping
COWA	Coupled Human–Climate–Water Model
CSPAC	Clarice Smith Performing Arts Center
EAA	Environmental Assessment Agency
ESSIC	Earth System Science Interdisciplinary Center
GCAM	Global Change Assessment Model
GDP	Gross Domestic Product
HANDY	Human and Nature Dynamics
HANDY1	Generation One of HANDY
IAM	Integrated Assessment Model
ICTP	Abdus Salam International Center for Theoretical Physics
IGSM	Integrated Global System Modeling framework
IIASA	International Institute for Applied Systems Analysis
IMAGE	Integrated Modelling of Global Environmental
IPCC	Intergovernmental Panel on Climate Change
IPST	Institute for Physical Science and Technology (UMD)
JGCRI	Joint Global Change Research Institute
MESSAGE	Model for Energy Supply Systems And their General Environmental impact
MIT	Massachusetts Institute of Technology
NASA	National Aeronautics and Space Administration
RRM	River Routing Module
SESYNC	National Socio-Environmental Synthesis Center
SPEEDY	Simplified Parameterizations, primitivE-Equation DYnamics
UN	United Nations
UMD	University of Maryland
US DOE	United States Department of Energy
VEGAS	VEgetation–Global–Atmosphere–Soil
WCC	Water Carrying Capacity

Chapter 1: Introduction

As apparent from its title, the focus of this dissertation is proposing a novel framework to couple Earth–Human Systems with bidirectional feedbacks, a partial implementation of the model in COWA and the introduction of Water Carrying Capacity as an example of Carrying Capacity in two-way Coupled Earth–Human Systems, a demonstration of the importance of renewable energy sources, and a study of their beneficial impacts on local climate due to climate–vegetation feedbacks in the Sahara.

Chapter 2 is a fairly detailed description of the key components and variables of the human system that interact bidirectionally with many variables of the Earth System. This chapter is a paper that I co-authored [Motesharrei et al., 2016] with a team of twenty distinguished scientists from multiple disciplines. In this paper, we argue that Population, Inequality, and Consumption are three key variables of the Human System that must be included endogenously in models that are used to inform environmental, economics, and climate policies. The paper explains that the Earth System (e.g., atmosphere, ocean, land, and biosphere) provides the Human System (e.g., humans and their production, distribution, and consumption) not only the sources of its inputs (e.g., water, energy, biomass, and materials) but also the sinks (e.g., atmosphere, oceans, rivers, lakes, and lands) that absorb and process its outputs (e.g., emissions, pollution, and other wastes).

The paper describes how the rapid growth in resource use, land-use change, emissions, and pollution has made humanity the dominant driver of change in most of the Earth's natural systems, and how these changes, in turn, have critical feedback effects on humans with costly and serious consequences, including on human health and well-being, economic growth and development, and even human migration and societal conflict. However, the paper argues that these two-way interactions ("bidirectional coupling") are not included in the current models. The study explains that increases in economic inequality, consumption per capita, and total population are all driving this rapid growth in human impact, but that the major scientific models of Earth–Human System interaction do not bidirectionally (interactively) couple Earth System Models with the primary Human System drivers of change such as demographics, inequality, economic growth, and migration.

Chapter 3 describes an implementation of the framework discussed in Chapter 2. The HANDY model [Motesharrei et al., 2014] constituted the core of my previous dissertation [Motesharrei, 2014]. HANDY includes some of the key bidirectional couplings that we propose in Motesharrei et al. [2016], but HANDY is a minimal model that is best suited for conducting "thought experiments". Thought experiments are quite essential to understand the underlying mechanisms of the system, and to detect the key factors that influence the dynamics of the system, especially over the long term. Therefore, building, and experimenting with, a minimal model is the best strategy to study new phenomena and investigate unexplored behaviors

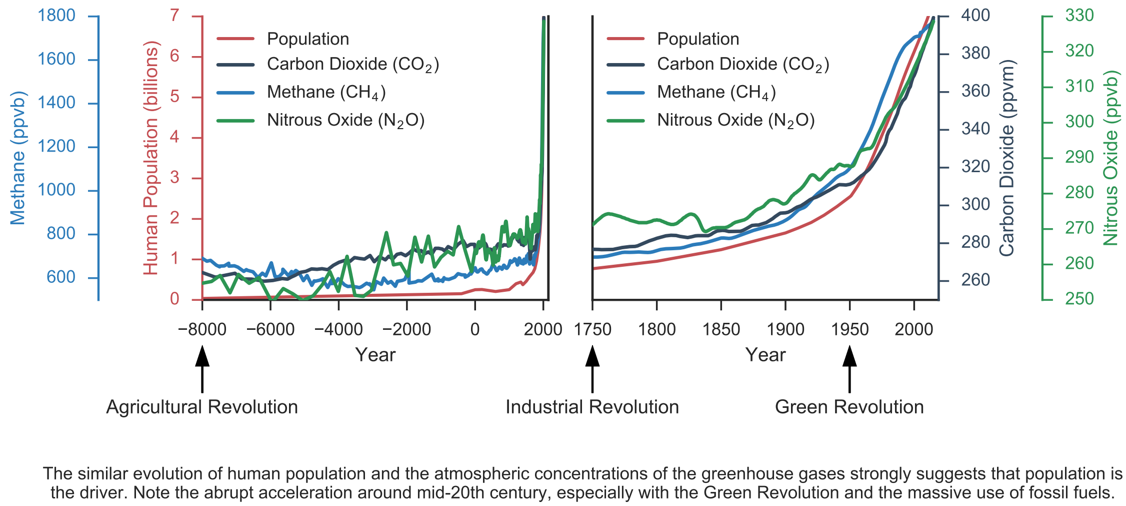

Figure 1.1: The similar evolution of world population and the atmospheric concentration of greenhouse gases over the past 10,000 years strongly suggests that human population is the driver. Note the abrupt acceleration after the Industrial Revolution (1750), and especially after the Green Revolution (1950), which required massive use of fossil fuels [Fu and Li, 2016].

of the systems. Moreover, minimal models are easier to understand, and perfect for educating students as well as the public.

In the real systems, however, we have many more variables and couplings, hence an attempt to capture changes of all those variables in the real system with a minimal model would be impossible. Of course, trying to represent all the variables and parameters in the real system requires infinite complexity of the model, and hence such an attempt would be futile by definition. Therefore, we must consider a trade-off between feasibility and complexity to build a model that can be validated for the major variables of a system, yet its complexity and computational requirements are reasonable and manageable.

The Coupled Human–Climate–Water Model (COWA) that I present in Chapter 3 is such a model. COWA was the logical second step (after HANDY) towards implementing the framework described in the first chapter [Motesharrei et al., 2016]. To be able to validate the model, we chose Phoenix Active Management Area (AMA) Watershed as our case study. Phoenix AMA Watershed is an example where freshwater resources are well managed, and past observations have been carefully recorded for many decades, providing an excellent source for the required long-term time-series to validate the model.

We have also built and validated a one-way coupled Human–Climate–Water model to compare and contrast its results to COWA's. An immediate conclusion was that one-way coupled models cannot capture any non-trivial evolution of the system, and can produce unrealistic projections. Consequently, we can miss important signals about the future — signals that may determine the fate of our environment and our species — if we rely on one-way coupled models for long-term projections.

COWA results include several surprising findings. The most surprising finding for us was the scenario where the freshwater storage and collection infrastructure expands over time (see Section 3.7.4). While an otherwise informed common sense tells us that expanding these infrastructures would always be a good decision, the scenario presented in Fig. 3.13 shows the long-term threat to the sustainability of the system. Population and freshwater consumption can grow very rapidly but at the cost of depleting Groundwater, resulting in a steeper collapse of the system, and many decades earlier. A decision that is seemingly beneficial in the short term can be detrimental in the long term. This is a counter-intuitive outcome that cannot be understood and predicted under any other framework.

A key measure that we develop in Chapter 3 for sustainability of freshwater system is Water Carrying Capacity (CC). Water CC is determined by multiple variables and factors of both the natural and the human systems. This should be contrasted to the traditional notion of Carrying Capacity as a predetermined parameter that is set by the modeler. Rather, we show that Water CC is a dynamic variable that could be calculated via simulations, and responds to changes of environmental and human system conditions. Finding a closed-form, analytical formula for Carrying Capacity is perhaps possible for a minimal system such as HANDY Motesharrei et al. [2014]. But a theoretical solution might be impossible for more complex systems such as COWA that aim to include, and validate, many variables of the real system. Hence the importance of numerical simulations to determine the future of Water CC under different policy choices. Nevertheless, we succeeded find a closed-form analytical expression for the Water CC in COWA via theoretical computations. An interesting result that we had not envisioned before was the case of a very large recycling capacity (R_M), where Water CC becomes independent of R_M. Theoretical computations brought to our attention that it is a possibility, and we confirmed this theoretical prediction through experiments.

In Chapter 4, we develop further the Cross Convergent Mapping (CCM) method [Sugihara et al., 2012] to allow detecting the leading variable in a strongly coupled dynamical system. We test our method with two Lorenz 63 systems [Lorenz, 1963] coupled with time-varying coefficients that would cause the leading subsystems to switch their dominance. We show that CCM can capture the leading subsystem under a wide set of coupling schemes: constant, periodic, Normal, and mixed Normal/non-Normal. We even show that CCM is robust under temporal uncertainties and additive normal noise. This method could be a valuable tool when modeling the feedbacks between coupled sub-systems of a dynamic system. One imminent application was to determine the dominant driver between global temperature and atmospheric CO_2 concentration [van Nes et al., 2015]

In Chapter 5, we investigate local climate impacts of large-scale wind and solar farms in the African Sahara and the neighboring Sahel region. The African Sahara is the largest desert in the world, with an area of 9.2 million square kilometers (US = 9.8). Due to its large surface area and proximity to equator, the Sahara has a great supply of solar and wind energy. It is close to sub-Saharan Africa and the Middle East, two of the driest regions in the world with fastest rates of population growth. The Sahel region, in particular, is one of the poorest regions in the world, with a projected population of over 600 million people by 2100. Large scale installations of solar panels and wind farms in this desert can produce 78 TW and 3 TW of electricity. To compare, world average power consumption is currently 18 TW. This energy will allow the economy to grow sustainably. Additionally, availability of clean energy can help with desalinating seawater and transporting it to the regions that suffer most from severe freshwater scarcity. Finally, availability of freshwater leads to improvement and expansion of agriculture and food availability. Moreover, increased precipitation will help to expand the current agriculture, which is predominantly rainfed, and increased vegetation will help with expanding livestock production. All of these effects could have major implications for bringing the region out of water and food scarcity and poverty.

The Sahara is sparsely inhabited, therefore, solar and wind farm installations will have minimal competition with natural and other human land uses like agriculture. This makes Sahara an ideal location for building massive solar and wind farms.

The first order effect of replacing fossil fuels with renewables as our source of energy would be reducing anthropogenic greenhouse gas emissions and the resulting climate change. The anthropogenic climate change is a subject that has been widely studied over the past several decades [Hansen et al., 2013]. However, large installations of solar and wind farms would change the land surface properties, and that could also result in climate change, which we find to be beneficial in this case. The mechanism would be friction–precipitation–vegetation for the wind farms and albedo–precipitation–vegetation feedback for both solar and wind farms. For the first time in our paper, we studied climate effects of large-scale renewable farms using a climate model that is coupled with vegetation through bidirectional feedbacks [Li et al., 2018].

Again, feedbacks can have fundamental impacts on the behavior of systems, and they are not confined to natural systems [Motesharrei et al., 2016, 2014]. In Li et al. [2018], we show that including these climate vegetation feedbacks is responsible for 80% of the precipitation increase for the wind farms, which means the effect would have been 5 times smaller had we not included this important feedback.

Our experiments for the combined solar and wind farms show that the precipitation can increase from 0.24 to 0.59 mm/day over the Sahara, and from 2.23 to 3.57 mm/day over the Sahel. This increase in precipitation of up to 500 mm/year is quite significant. This shows the importance of including key feedbacks in the models, and in particular, including the dynamic vegetation feedbacks in the climate models. As usual, feedbacks lead to surprising outcomes beyond what human mind is capable of perceiving.

Increase in rainfall will increase the vegetation growth. The vegetation cover fraction goes from 0.46 to 0.53, leaf area index goes from 0.64 to 1.12 m^2/m^2, and root carbon from 0.095 to 0.103 kgC/m^2. This is one side of the feedback. But when vegetation cover increases, surface albedo decreases, which will in turn further increase the vegetation through the vegetation–precipitation–albedo feedback.

The original idea behind our paper [Li et al., 2018] came to Professor Eugenia Kalnay about 10 years ago, inspired by the work of her PhD advisor Jule Charney at MIT. [1] The albedo–precipitation–vegetation feedback was originally proposed by Charney in 1975 to explain the extreme reduction of rainfall and drought in the Sahel [Charney, 1975].

The friction–precipitation–vegetation feedback was proposed by Sud and Smith in 1985 to explain how reduction in land surface roughness can lead to further reduction of rainfall [Sud and Smith, 1985]. Professor Kalnay suspected that solar panels might trigger the Charney mechanism but in the opposite direction, since they would reduce the albedo effectively, and wind farms might trigger the Sud mechanism in the opposite direction, since they increase the surface friction. We

[1] Charney is considered to be the father of modern dynamic meteorology.

confirmed these hypotheses in our paper through simulations with a bidirectionally coupled climate–land model [Li et al., 2018].

The Sahara is quite dry and its surface is covered with little vegetation. The additional rainfall and vegetation would certainly provide a much needed relief to this dry, bare desert.

We conducted additional experiments to investigate impacts in other deserts of the world. See Fig. S8 in the Supplementary Materials of the paper. The impacts seem to be much smaller in other world deserts because of their smaller area and scattered distribution. Also, albedo of the Sahara sand is about 0.4, which is higher than other world deserts, because the Sahara sand has a brighter color. This leads to a stronger change in effective albedo when solar panels are installed, and after vegetation cover increases.

We also conducted experiments for farms of smaller scales. Our results show that covering only the northwest quadrant of the Sahara would have almost the same precipitation and vegetation benefits as covering the whole Sahara (see Fig. S9 in the Supplementary Materials. Therefore, the impact depends on the specific location and scale of these installations. Nonetheless, the impact would increase with the size of wind/solar farms. A few studies have reported the impacts of the smaller scale wind and solar farms on local climate based on observations and models, for example, Zhou et al. [2012]; Roy et al. [2004]; Armstrong et al. [2016].

As we state in the paper, further studies with higher-resolution and more advanced climate models is necessary to more accurately investigate the local climate impacts of smaller farms.

There has been much research that shows satisfying the global energy demand via renewable sources is a realistic possibility [Jacobson et al., 2015]. From the perspective of total demand for energy, covering only 20% of the Sahara with solar panels would produce about 80 TW of electricity, more than 4 times the current global demand. Implementing such large-scale solar and wind farms has become increasingly possible but requires proper planning and visionary decision-making, plus co-operation of policymakers, companies, stakeholders, and people. It also requires development of energy storage technologies and large-scale storage facilities. But the obstacles, if any, are political and/or financial, not technological. We hope that all these local and global actors and stakeholders could co-operate to and make this kind of project a reality. This could be the best chance for sustaining life on this planet while improving the quality of life for everyone.

Chapter 2: Modeling Sustainability: Population, Inequality, Consumption, and Bidirectional Coupling of the Earth and Human Systems

Over the last two centuries, the impact of the Human System has grown dramatically, becoming strongly dominant within the Earth System in many different ways. Consumption, inequality, and population have increased extremely fast, especially since about 1950, threatening to overwhelm the many critical functions and ecosystems of the Earth System. Changes in the Earth System, in turn, have important feedback effects on the Human System, with costly and potentially serious consequences. However, current models do not incorporate these critical feedbacks. We argue that in order to understand the dynamics of either system, Earth System Models must be coupled with Human System Models through bidirectional couplings representing the positive, negative, and delayed feedbacks that exist in the real systems. In particular, key Human System variables, such as demographics, inequality, economic growth, and migration, are not coupled with the Earth System but are instead driven by exogenous estimates, such as UN population projections. This makes current models likely to miss important feedbacks in the real Earth–Human system, especially those that may result in unexpected or counterintuitive outcomes, and thus requiring different policy interventions from current models. The importance and imminence of sustainability challenges, the dominant role of the Human System in the Earth System, and the essential roles the Earth System plays for the Human System, all call for collaboration of natural scientists, social scientists, and engineers in multidisciplinary research and modeling to develop coupled Earth–Human system models for devising effective science-based policies and measures to benefit current and future generations. [1]

Significance Statement

The Human System has become strongly dominant within the Earth System in many different ways. However, in current models that explore the future of humanity and environment, and guide policy, key Human System variables, such as demographics, inequality, economic growth, and migration, are not coupled with the Earth System but are instead driven by exogenous estimates such as United Nations (UN) population projections. This makes the models likely to miss important feedbacks in the real Earth–Human system that may result in unexpected outcomes

[1] This chapter was published following peer-review as: Safa Motesharrei, Jorge Rivas, Eugenia Kalnay, Ghassem R. Asrar, Antonio J. Busalacchi, Robert F. Cahalan, Mark A. Cane, Rita R. Colwell, Kuishuang Feng, Rachel S. Franklin, Klaus Hubacek, Fernando Miralles-Wilhelm, Takemasa Miyoshi, Matthias Ruth, Roald Sagdeev, Adel Shirmohammadi, Jagadish Shukla, Jelena Srebric, Victor M. Yakovenko, and Ning Zeng. Modeling sustainability: population, inequality, consumption, and bidirectional coupling of the Earth and Human Systems. *National Science Review*, 3(4):470–494, December 2016.

requiring very different policy interventions. The importance of humanity's sustainability challenges calls for collaboration of natural and social scientists to develop coupled Earth–Human system models for devising effective science-based policies and measures.

Highlights

1. The Human System has become strongly dominant within the Earth System in many different ways.
   (a) Consumption, inequality, and population have increased extremely fast, especially since about 1950.
   (b) The collective impact of these changes threatens to overwhelm the viability of natural systems and the many critical functions that the Earth System provides.
2. Changes in the Earth System, in turn, have important feedback effects on the Human System, with costly and serious consequences.
3. However, current models, such as the Integrated Assessment Models, that explore the future of humanity and environment, and guide policy, do not incorporate these critical feedbacks.
   (a) Key Human System variables, such as demographics, inequality, economic growth, and migration, are instead driven by exogenous projections, such as the UN population tables.

(b) Furthermore, such projections are shown to be unreliable.

4. Unless models incorporate such two-way couplings, they are likely to miss important dynamics in the real Earth–Human system that may result in unexpected outcomes requiring very different policy interventions.

5. Therefore, Earth System Models must be bidirectionally coupled with Human System Models.

   (a) Critical challenges to sustainability call for a strong collaboration of both earth and social Scientists to develop coupled Earth–Human System models for devising effective science-based policies and measures.

   (b) We suggest using Dynamic Modeling, Input–Output Models, and Data Assimilation to build and calibrate such coupled models.

Description of Sections

Section 2.1 describes major changes in the relationship between the Earth System and the Human System, and key Human System factors driving these changes. Section 2.2 provides examples of fundamental problems in the exogenous projections of key Human System factors used in current models. Section 2.3 describes examples of changes in the Earth System that may impact the Human System seriously, as well as missing feedbacks from the Earth System onto the Human System. Section 2.4 argues for the need to bidirectionally couple both systems in order to model the future of either system more realistically, and proposes practical methods to implement this coupling.

One sentence Summary: In order to project future of both Earth and Human Systems more realistically, we must couple their models bidirectionally.

2.1 Dominance of the Human System within the Earth System

Humans impact the Earth System by extracting resources and returning waste and pollution to the system, and simultaneously altering land cover, fragmenting ecosystems, and reducing biodiversity. Planet Earth has been the habitat of humans for hundreds of thousands of years. Human life depends on the resources provided by the Earth System: air from the Earth's atmosphere; water from the atmosphere and rivers, lakes, and aquifers; fruits from trees; meat and other products from animals; and over the past 10,000 years, land for agriculture, and metals and other minerals from the Earth's crust. Until about 200 years ago, we used renewable biomass as the major source of materials and energy, but over the course of the past two centuries, we have instead become heavily dependent on fossil fuels (coal, oil, and natural gas) and other minerals for both materials and energy. These nonrenewable resources made possible both of the revolutions which drove the the growth in consumption per capita and population: the Industrial Revolution and the Green Revolution. Our relationship with our planet is not limited to consuming its resources. Waste is an inevitable outcome of any production process; what is produced must return to the Earth System in some form. Waste water goes back to the streams, rivers, lakes, oceans, or into the ground; greenhouse and toxic gases go into the atmosphere, land,

and oceans; and trash goes into landfills and almost everywhere else.

The level of this impact is determined by extraction and pollution rates, which in turn, are determined by the total consumption rate. Total consumption equals population multiplied by average consumption per capita, both of which are recognized as primary drivers of human environmental impact. Using Gross Domestic Product (GDP) per capita as a rough measure of consumption per capita, the extent of the impact of the Human System on the Earth System can be estimated from the total population and the average consumption per capita. This can be also seen from the defining equation for GDP per capita, i.e., GDP per capita = GDP / Population. One may rewrite this equation as GDP = Population × GDP per capita. By taking variations, we get:

$$\frac{\delta \text{GDP}}{\text{GDP}} = \frac{\delta \text{Population}}{\text{Population}} + \frac{\delta \text{GDP per capita}}{\text{GDP per capita}} \tag{2.1}$$

This equation simply means that the relative change in the total GDP is comprised of two components, i.e., the relative changes in population and GDP per capita. A graphical demonstration of this decomposition can be seen in the inset of Fig. 2.1.

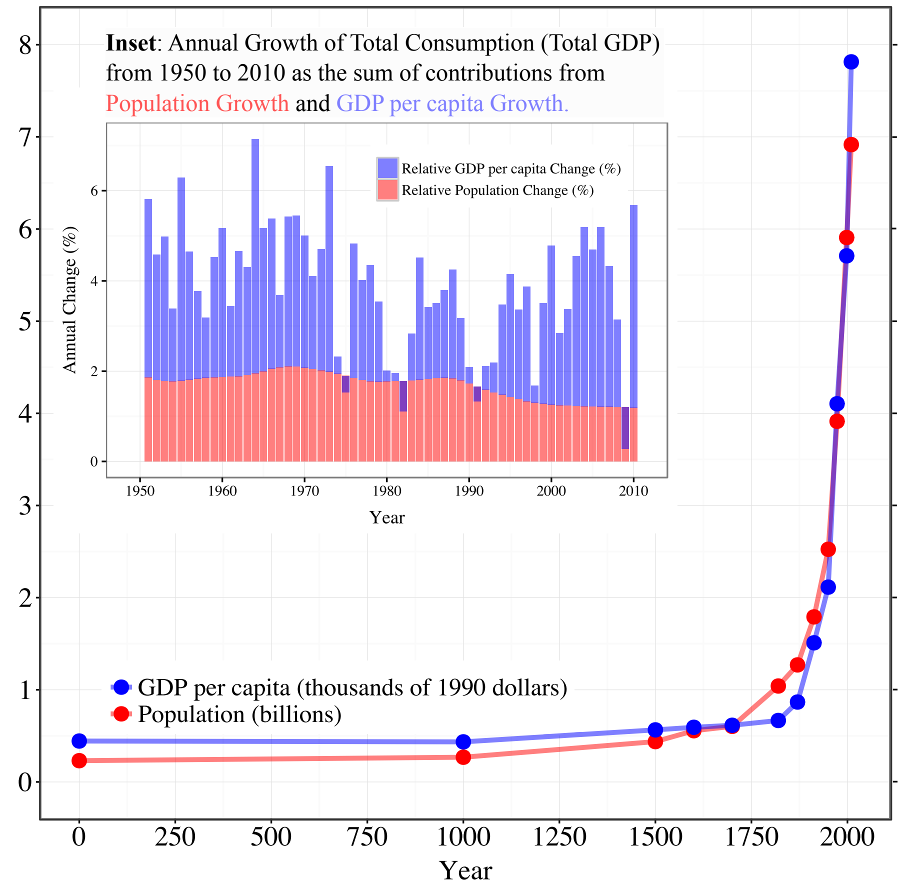

Population and GDP per capita (in the main graph) from year 1 to 2010 AD. *The total human impact is their product.*

Figure 2.1: World population and GDP per capita from year 1 to 2010 AD. *The total human impact is their product.* The inset shows the relative annual change of each between 1950 and 2010 [Maddison, 2001; Bolt and van Zanden, 2014; United Nations, 2013c]. Their averages were 1.69% and 2.21%, respectively, out of a total of ~4% (average annual change in GDP). Therefore, growth in population and consumption per capita have both played comparably important roles in the remarkable increase of human impact on planet Earth. This ~4% total growth corresponds to doubling the total impact every 17 years. Note that the contribution from population growth has been relatively steady, while the contribution from the relative change in GDP per capita has been much more variable from year to year (even negative for some years). See Eq. (2.1) for a description of the mathematical formula used to generate the inset. Data from Maddison [2001], with updates from the Maddison Project, 2013 (for the underlying methodology of the updates see Bolt and van Zanden [2014]). Population data for the inset from United Nations [2013c].

The rapid expansion of the human system has been a remarkably recent phenomenon (see Fig. 2.1). For over 90% of human existence, world population remained less than 5 million. After the Agricultural Revolution, it still took about 10,000 years to reach one billion, around the year 1800. About a century later the second billion was reached, around 1930. Thereafter, in less than a century, five billion more humans were added (within a single human lifetime). The peak in the *rate of growth* occurred in the 1960s, but because of the larger total population, the peak in *absolute growth* has persisted since the early 1990s [United Nations, 2015b]. To go from 5 to 6 billion took about 12 years (1987–1999), and from 6 to 7 billion also took about 12 years (1999–2011). The decline in the *rate* of growth over the past few decades has not significantly reduced the *absolute* number currently added every year, ~80 million (e.g., 83 million in 2016), equivalent to the population of Germany [Christenson, 2002; United Nations, 2013b].

A similar pattern holds for GDP per capita, but with the acceleration of growth occurring even more recently (see Fig. 2.1) and with the distribution of consumption becoming much more unequal. Thus, until the last century, population and GDP per capita were low enough that the Human System remained a relatively small component of the Earth System. However, both population and GDP per capita experienced explosive growth, especially after ~1950, and the product of these two growths — total human impact — has grown from relatively small to dominant in the Earth System.

Contrary to popular belief, these trends still continue for both population and consumption per capita. The world is projected to add a billion people every

13–15 years for decades to come. The current UN medium estimate expects 11.2 billion people by 2100, while the high estimate is 16.6 billion.[2] Similarly, while the highest rates of growth of global per capita GDP took place in the 1960s, they are not projected to decline significantly from their current rates (so that estimates of annual global growth until 2040 range from 3.3% (IMF and IEA) to 3.8% (US EIA), implying a doubling time of about 20 years). While there has been some reduction of the energy- and emissions-intensity of economic growth in wealthy countries, one has to be cautious about extrapolating recent improvements, as small as they may be, because these "improvements" have been at least partly due to the outsourcing of energy-intensive sectors to poorer countries [Sathaye et al., 2011; Feng et al., 2011a; Davis and Caldeira, 2010; Weber et al., 2008; Yu et al., 2013; Peters, 2008; Peters et al., 2011, 2012; Le Quéré et al., 2014; Muñoz et al., 2009; Bruckner et al., 2012; Wiedmann et al., 2015], and because there are basic physical limits to further efficiency improvements, especially in the use of water, energy, food, and other natural resources [Turral et al., 2010; Ruth, 1993, 1995a,b, 2006].

Two major factors enabled this demographic explosion. First, advances in public health, sanitation, and medicine significantly reduced mortality rates and lengthened average life-span. Second, the rapid and large-scale exploitation of fossil fuels [Krausmann et al., 2009] — a vast stock of nonrenewable resources accumulated by Nature over hundreds of millions of years that are being drawn down in just a few centuries — and the invention of the Haber–Bosch process to use natural gas

[2] In fact, the 2015 Revision has already raised the global total in 2100 by 360 million to 11.2 billion just from the last estimate published in 2013 [United Nations, 2015b].

to produce nitrogen fertilizer [Smil, 2004; Erisman et al., 2008] enabled increasingly higher levels of food and energy production. All these factors allowed fast growth of the human system [Warren, 2015; Smil, 1999]. For example, between 1950 and 1984, the production of grains increased by 250% due to the use of fossil fuels for fertilization, mechanization, irrigation, herbicides, and pesticides [Kendall and Pimentel, 1994]. These technological advances, together with the development of new seed varieties, are referred to as the "Green Revolution" that allowed global population to double in that period [Ramankutty et al., 2002].

Technological advances also allowed for the rapid increase in consumption per capita (see Fig. 2.1). This increase was made possible by a dramatic expansion in the scale of resource extraction, which, by providing a very large increase in the use of inputs, greatly increased production, consumption, throughput, and waste. During the fossil fuel era, per capita global primary energy and per capita global materials consumption have significantly increased over time. Despite tremendous advances in technological efficiencies, world energy use has increased for coal, oil, gas, and electricity since 1900, and global fossil fuel use per capita has continued to rise over the last few decades. There is no empirical evidence of reduction in use per capita, nor has there been an abandonment or long-term decline of one category through substitution by another. The same applies to global per capita use of materials for each of the major materials categories of minerals — industrial, construction, materials for ores, and materials derived from fossil energy carriers. Thus, while the rate of materials intensity of GDP growth has declined (very slowly: 2.5 kg/$ in 1950, 1.4 kg/$ in 2010), the per capita rate continues to increase. The only materials category whose per capita use has remained relatively stable is biomass [Krausmann et al., 2009; Schaffartzik et al., 2014], probably reflecting the physical limits of the planet's regenerating natural resources to continue to provide humans with ever-growing quantities of biomass [Seppelt et al., 2014; Cleveland and Ruth, 1998]. (See Motesharrei et al. [2014] for a conceptual model of regenerating natural resources.)

The rapidly growing size and influence of the Human System has come to dominate the Earth System in many different ways [Crutzen, 2006; Rockström et al., 2009; Barnosky et al., 2012; Crutzen, 2002]. Estimates of the global net primary production (of vegetation) appropriated by humans range as high as 55%, and the percentage impacted, not just appropriated, is much larger [Rojstaczer et al., 2001; Imhoff et al., 2004; Haberl et al., 2007; Lauk and Erb, 2009; Zeng and Yoon, 2009; Zeng et al., 2014; Liu et al., 2015; Haberl et al., 2011; Foley et al., 2005; Krausmann et al., 2013; Assessment, 2005]. Human activity has also had a net negative effect on total global photosynthetic productivity since the most productive areas of land are directly in the path of urban sprawl [Imhoff et al., 2000]. Human use of biomass for food, feed, fiber, fuel, and materials, has become a primary component of global biogeochemical cycles of carbon, nitrogen, phosphorous, and other nutrients. Land-use for biomass production is one of the most important stressors on biodiversity, while total biomass use has continued to grow and demand is expected to continue growing over the next few decades [Krausmann et al., 2008a]. Global food demand alone has been projected to double or more from 2000 to 2050 due to both rising population and rising incomes [Tilman et al., 2011]. Most agriculturally usable land has already been converted to agriculture [Tilman et al., 2002]. Most large mammals are now domesticated animals [Kareiva et al., 2007; Lyons et al., 2004]. Soils worldwide are being eroded, fisheries exhausted, forests denuded, and aquifers drawn down, while desertification due to overgrazing, deforestation, and soil erosion is spreading [Scholes and Scholes, 2013; Vitousek et al., 1997b; Döll et al., 2014; Aeschbach-Hertig and Gleeson, 2012]. Deforestation, in turn, affects local climate through evapotranspiration and albedo [Li et al., 2015, 2016a]. Since climate change is expected to make subtropical regions drier, desertification is expected to further increase, especially due to bidirectional albedo-vegetation feedback [Zeng and Yoon, 2009].

At the same time, greenhouse gases from fossil fuels, together with land-use change, have become the major drivers of global climate change [Hansen et al., 2013; Ciais et al., 2013; Crutzen, 2002]. Atmospheric levels of carbon dioxide, methane, and nitrous oxide not only exceed pre-industrial concentrations by about 40%, 150%, and 20%, respectively, they are now substantially above their maximum ranges of fluctuation over the past 800,000 years[3] [Ciais et al., 2013] while total carbon dioxide emissions continue to grow at a rapid rate [Marland et al., 2012]. Arctic sea ice, Antarctic and Greenland ice sheets, global glacier mass, permafrost area, and Northern Hemisphere snow cover are all decreasing substantially, while ocean surface temperatures, sea level, and ocean acidification are rising [Ciais et al., 2013]. Arctic sea ice is decreasing at an average rate of 3.0 ± 0.3 m^2 per metric ton of CO_2 emissions, and at the current emissions rate of 35 gigaton per year could completely

[3] In some estimates, as much as 10 to 15 million years for carbon [Tripati et al., 2009].

disappear by 2050 during Septembers [Notz and Stroeve, 2016]. The rate of ocean acidification, in particular, is currently estimated to be at least 100 times faster than at any other time in the last 20 million years [Rockström et al., 2009].

The Human System dominates the global nitrogen cycle, having produced a 20% rise in nitrous oxide (N_2O) in the atmosphere, now the third largest contributor to global warming, and a tripling of ammonia (NH_3) in the atmosphere due to human activities [Galloway et al., 2004]. In total, human processes produce more reactive nitrogen than all natural processes combined [Canfield et al., 2010; Rockström et al., 2009; Gruber and Galloway, 2008; Howarth et al., 2012; Vitousek et al., 1997a; Holtgrieve et al., 2011], altering the global nitrogen cycle so fundamentally that Canfield et al. [2010] estimate the closest geological comparison occurred about 2.5 billion years ago. Nitrogen and phosphorus fertilizer runoff, along with nitrogen oxides from fossil-fuel combustion (which is then deposited by rain over land and water) are causing widespread eutrophication in rivers, lakes, estuaries, and coastal oceans, and creating massive Dead Zones, with little or no oxygen, which are increasing in number and size in coastal waters and oceans globally, killing large swaths of sea life and damaging or destroying fisheries. This may be compounded further by potentially dangerous positive feedbacks between hypoxia, ocean acidification, and rising sea temperatures [Cai et al., 2011; Carstensen et al., 2014; Rabotyagov et al., 2014; Melzner et al., 2012; Rockström et al., 2009; Vaquer-Sunyer and Duarte, 2008; Ekstrom et al., 2015; Canfield et al., 2010; Tilman et al., 2001].

Human activities also dominate many regional hydrological cycles [Molle et al., 2010; Vörösmarty et al., 2000; Grasby, 2004; Molden, 2007; Meybeck, 2003; Gordon et al., 2008; Wagener et al., 2010; Barnett et al., 2008], with more than half of all accessible surface freshwater being used by humans, to such an extent that some major rivers are being so excessively depleted that they sometimes no longer reach the sea, while some major inland fresh and salty water bodies, such as Lake Chad, Lake Urmia, Lake Poopó and Aral Sea, are drying up. In many of the principal aquifers that support the world's agricultural regions and in most of the major aquifers in the world's arid and semi-arid zones, groundwater extraction is occurring at far greater rates than natural recharge. This includes aquifers in the US High Plains and Central Valley, the North China Plain, Australia's Canning Basin, the Northwest Sahara Aquifer System, the Guarani Aquifer in South America, and the aquifers beneath much of the Middle East and northwestern India [Famiglietti, 2014; Konikow, 2013; Castle et al., 2014; Famiglietti and Rodell, 2013; Voss et al., 2013; Famiglietti et al., 2011; Rodell et al., 2009; Scanlon et al., 2012]. Climate change can increase the frequency and severity of extreme weather events, such as hot and cold temperature extremes, heat waves, droughts, heavy precipitation, tropical cyclones, and storms [Mei and Xie, 2016; Wuebbles et al., 2013; Cai et al., 2015, 2014; Meehl and Tebaldi, 2004; Easterling et al., 2000]. In addition, more impervious surfaces together with other land cover changes increase runoff significantly, hence intensifying the adverse impacts of extreme hydrological events [Arnold and Gibbons, 1996; Di Baldassarre et al., 2009; Scanlon et al., 2006].

Many other socioeconomic trends and their impacts on the Earth System have accelerated synchronously since the 1950s with little sign of abatement [Steffen et al., 2015, 2006]. For example, human processes play a major role in virtually every major metal cycle, leading to atmospheric and direct contamination of terrestrial and aquatic environments by trace-metal pollutants. Coal combustion is the major source of atmospheric Cr, Hg, Mn, Sb, Se, Sn, and Tl emissions, oil combustion of Ni and V, and gasoline combustion of Pb, while non-ferrous metal production is the largest source of As, Cd, Cu, In, and Zn [Pacyna and Pacyna, 2001]. Surface mining has also become a dominant driver of land-use change and water pollution in certain regions of the world, where mountaintop removal, coal and tar sands exploitation, and other open pit mining methods strip land surfaces of forests and topsoils, produce vast quantities of toxic sludge and solid waste, and often fill valleys, rivers, and streams with the resulting waste and debris [Palmer et al., 2010]. All of these trends can have an impact on other species, and while the exact causes are difficult to establish, current animal and plant species extinction rates are estimated to be at least 100 times the natural background rate [Regan et al., 2001; Vitousek et al., 1997b; Mace et al., 2005; Kolbert, 2014]. Furthermore, ecosystems worldwide are experiencing escalating degradation and fragmentation, altering their health and provision of important ecosystem functions and services for humans and other species. Rates of deforestation and agricultural expansion have accelerated in recent years with extensive new infrastructure providing conduits for settlement, exploitation and development. Even within the remaining habitat, fragmentation is causing rapid species loss or alteration, and is producing major impacts on biodiversity, regional hydrology, and global climate, in particular in tropical forests, which contain over half of Earth's biodiversity and are an important driver in the climate system. Ongoing worldwide habitat fragmentation, together with anthropogenic climate change and other human pressures, may severely degrade or destroy any remaining ecosystems and their wildlife [Laurance et al., 2002; Laurance, 2004; Hanski et al., 2013; Lewis et al., 2015; Gibson et al., 2013; Powell et al., 2015; Bierregaard et al., 1992; Laurance et al., 1997; Ferraz et al., 2003; Laurance et al., 2000]. For example, the Living Planet Index, which measures biodiversity based on 14,152 monitored populations of 3,706 vertebrate species, shows a staggering 58% decline in populations monitored between 1970 and 2012 [WWF, 2016]. Continuation of these trends could result in the loss of two thirds of species populations by 2020 (only 4 years from now) compared to 1970 levels (i.e., in just half a century).

Thus, the Human System has fundamentally impacted the Earth System in a multitude of ways. But as we will show, these impacts on the Earth System also feed back onto the Human System through various factors and variables: human health, fertility, well-being, population, consumption, economic growth, development, migration, and even producing societal conflict. Rather than incorporate these feedbacks, current models simply use independent projections of these human system variables, often in a highly unreliable way.

2.2 Inequality, Consumption, Demographics, and Other Key Human System Properties: Projections vs. Bidirectional Coupling

These large human impacts on the Earth System must be considered within the context of the large global economic inequality to realize that current levels of resource extraction and throughput only support societies at First World living standards for about 17% of the world's current population [United Nations, 2015b]. The majority of the world's people live at what would be considered desperate poverty levels in developed countries, the average per capita material and energy use in developed countries is higher than in developing countries by a factor of 5 to 10 [Krausmann et al., 2008a], and the developed countries are responsible for over three quarters of cumulative greenhouse gas emissions from 1850 to 2000 [Baumert et al., 2005]. To place global resource-use inequality into perspective, it would require global resource-use and waste production at least 2 to 5 times higher than it is now to bring the average levels of the 82% of the world's people living in developing countries up to the average levels of developed countries today [Krausmann et al., 2008a]. The near-tripling in CO_2 emissions per capita in China from just 1990 to 2010 demonstrates the similar potential increases that could take place in the less developed world if this economic disparity is reduced [Balatsky et al., 2015]. Despite making China a focus of global concern because it became the single largest energy user and carbon emitter, China's 2010 per capita energy use (1.85 tonnes of oil equivalent) was actually still below the world average (1.87 toe) [OECD, 2014; Lawrence et al., 2013]. The rest of the developing world, with the potential to reach similar levels of per capita emissions, has more than three times China's population. Furthermore, China's 2010 per capita carbon emissions (6.2 metric tons) were still only about a third of the US (17.6 metric tons) [Bank, 2014a], indicating much more growth can still occur [Balatsky et al., 2015].

However, overall inequality in resource consumption and waste generation is greater than what these comparisons *between* countries demonstrate since resource consumption *within* countries is skewed towards higher income groups. In some countries, the Gini coefficient for carbon emissions (e.g. 0.49 in China and 0.58 in India [Hubacek et al., 2016]) is actually higher than the Gini coefficient for income (0.42 and 0.34 in 2010, respectively [Bank, 2014b]). Rather than disaggregating resource consumption within countries, using national per capita GDP calculations and projections provides a distorted understanding of the distribution and characteristics of resource-use and waste generation. Consumption patterns and associated per capita shares of resource-use and pollution differ enormously, and using a consumption-based calculation rather than a national territorial production-based approach demonstrates even further the extent of global economic and environmental inequality: About 50% of the world's people live on less than \$3 per day, 75% on less than \$8.50, and 90% on less than \$23 (US\$ at current Purchasing Power Parity). The top 10%, with 27.5 tons CO_2 per capita, produce almost as much total carbon emissions (46% of global total) as the bottom 90% combined (54%) with their per capita carbon emission of only 3.6 tons CO_2. [Hubacek et al., 2016; Lawrence et al., 2013]. (See Fig. 2.2).

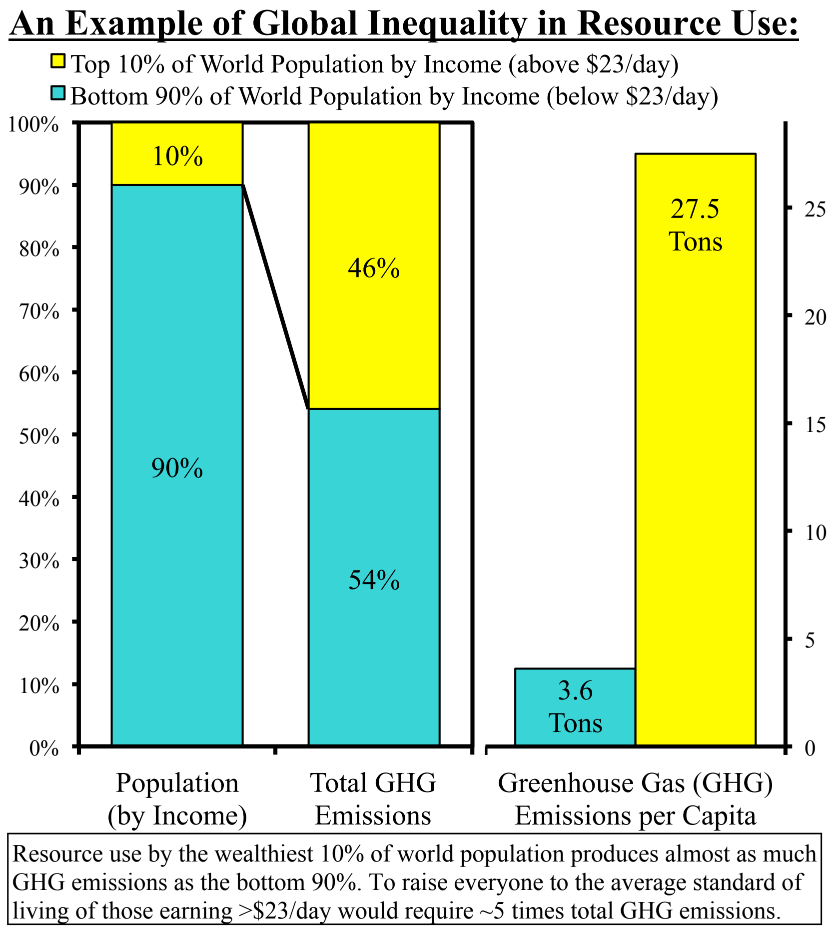

Figure 2.2: Global inequality in carbon emissions.

Furthermore, even if per capita emissions stabilize or decline in the developed countries, population growth in these wealthy countries will remain a major driver of future increases in resource-use and emissions. While some consider population growth a serious issue only in very poor countries, large population growth is still projected for some of the wealthiest countries today. For example, US, Canada, Switzerland, Sweden, Norway, Australia, and New Zealand are each projected to grow by about an additional 40 to 80%. The US, one of the highest resource-use per capita countries in the world (e.g., with an energy consumption per capita 4 times that of China and 16 times that of India in 2010 [Lawrence et al., 2013]), is projected to grow in population by about 50% from both natural increase and immigration, generating a very large increase in total resource-use and waste generation for the US alone.

Population growth in the developed countries is likely to be much higher than the UN estimates project because these estimates include arbitrary projections of very low future immigration from less developed countries. For example, while Africa's population is projected to rise over 6-fold from 366 million in 1970 to 2.4 billion in 2050, the UN's projection of annual net emigration from Africa remains about constant until 2050, at ~500,000, similar to the average from 1970 to 2000, thus the projected percentage emigrating declines sharply. (For comparison, between 1898 and 1914, ~500,000 people emigrated each year just from Italy alone, when its population was only 30-35 million.) Then, from 2050 to 2100, the annual net emigration is arbitrarily projected to smoothly decline to zero, even as Africa's projected population continues rising to over 4 billion [United Nations, 2013b]. However, recent international migration has increased on average with global population [Abel and Sander, 2014] and net migration to the developed countries has increased steadily from 1960 to 2010 [United Nations, 2013b] and more explosively recently. Thus, the UN projection of emigration seems unrealistically low, both relative to its increasing population and in the context of a rapidly aging, and supposedly shrinking, population in the developed countries, as well as recent migration pattern alterations following conflicts and associated social disruptions. The United Nations High Commissioner on Refugees (UNHCR) estimates that by the end of

2015, a total of 65.3 million people in the world were forcibly displaced, increasing at a rate of about 34,000 people per day. There are 21.3m refugees worldwide, with more than half from Afghanistan, Syria, and Somalia [UNHCR, 2016]. Yet this figure only reflects refugees due to persecution and conflict but does not include refugees as a result of climate change, famines, and sea level rise. Net migration in 2015 to Germany alone was 1.1m [DESTATIS, 2016].

The UN's 2012 projections of migration for other regions are similarly arbitrary and unrealistic. Net annual emigration from Latin America is projected to decline from nearly 1.2 million in 2000-2010 to about 500,000 by 2050, and then decline to zero by 2100. Net annual immigration to Europe rose from 41,000 in 1960-1970 to almost 2 million in 2000-2010, and explosively today due to increasing social strife, and yet, the UN's projection for 2010-2050 is a continuous decline in net immigration down to only 900,000 by 2050, and then a decline to zero by 2100 [United Nations, 2013b]. Even the UN Population Division itself admits, "We realize that this assumption is very unlikely to be realized but it is quite impossible to predict the levels of immigration or emigration within each country of the world for such a far horizon" [United Nations, 2013b].

A model that uses these UN population projections incorporates these arbitrary and unrealistic assumptions into their projections, undermining its reliability. This is one reason why it is essential to project demographic variables endogenously within the models. One result of such unrealistically low projections of future migration to the developed countries is to produce lower estimates of future total emissions of the developed countries, which means the developed countries are not required to make as much effort today to lower their own emissions. In order to limit the total increase in average global temperatures within the context of current climate change negotiations over carbon budgets, there is a maximum total amount of carbon that can be emitted globally, thus carbon emissions must be apportioned across countries and across time. Lower estimates of migration to developed countries means lower estimates of emissions in the future in developed countries, which means the developed countries are not required to make as much effort today to lower their own emissions [Stanton, 2011].

Furthermore, the UN projections of a relatively stable population for the whole of the developed world depend on dramatic, and highly unlikely, declines projected in a handful of key countries. Japan, for example, must decline by 34%, Germany by 31% and Russia by about 30% for the projected stability in total developed country population to be born out. These dramatic declines appear highly unlikely given that countries like Japan and Germany have not yet declined by more than about 1% [United Nations, 2013b], and already their governments have enacted a series of policies to encourage higher birth rates. In fact, there is evidence for the efficacy of various family policies in the recent fertility rebounds observed in several developed countries [Luci-Greulich and Thévenon, 2013]. Similarly, Russia, which saw its fertility rate plunge after 1989 (reaching a low of 1.19 in 1999 from 2.13 in 1988), enacted pro-natalist policies and liberalized immigration. The fertility rate has since rebounded, and the population decline reversed in 2009.

In addition, countries often highlighted for their low birth rates, like Italy and Spain, are not projected to decline by even 1% for decades. Small increases in fertility and/or immigration could extend that period for decades longer. Even without those increases in fertility or immigration, the total population of developed countries is not projected by the UN to peak until about 2050, and trajectories beyond that are very difficult to predict given their high dependence on future policies.

Despite widespread talk of population decline, it is important to emphasize that the only countries in the world to have experienced any declines beyond about 1% have all been associated with the special circumstances of the collapse of the former Soviet Bloc (and some microstates, such as a few island nations), and even in these cases, migration has played a major role in population changes. This is even true within Germany, where the only Länder (provinces) which have declined significantly in population are all from the former East Germany.

Since population is stabilizing in some countries, it is often thought that the human population explosion of the 20th century (growing by a factor of about 4) is over, and since rates of growth have been declining, family planning and population growth is no longer a concern. However, the UN projections of a stabilization in global population [United Nations, 2013b] are so far into the future (after 2100) that the projections are unreliable [Warren, 2015] and global stabilization itself is highly uncertain [Heilig et al., 2010]. In fact, alternate projection methodologies suggest with much more certainty that stabilization is unlikely to occur [Gerland et al., 2014]. Furthermore, even the UN projections are based on large assumed decreases in fertility rates in much of the world. If those projected decreases in fertility rates are off by only 0.5 births per woman (an error of less than 10% in many high fertility countries), the date at which the world reaches 11 billion will occur 5 decades earlier and will raise the global total population by 2100 to nearly 17 billion and still rapidly growing [United Nations, 2013b].

Current projections should be understood in the context of past projections that have overestimated fertility declines. For example, the 1999 UN projections significantly overestimated the time it would take to add the next billion people [United Nations, 1999]. Worse still, the 2015 estimate for the world's total population in 2100 [United Nations, 2015b] has gone up by over 2 billion just since the 2004 estimate [United Nations, 2004]. Even the 2010 UN projections had to be revised upwards in 2012 because previous estimates of total fertility rates in a number of countries were too low, and in some of the poorest countries the level of fertility appears to have actually risen in recent years [United Nations, 2013b; Lesthaeghe, 2014; NAS, 2016], and the 2012 estimates have again been revised upwards in 2015 [United Nations, 2015b]. To put all this in perspective, the 2004 estimates projected a peak in world population of 9.22 billion, but in the 2015 projection, 9.22 billion will be reached as early as 2041, and will still be followed by at least another 6 decades of growth.

Past mistaken projections reflect the use of highly questionable assumptions about fertility rate declines in developing countries [Heilig et al., 2010] that tend to reproduce a "natural" decline following the trajectory of more developed countries. Yet the empirical record shows that reductions (or increases) in fertility rates reflect a complex range of sociodemographic, economic, and policy conditions [Potts, 1997; Campbell et al., 2006; Lutz et al., 2014; Luci-Greulich and Thévenon, 2013;

Campbell et al., 2013; Bongaarts, 2016; Potts, 2014]. If those conditions are not present, the projected declines will not necessarily occur, as can be seen in countries like Niger (7.4 births per woman in 1970, 7.6 in 2012) [PRB, 2014; Potts et al., 2011]. Needless to say, the use of demographic projections with overestimated fertility declines again produces underestimated projections of future resource-use and emissions.

Even with these assumptions of large fertility declines in the projections, each additional billion humans added will not be spread evenly across the planet. The vast majority of the growth will be concentrated in countries that today continue to have very high rates of fertility (about 25 countries above 5, 45 above 4, and 65 above 3). These countries are also the lowest-income countries in the world, with the lowest resource-use per capita, which means that the majority of population growth is taking place precisely in regions with the highest potential for growth in resource-use per capita over the coming decades [Lawrence et al., 2013], and the growth of the total impact is the product of the two. For example, the lowest-income continent, Africa, which had 230 million people in 1950 and over a billion in 2010 (a four-fold increase in one lifetime) is currently on track to add another 3 billion in the next 85 years (another four-fold increase in one lifetime). Nigeria, by itself, is projected to reach almost 1 billion people. These high projections already assume very large decreases in fertility rates from their current average levels of approximately 5 children/woman in Sub-Saharan Africa. (Without this projected decrease in fertility rates, Africa alone would add 16 billion rather than 3 billion more people by 2100 [United Nations, 2013b].) The UN medium range projections show that the developing world (not including China) will grow by an additional 2.4 billion people in just the next three and a half decades, and a total of an additional 4 billion by 2100. Due to these uneven population growth rates, about 90% of the world's population will be living in today's less developed countries, with most of the growth in the poorest of these countries [United Nations, 2013b].

Poorer populations are expected to be more heavily impacted by climate change and other mounting environmental challenges despite having contributed much less to their causes [Ruth and Ibarrarán, 2009; IPCC, 2001, 2007; Group, 2014]. International and internal migration is increasingly being seen as an important component of adaptation and resilience to climate change and a response to vulnerabilities from other environmental risks. Given the aging social structures in some parts of the world, policies that support increased migration could be important not only for environmental adaptation, but also for the realization of other socioeconomic and demographic goals. Thus, migration will help both the sending and receiving countries. Of course, given the scale of projected population growth, migration alone is unlikely to be able to balance the regional disparities.

Current projections of future resource-use and greenhouse gas emissions used in the Intergovernmental Panel on Climate Change (IPCC) reports and Integrated Assessment Models (IAMs, discussed further in Section 2.3) also depend heavily on a continuation of high levels of global economic inequality and poverty far into the future. Projections that global resource-use and emissions will not rise very much due to rapid population growth in the poorest countries are based on the assumption that those countries will remain desperately poor by the standards of developed countries. (This assumption again provides the added benefit for today's wealthy countries that the wealthy countries have to make less effort today to reduce their own emissions. Given total global carbon emissions targets, projections of low economic growth in poor countries translate into less stringent carbon reduction requirements in wealthy countries [Raupach et al., 2014; Stanton, 2011].) However, China's recent rapid rise in emissions per capita shows this is a potential future path for the rest of the developing world. To argue otherwise requires assuming that today's developing countries will remain in desperate poverty, and/or will adopt technologies that the developed countries themselves have yet to adopt. Real world CO_2 emissions have tracked the high end of earlier emissions scenarios [Friedlingstein et al., 2014], and until the currently wealthy countries can produce a large decline in their own emissions per capita, it is dubious to project that emissions per capita in the less developed countries will not continue on a trajectory up to the levels of currently wealthy countries.

The scientific community has urged limiting the global mean surface temperature increase relative to pre-industrial values to 2°C. The economic challenges of staying on a 2°C pathway are greater the longer emission reductions are postponed [Iyer et al., 2015]. Given the role that developed countries have played historically in the consumption of fossil fuels, and their much higher per capita carbon emissions today, it is imperative that the developed countries lead the way and establish a successful track record in achieving such reductions. Thus, it is positive that at the United Nations Framework Convention on Climate Change (UNFCCC) Conference of the Parties (COP21) in Paris in December 2015, governments crafted an international climate agreement indicating their commitments to emissions reduction for the near term (to 2025 or 2030). Most importantly, the US committed to reduce economy-wide greenhouse gas (GHG) emissions below 2005 levels by 26–28% in 2025, and the EU has committed to reduce 2030 GHG emissions relative to 1990 by 40% (excluding emissions from land-use changes). Assuming that the goals of the Intended Nationally Determined Contributions (INDCs) are fulfilled, the results in Fawcett et al. [2015] and Iyer et al. [2015] show that a successful Paris agreement on near-term emissions reductions will be valuable in reducing the challenges of the dramatic long-term transformations required in the energy system to limit global warming to 2°C. The Paris framework will succeed even further if it enables development of subsequent pathways leading to the required additional global emissions reductions.

As we will show, all of these points raise the critical issue of the accuracy and reliability of the assumptions underlying the projections of key Human System variables, such as inequality, population, fertility, health, per capita GDP, and emissions per capita. These are the central elements in many of the standard models used to explore the future of humanity and the environment, such as various Integrated Assessment Models used to guide policy, and models used by the IPCC whose output guides international negotiations on energy use and emissions. Common to these models is their deficiency in capturing dynamic bidirectional feedbacks between key variables of the Human System and the Earth System; instead, they simply use independent projections of Human System variables in Earth System models.

2.3 Human System threatens to overwhelm the Carrying Capacity and Ecosystem Services of Earth System.

Economic theories that endorse limitless growth are based on a model of the economy that, in essence, does not account for the resource inputs and waste absorption capacities of the environment, and the limitations of technological progress and resource substitutability. In other words, these theories essentially model the economy as a perpetual motion machine [Daly, 1996]. But in the real world, economic activity both consumes physical material and energy inputs and produces physical waste outputs. The Earth System performs the functions ("ecosystem services") of providing both the *Sources* of these material and energy inputs to the human economy, as well as the *Sinks* which absorb and process the pollution and waste outputs of the human economy. See Figs. 2.3 and 2.4 [Daily, 1997; Kareiva et al., 2011; Assessment, 2005; Daly, 1996; Daily et al., 2009]. Since the scale of the Human System has grown dramatically relative to the Earth System's capacity to provide these ecosystem services, the problems of *depletion* and *pollution* have grown dramatically.

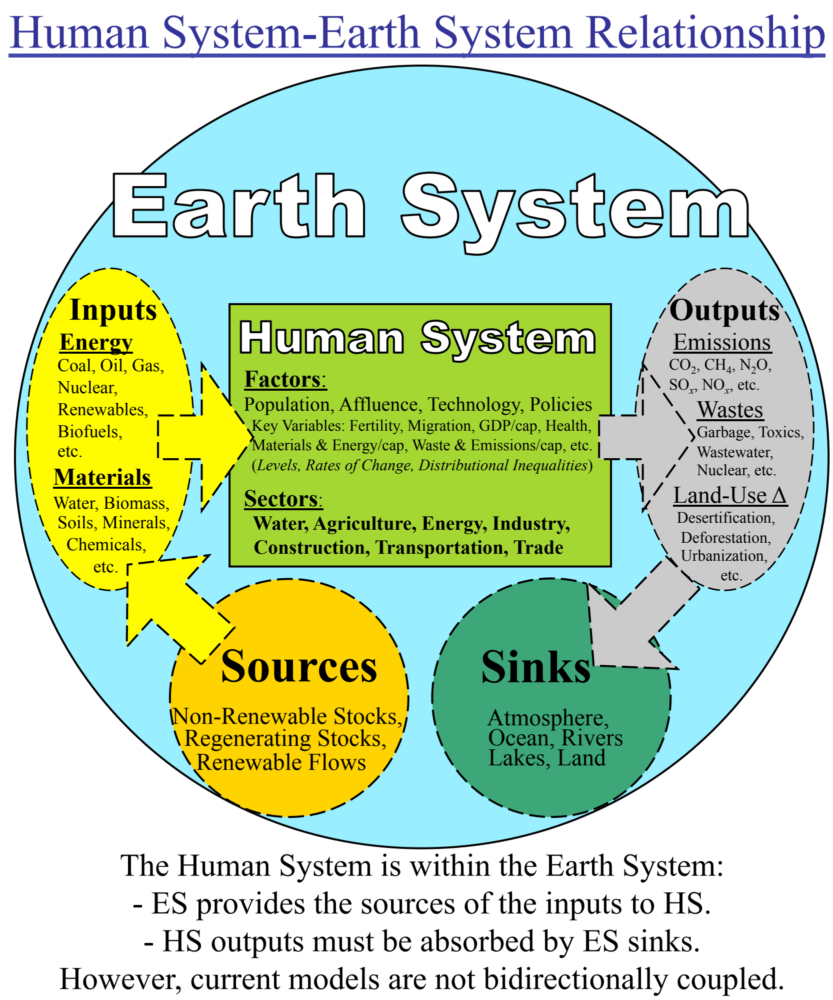

Figure 2.3: Relationship of the Human System within the Earth System, not separate from it (after Daly and Farley [2003]). The Earth System provides the sources of the inputs to, and the sinks that absorb the outputs of, the Human System.

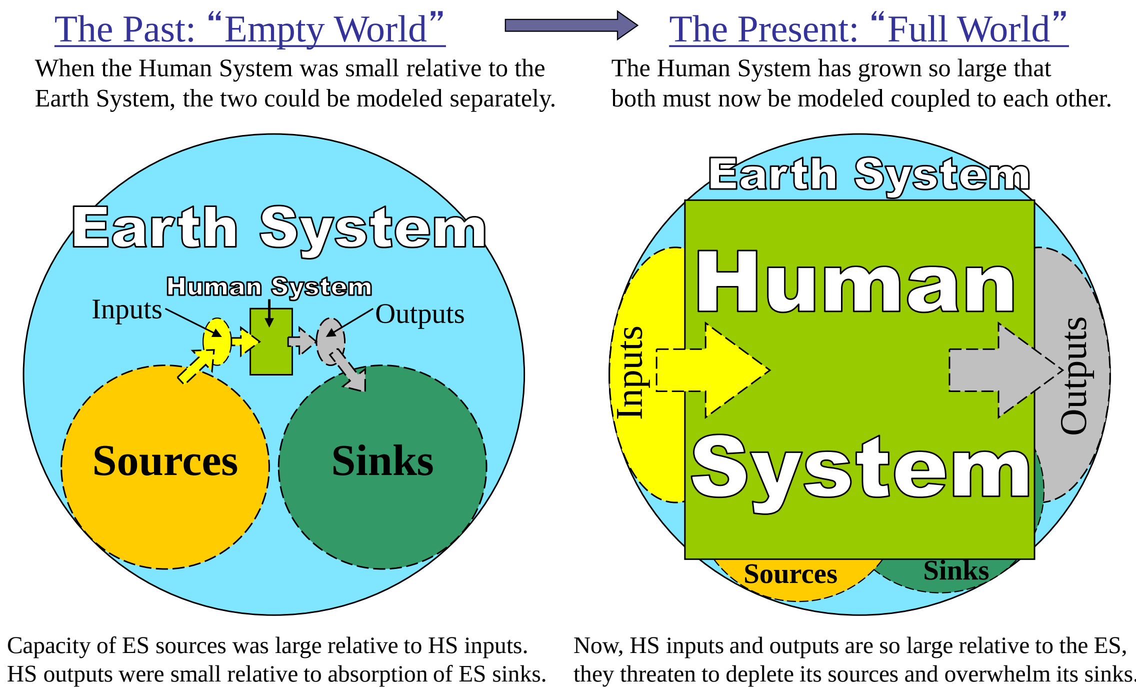

Figure 2.4: Growth of the Human System has changed its relationship with the Earth System and thus both must be modeled interactively to account for their feedback on each other.

Herman Daly has pointed out that the magnitude and growth rates of resource input and waste output are not sustainable: "We are drawing down the stock of natural capital as if it was infinite" [Daly and Farley, 2003]. For example, the rapid consumption of fossil fuels is releasing vast stocks of carbon into the atmospheric and ocean sinks at a rate about a *million times faster* than Nature accumulated these carbon stocks. As another example, millions of metric tons of plastic enter the oceans every year and accumulate throughout the world's oceans, especially in all subtropical gyres [Jambeck et al., 2015; Cózar et al., 2014]. Furthermore, while certain sectors of global society have benefited from the growth of the past 200 years, the environmental consequences are global in their impact, and the time scale of degradation of the resulting waste products (e.g., emissions, plastics, nuclear waste, etc.) is generally much longer than they took to produce or consume. Contrary to some claims within the field of Economics, physical laws do place real constraints on the way in which materials and energy drawn from the Earth System can be used and discharged by the Human System [Georgescu-Roegen, 1971; Ruth, 1993, 2006; Cleveland and Ruth, 1997]. To be sustainable, human consumption and waste generation must remain at or below what can be renewed and processed by the Earth System.

It is often suggested that technological change will automatically solve humanity's environmental sustainability problems [Solow, 1974; Nordhaus et al., 1973; Simon, 1981]. However, there are widespread misunderstandings about the effects of technological change on resource-use. There are several types of technological changes, and these have differing effects on resource-use. While some changes, such as in *efficiency* technologies, can increase resource-use efficiency, other changes, such as in *extraction* technologies and *consumption* technologies, raise the scale of resource extraction and per capita resource consumption. In addition, absent policy effects, even the increased technological efficiencies in resource-use are often compensated for by increases in consumption associated with the "Rebound Effect" [Polimeni et al., 2008; Greening et al., 2000; Ruth, 2009; Smil, 2008]. Furthermore, advances in *production* technologies that appear to be increases in productivity are instead very often due to greater energy and material inputs, accompanied by greater waste outputs. While the magnitude and even the sign of the effect of technological change on resource-use varies greatly, the empirical record shows that the net effect has been a continued increase in global per capita resource-use, waste generation, and emissions despite tremendous technological advances.

While per capita emissions of developed countries appear to be stabilizing when measured within the country of production, this is largely due to the shift in the location of energy-intensive manufacturing to developing countries, and estimates of developed countries' per capita emissions measured based on their consumption show that they continued to grow [Peters et al., 2011; Davis and Caldeira, 2010; Weber et al., 2008; Yu et al., 2013; Feng et al., 2011a; Peters, 2008; Peters et al., 2012; Le Quéré et al., 2014; Sathaye et al., 2011]. Even if today's industrialized societies can stabilize their resource-use (at probably already unsustainable levels), large parts of the world are in the midst of this industrial transition and the associated technological regime shift from agrarian to industrial society that greatly increases per capita resource-use and waste production [Krausmann et al., 2008b; Schaffartzik et al., 2014]. The effect of technological change can be observed in the transition from agrarian to industrial society. This industrialization raised agricultural yields largely due to increasing inputs, thereby allowing rapid human system expansion, but it also generated a societal regime shift that greatly increased per capita resource-use and waste generation [Krausmann et al., 2008b]. For example, from just 1971 to 2010, total primary energy use per capita in Korea increased by a factor of 10, from 0.52 to 5.16 tonnes of oil equivalent (toe) [OECD, 2014]. Therefore, technological advancement can add to the problems of global sustainability, rather than solve them. The question is not only whether technology can help solve environmental sustainability challenges, but also what policies and measures are required to develop the right technologies and adopt them in time. Technological advances could, and should, be part of the solutions for environmental and sustainability problems, for example, by transitioning to renewables, increasing use-efficiency, and fostering behavioral changes to cut resource-use and emissions, particularly in the high resource-using countries. But these technological solutions do not just happen by themselves; they require policies based on scientific knowledge and evidence to guide and support their development and adoption.

An important concept for the scientific study of sustainability is Carrying Capacity, the total consumption — determined by population, inequality, and per capita consumption — that the resources of a given environment can maintain over the long term [Catton, 1980; Daly and Farley, 2003]. One can generalize the definition of Carrying Capacity (CC) to any subsystem with different types of natural resources coupled with sociodemographic variables. For example, the subsystems for water, energy, and agriculture — each coupled bidirectionally to human sociodemographic variables and to each other — result in Water CC, Energy CC, and Agriculture CC. Water CC can be defined as the level of population that can be sustained at a particular per capita consumption and a given level of water sources and supply in the area under study. In general, this level depends on both human and natural factors. For example, Water CC is determined by the natural flow rate of water into and out of the area, precipitation and evaporation, withdrawal rate from water sources, dispensing technology, recycling capacity, etc. Moreover, Water, Energy, or Agriculture CC in a certain area can be imported from other regions to temporarily support a larger population and consumption [Feng et al., 2011a; Würtenberger et al., 2006; Rees, 1996]. Recent literature has emphasized the integrated nature of agricultural, energy, and water resources, and modeling the interactions of these subsystems is essential for studying the food-energy-water nexus [Bazilian et al., 2011; Waughray, 2011; Hussey and Pittock, 2012; Dale et al., 2011; Khan and Hanjra, 2009]. In order to understand and model either Human or Earth Systems, we must model all these natural and human subsystems interactively and bidirectionally coupled.

Consumption of natural resources by a population beyond the rate that nature can replenish overshoots the Carrying Capacity of a given system and runs the risk of collapse. Collapses in population are common in natural systems and have occurred many times in human societies over the last 10,000 years. A recent study focusing on the many collapses that took place in Neolithic Europe concluded that endogenous causes, i.e., overrunning Carrying Capacity and the associated social stresses, have been the root cause of these collapses [Shennan et al., 2013; Downey et al., 2016].

To study key mechanisms behind such collapses, Motesharrei et al. [2014] developed a two-way coupled Human and Nature Dynamic model, HANDY, by adding accumulated wealth and economic inequality to a predator-prey model of human-nature interaction. The model shows that both economic inequality and resource over-depletion can lead to collapse, in agreement with the historical record. Experiments presented in that paper for different kinds of societies show that as long as total consumption does not overshoot the Carrying Capacity by too much, it is possible to converge to a sustainable level. However, if the overshoot is too large, a collapse becomes difficult to avoid (see Fig. 2.5).

Collapses could also happen due to rapid decline of Carrying Capacity (CC) as a result of environmental degradation. Droughts and climate change can decrease natural capacities and regeneration rates, which in turn lead to a decline of CC. (Motesharrei et al. [2014] describe how to model these factors for a generic system, termed Nature Capacity and Regeneration Rate, and how they determine CC.) The resulting gap between total consumption and CC can lead to conflicts and the ensuing collapses. For example, see recent literature that shows the impacts of climate change on conflicts [Hsiang et al., 2011; Kelley et al., 2015; Hsiang et al., 2013], a potential precursor to collapses.

Modern society has been able to grow far beyond Earth's carrying capacity by using nonrenewable resources such as fossil fuels and fossil water. However, results from the model show that an unsustainable scenario can be made sustainable by reducing per capita depletion rates, reducing inequality to decrease excessive consumption by the wealthiest, and reducing birth rates to stabilize the population [Motesharrei et al., 2014]. The key question is whether these changes can be made in time.

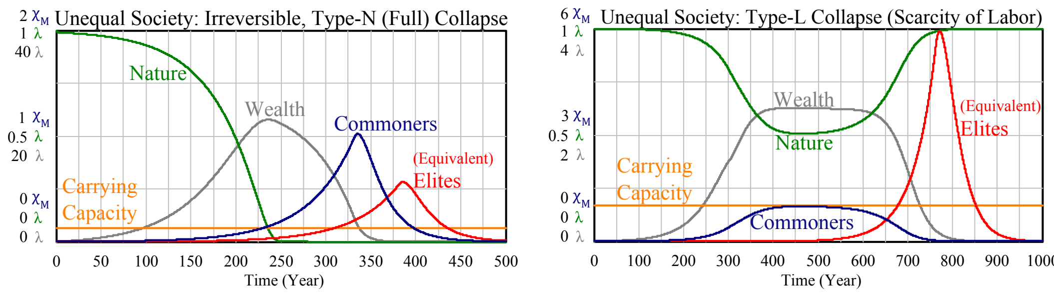

(a) A type-N (Nature) collapse due to both over-depletion of Nature and inequality.

(b) A type-L (Labor) collapse: after an apparent equilibrium, population collapses due to over-exploitation of Labor, although Nature eventually recovers.

Figure 2.5: Example results from Motesharrei et al. [2014].

Current models of climate change include sea level rise, land degradation, regional changes in temperature and precipitation patterns, and the consequences for agriculture, but without modeling the feedbacks that these significant impacts would have on the Human System, such as geographic and economic displacement, forced migration, destruction of infrastructure, increased economic inequality, nutritional sustenance, fertility, mortality, conflicts, and spread of diseases or other human health consequences [Ruth and Ibarrarán, 2009; Guzmán et al., 2009].

For example, nearly all features of the hydrologic system are now impacted by the human system [Wagener et al., 2010] with important feedbacks onto humans, e.g., snowpack decline due to climate change [Barnett et al., 2008] reduces water availability; agricultural processes further affect water availability and water quality [Gordon et al., 2008]; land use changes can reduce groundwater recharge [Scanlon et al., 2006], and thus many populations face both reduced water availability and increased flood frequency and magnitude [Di Baldassarre et al., 2009]. Moreover, increases in the frequency and magnitude of extreme weather events can impact agriculture and ecosystems [Rosenzweig et al., 2001; Easterling et al., 2000].

Furthermore, chemicals used in hydraulic fracturing, which involves cracking shale rock deep underground to extract oil and gas, can contaminate groundwater resources [Vaidyanathan, 2016; Jackson et al., 2015; DiGiulio and Jackson, 2016]. In addition, the injection of wastewater from oil and gas operations for disposal into deep underground wells is also altering the stresses of geologic faults, unleashing earthquakes [Shirzaei et al., 2016]. For example, "Until 2008 not a single earthquake had ever been recorded by the U.S. Geological Survey from the Dallas-Fort Worth (DFW) area…Since then, close to 200 have shaken the cities and their immediate suburbs. Statewide, Texas is experiencing a sixfold increase in earthquakes over historical levels. Oklahoma has seen a 160-fold spike in quakes…In 2014 the state's earthquake rate surpassed California's." [Kuchment, 2016].

Changes in the structure and functions of the ecosystem can also pose important threats to human health in many different ways [Myers et al., 2013]. Climate, climatic events (e.g., El Niño), and environmental variables (e.g., water temperature and salinity) can play a fundamental role in the spread of diseases [Colwell, 1996; Lipp et al., 2002; Pascual et al., 2000; Lobitz et al., 2000]. A recent report by the United States Global Change Research Program illustrates how climate change could affect human health through various processes and variables such as temperature-related death and illness, air quality, extreme events, vector borne diseases, water-related illness, food safety and nutrition, and mental health and wellbeing [Crimmins et al., 2016]. This USGCRP report states that "Current and future climate impacts expose more people in more places to public health threats... Almost all of these threats are expected to worsen with continued climate change."

Environmental catastrophes can result in the decline of national incomes for a few decades [Hsiang and Jina, 2014], and higher temperatures can severely affect human health [Romeo Upperman et al., 2015] and reduce economic productivity [Hsiang, 2010]. This effect is in addition to the well-established reduction in agricultural yields due to higher temperatures [Schlenker and Roberts, 2009; Peng et al., 2004; Lobell et al., 2011; Lobell and Field, 2007; Schlenker and Lobell, 2010; Moore and Lobell, 2015]. Climate could also be a strong driver of civil conflicts [Hsiang et al., 2011, 2013; Burke et al., 2009; Kelley et al., 2015; Ban, 2007]. Environmental change is also a known trigger of human migration [Myers, 2002; Feng et al., 2010b; Barbieri et al., 2010]. These, in turn, will significantly increase the unrealistically small future migration projections described in Section 2.2. In fact, climate change alone could affect migration considerably through the consequences of warming and drying, such as reduced agricultural potential, increased desertification and water scarcity, and other weakened ecosystem services, as well as through sea level rise damaging and permanently inundating highly productive and densely populated coastal lowlands and cities [Houghton et al., 1992; IPCC, 2001, 2007; Stern, 2007]. Furthermore, the impacted economic activities and migration could then feed back on human health [Ruiz et al., 2000]. Bidirectional coupling is required to include the effects of all of these feedbacks.

2.4 Bidirectional Coupling of Human System and Earth System Models is Needed. Proposed Methodology: Dynamic Modeling, Input–Output Models, Data Assimilation

Coupled systems can reveal new and complex patterns and processes not evident when studied separately. Unlike systems with only unidirectional couplings (or systems that just input data from extrapolated or assumed projections), systems with bidirectional feedbacks often produce nonlinear dynamics that can result in counterintuitive or unexpected outcomes [Liu et al., 2007]. Nonlinear systems often feature important dynamics which would be missed if bidirectional interactions between subsystems are not modeled. These models also may call for very different measures and policy interventions for sustainable development than those suggested by models based on exogenous forecasts of key variables.

The need for bidirectional coupling can be seen from the historical evolution of Earth System modeling. In the 1960s, atmospheric scientists developed the first mathematical models to understand the dynamics of the Earth's climate, starting with atmospheric models coupled to simple surface models (e.g., Manabe et al. [1965]). Over the following decades, new components such as ocean, land, sea-ice, clouds, vegetation, carbon, and other chemical constituents were added to make Earth System Models (ESMs) more physically complete. These couplings needed to be bidirectional in order to include feedbacks [Manabe et al., 1965]. The importance of accounting for bidirectional feedbacks is shown by the phenomenon of

El Niño-Southern Oscillation (ENSO), which results from the coupled dynamics of the ocean-atmosphere subsystems. Until the 1980s, atmospheric and ocean models were unidirectionally coupled (in a simple, "one-way" mode): the atmospheric models were affected by sea surface temperatures (SST) but could not change them, and ocean models were driven by atmospheric wind stress and surface heat fluxes, but could not change them. Such unidirectional coupling could not represent the positive, negative, and delayed feedbacks occurring in nature that produce ENSO episodes. Zebiak and Cane [1987] developed the first prototype of a bidirectional coupled ocean atmosphere model. This model, for the first time, allowed prediction of El Niño several seasons in advance [Cane et al., 1986]. Similarly, improving the modeling of droughts requires bidirectional coupling of the atmosphere and land submodels (see, for example, Koster et al. [2009]). Most current climate models have since switched to fully coupled atmosphere-ocean-land-ice submodels. This example shows that we can miss very important possible outcomes if the model fails to consider bidirectional feedbacks between different coupled components of systems that the model represent. Since the Human System has become dominant, it is essential to couple the Earth and Human Systems models bidirectionally in order to simulate their positive and negative feedbacks, better reflecting interactions in the real world.

It is important to note that such interactions take place not just at a global scale but also at the ecosystem and local habitat scales. Ecosystems at the regional and local scales provide critical habitat for wildlife species, thus preserving biodiversity, and are also an essential source of food, fiber, and fuel for humans, and forage for livestock. Ecosystem health, composition, function, and services are strongly affected by both human activities and environmental changes. Humans have fundamentally altered land cover through diverse use of terrestrial ecosystems at the local scale, which then impact systems at the global scale. Additional changes have taken place as a result of climate change and variability [Melillo et al., 2014]. Further human pressures are projected to have additional repercussions for species survival, biodiversity, and the sustainability of ecosystems, and in turn feedback on humans' food security and economic development [Rosenzweig et al., 2001]. Thus, a key challenge to manage change and improve the resilience of terrestrial ecosystems is to understand the role that different human and environmental forces have on them, so that strategies that target the actual drivers and feedbacks of coupled components of change can be developed and implemented. Understanding how terrestrial ecosystems function, how they change, and what limits their performance is critically important to determine their carrying capacity for accommodating human needs as well as serving as a viable habitat for other species, especially in light of anticipated increase in global population and resource-consumption for the rest of this century and beyond. Biodiversity and ecosystem services in forests, farmlands, grazing lands, and urban landscapes are dominated by complex interactions between ecological processes and human activities. In order to understand such complexity at different scales and the underlying factors affecting them, an integrated Human-Earth systems science approach that couples both societal and ecological systems is needed. Humans and their activities are as important to the changing composition and function of the Earth system as the environmental conditions and their natural variability. Thus coupled models are needed to meet the challenges of overcoming mismatches between the social and ecological systems and to establish new pathways toward "development without destruction" [Laurance, 2004; Hanski et al., 2013; Lewis et al., 2015; Gibson et al., 2013; Powell et al., 2015; Bierregaard et al., 1992; Laurance et al., 1997; Ferraz et al., 2003; Laurance et al., 2000].

This coupling process has taken place to a certain extent, but the coupling does not include bidirectional feedbacks between the Human and Earth Systems. Energy and Agriculture sectors have been added to Earth System Models (ESMs) creating comprehensive "Integrated Assessment Models" (IAMs). There are now several important, advanced IAMs, including MIT's IGSM, US DOE's GCAM, IIASA's MESSAGE, the Netherlands EAA's IMAGE, etc.[4] [Prinn et al., 1999; Sokolov et al., 2005; Edmonds et al., 1994; Calvin et al., 2013; Nakicenovic and Riahi, 2003; Bouwman et al., 2006]. However, in the IAMs, many of which are used in producing the IPCC reports, population levels are obtained from a demographic projection like the United Nations' population projections discussed in Sections 2.1 and 2.2, which do not include, for example, impacts that climate change may have on the Human System [Nobre et al., 2010].

In today's IAMs, tables of projected demographic and socioeconomic vari-

[4]MIT: Massachusetts Institute of Technology; IGSM: Integrated Global System Modeling framework; US DOE: United States Department of Energy; GCAM: Global Change Assessment Model; IIASA: International Institute for Applied Systems Analysis; MESSAGE: Model for Energy Supply Systems And their General Environmental impact; EAA: Environmental Assessment Agency; IMAGE: Integrated Modelling of Global Environmental Change.

ables determine changes in resource-use and pollution/emission levels, which in turn can determine Earth System variables such as atmospheric temperature. However, changes in resource levels, pollution, temperature, precipitation, etc. estimated by the IAMs cannot, in turn, impact levels of these Human System variables and properties because they are exogenous to the IAMs. This is true even for the scenarios of the IPCC, which are constructed without full dynamic coupling between the human and natural systems. Although there are certain IAMs that include some couplings within human subsystems, critical feedbacks from natural systems onto demographic, economic, and human health variables are missing, so that the coupling between human subsystems and the Earth System in most current modeling is unidirectional, whereas in reality, this coupling is bidirectional [Nobre et al., 2010].

Without including such coupled factors, the independent projections of population levels, economic growth, and carbon emissions could be based on inconsistent or contradictory assumptions, and hence could be inherently incorrect. For example, the United Nations' population projections assume fertility declines in today's lowest-income countries that follow trajectories established by higher income countries. However, the economic growth projections and, therefore, per capita carbon emission projections, assume today's poorest countries will not grow close to anywhere near the level of today's wealthy countries. The 45 lowest income countries are projected to grow to about $6,500 GDP per capita by 2100 [Stanton, 2011] but the average GDP per capita of today's high-income countries is about $45,000. Rather than relying on projections, the demographic component of any coupled model must include the factors that contributed to the demographic transition in other countries, such as education, family planning, health care, and other government policies and programs [Cohen, 2008; Potts and Marsh, 2010; Lutz et al., 2014; Sulston et al., 2012].

Projections of key variables in a realistic model should not be based on mechanistic time-extrapolations of those variables but rather on the intrinsic internal dynamics of the system. Specifically, key parameters of the Human System, such as fertility, health, migration, economic inequality, unemployment, GDP per capita, resource-use per capita, and emissions per capita, must depend on the dynamic variables of the coupled Human–Earth system. Not including these feedbacks would be like trying to make El Niño predictions using dynamic atmospheric models but with sea surface temperatures as an external input based on future projections independently produced (e.g., by the UN) without feedbacks.

Furthermore, the use of GDP as a key measure and determinant in these future projections is itself highly problematic, because it is a very weak measure of human well-being, economic growth, or societal prosperity [Costanza et al., 2014]. GDP neither accounts for the value of natural capital nor human capital, ignores income and wealth inequality, neglects both positive and negative externalities, and only captures social costs and environmental impacts to the extent that prices incorporate them. Any economic activity, whether deleterious or not, adds to GDP as long as it has a price. For example, labor and resources spent to repair or replace loss due to conflicts or environmental damages are counted as if they add to — rather than subtract from — total output. Alternative measures, such as the Genuine Progress Indicator (GPI), the Sustainable Society Indicator (SSI), the Human Development

Index (HDI), and the Better Life Index (BLI) of the Organization for Economic Co-operation and Development, have been developed [Talberth et al., 2007; Van de Kerk and Manuel, 2008; Anand and Sen, 1994]. These measures show that, especially since the 1970s, the large increases in GDP in the developed countries have not been matched by increases in human well-being. Integrated and coupled Human–Earth system models will allow for the development of much more accurate and realistic measures of the actual productivity of economic activity and its costs and benefits for human well-being. Such measures will allow for the valuation of both natural and human capital and for defining and developing sustainability metrics that are inclusive of the wealth of natural and human capital. They will also bring together the current disparate debates on environment/climate, economics, demographics, policies, and measures to put the Human-Earth System on a more sustainable path for current and future generations.

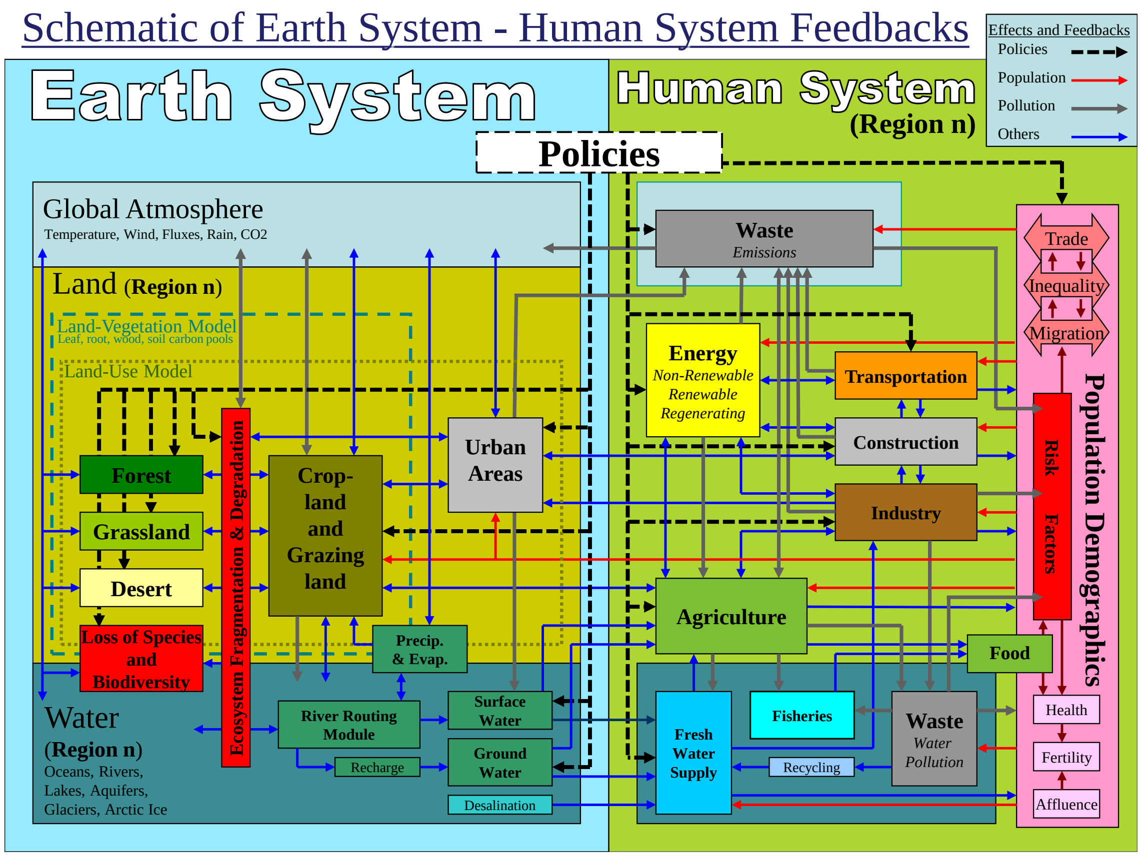

Figure 2.6: Schematic of a Human-Earth System with Drivers and Feedbacks.

To address the above issues, the development of coupled global Human-Earth System frameworks that capture and represent the interactive dynamics of the key subsystems of the coupled human-nature system with two-way feedbacks are urgently needed. The global Human-Earth System framework we propose, and represent schematically in Fig. 2.6, combines not only data collection, analysis techniques, and Dynamic Modeling, but also Data Assimilation, to bidirectionally couple an Earth System Model containing subsystems for Global Atmosphere, Land (including both Land-Vegetation and Land-Use models) and Ocean and Ice, to a Human

System Model with subsystems for Population Demographics, Water, Energy, Agriculture, Industry, Construction, and Transportation. The Demographics subsystem includes health and public policy factors that influence key variables such as fertility, disease, mortality, and immigration rates, while the Water, Energy, Agriculture, Industry, Construction, and Transportation subsystems include cross-national input-output modeling to provide the consumption-based resource-input and waste-output "footprint" accounting analyses missing from the territorial-based methods.

Input-output (IO) analysis can account for the flows of resource-inputs, intermediate and finished goods and services, and waste-outputs, along the production chain [Miller and Blair, 2009; Murray and Wood, 2010]. By accounting for the impacts of the full upstream supply chain, IO analysis has been used in life-cycle analysis [Hendrickson et al., 1998] and for linking local consumption to global impacts along global supply chains [Hubacek et al., 2014; Davis and Caldeira, 2010; Lenzen et al., 2012; Peters et al., 2011]. IO models can be extended with environmental parameters to assess different environmental impacts from production and consumption activities, including water consumption [Feng et al., 2011a,b; Guan and Hubacek, 2007], water pollution [Guan and Hubacek, 2007, 2008], carbon dioxide emissions [Feng et al., 2010a; Hertwich and Peters, 2009; Guan et al., 2009], land use and land cover change [Weinzettel et al., 2013; Hubacek and Sun, 2001; Yu et al., 2013], and biodiversity [Lenzen et al., 2012]). Such models have been developed and applied at various spatial and temporal scales. Since emissions embodied in trade have been growing rapidly, resulting in an increasing divergence between territorial-based and consumption-based emissions, territorial measures alone cannot provide a comprehensive and accurate analysis of the factors driving emissions nor the effectiveness of reduction efforts [Barrett et al., 2013]. IO models can provide these consumption-based calculations and have been employed to identify and quantify key drivers for emissions and energy consumption (such as population growth, changes of consumption patterns, and technical progress [Feng et al., 2012; Guan et al., 2008, 2009]) as well as the environmental impacts of social factors (such as urbanization and migration) reflecting consumption patterns of different categories of households with high spatial detail [Baiocchi et al., 2010; Hubacek et al., 2014]. IO analysis can also be used for simulating potential future states of the economy and the environment (e.g., Duchin [1994]), through dynamically updating technological change and final demand, or employing recursive dynamics to explore explicit scenarios of change.

The need for global Earth System frameworks coupled to population drivers has been recommended since the 1980s, in the pioneering report by the Earth System Sciences Committee of the NASA Advisory Council, chaired by Francis P. Bretherton [NASA, 1988]. While Earth System components and needed feedbacks were described and interaction of the Earth System and the Human System was shown in the report, multiple subsystems of the Human System and feedbacks between those subsystems and with the Earth System were not fully included. The coupled framework proposed here includes the major subsystems and components of the Human System as well as their major feedbacks and risks, and explicitly recognizes policies as a major driver of the full system.

Earth System models have long been based on integrating their dynamical equations numerically (e.g., numerical weather prediction models used by Weather Services). For Human Systems, Dynamic Modeling is also a powerful tool that scientists have successfully applied to many systems across a range of economic, social, and behavioral modeling [Hannon and Ruth, 2009; Ruth and Davidsdottir, 2009; Ruth and Hannon, 2012; Hannon and Ruth, 2014; Ruth, 1993]. The ability of dynamic models to capture various interactions of complex systems, their potential to adapt and evolve as the real system changes and/or the level of the modelers' understanding of the real system improves, their ability to model coupled processes of different temporal and spatial resolutions and scales, and their flexibility to incorporate and/or couple to models based on other approaches (such as agent-based modeling, stochastic modeling, etc.) render them as a versatile and efficient tool to model Coupled Earth–Human Systems [Costanza and Ruth, 1998; Hannon and Ruth, 1994; Meadows, 2008; Sterman et al., 2012]. Since Earth System models are already dynamic, a Dynamic Modeling platform would be a natural choice to model coupled Earth–Human Systems.

Fig. 2.7 is a schematic showing an example of a model to couple energy and water resources at the local and regional scales to human population. Many of the variables in such a model are affected by processes at the global scale, while decisions are often made at a local scale. Choosing variables from the subsystems depends on the specific goals of the model. Reconciling various scales spatially or temporally can be done through downscaling, aggregating, and averaging for variables defined at smaller scales. Moreover, the human system strongly influences consumption even at these smaller local scales. For example, Srebric et al. [2015] show that not only population size but also behavior of people at the community scale strongly affects local energy consumption. This example shows that coupled human system models are needed at various scales to project consumption patterns, especially for energy and water. [5]

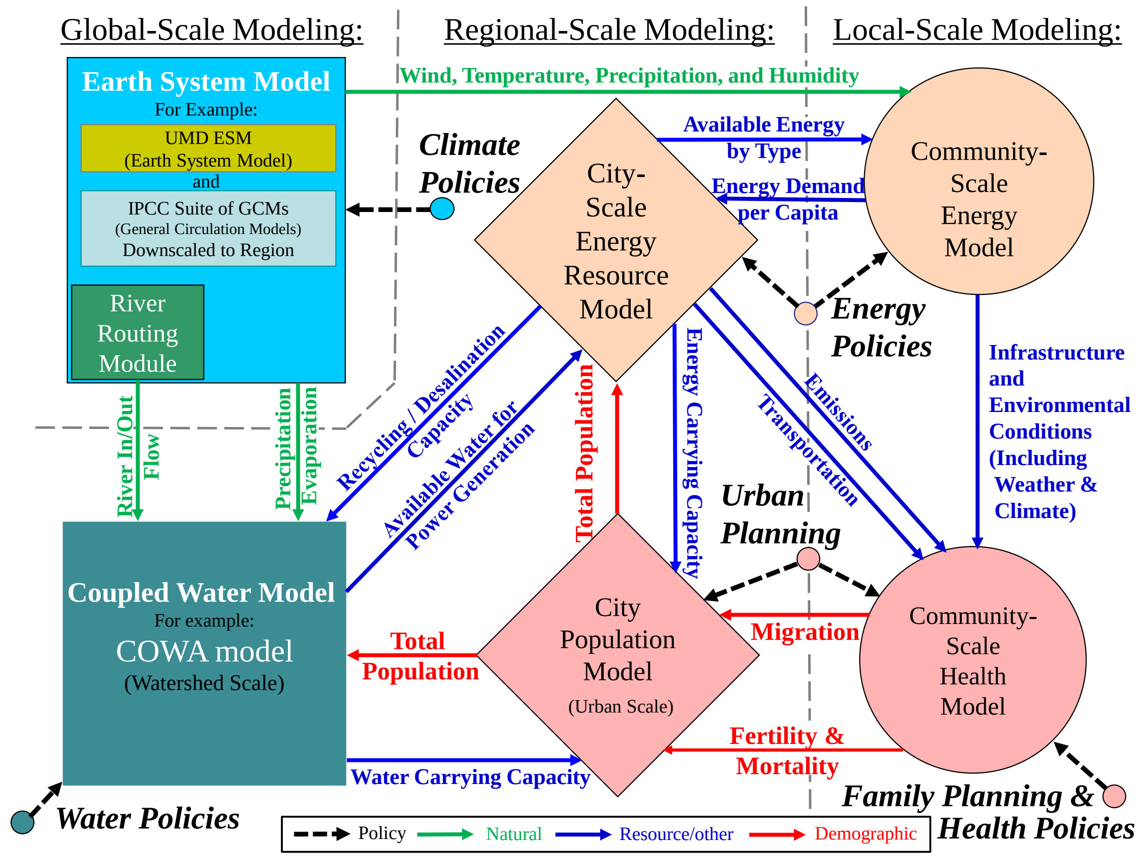

Figure 2.7: An example of a model schematic integrating water and energy resources with human population and health at the local and regional scales, coupled to an Earth System Model at the global scale.

A major challenge in implementing such a framework of a coupled Earth–

[5]We thank the anonymous Reviewer No. 2 for emphasizing the importance of coupling across various scales, and for many other helpful comments.

Human System is that it requires tuning many parameters to approximately reproduce its past observed evolution. This task has become easier over the last decade with the development of advanced methods of Data Assimilation commonly used in atmospheric sciences to optimally combine a short forecast with the latest meteorological observations in order to create accurate initial conditions for weather forecasts generated several times a day by the National Weather Services (e.g., [Kalnay, 2003; Anderson, 2001; Hunt et al., 2007; Lorenc, 2003; Whitaker and Hamill, 2002]). The most advanced methods (known as 4D-Var and Ensemble Kalman Filter) are able to go over many years of observations using a dynamic forecasting model and estimate the optimal value of model parameters for which there are no observations (e.g., Annan and Hargreaves [2004]; Liu et al. [2014a,b]; Kang et al. [2011, 2012]; Annan et al. [2005]; Evensen [2009]; Ruiz et al. [2013]).

Uncertainty is another important challenge in producing future behavior and scenarios with models. This problem has been addressed successfully in meteorology by using, instead of a single forecast, an ensemble of typically 20-200 model forecasts created by adding perturbations in their initial conditions and in the parameters used in the models. These perturbations are selected to be compatible with estimated uncertainties of the parameters and initial conditions [Toth and Kalnay, 1993; Tracton and Kalnay, 1993; Buizza et al., 1993, 1999]. The introduction of ensemble forecasting in the early 1990s provided forecasters with an important measure of uncertainty of the model forecasts on a day-to-day and region-to-region basis. This made it possible to extend the length of the US National Weather Service's weather forecasts made available to the public from 3 days to 7 days (e.g., Kalnay [2003]). A similar approach, i.e., running ensembles of model projections with perturbed parameters, could be used with coupled Earth–Human System models to provide policymakers with an indicator of uncertainty in regional or global projections of sustainability associated with different policies and measures. Calibration and tuning of coupled Human–Earth System models, as indicated above, could take advantage of optimal parameter estimation using advanced Data Assimilation, rather than following the more traditional approach of tuning individual parameters or estimating them from available observations.

Our proposed framework, together with Data Assimilation techniques, allows developing, testing, and optimizing measures and policies that can be implemented in practice for early detection of critical or extreme conditions that will lead to major risks to society and failure of supporting systems and infrastructure, and aid in the estimation of irreversible thresholds or regime-shifting tipping points [Nobre and Borma, 2009; Lenton et al., 2008; Schellnhuber, 2009]. Moreover, it allows for detecting parameters and externalities (such as inadequate measures or policies) that may play a significant role in the occurrence of catastrophes and collapses [Scheffer et al., 2001; Scheffer and Carpenter, 2003; Ruth et al., 2011; Downey et al., 2016]. By adjusting the values of those parameters found to be influential through numerical experiments and simulations, short-term and long-term policy recommendations that can keep the system within optimum levels or sustainable development targets (e.g., Millennium Development Goals or the Post-2015 Development Agenda) can be designed and tested. This approach would allow policies and measures that have been found to be successful in specific cases to be modeled under different conditions or more generally.

There are numerous examples of policies successfully tackling many of the challenges identified in this paper. For example, the province of Misiones, Argentina, with policies for forest protection and sustaining local incomes, stands out by having very high, remotely-sensed values of NDVI (vegetation index) compared to the neighboring regions [Izquierdo et al., 2008]. The state of Kerala, India, despite a very low GDP per capita (under $300 until 1990s), through policies expanding access to education and medical care, enjoys higher life expectancy, lower birth rates, lower inequality, and superior education compared to the rest of India [Jeffrey, 1992; Singh, 2011; Susuman et al., 2016]. Formal primary, secondary, and tertiary education can also reduce societal inequalities and improve economic productivity [Sulston et al., 2012; Lutz et al., 2014; Cohen, 2008; Lutz and Kc, 2011]. Education itself can also be offered in other forms. For example, education through mass media can be influential for changing long-term cultural trends and social norms, as can be seen in the successful attempt to reduce fertility rates in Brazil using soap operas [La Ferrara et al., 2012]. There have also been other extremely successful non-coercive family planning policies, e.g., in Thailand, Mexico, and Iran [Pritchett, 1994; Potts, 1997; Potts and Marsh, 2010; Vahidnia, 2007; Roudi-Fahimi, 2002; Lutz et al., 2010; Abbasi-Shavazi et al., 2009; Bongaarts, 2016]. A recent paper in PNAS [O'Neill et al., 2010] showed that slowing population growth could provide 16–29% of the emissions reductions needed by 2050 and by 37–41% by 2100, and a study by Wire [2009] shows family planning is four times as efficient as adopting low-carbon technologies for reducing carbon in the atmosphere and ocean.

Successful local and regional policies on air quality include California sharply reducing NO_2 in Los Angeles by 6.0 ± 0.7 % per year between 1996 and 2011 through strict policies on vehicular emissions [Hilboll et al., 2013]. Maryland succeeded in reducing SO_2 emissions per unit energy produced from power plants by ~90% [He et al., 2016]. Regulations have reduced levels of SO_2 and NO_2 over the eastern US by over 40% and 80%, respectively, between 2005 and 2015. Over a similar period in India, these levels grew by more than 100% (SO_2) and 50% (NO_2), showing the possible dangers ahead absent effective policies [Krotkov et al., 2016].

Effective policies and measures are needed for all sectors of the Human–Earth System Model described above [Brundtland et al., 2012; Sulston et al., 2012]. A dynamical model of such systems should be capable of testing the effects of various policy choices on the long-term sustainability of the system [Ruth et al., 2011].

The track record until recently on climate change shows policy inaction is both dangerous and can be very costly [Ruth, 2010; Stern, 2007; Sterman et al., 2012]. Anthropogenic climate change driven by carbon emissions, water vapor, and surface albedo was theorized as early as the 19th century, and an empirical warming trend was measured by the 1930s. Scientists came to understand the fundamental mechanisms of climate change by the 1950s and 60s (e.g., Budyko [1961]; Manabe and Wetherald [1967]). The first international scientific Conference on the Study of Man's Impact on Climate was held in 1971 and issued a report warning about the possibilities of melting polar ice, reduced albedo, and other unstable feedbacks that could lead to accelerated climate change "as a result of man's activities" [Matthews et al., 1971]. By 1979, a US National Academy of Sciences panel, chaired by Jule

Charney, issued a report confirming the findings of climate change models [Charney et al., 1979], and over the course of the 1980s the empirical evidence confirming ongoing climate change grew very rapidly. In 1988, James Hansen testified before the US Congress about the near certainty of climate change. The first IPCC Assessment Report was completed in 1990, and the Fifth in 2014, with each report successively warning of the increasingly grave consequences of our current trajectory. The latest report warns that without new and effective policies and measures, increases in global mean temperature of 3.7 to 4.8°C are projected by 2100 relative to pre-industrial levels (median values; the range is 2.5 to 7.8°C) [IPCC, 2014]. Other national and global institutions have also warned of the disastrous consequences of such warming (e.g., Melillo et al. [2014]). As a recent World Bank assessment [Group, 2014, p. xvii] states, "The data show that dramatic climate changes, heat and weather extremes are already impacting people, damaging crops and coastlines and putting food, water, and energy security at risk... The task of promoting human development, of ending poverty, increasing global prosperity, and reducing global inequality will be very challenging in a 2°C [increase] world, but in a 4°C [increase] world there is serious doubt whether this can be achieved at all... the time to act is now." Scientists have also long warned about the consequences of climate change for international security (e.g., Sagdeev and Eisenhower [1990]; Brown [1989]; Barnett [2003]).

And yet, despite a long history of scientific warnings, the many current ecological and economic impacts and crises, the future risks and dangers, the large number of international meetings and conferences on the urgent need for climate policies and measures, and the adoption of some national and regional climate policies, growth in global CO_2 emissions from fossil fuels and cement has not only remained strong but is actually accelerating. The average annual rate of growth from 2000–2009 (~2.9%) was almost triple the rate of the previous two decades, 1980–1999 (~1.1%), while the most recent years, 2010–2012, have been even higher (~3.4%) [Boden et al., 2013; Peters et al., 2011].

The sobering fact is that very little has been accomplished in establishing effective carbon reduction policies and measures based on science. The development and implementation of policies promoting sustainable technologies for the future (e.g., renewable energy sources) becomes even more challenging because of intervention and obstruction by a number of vested interests for continued and expanded use of their existing non-renewable technologies and resources (e.g., some in the coal, oil, and gas industries). This is further complicated by some political rejection of science-based future climate projections and unwillingness to consider alternative economic development pathways to lowering the emission of carbon dioxide and other greenhouse gases from the Human-Earth systems. However, the commitments to reduce carbon emissions by the vast majority of the world's countries in the recent agreement from the COP21 in Paris could signify a major policy turning point.

With more than 180 countries, covering ~90% of global emissions, having committed to submit Intended Nationally Determined Contributions (INDCs), the Paris framework forms a system of country-level, nationally-determined emissions reduction targets that can be regularly monitored and periodically escalated. While analysis [Fawcett et al., 2015] of the INDCs indicates that, if fully implemented, they can reduce the probability of reaching the highest levels of temperature change by 2100 and increase the probability of limiting global warming to 2°C, achievement of these goals still depends on the escalation of mitigation action beyond the Paris Agreement. Even if the commitments are fulfilled, they are not enough to stay below the 2°C pathway [Kintisch, 2015; Iyer et al., 2015; Fawcett et al., 2015], but the Paris framework is an important start for an eventual transformation in policies and measures. Thus, the INDCs can only be a first step in a deeper process, and the newly created framework must form an effective foundation for further actions on emissions reductions.

One of the anonymous reviewers pointed out that the failure of policymakers to react sufficiently to the scientific understanding of global warming is paralleled by a similar failure with regards to scientific knowledge about population trajectories. Family planning policies have been pushed off policy agendas for the last few decades, and the subject of population has even become taboo. There are numerous non-evidence-based barriers that separate women from the information and means necessary to plan childbirths. The total fertility rate remains high in many countries not because women want many children but because they are denied this information and technologies, and often even the right to have fewer children. Access to family planning information and voluntary birth control is a basic human right and should be treated as such by international institutions and policy frameworks. Similarly, there is also an urgent need for improved educational goals worldwide. While these goals are repeatedly supported by both researchers and policymakers, policy implementation continues to be lacking. As a recent report by the Royal Society explains, improved education (especially for women) and meeting the large voluntary family planning needs that are still unmet in both developed and developing countries are fundamental requirements of future economic prosperity and environmental sustainability. This again emphasizes the critical need for science-based policies [Sulston et al., 2012; Lutz et al., 2014; Cohen, 2008; Brundtland et al., 2012; NAS, 1986; NAS and Society, 1992; NAS, 1963; Turner, 2009; NAS, 1999, 1971, 1993].[6]

The importance and imminence of sustainability problems at local and global scales, the dominant role that the Human System plays in the Earth System, and the key functions and services the Earth System provides for the Human System (as well as for other species), all call for strong collaboration of earth scientists, social scientists, and engineers in multidisciplinary research, modeling, technology development, and policymaking. To be successful, such approaches require active involvement across all disciplines that aim to synthesize knowledge, models, methods, and data. To take effective action against existing and potential socio-environmental challenges, global society needs scientifically-based development of appropriate *policies*, *education* that raises collective awareness and leads to actions, investment to build new or improved *technologies*, and changes in *economic* and *social structures*. Guided by such knowledge, with enough resources and efforts, and only if done in time, human ingenuity can harness advances in science, technology, engineering, and policy to develop effective solutions for addressing the challenges of environment and climate, population, and development. Only through well-informed decisions and

[6]We thank anonymous Reviewer No. 1 for guiding us to add all the important points in this paragraph and the associated citations.

actions can we leave a planet for future generations in which they can prosper.

Acknowledgements

This work was supported by the University of Maryland Council on the Environment 2014 Seed Grant, award number 1357928. The authors would like to acknowledge the following grants and institutions: S.M., K.F., and K.H.: National Socio-Environmental Synthesis Center (SESYNC) — National Science Foundation (NSF) award DBI-1052875; J.R.: The Institute of Global Environment and Society (IGES); G.R.A.: Laboratory Directed Research and Development award by the Pacific Northwest National Laboratory, which is managed by the Battelle Memorial Institute for the U.S. Department of Energy; M.A.C.: Office of Naval Research, research grant MURI N00014-12-1-0911; F.M.W.:NSF award CBET-1541642; V.M.Y.: The Institute for New Economic Thinking (INET).

We benefited from many helpful discussions with many colleagues including Professors Mike Wallace, Jim Carton, Inez Fung, Deliang Chen, Jim Yorke, Ross Salawitch, Margaret Palmer, Russ Dickerson, Paolo D'Odorico, and Steve Penny.

Thank you to Ian Munoz and Dr. Philippe Marchand for technical assistance in producing Fig. 2.1.

As is the case with all independent peer-reviewed research, the views and conclusions in the paper are those of the authors alone. The funding organizations did not have any role in writing the paper and did not review it.

Chapter 3: COWA: a Two-way Coupled Human–Climate–Water Model to explore water management options

Existing studies of freshwater systems generally focus on hydrological flows without considering impacts from human feedbacks on these natural flows. However, the human system has become the major driver of changes in freshwater systems. The Coupled Human–Climate–Water model (COWA) is a minimal dynamic model that aims to capture these bidirectional positive, negative, and delayed feedbacks. The results show remarkable differences between simulation outputs of two-way and one-way coupled models, showing that projecting both human and natural system variables without feedbacks over long periods of time yields unrealistic results. COWA shows that Carrying Capacity is not static but rather evolves in response to the dynamic interactions and feedbacks in a changing system of many human and natural factors. COWA allows to determine the Water Carrying Capacity (WCC) of a region, i.e., the level of population and water consumption that a region's natural hydrological regime can support over the long term. Additionally, it shows that implementing effective water management policies — such as recycling and conservation technologies — can expand WCC of a region. An unexpected result of including bidirectional coupling is that expanding reservoir size and water collection capacity produces short-term population growth without expanding WCC, but because groundwater stocks are depleted more rapidly, it leads to an earlier and steeper collapse of the water resources and population. Lack of a dynamic understanding of a system can lead to the opposite conclusion about its behavior. COWA shows the critical importance of long-term policies for sustaining water resources, especially when demand rises and when estimates of available groundwater or potential for contamination of freshwater sources are highly uncertain. Significant signals of potential collapse (or unsustainability) can be missed if we limit the horizon to short term and neglect bidirectional feedbacks.

Significance Statement

A novel understanding for the *Carrying Capacity* of the system emerges thanks to Human–Climate–Water feedbacks modeled in COWA. Water Carrying Capacity is a simple yet powerful measure that allows monitoring, and planning for, the viability of the system decades in advance.

Highlights

1. The Human System and its impact on the Earth System have grown rapidly since 1750, and explosively after 1950. The Human System has become the dominant driver of changes in the natural environment.

2. Current models that are used to project the future of the Human System and

the Earth System do not model bidirectional Human–Earth feedbacks. Hence significant signals that may determine the fate of the environment and our species can be missed.

3. The Coupled Human–Climate–Water Model (COWA) includes bidirectional feedbacks between the Human and Freshwater systems, hence allowing to capture nonlinear, non-trivial behavior of these systems.

4. A comparison of results from COWA with a one-way coupled Human–Climate–Water Model shows the inherent inability of one-way coupled models to capture major, non-trivial, long-term changes in the Human–Nature systems.

5. Groundwater depletion is severe in many watersheds around the world and in the US, e.g., Central Valley and High Plains. But COWA shows visionary policies in Phoenix AMA have saved over 40 cubic kilometers (ckm) of groundwater in this watershed over the past three decades.

6. Because of modeling bidirectional couplings, COWA can estimate the Water Carrying Capacity (WCC) for the region through simulations. WCC depends on multiple variables in both the human and natural systems, and provides a simple, clear measure for sustainability of the freshwater system in a region.

7. COWA can test the impact of groundwater withdrawal restriction policies in the long term. Without such policies, consumption can overshoot its sustainable levels and lead to a catastrophic collapse of the system.

8. COWA can also simulate the result of uncertainties in groundwater estimates, which could be exacerbated by potential contaminations, e.g., due to fracking.

9. Developing water recycling capacity and improving water consumption efficiency are shown to increase WCC. But without policies to restrict groundwater withdrawal, they cannot prevent an overshoot of the WCC and therefore the resulting collapse.

10. Increasing the freshwater storage and withdrawal capacity allows consumption to increase at a faster rate and reach a peak sooner. But that would result in a steeper collapse of the system several decades earlier. This is a surprising, counter-intuitive result that cannot be predicted and understood without including bidirectional feedbacks in the model.

11. Due to accelerated loss of groundwater and accelerated droughts due to climate change, the system may reach its peak by 2050, much earlier than expected. Developing policies for resilience requires long-term analysis performed by bidirectionally coupled models.

12. WCC can be calculated for various scenarios by simulating with COWA. WCC can simplify the complexities of the full system for policymakers and allow them to propose, design, develop, and test efficient, effective policies.

13. By building up resilience of the system and implementing evidence-based, long-term policies, we show that the system can smoothly converge to WCC, hence ensuring a safe, prosperous future for the environment, economy, and

people.

3.1 Introduction

Over the last two centuries, the impact of the Human System has grown dramatically, becoming strongly dominant within the Earth System in many different ways. Both population and per capita consumption have grown rapidly, especially since about 1950, putting tremendous pressure on natural resources [Fu and Li, 2016; Ceballos et al., 2017; Motesharrei et al., 2016; Sulston et al., 2012]. The changes in the Earth System have important feedback effects on the Human System. However, current models that project the future of resources and humanity do not include such feedbacks that exist in reality. To address this problem, we followed the framework proposed in Motesharrei et al. [2016] to develop a model for Freshwater and Human Systems that includes bidirectional feedbacks.

Over the past few decades, an increase in global water resource awareness [United Nations, 1992, 2003; Food and Agriculture Organization, 2007; World Bank, 2008a,b; United Nations, 2009; UNEP, 2012; Food and Agriculture Organization, 2013; United Nations, 2013a, 2015a] has driven national concern [ACE, 2016; GAO, 2012; DOE, 2016; EPA, 2010] for regional freshwater sustainability and sparked a wave of studies at the local level as well. However, there has been no clear consensus over how to move forward, only that collaboration and communication among sectors will be necessary. This recent push to further understand complexities of the hydrological system has made it increasingly apparent that sustaining the quality and quantity of our freshwater resources, in the midst of increasing human population and climate uncertainties, has become a complex and challenging management problem.

As a result of the basic need of freshwater for survival, water resources are typically considered a common good, and its use a human right. However, the sustainability of this good, and therefore the future exercising of this right, has been called into question. It has been suggested that the issue of available freshwater for human use has been underestimated in previous research [Rodell et al., 2018]. Furthermore, water scarcity is a widespread problem, already impacting two-thirds of the global population, likely to be exacerbated with the uncertainties associated with climate change [Mekonnen and Hoekstra, 2016]. This widespread scarcity, combined with an underestimated perception of water resources, can lead to a highly stressful and potentially dangerous situation [Udall and Overpeck, 2017].

As we write in our *Modeling Sustainability* paper [Motesharrei et al., 2016], human activities dominate many regional hydrological cycles [Molle et al., 2010; Vörösmarty et al., 2000; Grasby, 2004; Molden, 2007; Meybeck, 2003; Gordon et al., 2008; Wagener et al., 2010; Barnett et al., 2008], with more than half of all accessible surface freshwater being used by humans, to such an extent that some major rivers are being so excessively depleted that they sometimes no longer reach the sea, while some major inland fresh and salty water bodies, such as Lake Chad, Lake Urmia, Lake Poopó and Aral Sea, are drying up. In many of the principal aquifers that support the world's agricultural regions and in most of the major aquifers in the world's arid and semi-arid zones, groundwater extraction is occurring at far greater rates than natural recharge. This includes aquifers in the US High Plains and Central Valley, the North China Plain, Australia's Canning Basin, the Northwest Sahara Aquifer System, the Guarani Aquifer in South America, and the aquifers beneath much of the Middle East and northwestern India [Famiglietti, 2014; Konikow, 2013; Castle et al., 2014; Famiglietti and Rodell, 2013; Voss et al., 2013; Famiglietti et al., 2011; Rodell et al., 2009; Scanlon et al., 2012]. In addition, the increase of impervious surfaces and other land cover changes increase runoff significantly, hence intensifying the adverse impacts of extreme hydrological events [Arnold and Gibbons, 1996; Di Baldassarre et al., 2009; Scanlon et al., 2006].

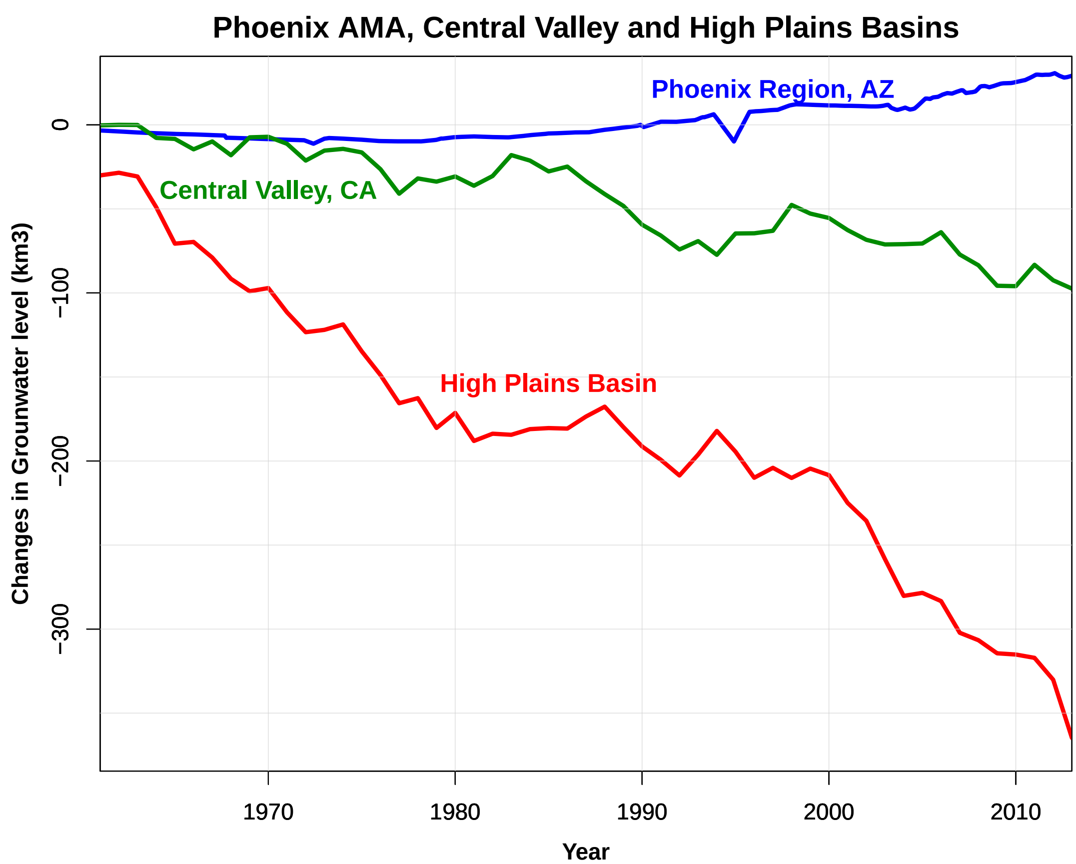

Figure 3.1: Groundwater depletion is severe in many watersheds around the world. The fast depletion in Central Valley and High Plains in the US is shown here. This should be contrasted with Phoenix AMA, where effective policies not only slowed growth in consumption and prevented GW depletion but allowed GW to increase.

We further describe in Motesharrei et al. [2016] that nearly all features of the hydrologic system are now impacted by the human system [Wagener et al., 2010], with important feedbacks onto humans, e.g., snowpack decline due to climate change [Barnett et al., 2008] reduces water availability; agricultural processes further affect water availability and water quality [Gordon et al., 2008]; land use changes can reduce groundwater recharge [Scanlon et al., 2006], and thus many populations face both reduced water availability and increased frequency and magnitude of floods [Di Baldassarre et al., 2009]. Furthermore chemicals used in hydraulic fracturing, which involves cracking shale rock deep underground to extract oil and gas, can contaminate groundwater resources [Vaidyanathan, 2016; Jackson et al., 2015; DiGiulio and Jackson, 2016].

Traditionally, studies regarding freshwater systems primarily focus on natural hydrological flows, while more recent studies regarding sustainability primarily focus on the balancing of uncertain future human demands upon natural supplies. However, the impact of human feedbacks on natural water flows is often not considered and, thus, the notion of the human system as a major driver of changes in the freshwater system and associated sustainability is frequently ignored.

Despite such important impacts of the Human System on the Freshwater System and vice versa, current models of the Freshwater System often focus on the physical and natural dynamics of the hydrologic system. Even in models where the Human System impact on the Freshwater system is considered, for example, Global Climate Change Assessment Model (GCAM) [Kim et al., 2016], the feedback from the Freshwater System on the Human System is not modeled.

3.2 Method

Following the framework proposed in Motesharrei et al. [2016], we developed the coupling scheme shown in Fig. 3.2. By modeling bidirectional feedbacks between Human System, Water Resources, and Climate, COWA allows a new understanding of their complex interplay, and the resulting non-trivial dynamics. The resulting vision into the dynamics of the system that spans several decades, and up to a few centuries, helps with addressing the sustainability challenges of freshwater resources.

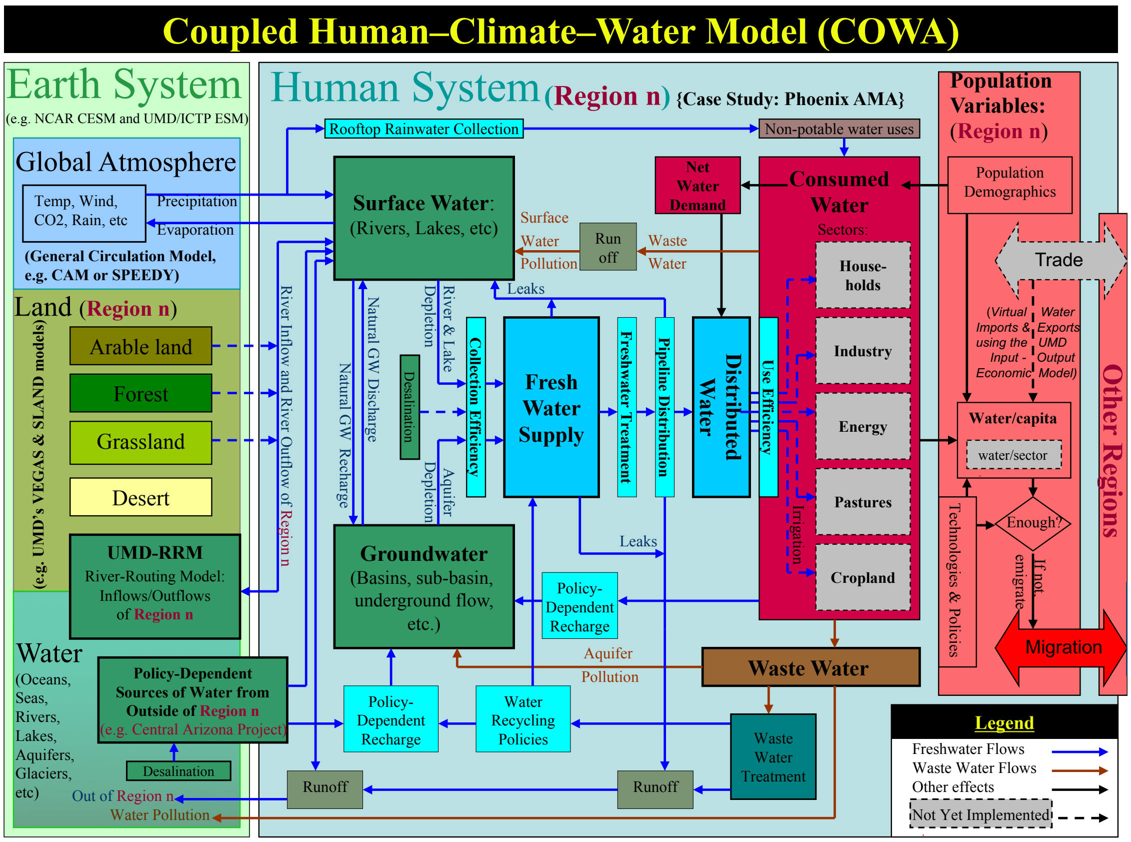

Figure 3.2: A schematic of the Coupled Water Model, including the Earth System Model (ESM) and the River Routing Module (RRM).

The Coupled Human–Climate–Water model, COWA, is a dynamic model used to study various effects of the human system on water resources and water supplies over time, and the feedbacks of these water resources on the human system. COWA includes demographic characteristics of the human system, such as population, growth rate, regional net migration, and water demand per capita, as well as the influence of human decisions on the management of water systems. An Earth System Model (ESM) and a River Routing Module (RRM) provide exogenous inputs into COWA to provide climatic (i.e., precipitation and evapotranspiration) and hydrologic (i.e., river inflow and river outflow) flows. By coupling the ESM and RRM to COWA, we can simulate future availability of water supplies under changing climate and water policies.

Our model shows that Water Carrying Capacity (CC) is a result of the dynamic interaction of several factors, both natural and human: The flows of water (which are the net sum of precipitation, evaporation, and inflows and outflows above surface and underground), population, minimum threshold of per capita consumption, the unequal distribution of water consumption, water recycling, consumption efficiency technology, system leakages, and other distributional properties and characteristics of the freshwater system. We note that the stock of GW does not determine the Water CC because GW recharge is taking place very slowly, rendering GW effectively a nonrenewable stock of water, and because the recharge is emanated from the *flows* of water. Therefore, CC is not static due to this dynamic interplay of various natural and human factors. This complexity has led some scholars to argue that CC cannot be estimated for humans and therefore they conclude that we should abandon efforts to do so [National Research Council, 2014; Cohen, 1995]. In response, this paper and our model show that CC is not only a critical concept for sustainability research and planning, but also that it *can* be estimated even though it is dynamic and created by the complex interaction of several factors. Here, with COWA, we show how CC can be estimated for water.

3.3 Modeling Approach

The four primary state variables in COWA are Population, x, Surface Water Sources, y_S, Groundwater Sources, y_G and (stored) Freshwater Supply, z. Population is controlled by the death rate, α, birth rate, β, and net immigration rate, I. Death rate is not constant but increases as water consumption per capita decreases below a threshold value. Immigration rate is proportional to the consumption per capita, and becomes negative if it drops below a certain threshold, C_{th}, due to water scarcity. Surface water stock, y_S, is controlled by several flows: river inflow, Φ, river outflow, Ψ, precipitation, P, evapotranspiration, E, withdrawal of water from surface water sources into the freshwater supply, W_S, groundwater recharge, G, leak to sources, Λ, flow of non-recycled water to sources, N, and runoff to sources, Ω. Groundwater stock, on the other hand, has only one incoming flow, groundwater recharge, G, and one outgoing flow, withdrawal of groundwater into the freshwater supply, W_G. Freshwater supply is controlled by three inflows, withdrawals, W_S+W_G, and recycling, R, and two outflows, supply collection, K, and leakage, L. Rooftop collection rate, Γ, is directly available for consumption and therefore, is deducted from the total precipitation when calculating net inflow of water to (surface water) sources.

COWA couples natural and human water flows and stocks. COWA inputs the physical/natural hydrological flows as exogenous variables by coupling with natural system models: an Earth System Model (ESM) and a River Routing Model (RRM). ESM and RRM provide data for four key hydrological flows that drive the model:

(1) precipitation, P, (2) evapotranspiration, E, (3) river inflow, Phi, and (4) river outflow, Psi. A full description of the ESM and RRM used for generating these exogenous input data can be found in Supplementary Information.

The key interactions and flows between state variables of COWA are shown in Fig. A.1.

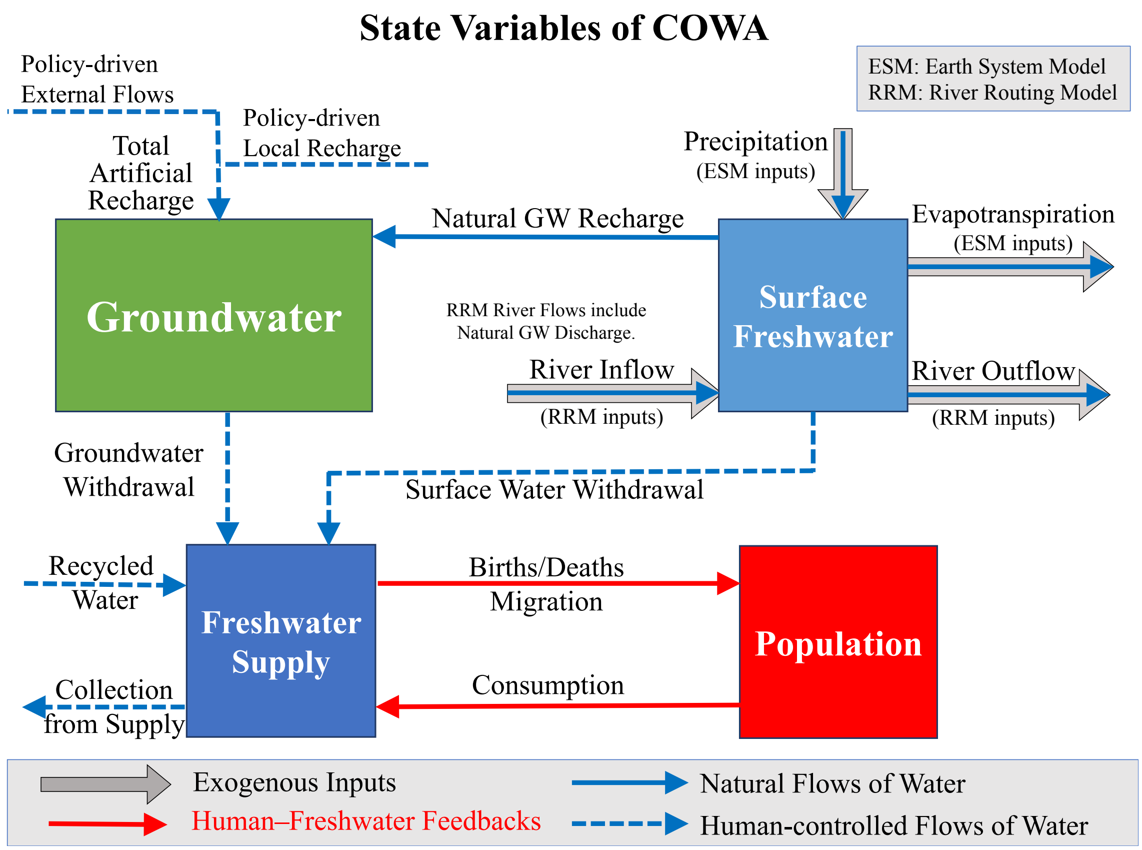

Figure 3.3: A schematic of the state variables of COWA, including the flows among them as well as the linkages to the Earth System Model (ESM) and the River Routing Model (RRM). Hard Caption: Red arrows show feedbacks while blue arrows show flow of water.

The equations governing state variables of COWA can be summarized as:

$$
\begin{cases}
\dot{x} &= \beta x - \alpha x + I(t) \\
\dot{y}_S &= \Phi(t) + P(t) - \Psi(t) - E(t) - W_S(t) + \Omega(t) + \Lambda(t) + N(t) - G(t) - O(t) \\
\dot{y}_G &= G(t) - W_G(t) - G_C(t) + O(t) + A(t) \\
\dot{z} &= W_S(t) + W_G(t) + R(t) - K(t) - L(t)
\end{cases}
\tag{3.1}
$$

A full description of the functions and parameters in (3.1) can be found in SI.

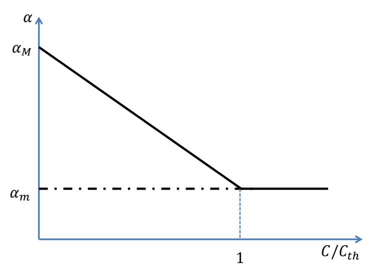

(a) Death rate as a function of consumption per capita and demand per capita. HARDCAPTION: Note that the minimum threshold of consumption per capita, C_{th}, is directly proportional to demand per capita, δ.

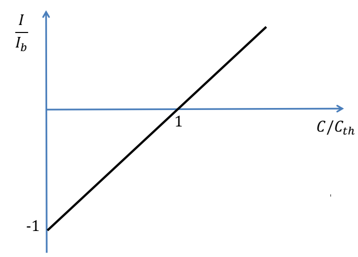

(b) Immigration rate as a function of consumption per capita. If consumption is above its threshold level, there is immigration into the region. However, when it drops below the threshold value, people start to emigrate from the region.

Figure 3.4: Feedbacks between the Freshwater consumption and population growth.

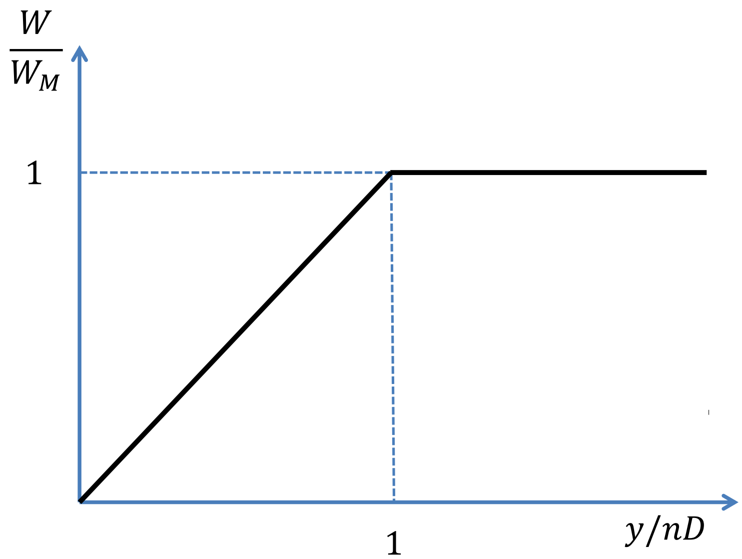

Figure 3.5: Withdrawal rate as a function of available freshwater sources, y, effective demand, D, and number of reserve months, n. The latter parameter is a strong policy knob with important implication for sustaining water sources. By choosing a large n, we can insure long-term availability of water, however, it implies a mandatory reduced consumption for the short-term in the event of a drought.

Fig. 3.5 an important mechanism in COWA that, as we will show below, can play a critical role in preventing fast, catastrophic declines of population and consumption when freshwater becomes scarce, particularly when the stock of Groundwater is depleted. For Groundwater, a typical value of $n = 60$ months, i.e., 5 years can be chosen. But to achieve a soft, smooth landing to the level of Water Carrying Capacity, we need to keep enough water for many decades, say, 50–100 years in the groundwater stocks. This is demonstrated in 3.7.5, 3.7.6, and 3.7.8.

3.4 Theoretical derivation of Water Carrying Capacity for COWA

Carrying Capacity (CC) for a coupled human–natural system is a complex variable that is determined by multiple human and natural system factors. It is important to emphasize that Carrying Capacity is a not a predetermined value but rather is produced by the dynamics of the system. For a minimal model, such as HANDY [Motesharrei et al., 2014], with only a few equations, it is possible to calculate the Carrying Capacity theoretically given the parameters and governing equations of the system. However, for a more complex system, a theoretical calculation of Carrying Capacity becomes more daunting. It might be even impossible in certain cases to find a closed-form analytical expression for Carrying Capacity. This is why it is important to determine the value of Carrying Capacity under various conditions through simulations. This is only possible if the bidirectional feedbacks between the key Human System variables and Natural System components are modeled.

Here we derive an analytical formula for Water Carrying Capacity as determined by the endogenous dynamics of COWA.

To begin, let us assume that the system has reached a near-equilibrium state. The system will not reach a full equilibrium since the natural flows, such as precipitation, vary all the time due to natural variability. However, we can assume an average value for such flows, and the system will vary around the equilibrium point established by these averages.

When the system has reached its near-equilibrium state, the rate of the change of the state variables tend to zero. From Eq. (3.1), we have:

$$\begin{cases} \dot{x} &= \beta x - \alpha x + I(t) = 0 \\ \dot{y}_S &= \Phi(t) + P(t) - \Psi(t) - E(t) - W_S(t) + \Omega(t) + \Lambda(t) + N(t) - G(t) - O(t) = 0 \\ \dot{y}_G &= G(t) - W_G(t) - G_C(t) + O(t) + A(t) = 0 \\ \dot{z} &= W_S(t) + W_G(t) + R(t) - K(t) - L(t) = 0 \end{cases} \tag{3.2}$$

Substituting for α and $I(t)$ from Table A.2 (and Figs. 3.4a and 3.4b), the first equation of (3.2) becomes:

$$\beta - \alpha_M + (\alpha_M - \alpha_m)\frac{C}{C_{th}} + I_{br}\big(\frac{C}{C_{th}} - 1\big) = 0. \tag{3.3}$$

We can solve this equation for C/C_{th} by introducing a dimensionless parameter ξ that incorporates birth, death, and immigration rates:

$$\xi := \frac{I_{br} + \alpha_M - \beta}{I_{br} + \alpha_M - \alpha_m}. \tag{3.4}$$

Note that ξ is analogous to the dimensionless variable η defined in Eq. 7 of the HANDY paper [Motesharrei et al., 2014]. (In COWA, η represents the parameter "transfer efficiency", as explained in Table A.3.) As immigration $I_{br} \to 0$, η of HANDY approaches ξ defined above in Eq. (3.4).

Substituting for C and C_{th} from Table A.2 and rearranging Eq. (3.3) we obtain:

$$\frac{K}{\mu\frac{\delta}{\tau}x} = \xi. \tag{3.5}$$

Denoting Water Carrying Capacity as χ, and assuming no rooftop rainwater collection ($\Gamma = 0$) for simplicity, we can rearrange Eq. (3.5) to derive an equation for Water Carrying Capacity in terms of the collection rate, K:

$$\chi = \frac{K}{\mu\xi\frac{\delta}{\tau}}. \tag{3.6}$$

We will proceed by attempting to determine K from the remaining three equations of 3.2. First, let us denote the average net natural flow of water into the system by F:

$$F := < P - E + \Phi - \Psi >, \tag{3.7}$$

where $< . >$ denotes time average over a long period of time. For the near-equilibrium state, reservoir overflow $O \to 0$, and groundwater recharge G becomes negligible. Moreover, as $y_G \to 0$, groundwater contamination also becomes negligible, i.e., $G_C = 0$. Finally, let us denote the average bonus flows by $A =< A(t) >$. In reality, $A = 0$ after a long time, however, we will keep it in the computations below to be able to theoretically calculate its impact on Water Carrying Capacity. Therefore, we obtain from the remaining three equations of 3.2:

$$\begin{cases} F + \Omega + \Lambda + N - W_S &= 0 \\ A - W_G &= 0 \\ W_S + W_G + R - L - K &= 0 \end{cases} \tag{3.8}$$

Note that in (3.8), we have dropped the dependence on time, t, since we can take time-averages for all the functions in 3.2 in the near-equilibrium state.

We now have to combine and simplify the three equations in (3.8). The second equation gives $W_G = A$, which can be substituted into the third equation, therefore reducing (3.8) to two equations. We will use the equations in Table A.2 to replace Ω, Λ, N, R, and L. The tricky step here is to choose the recycled water rate, R, correctly. There will be two possibilities: if the maximum recycling capacity, R_M, is small, then R will be capped by R_M, i.e., $R = R_M$. If, on the other hand, R_M happens to be very large, then R will be constrained by the maximum available water for recycling, i.e., $R = \Sigma$. In the latter case, since all the consumed water that has gone to sewer would be recycled, there will be no nonrecycled water left, i.e., $N = \nu(\Sigma - R) = 0$. In the former case, $N = \nu(\sigma K - R_M)$. We must consider each case separately.

First, let us continue the calculations for the first case, $R = R_M$. This will be more probable in most situations, since there are few places in reality where the recycling capacity dominates the natural flow rate of freshwater into the region. The computation goes as the following:

$$
\begin{cases}
W_S = F + \omega(1-\sigma)K + \lambda\dfrac{1-\eta}{\eta}K + \nu(\sigma K - R_M) \\
W_S = K + \dfrac{1-\eta}{\eta}K - A - R_M
\end{cases}
\tag{3.9}
$$

By eliminating W_S between the two equations and some further simplifications, we obtain:

$$
K = \frac{F + A + (1-\nu)R_M}{\lambda - \omega + \sigma(\omega - \nu) + \eta^{-1}(1-\lambda)}. \tag{3.10}
$$

Repeating the similar computation for large R_M, where $R = \Sigma$, we obtain after simplification:

$$
K = \frac{F + A}{(1-\omega)(1-\sigma) + (1-\lambda)(\eta^{-1} - 1)}. \tag{3.11}
$$

Combining Eqs. (3.10) and (3.11) with (3.6), we obtain the analytical form of the Water Carrying Capacity, χ, as well as χ_+ for when R_M is very large:

$$
\chi = \frac{F + A + (1-\nu)R_M}{\lambda - \omega + \sigma(\omega - \nu) + \eta^{-1}(1-\lambda)} \cdot \frac{\tau}{\mu\delta\xi}. \tag{3.12}
$$

$$
\chi_+ = \frac{F + A}{(1-\omega)(1-\sigma) + (1-\lambda)(\eta^{-1} - 1)} \cdot \frac{\tau}{\mu\delta\xi}. \tag{3.13}
$$

The χ_+ for large recycling capacity was a case that we had not envisioned in our experiments, and only considered it when attempting to derive Water Carrying Capacity theoretically. We then confirmed this theoretical derivation with numerical experiments with COWA.

3.5 Model Validation

It is best practice to use hydrological boundaries, as opposed to administrative boundaries, when modeling systems concerning hydrological processes. Therefore, for the purpose of this research, the COWA model was applied to the Phoenix Active Management Area (AMA) located in south-central Arizona. This region surrounding the city of Phoenix consists of seven groundwater sub-basins (i.e., West Salt River Valley, East Salt River Valley, Hassayampa, Fountill HIll, Rainbow Valley, Lake Pleasant, and Carefree basins), five major natural river systems (i.e., Agua Fria, Gila, Salt, Verde, and Hassayampa rivers), one major artificial surface water system (i.e., the Central Arizona Project (CAP)). Phoenix AMA includes portions of three counties, i.e. Maricopa, Yavapai, and Pinal counties. Furthermore, the Phoenix region has experienced one of the largest population growth rates in the past two decades in comparison to other major U.S. metropolitan areas, as well as some of the worst water scarcity conditions, alongside with intensive and proactive conservation efforts within Arizona as well as across state lines.

These characteristics of the Phoenix region allow us to carry out an in-depth study of natural and human dynamics impacting the balance of the hydrologic cycle in the presence of extensive human interference. Furthermore, the existence of a long history of water records provides an opportunity to minimize data gaps. Applying the model to this region allows "thought experimentation" of the impact of various policy decisions concerning current practices, implementation of new practices or the impacts of climate change (i.e., changes in precipitation or evaporation rates) on current or new practices. Such scenarios are simulated, analyzed, and discussed in the following sections. However, we first use observed values to make a goodness-of-fit analysis of simulated behaviors to validate the model and provide evidence of the model's ability to capture dynamic trends of the real system.

A map of the Phoenix Active Management Area can be found in Fig. A.2

3.5.1 Validation of COWA (the two-way coupled Human–Climate–Water model)

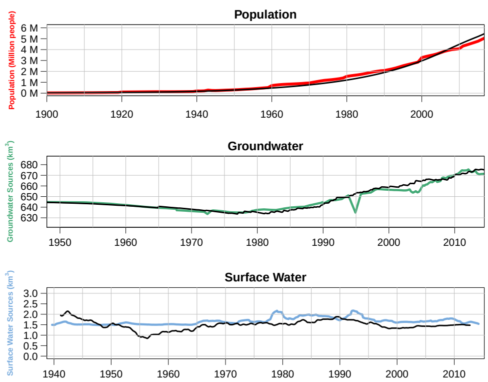

(a) Validation of COWA for the three state variables Population, Groundwater, and Surface Water using available past observations.

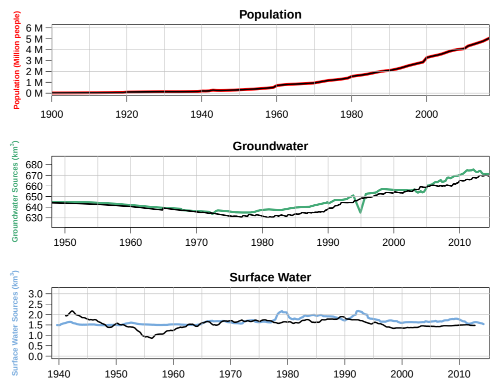

(b) Validation of the one-way coupled model for the three state variables Population, Groundwater, and Surface Water using available past observations.

Figure 3.6: COWA and the one-way coupled Human–Climate–Water model are two separate models, with different model structures and optimal parameters, therefore, they have to be validated separately. Capturing the past trend of Groundwater with the one-way model is more difficult due to lack of feedbacks. Population in the one-way model is an exogenous driver, hence the perfect fit. Surface water varies on a much smaller time scale due to variation in precipitation and natural flows (surface and subsurface), and is hence more difficult to validate with a model whose major skill is in capturing long-term trends.

COWA is validated by comparing the time-series for three main state variables as a result of model simulation against past observations. Validations are constrained by availability of data. Population data has been available since 1900, hence validation is shown between 1900 and 2015. The errors are rather small.

The Population stock, x, is simulated (see (3.1)) in units of people (ppl) and is computed for each one month time step in the model from 1900–2100. Therefore, regional monthly population data from 1900–present was needed to make the comparison of simulated to observed population stocks. The data came from the U.S. Census Bureau's (USCB) State Population Estimates and Demographic Components of Change: 1900 to 1990, supplemented for more recent years with USCB's Counties Population Totals Tables: 2010-2016 and County Intercensal Tables: 2000-2010.

Groundwater is validated between 1947 and 2013. Note that there is an erroneous sudden drop in the "observed" value in 1994, which seems to be due to either a measurement error or a reporting error. [1]

In order to determine historically observed groundwater in volumetric units (i.e., cubic kilometers, ckm) per time step (i.e., months, mo), we used the Water-level Change and Storativity method [Konikow, 2013]. The water level data used in the approximation was obtained from the Arizona Department of Water Resources' (ADWR's) database, the Groundwater Site Inventory (GWSI).

Surface Water is more difficult to validate because changes in Surface Water occur over much shorter time scales, and at a much higher frequency, compared

[1] We have notified Arizona Department of Water Resources about this irregular data point.

to Groundwater. COWA's strength is in capturing trends that emerge as a result of coupling with the Human System, and hence its excellent skill at decadal time scales. But changes in Surface Water could be even significant over daily time scales. Therefore, we show the running average time-series for the Surface Water in Fig. 3.6. Although the difference between simulated and observed time-series is larger compared to Groundwater or Population, the comparison is reasonable, i.e., COWA can capture the trends in Surface Water change.

Similarly to observed groundwater values, the observed surface water values would need to be in volumetric (ckm) units at monthly temporal intervals. In order to approximate these values, this research used monthly mean river flow and total monthly reservoir storage data from the the USGS Surface Water Monthly Statistics database and the Arizona Department of Water Resources Phoenix AMA Master Water Budget Historical Template for total annual CAP deliveries.

First, all major river systems within the Phoenix regions were identified, including five natural (i.e., Hassayampa, Gila, Agua Fria, Verde, and Salt rivers), as well as one artificial (i.e., Central Arizona Project, CAP) surface water system. For each natural river system, the river gauge station most upstream yet still within the boundaries of the Phoenix regions was the designated inflow point, while the most downstream station (within the region's boundaries) was designated the point of outflow. The geographical locations and USGS identification numbers of each river station used in these estimation are depicted in Fig. A.2

3.5.1.1 Validation of the one-way coupled version of COWA

The validation process is repeated here for the model with only one-way couplings of population and per capita consumption to freshwater resources. The validation for one-way and two-way models has to be carried out differently because they have essentially different model structures. Thus, the choice of parameters to produce these validation results differ. The Population variable in the one-way model exactly matches the observed population, since it is an exogenous variable read into the model.

The error for Groundwater for the one-way model could not be reduced to a level comparable to that of the two-way coupled model, and there are larger differences especially after 1980, probably because the variations in the level of Groundwater because feedbacks cannot be captured in a one-way coupled simulation scheme. The observed surface water, whose variations occur at a much finer time scale compared to groundwater, is reproduced with a similar level of error as in the coupled model.

3.6 One-way coupled model vs. COWA (Two-way coupled model)

In Section 3.1, we discussed the importance of feedbacks in the coupled models. In this section, we first compare the simulation output of COWA with the output of its one-way coupled counterpart, and discuss their fundamental difference. Note that in the one-way coupled model, the feedback from the water system on population change and immigration does not exist. Instead, population projection is derived from an independent statistical demographic projection as an exogenous variable to drive the model, as is done in most existing models. By comparing the one-way coupling standard practice and the two-way coupling of our model, we show that the standard one-way coupling produces unrealistic projections, because essential feedbacks found in reality are not modeled. We continue by analyzing a series of different scenarios from COWA.

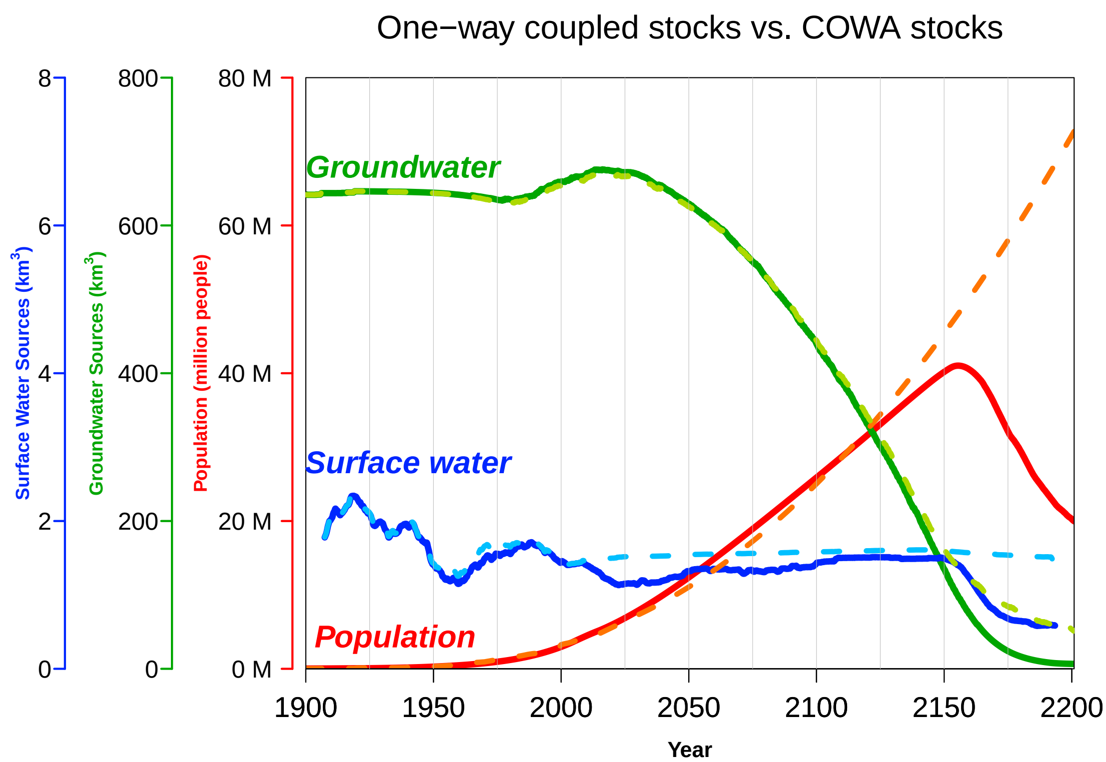

Figure 3.7: A comparison of the one-way coupled model vs. COWA. The collapse of the Population in COWA is a behavior that the one-way coupled model, due to its structure, cannot produce, because it is missing the bidirectional feedbacks that exist in reality. HARDCAPTION: Without two-way feedbacks, the one-way coupled model cannot predict a collapse of Population. (arrows to one-way and COWA (two-way) population lines)

To show the fundamental difference of one-way vs. two-way coupling, we show in Fig. 3.7 the 200-year projections produced by both models. As can be seen, after about 2150, Population in the two-way coupled model differs fundamentally from that in one-way model, i.e, from the independently projected population used to exogenously drive the one-way model. The statistically projected population in the one-way coupled model continues to grow. However, when feedbacks are introduced in the two-way coupled model, the population growth slows, and eventually reverses, because the freshwater resources that are necessary for growth to be maintained become insufficient. Population declines and eventually stabilizes to the level of Carrying Capacity around 2215, and is maintained at Carrying Capacity by the natural flows beyond that point. Note that this shows that Carrying Capacity is set by these flows of water and not by the available stocks of water. In fact, a large stock of Groundwater, absent strict withdrawal restriction policies, allows Population to grow to several times its Carrying Capacity, but then this high population level cannot be maintained since the stock of Groundwater is depleted and the remaining flows are too small to maintain the high level of consumption. This also highlights that if water consumption is greater than the available flows, Groundwater stocks are essentially a non-renewable resource which do not determine the Water Carrying Capacity. This is a very important point that is not widely understood or recognized.

3.6.1 Population Projections: Made with COWA vs. statistical, demographic projections

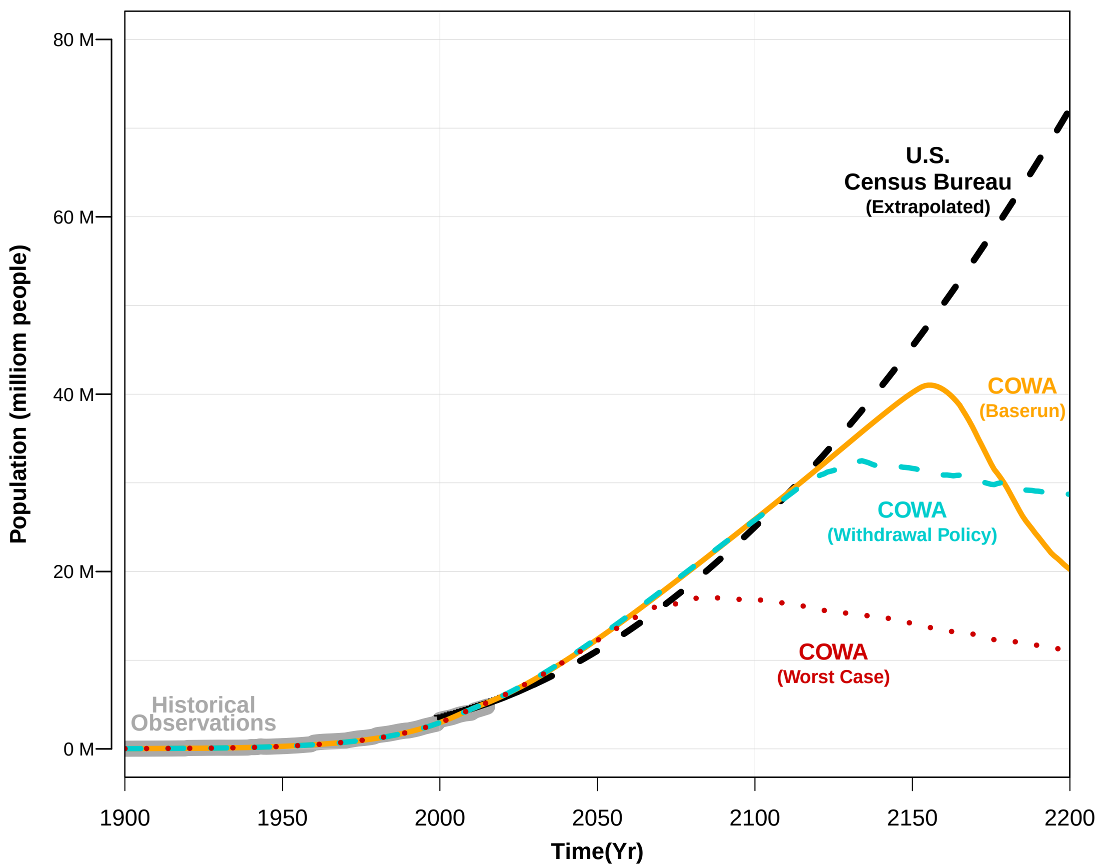

Figure 3.8: A comparison of the Population projections produced by COWA vs. demographic projections. The collapse of the Population in COWA is a behavior that statistical extrapolation models, inherent to their design, cannot produce, because it is a result of bidirectional feedbacks missing in static models.

A collapse of the population is a non-trivial, nonlinear behavior that cannot be produced by any static projection. The only way to produce this behavior is for the model to include the two-way interactions that exist in reality between the freshwater resources, consumption level, migration, and population growth. Therefore, it is crucial to use a model that includes bidirectional feedbacks with the key Human System variables if we aim to make long term projections, and use the models to propose, develop, and test various policies.

3.7 Scenarios

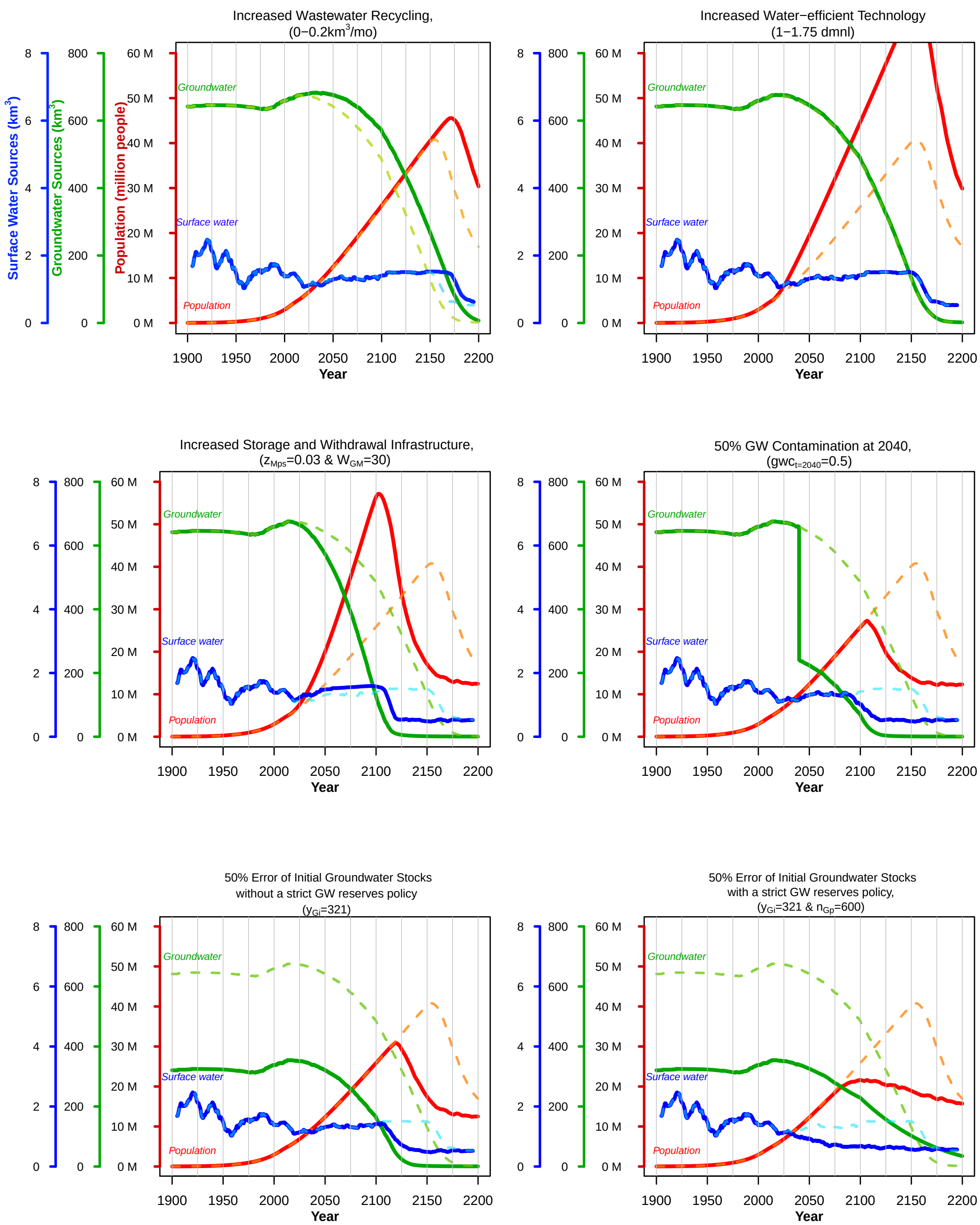

Figure 3.9: A summary of various simulation scenarios from COWA.

An essential purpose of modeling is to be able to test the various effects of different policy interventions on the dynamics of a system. Here we use COWA to evaluate the impact of various water management policies in the long run. We compare each scenario to the base run, as shown in Fig. 3.7.

3.7.1 Removal of "Bonus" Flows

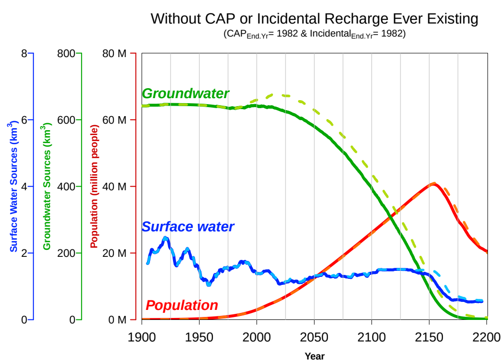

(a) A scenario with no bonus flows.

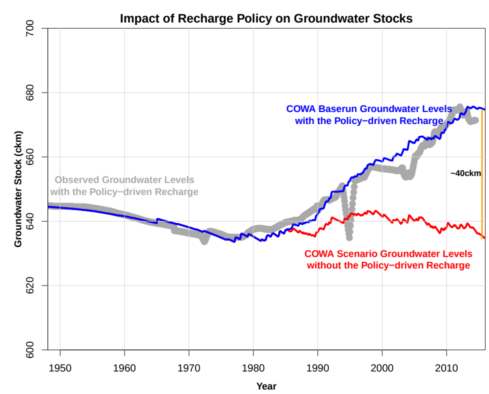

(b) The comparison of observed Groundwater to the scenario where bonus flows are removed.

Figure 3.10: Here we show the hypothetical situation that bonus flows from the Central Arizona Project (CAP) and Incidental Recharge never existed. The rebound of Groundwater levels that started in early 1980s would have never happened without these intervention policies and the associated infrastructures that were built to direct these bonus flows into the region.

Here we have a prime example of successful past water management policies producing a recovery of the declining natural resources of a region. The difference between Groundwater in the scenario shown in Fig. 3.10 with the base run is due to successful projects that began with insightful long-term water management policies.

3.7.2 Consumption Technology

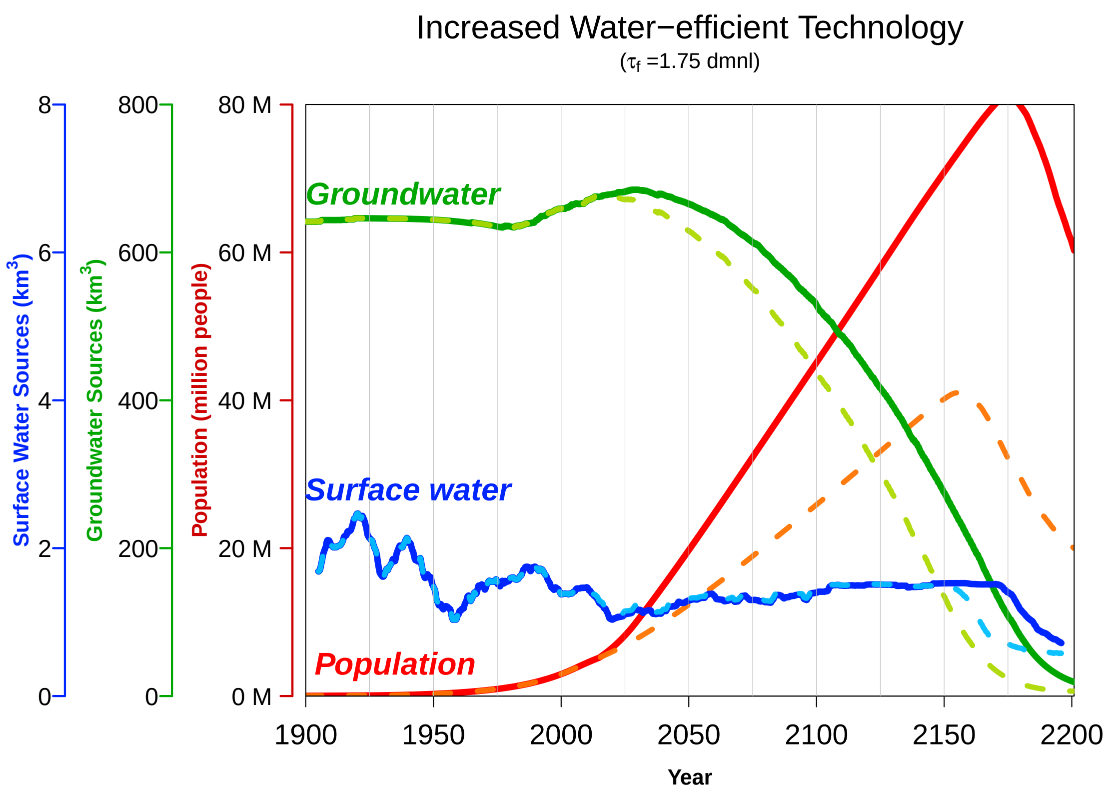

Figure 3.11: Improving the technology for more efficient consumption of freshwater will allow more consumption with the same amount of resources. This results in a higher Water Carrying Capacity proportional to the efficiency improvements and a faster population growth and decline. However, improvements in water use technologies do not change Freshwater resources relative to the base run. Note that we do not consider the Rebound Effect in our model.

There are many types of technology. Technological advances in *Extraction, Production, Consumption, and Efficiency* can affect lifetime of resources positively or negatively [Motesharrei et al., 2016]. Therefore, it is important to accurately define the type of technology when we discuss the impact of the technological change on a system.

Here, we consider efficiency and conservation improvements to Consumption Technology in COWA. Examples of these would be using efficient toilets and showerheads, or changing from flood irrigation to drip irrigation.

Improvements in consumption technology increases Water CC, but it does not change the Groundwater or Surface Water levels compared to the base run. This is because effectively, a technological change allows more total consumption, hence a higher Population, to subsist with the same amount of resources.

It is important to emphasize that we do not model the Rebound Effect (Jevons paradox) [citations from our other papers] here. In the presence of the Rebound Effect, the effect of of introducing such efficiency technologies will be lower than expected, as people will increase their consumption patterns as freshwater availability improves. In many cases, the Rebound Effect can more than cancel out the increase in efficiency.

3.7.3 Wastewater Recycling

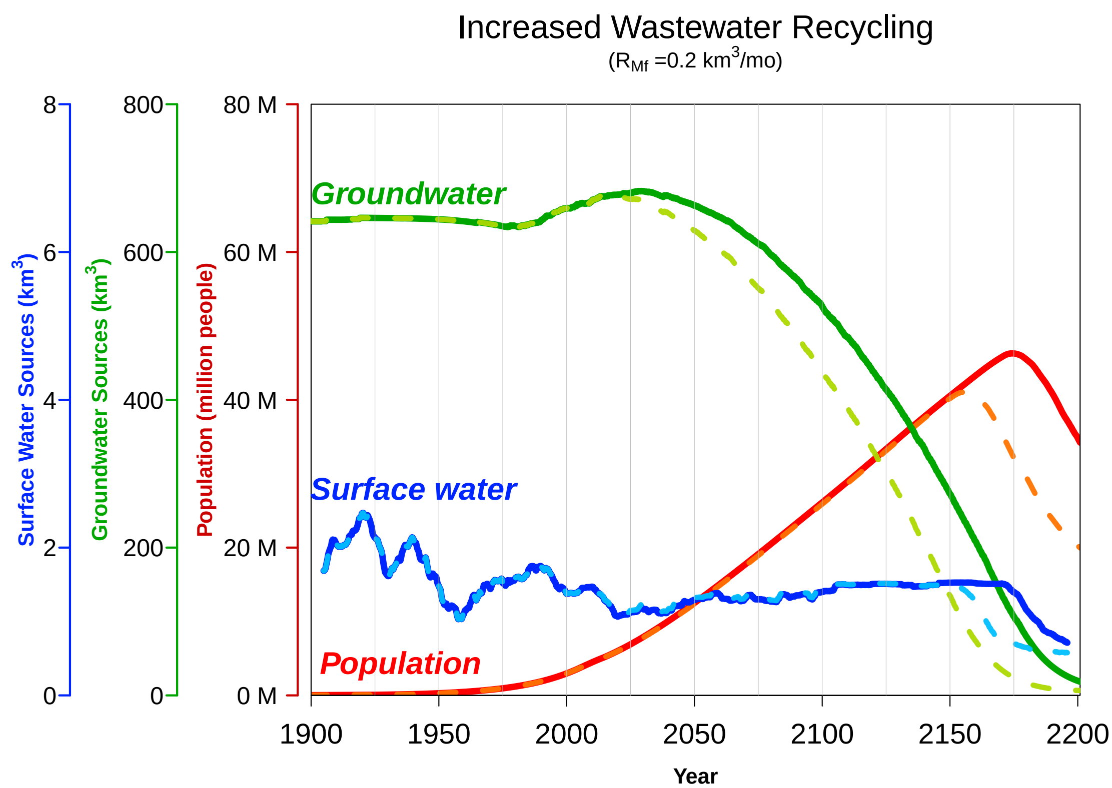

Figure 3.12: By recycling wastewater, we can reduce the reliance on Groundwater, hence slowing its depletion and improving the Water Carrying Capacity of the region.

Recycling is a major way to boost freshwater availability. It has been used successfully in many water-scarce regions of the world.

As seen in Fig. 3.12, recycling enhances Water CC in the long run. It also increases the peak population, and can postpone the population decline by slowing the depletion of Groundwater. Its impact is equivalent to increasing the natural flow.

3.7.4 Infrastructure Improvements: Reservoir Capacity and Groundwater Withdrawal Capacity

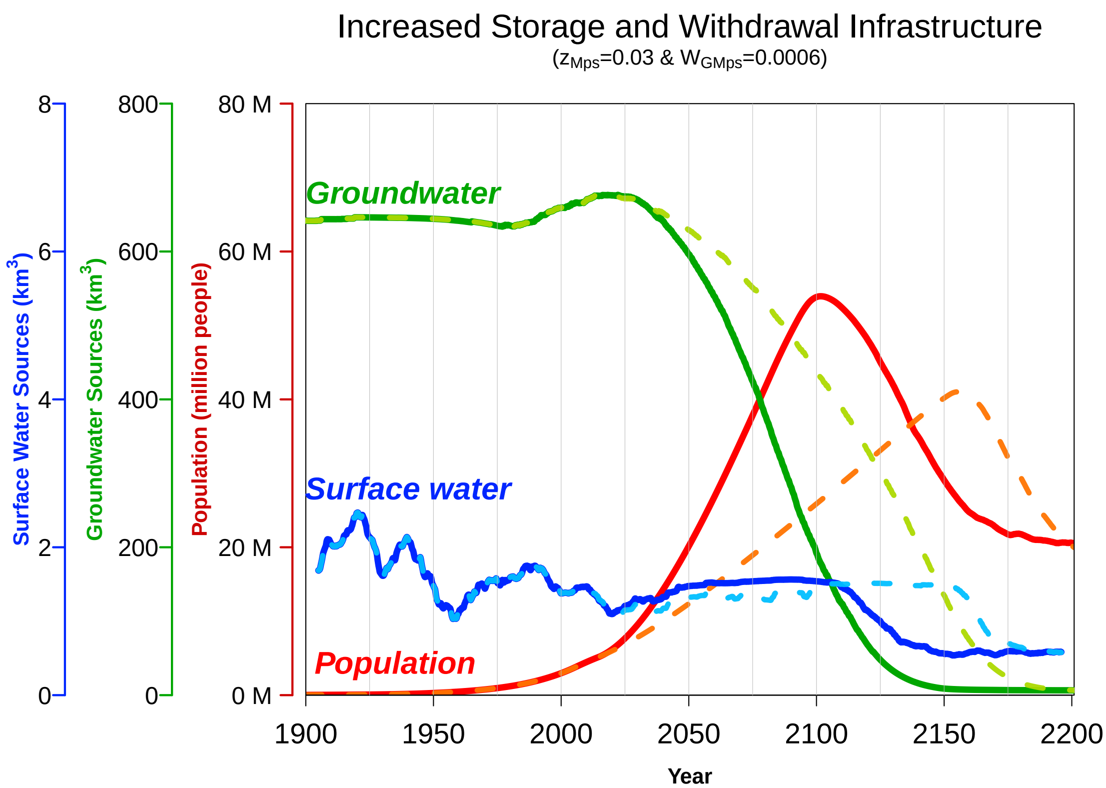

Figure 3.13: By expanding the reservoir capacity and increasing the groundwater withdrawal capacity, the increased availability of water allows for faster growth in water consumption, and hence faster growth in population. But that comes at the expense of more rapidly depleting groundwater, hence leading unexpectedly to a sooner, steeper collapse of the system.

The results of this scenario show a striking contrast between the effects of increasing wastewater recycling and water-efficient technologies on the one hand, and increasing Reservoir Capacity or Groundwater withdrawal capacity on the other. By increasing both the Reservoir Capacity and the withdrawal rate from the groundwater — and absent strict withdrawal restriction policies — Population can grow at a much faster pace and to a much higher level. Thus one might at first think that building and expanding these water infrastructures can be a helpful improvement to the region's Water Carrying Capacity. However, by ignoring the impact on the freshwater resources, the "improvement" would drive the system to a much sooner and steeper collapse. This happens because the fast growth comes at the expense of over-depleting groundwater, an effectively non-renewable resource stock. While increasing the water storage infrastructure does not improve the Carrying Capacity, it can increase the resilience of the system to temporary drought conditions.

Thus, the model results emphasize a striking finding that may seem counter-intuitive at first: neither increasing reservoir capacity nor increasing water withdrawal capacity can increase the water Carrying Capacity of a region. This is because the natural water supply factors determining Carrying Capacity are the flows of water, which are the net sum of the precipitation, evaporation, and river inflows and outflows (above surface and underground) of a region (plus any "bonus" flows). The human factors determining the water Carrying Capacity of a region are population growth rates, minimum threshold of per capita consumption, the unequal distribution of water consumption, water recycling, consumption efficiency and conservation technologies, and leakages. In contrast, the stock of Groundwater is **not** a determinant of the Water CC of a region. Groundwater is essentially a natural reservoir for water, filled by recharge (which itself comes from flows or wastewater treatment) and depleted by withdrawals, both of which can be heavily influenced by deliberate policies. If the water withdrawal is higher than the recharge, the stock will be depleted. Increasing reservoir size reduces the time to depletion (i.e., the exhaustion of the Groundwater stock). Thus, building infrastructure that enhances accessing more water within a region does not increase that region's water CC, but instead actually accelerates its depletion. Similarly, while building greater reservoir capacity can increase resilience in the system to manage short periods of drought, it does not increase the region's final water carrying capacity. In fact, as the model shows, it too can reduce the time to depletion as a result of higher levels of consumption by encouraging population growth and per capita consumption. The results of this scenario show a striking contrast between the effects, on the region's Water Carrying Capacity, of increasing wastewater recycling and water-efficient technologies versus increasing Reservoir Capacity or Groundwater withdrawal capacity. Here we have an example of a significant surprising result that could be easily missed if we do not consider the bidirectional feedbacks between the Human System and the natural resources. This shows the importance of taking into account these two-way interactions before making major policies and decisions that may impact the system in the long term.

3.7.5 Large Uncertainties in Estimates of Groundwater

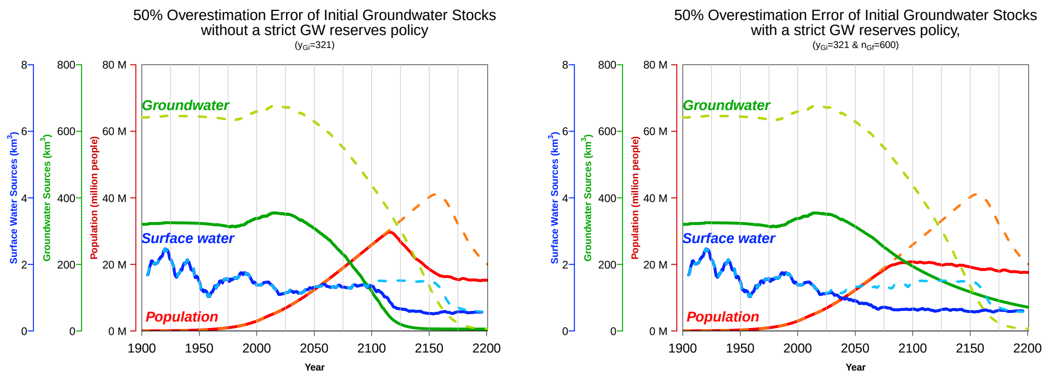

(a) A 50% uncertainty in the volumetric estimates of the total Groundwater could mean reaching critically low levels of Groundwater 40–60 years earlier.

(b) Stricter groundwater withdrawal restriction policies could prevent a catastrophic state of groundwater depletion and population collapse.

Figure 3.14: The impact of large uncertainties in the estimates of Groundwater.

Groundwater plays a major role in the dynamic of the system and the growth of consumption. However, existing estimates of the total volume of groundwater are highly uncertain. Here we consider two scenarios where the actual groundwater is not as abundant as the estimates that form the basis for the base run.

In Fig. 3.14a, we show what happens if our initial estimates of groundwater are off by 50%, which is in the range of uncertainty for the volumetric estimates of groundwater. Obviously, the result is that the near total depletion (reaching close to zero) of groundwater takes place 30–40 years earlier, which leads to a population collapse much earlier. Also, the peak population decreases by about 10–15 million people (25–30% lower peak).

The results in Fig. , with the addition of strict GW withdrawal restriction policies, also show that such extreme depletion of groundwater levels can be avoided by introducing stricter groundwater withdrawal restriction policies. A policy requiring that at least 50 years of current demand be kept in the ground, instead of just 5 years, can assure that the final groundwater levels would not reach catastrophically low levels. These restrictions can also avoid the sharp decline from the peak population, which happens in the absence of such policies after groundwater resources reach a very low level, and thus a major demographic, economic, and environmental crisis can be avoided.

3.7.6 Groundwater Contamination

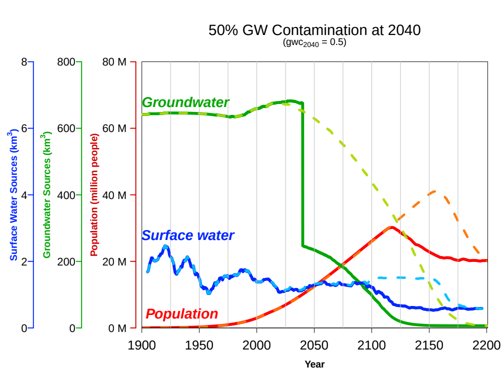

(a) A major depletion of groundwater could mean reaching the critically low levels of groundwater several decades earlier since we could lose access to a major portion of this freshwater resource.

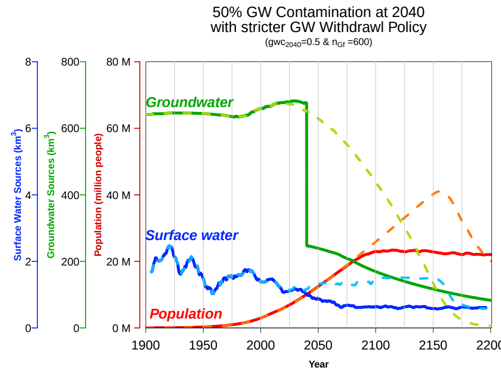

(b) Stricter groundwater withdrawal restriction policies could prevent a catastrophic state of groundwater depletion and population collapse.

Figure 3.15: The impact of a major contamination, which can occur either suddenly (shown above) or over a longer period of time. The overall result, i.e., losing access to major portion of groundwater resources, would be almost the same.

Another scenario we consider is contamination of groundwater at some point in the future. This corresponds, for example, to a massive chemical contamination as a result of a hydraulic fracturing operation.

In reality, the contamination can happen gradually over many years, suddenly over a short period of time, or a combination of the two scenarios. It would be difficult to foretell how contamination is going to take place at any certain geographical location. Moreover, groundwater treatment could partially restore the lost stock of groundwater. The combined effect of sudden or gradual contamination, plus possible treatment, is a partial loss of the stock of groundwater. Therefore, we model the contamination as a sudden decline of the GW stock, with the loss equal to a portion of the total GW stock at the contamination year. This allows for simpler and clearer experiments about the potential future contamination scenarios. Needless to say, it would be trivial to adjust the model to implement the gradual change and treatment; however, the end result would not be substantially different.

The eventual effects are similar: earlier decline of Groundwater leads to earlier decline of Population, as well as a lower peak value. In Fig. 3.15b, administering stricter withdrawal policies would save the system in a similar fashion as in the previous scenario.

3.7.7 A scenario with multiple realistic challenges

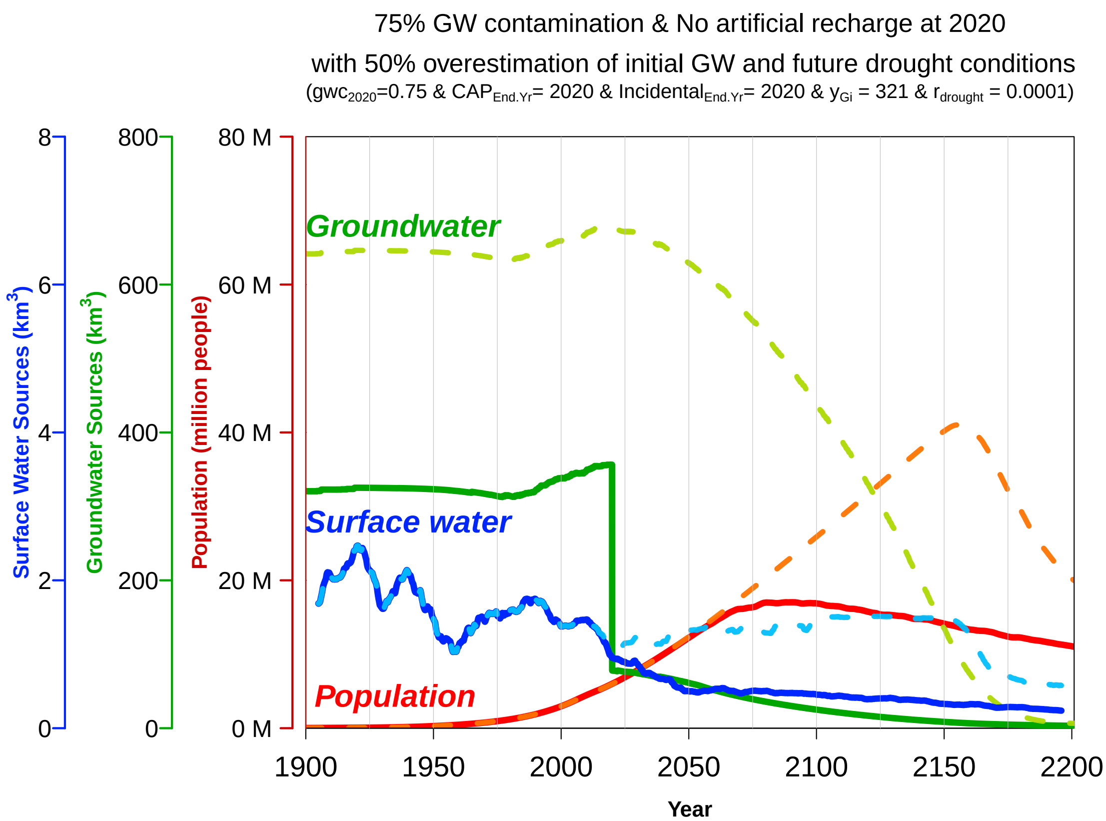

Figure 3.16: The prospects of continuous growth for another century and reaching a relatively large peak population is only possible because of a very large stock of "fossil" water (Groundwater). Taking into account the large uncertainty in volumetric estimates, as well as possibility of a major contamination in the near future completely changes that picture. Here we show that picture, adding the increased droughts due to climate change, as well as the end of bonus flows (CAP) from outside the region starting in 2020. Under such conditions, population will reach a peak by mid-century, and will continue to shrink because of decreases in precipitation and natural flows. Most importantly, this figure shows how Water Carrying Capacity changes as a function of precipitation.

In Fig. 3.16, we see how a combination of various factors can cripple the system within a few decades. Such a scenario is certainly possible, therefore the need for well-designed policies to build resilience and longevity into the system. Designing a resilient system requires understanding factors that can bring about this state, and developing long-term policies that ensure these factors cannot devastate the system. These policies should include stricter withdrawal restrictions, building infrastructure for recycling water, preventing leaks in the system, and improving water consumption efficiency.

3.7.8 Preventing Collapses with long-term policies

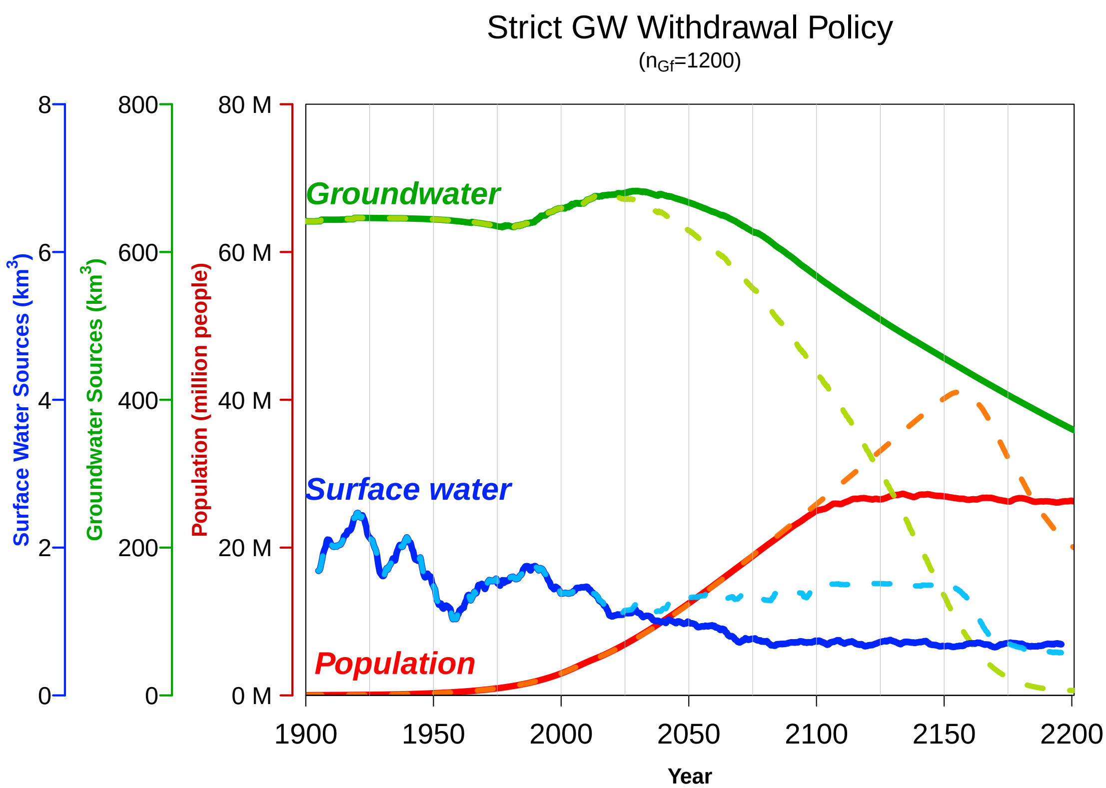

Figure 3.17: Future collapses that may happen with major depletion of Freshwater sources, especially Groundwater, could be avoided by enacting policies that protect the system in the long run. Hard Caption: Policies can prevent the catastrophic outcome observed in the base run. But making such long-term policies requires a long-term (multiple decades) thinking framework, whereas most current policies are driven by short-term goals.

By designing policies with the long-term health of the system in mind, an overshoot of the Water Carrying Capacity that can otherwise take place could be avoided. Instead, the system could smoothly converge to its Carrying Capacity without experiencing any steep, catastrophic changes.

3.7.9 Water Carrying Capacity from COWA simulations

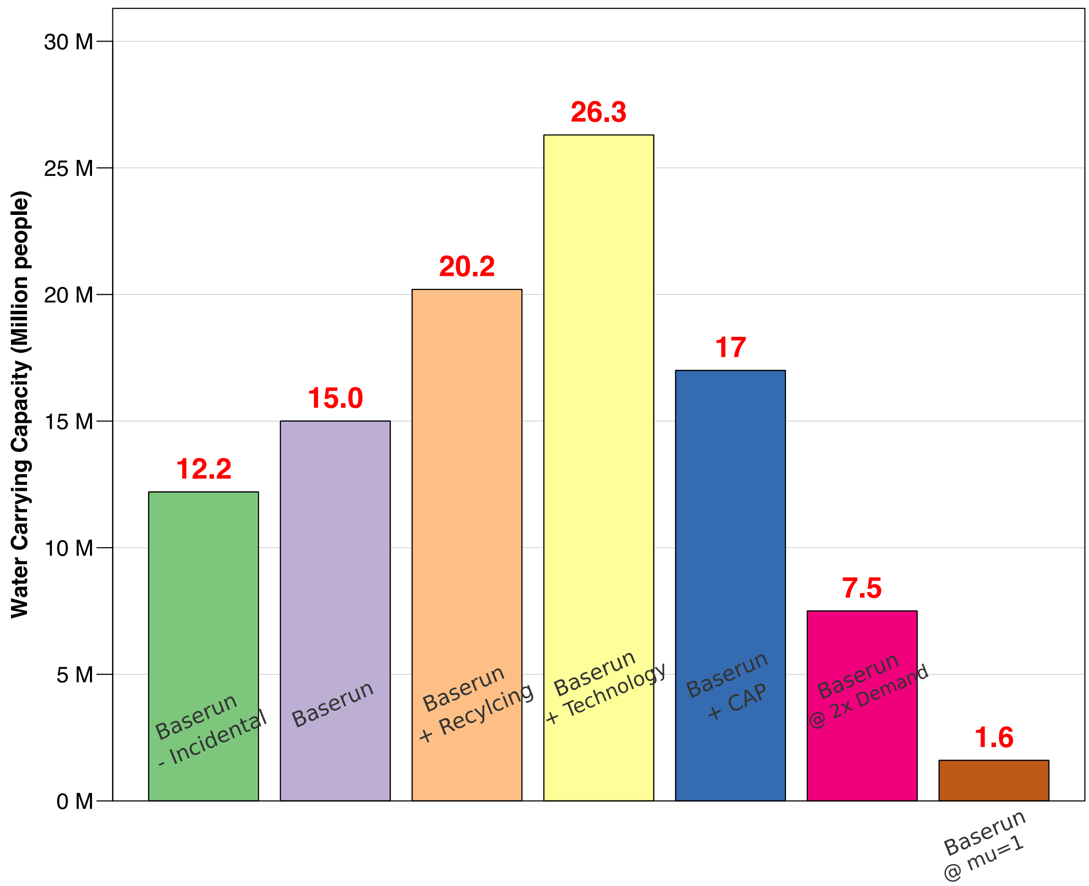

Figure 3.18: Calculation of the Water Carrying Capacity with COWA for the study region under various scenarios. Indefinite CAP assumes that the diversion of water from the Colorado River to Arizona will continue forever at its present rate.

To compare the impact of the various policies in the long run, we show a comparison of the Carrying Capacity as changed by each management option. We also show the impact on the Carrying Capacity of the “bonus” policy flows, i.e., the artificial and extra-regional sources of water added to the region’s water supply due to earlier policymaking (the Central Arizona Project, which brings water into the region from outside, and what is called ”Incidental Recharge”, which refers to policy-driven recharge from several sources, including agricultural irrigation water and treated wastewater which is redirected to replenish GW stocks.). For each management option scenario in the figure, the different bars show the Water CC depending on different policy scenarios. The last bar shows the Water CC if people can accept half the current minimum “threshold consumption per capita” (μ). This shows how critical this parameter is in determining Water CC: as people can tolerate higher level of water scarcity (corresponding to lower μ), the natural flows can sustain a larger number of people. Note that a lower mu could also represent moving water-intensive economic activities out of the region and importing the virtual water instead.

3.8 Discussion

It is important to remember that Groundwater depletion, even if there is GW still available, can greatly increase the expense of obtaining it due to the fact that it is at much deeper levels. As the water table declines, the cost and the capital equipment required increases, as existing wells run dry and have to be drilled deeper, and pumping equipment has to be upgraded and replaced with more expensive equipment that can draw water from a much deeper source. The situation in California’s

Central Valley is a good example of this, where wells have to be dug incredibly deep, new capital equipment has to be installed in order to reach the declining water level in the wells. In fact, many well-users end up with dry wells and when accessing the water at lower levels becomes cost-prohibitive they are forced to move due to lack of water.

The stock of Groundwater and the built infrastructure for storage of Freshwater are analogous to each other in that neither increases the Water Carrying Capacity of the region but they can improve the resilience of the region to drought conditions. With a larger stock of Groundwater compared to available water in the reservoir, built infrastructure can shield against drought over a shorter time period while groundwater can do that over the longer time scales. Since Groundwater stocks are generally much larger than many years of surface flows, their availability can encourage higher consumption and unsustainable growth (absent restriction policies like in Phoenix AMA).

Another empirical fact demonstrated by COWA, which we emphasize in this paper, is the fundamental importance of policies forto water resource management, and that these policies can be quite successful. Conversely, the lack of policies, particularly long-term policies, can jeopardize a region's sustainability, and even result in disastrous outcomes. In contrast to many other basins, such as the US High Plains and Californias Central Valley, groundwater stocks in the Phoenix AMA have not been declining. The fundamental reasons for this success in groundwater management in the Phoenix AMA are the public water management policies explicitly designed to reduce groundwater withdrawals and instead artificially recharge the groundwater stocks. These usage and recharge policies are combined with policies to encourage higher efficiency in water use, reduced leakage and waste, and a transition away from higher-water intensity to lower-water uses in economic activities and in residential design.

In Arizona, groundwater had been pumped for decades from aquifers at higher rates than it was naturally recharged back into the underground stocks, significantly depleting many of the aquifers. As early as the 1950s, groundwater depressions had developed due to well extraction exceeding natural recharge, hence depleting groundwater stocks. In order to meet the challenges of this imbalance, state and local governments responded with policies to artificially recharge groundwater stocks using both artificial flows from outside the region as well as diversion of treated wastewater back into the aquifers. These groundwater recharge policies use Percolation Basins (depressed areas of land specifically designed to hold water over a permeable substrate causing the water to percolate back into the ground to recharge groundwater stocks) and Injection Wells (wells constructed for the purpose of injecting water back into the aquifer). Water use policies have also been designed to encourage the use of renewable flows for direct usage rather than rely on non-renewable stocks for direct usage.

Artificial recharge has become a critical component of Arizonas water supply management, driven by the need to meet the targets of the 1980 Groundwater Management Code and many other state and local statutes and policies, including the Underground Water Storage and Recovery program established in 1986 and the Underground Water Storage, Savings, and Replenishment Act, enacted in 1994 by the Arizona Legislature. The recharge management policies and programs are administered by Arizona Department of Water Resources. The Phoenix AMA is mandated to combine efficient water uses with decreased groundwater withdrawals to be replaced by the increased use of renewable water supplies in order to reach "safe-yield" levels by the year 2025.

These policies are designed to store current excess flows of water underground through artificial recharge in order to replenish over-withdrawal and ensure an adequate supply for the future. Both the geology and desert environment of Arizona makes artificial recharge of water underground both practical and cost-effective. The current excess flows that are used for this artificial recharge themselves are also a product of other policies and programs. Arizona is allotted 1.85 km^3/yr diverted from the Colorado river system located outside the basin and channeled to the basin through the Central Arizona Project (CAP) by 540 km of artificial canals and pumping stations [ADWR, 2010]. According to US Census Bureau, 2010 population in Arizona was about 5 million, and is projected to double by 2030. Further, in a 2017 Census study, Maricopa county (which accounts for 80% of the Phoenix AMAs surface area) was found to be the fastest growing county in the entire nation [USCB, 2017]. Without these past policies, Arizona would not have been able to sustain the population it currently has, much less an expanded population in the future.

3.9 Author Contributions

JR designed the initial Coupled Human-Water System schematic. JR, SM, EK, KCG, and FMW developed the conceptual framework for COWA. SM designed the mathematical model of COWA, as well as the one-way coupled water model, and implemented them in VENSIM, with additions by KCF, EK, JR, and FMW. KCG collected the datasets for simulating and validating COWA and processed them with guidance from FMW. FZ developed and validated COWA-RRM for surface and subsurface flows, and then FZ generated the climate time-series from Earth System Models, all with guidance from HW, NZ, and EK. KCG and SM validated COWA. SM, JR, and EK designed the COWA experiments. KCG and SM ran the experiments. KCG visualized the results. SM, JR, and EK analyzed the results. SM, JR, and EK developed the concept of Dynamic Carrying Capacity, and SM derived the theoretical formula for COWA's Dynamic Water Carrying Capacity. SM, JR, KCG, and FZ drafted the manuscript. All co-authors contributed to the discussion of the results and improving the manuscript.

Chapter 4: Causality Analysis: Identifying the Leading Element in a Coupled Dynamical System

Physical systems with time-varying internal couplings are abundant in nature. While the full governing equations of these systems are typically unknown due to insufficient understanding of their internal mechanisms, there is often interest in determining the leading element. Here, the leading element is defined as the sub-system with the largest coupling coefficient averaged over a selected time span. Previously, the Convergent Cross Mapping (CCM) method has been employed to determine causality and dominant component in weakly coupled systems with constant coupling coefficients. In this study, CCM is applied to a pair of coupled Lorenz systems with time-varying coupling coefficients, exhibiting switching between dominant sub-systems in different periods. Four sets of numerical experiments are carried out. The first three cases consist of different coupling coefficient schemes: I) Periodic–constant, II) Normal, and III) Mixed Normal/Non-normal. In case IV, numerical experiment of cases II and III are repeated with imposed temporal uncertainties as well as additive normal noise. Our results show that, through detecting directional interactions, CCM identifies the leading sub-system in all cases except when the average coupling coefficients are approximately equal, i.e., when the dominant sub-system is not well defined. [1]

4.1 Introduction

Identifying the leading [sub–]system from a pair of coupled dynamical systems using only time–series is challenging when nothing or little is known of the underlying dynamics. The definitive approach to detect causal relationships between components of a system is to fully identify the underlying physical mechanisms and governing equations. However, in most cases we only have a partial knowledge about the internal physical mechanisms. In these cases we must resort to observed data to establish the existing causal relationships.

In linear systems, lead time of the driver (or equivalently, latency of the response) may indicate a causal relationship, which hence could be identified by [linear] lag–correlation analysis. In a nonlinear system, however, there may be no persistent lead–lag between the two signals, due to feedback loops between the variables. Therefore, a simple linear lag–correlation analysis may not reliably determine the correct causal relationship in a general nonlinear system [Chatfield, 2013]. For example, Figure 4.1 shows lead–lag switching between two coupled variables. If one considers short intervals of the time–series and take lead time and high correlation as the indicators of causation, an incorrect conclusion about the causal relationship between the variables will be made. In this condition, one can analyze the

[1]This chapter was published following peer-review as: Amir E. BozorgMagham, Safa Motesharrei, Stephen G. Penny, and Eugenia Kalnay. Causality Analysis: Identifying the Leading Element in a Coupled Dynamical System. *PLoS ONE*, 10(6):e0131226, June 2015.

signal phases to establish temporal precedence and exploit the phase slope index to estimate the flow direction of information flux [Nolte et al., 2008].

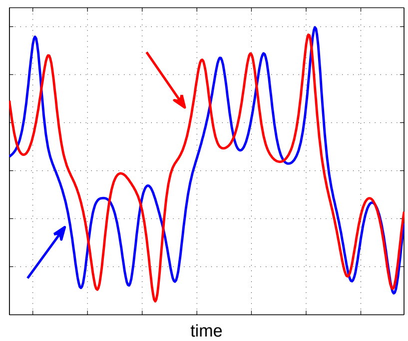

Figure 4.1: **An example of lead–lag switching between two signals of a nonlinear system.** Observation of the leading signals, shown by the colored arrows, in short intervals may result in an incorrect conclusion about the cause–effect relationship. (The time–series in this figure are generated by (4.9).)

The concept of information transfer has been used as an indication of causality. A practical measure of information transfer is the transfer entropy [Schreiber, 2000] which distinguishes directional communications between variables of a system. This probabilistic measure has been used in a variety of fields such as neuroscience [Vicente et al., 2011; Ding et al., 2006], the study of chemical processes [Bauer et al., 2007] and cellular automata [Lizier et al., 2008]. A more general form of the transfer entropy that has an augmented time–delay parameter can detect the propagation time in addition to the asymmetric information transfer between observed signals [Wibral et al., 2013].

Before establishing the general notion of information transfer [and transfer entropy], a practical definition of causality was proposed by Wiener [Wiener, 1956] and later adopted and formalized in terms of linear autoregression by Granger [Granger, 1969, 1980]. Later, it was shown that Granger causality can be considered in the context of information transfer, and is equivalent to transfer entropy for Gaussian variables [Barnett et al., 2009]. Although the standard [linear] Wiener–Granger method was first introduced for economic systems, the method and its extended nonlinear versions gained widespread use in other fields like neuroscience and financial market [Hlavkov-Schindler et al., 2007; Bressler and Seth, 2011; Barnett and Seth, 2014; Chen et al., 2004; Marinazzo et al., 2008; Hiemstra and Jones, 1994]. According to Wiener–Granger causality definition, a candidate driver is among the drivers of a response signal if the response prediction error increases significantly by removing the candidate driver data from the universe of all drivers. More precisely, given sets of interdependent variables X and Y, it is said that "X causes Y" if, in an appropriate statistical sense, X assists in predicting the future of Y beyond the degree to which Y already predicts its own future [Barnett et al., 2009]. The Granger method is a forward method as it uses the driver data to *predict* the response. An important characteristic of the Granger method is that it requires the signals to be separable and have non–zero entropy rates [Cover and Thomas, 2012]. In a separable system it is possible to separate a candidate driver's data from other factors, thus enabling prediction to be conducted using data sets including and excluding the candidate driver. Separability is a restrictive conditions since many observed signals of interest are from deterministic nonlinear systems with interdependence and feedbacks between state variables, resulting in mixed information from different sources.

Although the transfer entropy and Granger causality provide valuable statistical information about the observed signals and their asymmetric connectivity, the true causal relationship between variables of a system can only be identified by intervention, i.e., perturbing the candidate cause variable to investigate its direct influence on the response variable. Information flow was proposed as a quantitative measure of intervention. This Bayesian probabilistic measure quantifies the distribution of a response variable as a result of "imposing" conditions. However, there are some practical limitations for applying this measure and detecting real causal relationships in realistic systems. For example one may need to know about the structure of causal links of a network or the underlying rules of the causal interactions which are the purpose of a causality study (the back–door adjustment criterion was proposed to solve this problem in certain condition) [Pearl, 2000; Ay and Polani, 2008; Lizier and Prokopenko, 2010].

Sugihara et al. [2012] investigated the problem of causality from a new perspective, proposing the Convergent Cross Mapping (CCM) method for deterministic nonlinear systems with smooth manifolds. The fundamental idea of the CCM method is that if Y is causally influenced by X, then Y has signatures of X such that the historical record of Y can reliably estimate the state of X. Therefore, a better estimate of the driver variable, X, shows stronger causal influence on the response variable, Y.

It is important to note that: (i) unlike Granger causality that uses prediction as its fundamental basis, the CCM method is not based on prediction of a variable,

(ii) the CCM method does not apply Bayesian probability, the core concept of the transfer entropy and information flow measures, and (iii) true causality can only be established using interventions and all other methods, including CCM, Granger and information transfer, just deliver a "best guess".

Sugihara et al. [2012] showed that CCM can identify unidirectional and bidirectional causation, and dominant driver, in *weakly* coupled nonlinear systems with *constant* coupling coefficients. They presented successful applications of the CCM method in ecology, biology and geoscience [Sugihara et al., 2012; Deyle et al., 2013; van Nes et al., 2015]. Our study is motivated by the need to identify the dominant constituent in systems that are speculated to have time–varying interconnections such that switching happens between the dominant elements in different time periods. As an example we may refer to the challenging problem of identifying the driver–response or dominant variables of the global climate system from geophysical records of greenhouse gases such as CO_2 concentration and temperature proxy [Monnin et al., 2001; Caillon et al., 2003; Shakun et al., 2012]. For this purpose, we consider coupled systems that (i) have *variable* coupling parameters in sequential periods, and (ii) the larger coupling coefficient is not fixed for a specific sub–system. Thus, we may observe switching between the dominant sub–systems during successive periods. We investigate whether CCM can identify the leading sub–system [2] from a pair of coupled sub–systems under different conditions of our interest. To do that, we perform numerical experiments with different [linear] coupling schemes of

[2] The *leading sub–system* is defined as the system with a larger average coupling coefficient over specified intervals of the time–series assuming that the coupled systems have the same time scales.

Lorenz system [Lorenz, 1963] with asymptotic synchronization [Yang et al., 2006]. We consider periodic–constant (case I), normally distributed (case II), and mixed normally/non–normally distributed (case III) coupling coefficients. We also investigate the CCM results in presence of temporal uncertainties and additive noise (case IV). Our results indicate that CCM can identify the leading sub–system, except when the average coupling coefficients are approximately equal and the leading sub–system is not well-defined.

This article is organized as follows. Section §4.2 covers mathematical details of the CCM method, and section §4.3 describes the coupling schemes. In section §4.4 we show results of the numerical experiments. In section §4.5 we summarize and discuss our findings.

4.2 Method

In the CCM method, it is assumed that a response signal has signatures from its driver so that the approximate behavior of the driver can be estimated (or recovered) from the response signal. Thus, a better estimate of the driver shows stronger causal influence on the response variable. To implement the CCM method, we use the concept of one–to–one mapping between the original smooth manifold of the [full] system and the compact reconstructed phase spaces (shadowing manifolds) of the observed signals [Takens, 1981; Sauer et al., 1991]. If the two observed signals belong to a same dynamical system, by considering the original manifold as an interface, it is known that there is a one–to–one mapping between the two reconstructed phase spaces. If the dimension of the reconstructed phase spaces are selected based on the false neighborhoods method criteria [Cao, 1997], arbitrary nearby points on the driver's reconstructed phase space map to nearby points on the original attractor. Because of causal influence of the driver, the nearby points on the original manifold stay close on the reconstructed phase space of the response signal. The stronger causal influence of the driver on the response, the closer would be the mapped points of the response signal on its shadowing manifold [Sugihara et al., 2012].

In this section, we assume without loss of generality that $x(t)$ is the driver and $y(t)$ is the response. The time–series $x(t)$ and $y(t)$ are sampled at equally spaced times Δt,

$$\begin{cases} x_n = x(t) = x(t_0 + (n-1)\Delta t) \\ y_n = y(t) = y(t_0 + (n-1)\Delta t) \end{cases} \tag{4.1}$$

where $n = 1, 2, \cdots, N$, and N is the total number of data points in each time–series. We set $t_0 = 0$ to simplify the notation. We use $[x(t), y(t)]$ and $[x_n, y_n]$ notations interchangeably.

CCM uses the time–delay coordinates to reconstruct the phase spaces of the *L-point windows* from the time–series $x(t)$ and $y(t)$ [Deyle and Sugihara, 2011]. The L-point windows are defined as

$$\begin{cases} W_x^{i,L} = \{x_i, x_{i+1}, \cdots, x_{i+L-1}\} \\ W_y^{i,L} = \{y_i, y_{i+1}, \cdots, y_{i+L-1}\} \end{cases} \tag{4.2}$$

for $i = 1$ to $i = N + 1 - L$ and $L_{min} \leqslant L \leqslant L_{max}$. We define L_{min} and L_{max} below. The L-point windows sweep the entire time–series $x(t)$ and $y(t)$ (see Fig. 4.2a).

We use the average mutual information measure I, a nonlinear generalization of the correlation function, to select the time lags τ as an integer multiple of Δt. This measure shows the average amount of information about a signal at $t + t'$, i.e., $s(t + t')$, when $s(t)$ is observed

$$I(t') = \sum_{n=1}^{N} P(s(t), s(t + t')) \log_2 \left[\frac{P(s(t), s(t + t'))}{P(s(t)), P(s(t + t'))} \right], \tag{4.3}$$

where $P(s(t), s(t + t'))$ is the joint probability of measuring $s(t)$ and $s(t + t')$. We choose τ where the first minimum of $I(t')$ occurs [Takens, 1981; Fraser and Swinney, 1986; Abarbanel, 1996].

We employ the false neighborhood method to determine the embedding dimension, E. The correct embedding dimension prevents self overlapping of the projected manifold. Therefore, "if E is qualified as an embedding dimension by the embedding theorem [Takens, 1981; Sauer et al., 1991], then any two points which stay close in the E-dimensional reconstructed space will be still close in the $(E + 1)$-dimensional reconstructed space. Such a pair of points are called true neighbors, otherwise, they are called false neighbors" [Cao, 1997].

By these two parameters, i.e., τ and E, we generate the time–delay coordinates as well as the reconstructed phase space resembling the original manifold of the attractor. The E-dimensional time–delay coordinate vectors corresponding to $W_x^{i,L}$ and $W_y^{i,L}$ are shown as

$$\begin{cases} m_x^{i,L}(t) = [x(t - (E - 1)\tau), \cdots, x(t - \tau), x(t)] \\ m_y^{i,L}(t) = [y(t - (E - 1)\tau), \cdots, y(t - \tau), y(t)] \end{cases} \tag{4.4}$$

for $t = (i-1)\Delta t + (E-1)\tau$ to $t = (i+L-2)\Delta t$. Limits of t are chosen such that the first/last component of $m^{i,L}$ vectors corresponds to the first/last point of $W^{i,L}$ windows. The reconstructed phase spaces are

$$\begin{cases} M_x^{i,L} = \left\{m_x^{i,L}(t)\right\} \\ M_y^{i,L} = \left\{m_y^{i,L}(t)\right\} \end{cases} \tag{4.5}$$

each containing $L - (E-1)(\tau/\Delta t)$ vectors.

After reconstructing the phase spaces, sufficient numbers of nearest neighbor points are selected for each E-dimensional vector in $M_y^{i,L}$, referred to as a Y–central point, Y_c (see Figure 4.2b). The neighbor points are denoted by Y_j, ordered by their distance, d_j, to Y_c, from nearest to farthest. Therefore Y_1 is the nearest neighbor to Y_c. The number of selected neighbor points should be equal or larger than $E+1$ so the simplex method can represent the dynamics on an E-dimensional manifold [Farmer and Sidorowich, 1987]. This requirement specifies $L_{min} = (E+2) + (E-1)(\tau/\Delta t)$. We use the corresponding contemporaneous points of the Y_j in M_x, denoted by X_j, to calculate the position of a single point that represents them, $\widehat{X}$. We define the exponentially decaying weights based on the distances between the Y_c and its neighbor points, d_j, as

$$\begin{cases} u_j = \exp\left(-\dfrac{\|d_j\|}{\|Y_c - Y_1\|}\right) \\ \omega_j = \dfrac{u_j}{\sum u_j} \end{cases} \tag{4.6}$$

where $\|\cdot\|$ is the Euclidean norm. The position of the representative point in M_x is calculated as

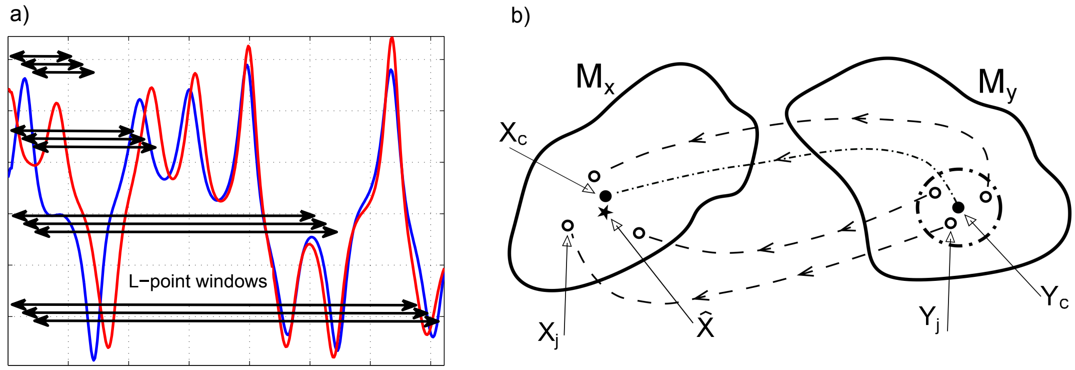

Figure 4.2: **(a) Two time–series $x(t)$ and $y(t)$ and a schematic of the L-point windows with different lengths sweeping the whole span of the time–series.** (b) A schematic of the reconstructed phase spaces of the L-point windows corresponding to two time–series. For each E-dimensional Y–central point, Y_c, in the response reconstructed phase space, M_y, a sufficient number of nearest neighbor points are selected (empty circles, Y_j, right) and their distances, d_j, to Y_c are determined. For each neighbor point its contemporaneous point in the driver reconstructed phase space, M_x, is determined (empty circles, X_j, left). The weighted average of these points, $\widehat{X}$, is compared with X_c, the true contemporaneous point in M_x corresponding to Y_c. The CCM coefficient, $\rho(L)$, is defined as the correlation coefficient between $\widehat{X}$ and X_c, *averaged* over all possible L-point windows.

$$\widehat{X} = \sum \omega_j X_j. \tag{4.7}$$

The set of these recovered points, $\left\{\widehat{X}\right\}$ is the *recovered phase space*. If $x(t)$ and $y(t)$ are dynamically coupled, $\left\{\widehat{X}\right\}$ should be strongly correlated to $M_x = \{X_c\}$, where X_c is the correspondent point to Y_c (see the star and black filled circle in

Fig 4.2b). In addition, as L increases, the density of the points in the reconstructed phase space increases, hence the distances between the nearest neighbors shrink. Thus, $\widehat{X}$ converges to a vicinity of X_c that becomes smaller as the causal effect of the driver increases. Therefore, the CCM coefficient, $\rho(L)$, as a measure of causal relationship between the [candidate] driver and the response signal is defined as the correlation coefficient between $\widehat{X}$ and X_c, *averaged* over all possible L-point windows,

$$\rho_{\widehat{X}|M_y}(L) = \left\langle \frac{\operatorname{cov}(\widehat{X}, X_c)}{\sigma_{\widehat{X}}\sigma_{X_c}} \right\rangle_L . \tag{4.8}$$

Providing a causal relationship between the signals, ρ converges to a constant equal or less than one. Note that $\langle\cdot\rangle_L$ indicates averaging over all L-point windows, and $\widehat{X} \mid M_y$ emphasizes that $\widehat{X}$ is estimated given M_y. If we study the opposite roles, that is $y(t)$ as the driver and $x(t)$ as the response, the CCM coefficient would be shown by $\rho_{\widehat{Y}|M_x}$. In section §4.3 we simplify this notation by setting $\rho_{\widehat{X}|Y} = \rho_{\widehat{X}|M_y}$ and $\rho_{\widehat{Y}|X} = \rho_{\widehat{Y}|M_x}$.

It is important to note that: (i) the CCM method can investigate causal relationship over any window of the time–series that contains sufficient information about the attractor of the dynamical system. In case of nonstationary signals, the CCM results during the considered time interval are presumably valid if the original manifold and the reconstructed phase spaces do not have significant changes, that is near–stationary condition holds. A general case of nonstationary signals analysis with the CCM method is left for future work. (ii) CCM only considers the past data and does not attempt to predict the signals. Therefore, CCM could be robustly applied to chaotic systems, where predictions may rapidly diverge from the true/observed states. (iii) The identified causal relationship by the CCM method is not exclusive, i.e., the identified driver might be one of the many drivers of the system. Therefore, in systems with multiple variables the CCM method can be applied and repeated for different combination of candidate driver and response signals. (iv) Our results (not shown here) show that the CCM method is not sensitive to increases in the embedding dimension if that parameter is chosen with respect to the results of the false neighborhood method. By increasing the embedding dimension beyond what is prescribed by the false neighborhood method, computation cost increases because the search process for the nearest neighbors should be performed in a larger space dimension but the CCM results remain almost unchanged because the extra dimensions do not add new information. In addition, the CCM results are not sensitive to small changes of τ if that embedding parameter remains in the vicinity of the first minimum of the average mutual information measure.

4.3 Experiment design with coupled Lorenz systems

In order to study the applicability of the CCM method to [strongly] coupled systems with variable coupling coefficients, we apply it to a pair of identical Lorenz systems [Lorenz, 1963], $\mathfrak{L}_X$ and $\mathfrak{L}_Y$, coupled with different coupling schemes. We choose to study synchronized dynamical systems, in which the coupling is canonically between two identical [sub-]systems coupled simultaneously with a linear coupling term where the dominant element is clearly identified by its larger coupling coefficient. Study of synchronized dynamical systems has expanded beyond the canonical case to included "generalized synchronization" [Hunt et al., 1997], in which the two systems differ. Other work in synchronized dynamical systems has studied "lagged synchronization" [Pecora et al., 1997]. Since this application of the CCM method is new, we choose to focus on the canonical representation of the problem and allow for similar extensions in future work to address these more complex variations of the general problem.

The general form of $\mathfrak{L}_X$ and $\mathfrak{L}_Y$ is given by (4.9).

$$
\begin{aligned}
&\mathfrak{L}_X \begin{cases} \dot{x_1} = \sigma\left(x_2 - x_1\right) + k_\mu \mu\left(y_1\right) \\ \dot{x_2} = x_1\left(\rho - x_3\right) - x_2 \\ \dot{x_3} = x_1 x_2 - \beta x_3 \end{cases} \\
&\mathfrak{L}_Y \begin{cases} \dot{y_1} = \sigma\left(y_2 - y_1\right) + k_\eta \eta\left(x_1\right) \\ \dot{y_2} = y_1\left(\rho - y_3\right) - y_2 \\ \dot{y_3} = y_1 y_2 - \beta y_3 \end{cases}
\end{aligned}
\tag{4.9}
$$

The parameters of the Lorenz–63 systems are $(\sigma, \rho, \beta) = (16, 45.92, 4)$ throughout this paper. μ and η are the coupling coefficients, and k_μ and k_η are the binary on–off switches. Variations of the coupling coefficients, activation of the on–off switches, and duration of successive periods are discussed in section §4.4.

We investigate whether CCM can distinguish the leading system by detecting the difference between the CCM coefficients $\rho_{\widehat{X}|Y}$ and $\rho_{\widehat{Y}|X}$. We probe one signal from each system, $x_1(t)$ and $y_1(t)$ in the following experiments. When the two systems are strongly correlated, for example, due to a strong feedback loop, $\rho_{\widehat{X}|Y}$ and $\rho_{\widehat{Y}|X}$ are close to each other for large L's. Thus, one must investigate *small differences* between $\rho_{\widehat{X}|Y}$ and $\rho_{\widehat{Y}|X}$.

A brief description of the four experiments is as follows. In case I, $\mathfrak{L}_X$ and $\mathfrak{L}_Y$ are coupled by a periodic on–off switching mechanism and constant coupling coefficients during all periods. We cover 100 different combinations of coupling coefficients. In case II, both coupling coefficients in all periods are normal random variables with specified mean and standard deviation. In case III, one of the coupling coefficients is a normal random variable and the other one is from a Weibull (skewed non–normal) distribution [Rinne, 2008]. In case IV, we consider the original pairs of signals from cases II and III and impose relative temporal shifts (representing temporal uncertainties) and also additive Gaussian noise. It is notable that, in all cases, due to bidirectional coupling in system (4.9), we observe quite high degree of correlation between the probed signals $x_1(t)$ and $y_1(t)$, unless the two systems have different amplitudes and scales, as in the case of the ocean–atmosphere model [Peña and Kalnay, 2004].

As discussed in section §4.2, by increasing the length of the L-point windows $\rho(L)$ converges to a constant provided that the two signals are dynamically connected. In our experiments, convergence of $\rho(L)$ over the range $L = 25$ to 500 is tested. We observe negligible variations in the CCM coefficients for $L \geqslant 300$. To be on the safe side, we choose $L = 500$ to report all the CCM coefficients. This choice of L is equivalent to 0.5 time unit since we sample the signals 1000 times per non–dimensional time unit.

4.4 Experiment results

Below we present the results of four sets of numerical experiments with the system (4.9).

4.4.1 Case I: Coupled Lorenz systems, periodic–constant coupling coefficients

In this case, coupling coefficients μ and η assume constant integers 1 to 10, resulting in 100 combinations, during 10 consecutive periods of the time–series, each spanning 10 non–dimensional time units. The switching mechanism is controlled by k_μ and k_η, such that in odd periods $k_\mu = 0$ and $k_\eta = 1$ and in even periods $k_\mu = 1$ and $k_\eta = 0$ as described in (4.10).

$$\begin{cases} (\eta, \mu) = \text{int}[1:10] \times \text{int}[1:10] \\ k_\eta = 1 \text{ odd periods}, 0 \text{ even periods} \\ k_\mu = 0 \text{ odd periods}, 1 \text{ even periods} \end{cases} \tag{4.10}$$

Figure 4.3a shows $\rho_{\widehat{Y}|X}$ at $L = 500$ for different values of μ and η and random initial conditions. We observe similar patterns in $\rho_{\widehat{Y}|X}$ and $\rho_{\widehat{X}|Y}$ (not shown here) such as vertical and horizontal bands. For example, we see a blue horizontal band near $\mu = 1$ in Fig. 4.3a. Showing that the influence of $\mathfrak{L}_Y$ on $\mathfrak{L}_x$ is small. Therefore, $\left\{\widehat{Y}\right\}$ (the recovered phase space of $\mathfrak{L}_Y$ from $\mathfrak{L}_X$), is poorly correlated to M_y (the reconstructed phase space of $\mathfrak{L}_Y$), hence the small values for $\rho_{\widehat{Y}|X}$ on the band. Another observed pattern is the high values of ρ in the regions with the strongest coupling between the two sub–systems (high μ and η), showing the large mutual influence between the two systems.

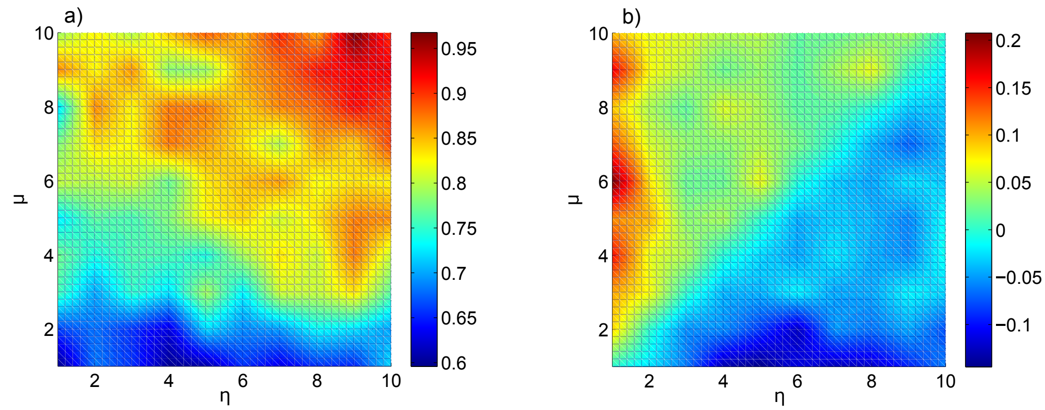

Figure 4.3: **Case I.** (a) $\rho_{\widehat{Y}|X}$ at $L = 500$ over the range of μ and η given by (4.10) and for random initial condition. (b) Difference between the CCM coefficients, $\Delta\rho = \rho_{\widehat{Y}|X} - \rho_{\widehat{X}|Y}$, at $L = 500$ over the specified range of μ and η.

To address the main question of this study we investigate $\rho_{\widehat{Y}|X} - \rho_{\widehat{X}|Y}$. We expect that if $\mathfrak{L}_Y$ is the leading sub–system, then $\rho_{\widehat{Y}|X}$ is larger than $\rho_{\widehat{X}|Y}$ and similarly, $\rho_{\widehat{X}|Y}$ is larger than $\rho_{\widehat{Y}|X}$ if $\mathfrak{L}_X$ is the dominant sub–system. Referring to Fig. 4.3b, when $\mu > \eta$ we observe that $\rho_{\widehat{Y}|X} > \rho_{\widehat{X}|Y}$ (upper diagonal of Fig. 4.3b) and when $\eta > \mu$, $\rho_{\widehat{X}|Y} > \rho_{\widehat{Y}|X}$ (lower diagonal of Fig. 4.3b).

This numerical experiment with 100 combinations of coupling coefficients shows that even when ρ values are close to each other ($\rho_{\widehat{Y}|X} \approx \rho_{\widehat{X}|Y}$), CCM can capture the leading system through small differences between the CCM coefficients, except for $\mu \approx \eta$ where neither system is leading.

4.4.2 Case II: Coupled Lorenz systems, normally distributed coupling coefficients

In section §4.4.1, we studied CCM's capability to identify the leading system in coupled systems with periodic constant coupling coefficients. A more general and realistic case is a system with randomly distributed coupling coefficients and with random period's length. Therefore, in this section we choose the coupling coefficients from normal distributions. Note that these coefficients are constant during each period. In equation (4.9) we set $\eta = \eta_N$ and $\mu = \mu_N$ where subscript N stands for normal random variables. We set the mean and standard deviation of the coupling coefficients such that the ratio of the averaged coupling coefficients $\overline{\eta}_N/\overline{\mu}_N$ covers the approximate range $(0.5, 5)$. The switching coefficients, k_η and k_μ, are kept on for all periods in order to have bidirectional communication between the two sub–systems. We also choose the duration of each period, T_i, from a normal distribution as described in (4.11).

$$\begin{cases} k_\eta = 1, k_\mu = 1 \text{ for all periods} \\ \eta = \eta_N = \mathcal{N}(5.5, 2) \\ \mu = \mu_N = \mathcal{N}(\alpha, 2) \mid \alpha \in \text{int}[1:10] \\ T_i = \mathcal{N}\left(\overline{T} = 10, \sigma = 2\right) \mid i \in \text{int}[1:20] \end{cases} \tag{4.11}$$

Again, to address the main question of this study we investigate the difference between the CCM coefficients, $\Delta\rho = \rho_{\widehat{X}|Y} - \rho_{\widehat{Y}|X}$, at $L = 500$ as a function of $\overline{\eta}_N/\overline{\mu}_N$, where $\overline{\eta}_N$ and $\overline{\mu}_N$ are the mean values of η_N and μ_N over the entire time–

series. Fig. 4.4a shows that the difference between the CCM coefficients is negative for $(\overline{\eta}_N/\overline{\mu}_N) < 1$ and positive for $(\overline{\eta}_N/\overline{\mu}_N) > 1$. We also observe a close to linear relationship between $\overline{\eta}_N/\overline{\mu}_N$ and the difference between the CCM coefficients $(\Delta\rho)$ in the considered range of the coupling coefficients.

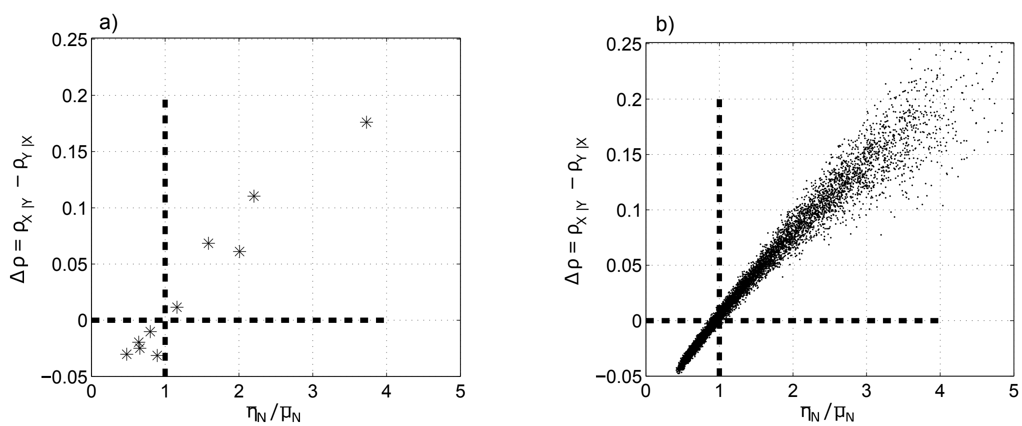

Figure 4.4: **Case II.** (a) The difference between the CCM coefficients, $\Delta\rho = \rho_{\widehat{X}|Y} - \rho_{\widehat{Y}|X}$, at $L = 500$ as a function of the ratio of the averaged coupling coefficients, $\overline{\eta}_N/\overline{\mu}_N$. (b) Monte Carlo simulation of 1000 independent realizations of (4.11) to calculate $\Delta\rho$ at $L = 500$ as a function of $\overline{\eta}_N/\overline{\mu}_N$. $\overline{\eta}_N$ and $\overline{\mu}_N$ are the mean values of η_N and μ_N over the span of the time–series. Quadrants are shown by the bold lines.

We extend this analysis using the Monte Carlo method. We generate 1000 independent realizations of the coupled system for each $\alpha \in \text{int}[1 : 10]$ (thus, we have 10,000 individual data points) and calculate the difference between the CCM coefficients at $L = 500$. As we observe in Figure 4.4b, $\Delta\rho$ is negative for almost all realizations when $(\overline{\eta}_N/\overline{\mu}_N) < 1$ and positive when $(\overline{\eta}_N/\overline{\mu}_N) > 1$. Note that the distribution of the points on two sides of $(\overline{\eta}_N/\overline{\mu}_N) = 1$ depends on the definitions of η_N and μ_N in (4.11).

The placement of the data points on the first and the third quadrants in Figs. 4.4a and 4.4b shows that CCM can determine the leading system when the coupling coefficients are normally distributed except when $\overline{\eta}_N \approx \overline{\mu}_N$ which means that the leading sub–system is not well–defined.

Referring to (4.8), $\rho(L)$ is obtained by averaging over all possible L-point windows. Thus, one might be concerned whether the difference between ρ values, i.e., $\Delta\rho = \rho_{\widehat{X}|Y} - \rho_{\widehat{Y}|X}$, is statistically significant and meaningful. To address this concern we perform a non–parametric one–sample Kolmogorov–Smirnov test for all data points of Fig. 4.4a. Results of this test, for $\rho_{\widehat{X}|Y}$ and $\rho_{\widehat{Y}|X}$, fail to reject the null hypothesis that the data in vector ρs comes from a standard normal distribution at 0.1% significance level. Next, a group t-test show that for all the data points the obtained t values exceed the required minimum corresponding to a critical *p–value* of 0.01 and therefore we can say that the differences are significant at that level. For example for the smallest absolute value of $\Delta\rho$ in that figure, the calculated t value equals 3.16 which is larger than 2.58 corresponding to 0.01 critical *p–value*. These numerical values correspond to the sample size of the L-point windows at $L = 500$. Therefore, we can reject the null hypothesis (no significant difference between the mean value of ρ).

4.4.3 Case III: Coupled Lorenz systems, normally and non–normally distributed coupling coefficients

For numerical experiments §4.4.1 and §4.4.2, we considered constant and normally distributed coupling coefficients, respectively. In case II, the difference between the two coupling coefficients is also a normal variable because both coefficients are normal variables. In case III to further generalize our study, we break the symmetry of the coupling coefficients by choosing one of them from a normal and the other from a non–normal random distribution. By this selection, the difference between the coupling coefficients is not a normal variable. We set $\eta = \eta_N$ as in §4.4.2 but choose $\mu = \mu_{Wb}$ from Weibull distributions [Rinne, 2008]. As before, each time–series consists of twenty periods with normally distributed length (during each period, the coupling coefficients are constant). The current setting is summarized in (4.12).

$$\begin{cases} k_\eta = 1, k_\mu = 1 \text{ for all periods} \\ \eta = \eta_N = \mathcal{N}(5, 2) \\ \mu = \mu_{Wb} = \text{Weibull}(\alpha, 1.2) \mid \alpha \in \text{int}[1:11] \\ T_i = \mathcal{N}\left(\overline{T} = 10, \sigma = 2\right) \mid i \in \text{int}[1:20] \end{cases} \tag{4.12}$$

Parameters of the Weibull distribution are chosen in order to have sufficient values of $\overline{\eta}_N/\overline{\mu}_{Wb}$ both below and above one. The same reasoning also applies to setting (4.11) of experiment case II. Figure 4.5 shows the asymmetric Weibull probability density function for the parameters of (4.12).

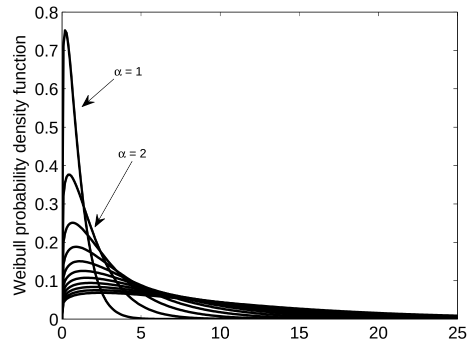

Figure 4.5: **Weibull probability density function for $\alpha \in \textbf{int}[1:11]$ and shape factor equal to 1.2 in 4.12.**

Similar to cases I and II we investigate the $\Delta\rho = \rho_{\widehat{X}|Y} - \rho_{\widehat{Y}|X}$ as a function of $\overline{\eta}_N/\overline{\mu}_{Wb}$ at $L = 500$ (see Fig. 4.6a). Similar to Fig. 4.4a, we observe that $\Delta\rho$ is negative for $(\overline{\eta}_N/\overline{\mu}_{Wb}) < 1$ and is positive for $(\overline{\eta}_N/\overline{\mu}_{Wb}) > 1$ that supports our expectation about the ability of the CCM method to distinguish the leading sub–system.

We employ the Monte Carlo method to generate 1000 independent realizations of the coupled Lorenz systems with setting (4.12) (thus, we have 11,000 individual data points). Then we calculate $\Delta\rho$ for each realization at $L = 500$, shown in Fig. 4.6b. We again observe that $\Delta\rho$ is negative for $(\overline{\eta}_N/\overline{\mu}_{Wb}) < 1$ and positive for $(\overline{\eta}_N/\overline{\mu}_{Wb}) > 1$ except for a small fraction of points around $\overline{\eta}_N/\overline{\mu}_{Wb} \approx 1$ where essentially the leading system is not well–defined. Therefore, CCM can distinguish the leading sub–system in a coupled system with normal/non–normal coefficients, except when the two sub–systems have almost equal coupling coefficients. We also note that in both cases II and III, detection of the leading sub–system is more

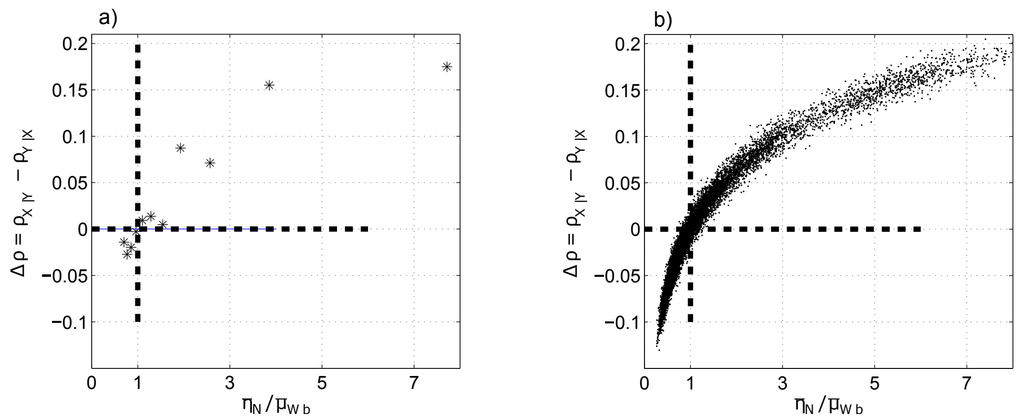

Figure 4.6: **Case III**. (a) $\Delta\rho = \rho_{\widehat{X}|Y} - \rho_{\widehat{Y}|X}$ at $L = 500$ as a function of $\overline{\eta}_N/\overline{\mu}_{Wb}$. (b) 1000 independent realizations of (4.12) and the corresponding $\Delta\rho$ at $L = 500$ as a function of $\overline{\eta}_N/\overline{\mu}_{Wb}$. $\overline{\eta}_N$ and $\overline{\mu}_{Wb}$ are the mean values of η_N and μ_{Wb} over the span of the time–series. Quadrants are shown by the bold lines.

reliable for larger values of $(\overline{\eta}/\overline{\mu})$.

Here in contrast to the case II, we notice a nonlinear relationship between $\Delta\rho$ and $\overline{\eta}_N/\overline{\mu}_{Wb}$, i.e., the rate of change of $\Delta\rho$ decreases rapidly as $\overline{\eta}_N/\overline{\mu}_{Wb}$ increases. Thus, we see a faster saturation in Figure 4.6 compared to Figure 4.4. Also, non–symmetric distribution of the data points around the vertical line $\overline{\eta}_N/\overline{\mu}_{Wb} = 1$ in Fig. 4.6b is due to the range of $\overline{\eta}_N/\overline{\mu}_{Wb}$ according to (4.12), which has a longer tail on the right hand side ($\overline{\eta}_N/\overline{\mu}_{Wb} > 1$). If we plot $-\Delta\rho = \rho_{\widehat{Y}|X} - \rho_{\widehat{X}|Y}$ vs. $\overline{\mu}_{Wb}/\overline{\eta}_N$, we would see a similar trend as in Fig. 4.6b, although some ranges are non overlapping due to asymmetric distribution of the coupling coefficients.

Similar to case II, we repeat the statistical one–sample Kolmogorov–Smirnov and t-test for $\Delta\rho$ values of Fig. 4.6a. In this case, except one data point, which is the closest one to the vertical axis $\overline{\eta}_N/\overline{\mu}_{Wb} = 1$, all other data points have t

values larger than the required minimum corresponding to a critical *p–value* of 0.01. Therefore we can say that the differences are significant at that level and reject the null hypothesis.

4.4.4 Case IV: Coupled Lorenz systems, temporally shifted and noisy signals

In this section, we investigate the ability of the CCM method for detecting the leading system in the presence of chronological uncertainties (temporal uncertainty between the two time–series) and also additive Gaussian white noise. We simulate the chronological uncertainties by relative shifting of the two time–series. We take the signals from case II and III and apply relative shifts of 2.5 and 5% of the full length of the time–series.

For the additive Gaussian white noise we consider a normal random variable with zero mean and standard deviation of 5 and 10% of the standard deviation of the original signals of cases II and III. By this choice, the signal–to–noise ratios (SNR) are equal to 400 and 100 respectively, that show moderate noise levels.

As before, we compute $\Delta\rho$ with respect to the ratio of the averaged coupling coefficients, i.e. $(\overline{\eta}/\overline{\mu})$, for different conditions. Results of the experiments with chronological uncertainties and additive noise (see Figs. 4.7 and 4.8) show the same features of Figs. 4.4a and 4.6a. For example $\Delta\rho$ is negative when $(\overline{\eta}/\overline{\mu}) < 1$ and positive when $(\overline{\eta}/\overline{\mu}) > 1$ with few exceptional data points in each figure that are close to $(\overline{\eta}/\overline{\mu}) = 1$. Also, we observe almost linear distribution of the data points in Figs.

4.8a and 4.8a similar to the results of case II, Fig. 4.4a, and nonlinear distribution of the data points in Figs. 4.8b and 4.8b similar to case III, Fig. 4.6a. These results show that the CCM results are robust to the imposed temporal uncertainties and additive white noise especially for larger ratio of the coupling coefficients.

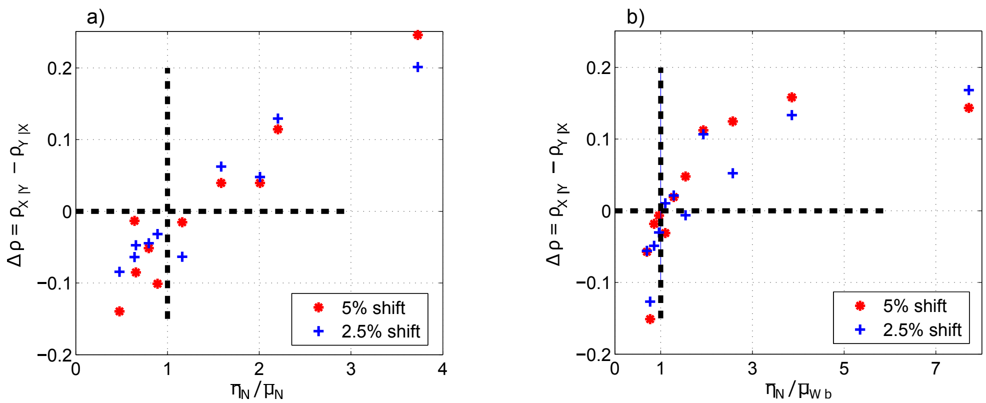

Figure 4.7: **Case IV. The experiments with temporal uncertainties**. (a) $\Delta\rho$ at $L = 500$ as a function of $\overline{\eta}_N/\overline{\mu}_N$ for shifted signals of case II. (b) $\Delta\rho$ at $L = 500$ as a function of $\overline{\eta}_N/\overline{\mu}_{Wb}$ for shifted signals of case III. Quadrants are shown by bold lines.

4.5 Summary

There is general interest in determining causal relationship between variables of a physical system. Therefore, establishing a method for causality analysis is of paramount importance [Pearl, 2000]. Linear lead–lag analysis is commonly applied to underpin causal relationship when there are some evidences about the internal mechanisms of the system. But quite frequently, two signals show inconsistent lead–lag behavior in different time windows due to nonlinearities of the system. Therefore,

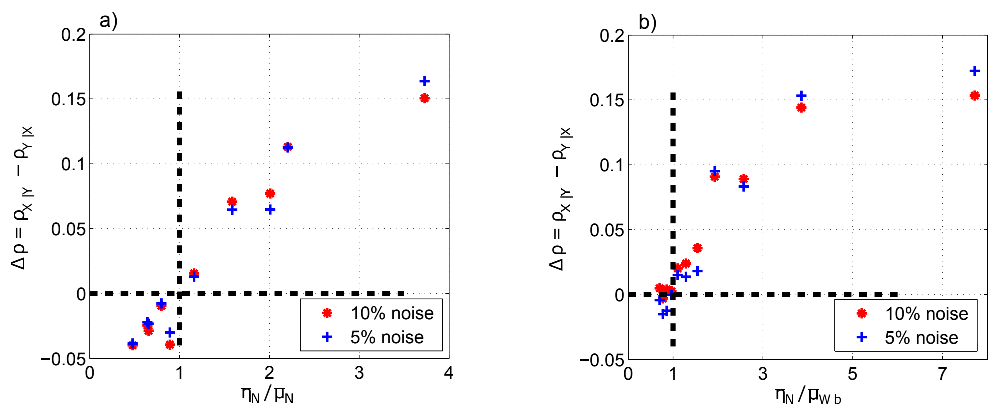

Figure 4.8: **Case IV. The experiments with two levels of additive Gaussian noise**. (a) $\Delta\rho$ at $L = 500$ as a function of $\overline{\eta}_N/\overline{\mu}_N$ for signals of case II. (b) $\Delta\rho$ at $L = 500$ as a function of $\overline{\eta}_N/\overline{\mu}_{Wb}$ for signals of case III. Quadrants are shown by bold lines.

this method can not conclusively determine causality over the full time span of observed signals. Introducing Granger causality [Granger, 1969] was a turning point in that field. Granger proposed his practical method based on Wiener's definition of causality that is founded on the idea of predictions of a variable both with and without a candidate driver. If forecast is significantly improved when the information of candidate driver is included in the set of predictors, the Granger method concludes that the candidate signal is a driver. The concept of information transfer and transfer entropy as a measure of directional communication between elements of a system [Schreiber, 2000] was an important achievement that opens the door to many practical causality investigations. Later, it was found that Granger causality and transfer entropy are equivalent for Gaussian variables [Barnett et al., 2009]. Although information transfer measures provide important understanding about the directional interconnections of a system, they do not identify true instantiated causal relationship in a system. It was shown that interventional methods and information flow are the appropriate concept and measure to identify micro–level causal relationships [Lizier and Prokopenko, 2010].

Sugihara et al. [2012] proposed a new idea about causality analysis applicable to deterministic nonlinear systems based on cross convergent mapping between shadowing manifolds. They successfully applied the CCM method to analyze causality in weakly coupled systems with constant coupling coefficients.

This study was inspired by identifying the leading element in systems that are speculated to have time–varying internal connections with probable change of dominant sub–system in different periods (e.g., the global climate and the earth system that has several interconnected sub–systems). For the first time, we addressed applicability of the CCM method to coupled systems with time–varying coupling coefficients and switching between dominant elements in different periods. We conducted four sets of numerical experiments: I) periodic–constant coupling coefficients, II) normally distributed coupling coefficients, III) mixed normally and non–normally distributed coupling coefficients and IV) imposed temporal uncertainties and additive noise to the observed time–series of cases II and III. We investigated whether the CCM method can identify the leading sub–system that has a larger average coupling coefficient over the entire span of the time–series.

Our main conclusions are:

1. If the averaged coupling coefficients are not approximately equal, i.e., $\overline{\eta} \not\approx \overline{\mu}$,

and a leading system exists, then the CCM coefficient of the leading system is significantly larger than the CCM coefficient of the system with a smaller average coupling coefficient.

2. If the ratio of the average coupling coefficients is close to one ($\overline{\eta}/\overline{\mu} \approx 1$), the leading system is not well–defined and the CCM method is not applicable.

3. The CCM results are quite robust to temporal uncertainties and also moderate level additive Gaussian noise.

4. For normally distributed coupling coefficients (case II), a [close to] linear relationship between $\Delta\rho$ and the ratio of the average coupling coefficients is observed (in the range of the selected coefficients).

5. For mixed normally and non–normally distributed coupling coefficients (case III), a nonlinear relationship between $\Delta\rho$ and the ratio of the average coupling coefficients is observed (in the range of the selected coefficients).

According to these observations, we conclude that when the ratio of the average coupling coefficients is not close to one, the CCM method can detect the leading sub–system in a set of two coupled systems with time–varying coupling coefficients — even in the presence of chronological uncertainties or additive Gaussian noise. We anticipate the CCM method can be applied in atmospheric science, biology, ecology, epidemiology, and sociology.

Acknowledgments

We greatly benefited from many discussions with Professors James Yorke, Brian Hunt and Shane Ross. We thank the reviewers for their insightful comments and suggestions.

Author Contributions

Conceived and designed the experiments: AEBM SM SGP EK. Performed the experiments: AEBM SM SGP EK. Analyzed the data: AEBM SM SGP EK. Contributed reagents/materials/ analysis tools: AEBM SM SGP EK. Wrote the paper: AEBM SM SGP EK.

Chapter 5: Climate model shows large-scale wind and solar farms in the Sahara increase rain and vegetation

Wind and solar farms offer a major pathway to clean, renewable energies. However, these farms would significantly change land surface properties, and, if sufficiently large, the farms may lead to unintended climate consequences. In this study, we used a climate model with dynamic vegetation to show that large-scale installations of wind and solar farms covering the Sahara lead to a local temperature increase and more than a twofold precipitation increase, especially in the Sahel, through increased surface friction and reduced albedo. The resulting increase in vegetation further enhances precipitation, creating a positive albedo–precipitation–vegetation feedback that contributes ~80% of the precipitation increase for wind farms. This local enhancement is scale dependent and is particular to the Sahara, with small impacts in other deserts. [1]

[1] This chapter was published following peer-review as: Yan Li, Eugenia Kalnay, Safa Motesharrei, Jorge Rivas, Fred Kucharski, Daniel Kirk-Davidoff, Eviatar Bach, and Ning Zeng. Climate model shows large-scale wind and solar farms in the Sahara increase rain and vegetation. *Science*, 361(6406):1019–1022, September 2018.

Editor's Summary: More energy, more rain

Energy generation by wind and solar farms could reduce carbon emissions and thus mitigate anthropogenic climate change. But is this its only benefit? Li *et al.* conducted experiments using a climate model to show that the installation of large-scale wind and solar power generation facilities in the Sahara could cause more local rainfall, particularly in the neighboring Sahel region. This effect, caused by a combination of increased surface drag and reduced albedo, could increase coverage by vegetation, creating a positive feedback that would further increase rainfall.

Main Text

Limiting global warming to 2°C is essential for mitigating excessive damages from climate change [McGlade and Ekins, 2015; Shindell et al., 2016; Seneviratne et al., 2016]. Major global efforts and long-term policies are needed to attain the corresponding level of decarbonization [Motesharrei et al., 2016; Jakob et al., 2014; Millar et al., 2017]. Renewable energy sources such as wind and solar power have become viable options (7) because of their abundant supply and wide availability on Earth [MacDonald et al., 2016; Barthelmie and Pryor, 2014]. Extracting a small fraction of the solar and wind energy available on Earth would be more than enough to meet the total global demand of energy in all forms. This opens the possibility of powering the world entirely with wind and solar energy, which is possible and has been discussed in the literature [Miller et al., 2011; Hu et al., 2016; Lu et al., 2009;

Marvel et al., 2013].

To substitute for the fossil fuels that currently still dominate worldwide electricity generation, as well as transportation, heating, and industrial energy demands, more large-scale wind and solar farms would need to be installed throughout the world. The installed wind turbines and photovoltaic panels would cover the land and modify land surface properties (in particular, surface roughness and albedo, respectively) and, if large enough, could have unintended consequences on local and regional climate [Roy et al., 2004; Hernandez et al., 2014; Zhou et al., 2012]. Previous modeling studies have shown that large-scale implementation of wind and solar farms can produce significant climate change at continental scales [Hu et al., 2016; Keith et al., 2004]. However, in those studies, vegetation is prescribed rather than dynamic — that is, either vegetation types and properties do not respond to the changing climate caused by the large wind and solar farms or the vegetation changes do not feed back onto climate. The lack of vegetation feedbacks could make the modeled climate impacts very different from their actual behavior [Wang and Eltahir, 2000a,b], as vegetation dynamics [e.g., albedo, evapotranspiration, roughness, and leaf area index (LAI)] have been proven to play a key role in the land-climate interaction [Zeng et al., 1999]. Vegetation feedbacks can either enhance or suppress the initial climate changes triggered by land change [Kucharski et al., 2013; Zeng and Yoon, 2009].

In our study, we used a climate model with dynamic vegetation to investigate the climate impacts of large-scale wind and solar farms installed in the world's largest deserts. We primarily focused on the effect of such large wind and solar farms in the Sahara region (including the most arid parts of the Arabian Desert) and the neighboring Sahel region for several reasons: (i) The Sahara is the largest desert in the world and has a great supply of solar and wind energy. (ii) The Sahara is sparsely inhabited, and thus the development of wind and solar farms would have minimal competition for land surface area against natural and other human land uses, such as agriculture [Hernandez et al., 2014]. (iii) The Sahel is a transition region between desert and wooded savanna and, as such, is highly sensitive to land changes [Wang and Eltahir, 2000a,b; Charney, 1975]. (iv) Both regions are near Europe and the Middle East, areas with enormous current energy demand, and sub-Saharan Africa, which has a large projected growth in energy demand (see supplementary text). (v) Massive investment in solar and wind generation could promote economic development in the Sahel, one of the poorest regions in the world, as well as provide clean energy for desalination and provision of water for cities and food production [Battisti and Naylor, 2009]. The wind and solar farms simulated in this study would generate approximately 3 and 79 TW of electrical power, respectively, averaged over a typical year (see supplementary text).

Our results show that the effects of the large-scale wind and solar farms in the Sahara are most significant locally — i.e., at or near the locations of wind and solar farms — with limited remote impacts (Fig. 1). The wind farm causes significant regional warming on near-surface air temperature (+2.16 K), with greater changes in minimum temperature than maximum temperature (+2.36 versus +1.85 K) (fig. S1). This asymmetric temperature impact has been reported in both empirical [Zhou et al., 2012] and modeling studies [Roy et al., 2004; Vautard et al., 2014].

The greater nighttime warming takes place because wind turbines can enhance the vertical mixing and bring down warmer air from above to the lower levels, especially during stable nights [Roy et al., 2004; Roy and Traiteur, 2010]. Wind farms also increase precipitation as much as +0.25 mm/day, averaged over areas with wind farm installations, which results in the doubling of precipitation compared with the control experiment (0.24 mm/day), particularly in the Sahel region, which features an average increase of +1.12 mm/day (table S1). This is because the increased surface friction reduces wind velocity and the associated Coriolis force, which leads to a more dominant pressure gradient force toward the Saharan heat low that is enhanced by the warming induced by wind farms. This produces surface convergence and upward motion as well as moisture convergence and higher humidity (figs. S3 to S5). The increase in precipitation, in turn, leads to increases in vegetation cover fraction (+0.084), LAI (+0.50 m2/m2), and root carbon (+0.08 kgC/m2) that further reduce surface albedo (figs. S2 and S5). These changes together trigger a positive albedo–precipitation–vegetation feedback (21, 22). Additionally, the recovered vegetation increases evaporation, surface friction, cloud cover (fig. S3), and consequently, precipitation. The increased evaporation, which partially compensates the increased net surface solar radiation, also plays an important role in local precipitation enhancement (21). A slight cooling is observed in the wetter Sahel region because recovered vegetation increases evaporation and decreases sensible heat flux. As expected, the increased drag at the surface due to wind turbines reduces wind speed by ~36% (fig. S1).

Impacts of solar farms on temperature and precipitation are markedly sim-

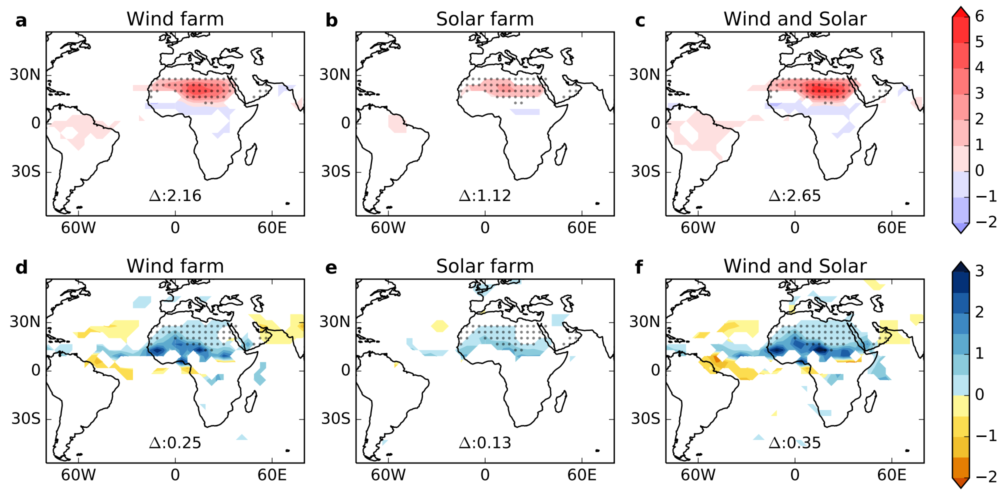

Figure 5.1: Impacts of wind and solar farms in the Sahara on mean near-surface air temperature (kelvin) and precipitation (millimeters per day). The impacts of wind farms (A and B), solar farms (C and D), and wind and solar farms together (E and F), respectively, are shown. Only areas where changes are significant at the 95% confidence level (t test) are displayed on the map. Gray dots denote the location of wind and/or solar farms. At the bottom of each plot, the number after Δ represents the changes in climate (in either kelvin or millimeters of precipitation per day) averaged over areas covered by wind and solar farms.

ilar to those of wind farms in terms of spatial patterns. This is because solar panels directly reduce surface albedo and thus trigger a similar positive albedo–precipitation–vegetation feedback to that of wind farms, and this feedback leads to temperature and precipitation increase. The resulting warming is stronger in maximum temperature (+1.28 K) than in minimum temperature (+0.97 K) because albedo reduction mainly affects net radiation during daytime (fig. S1). Compared with the control experiment, a 50% increase in precipitation (+0.13 mm/day) is observed in solar farm locations in the Sahara, and an increase of +0.57 mm/day is recorded in the Sahel (table S1). Unlike the wind farm experiment, the solar farm experiment produces very little change in wind speed (fig. S1).

When wind and solar farms are deployed together in the Sahara, changes in climate are enhanced. The precipitation in the Sahara increases from 0.24 mm/day in the control run to 0.59 mm/day in the case of combined wind and solar farms, a ~150% increase, whereas the temperature increase (+2.65 K) is only slightly larger compared with that for the solar farm alone. Although the absolute amount of precipitation change averaged over the entire Sahara is low from these experiments (up to +0.35 mm/day for the combined wind and solar farms), it should be emphasized that the precipitation impact is not uniform across space. The most substantial precipitation increase occurs in the Sahel, with a magnitude of change between +200 to +500 mm/year (table S1), which is large enough to have major ecological, environmental, and societal impacts.

Our simulations show that both the wind and solar farms in the Sahara contribute to increased precipitation, especially in the Sahel region, through the positive albedo–precipitation–vegetation feedback. This positive feedback is established through different mechanisms for wind and solar farms. For wind farms, the higher surface roughness strengthens low-level convergence, leading to precipitation increase in the Sahara [Sud and Smith, 1985]. For solar farms, the decreased albedo associated with solar panels (i.e., the lower effective albedo of solar panels compared with the sand in the Sahara) results in more absorption of solar radiation and, hence, surface warming, which leads to low pressure at the surface, as well as convergence, rising motion, and consequently, more precipitation [Charney, 1975; Charney et al., 1977]. The precipitation increase induced by either wind or solar farms, in turn, increases vegetation cover and LAI, leading to further reduction in albedo and increase in roughness, both of which help organize the moisture convergence that drives the change in precipitation. These friction–precipitation–vegetation feedbacks (wind farms) and albedo–precipitation–vegetation feedbacks (wind and solar farms) are known as the Sud [Sud and Smith, 1985] and Charney mechanisms [Charney, 1975; Charney et al., 1977], respectively. To quantify the contribution of these two mechanisms, we carried out additional wind farm experiments in which both mechanisms are present that can separate the climate changes induced by the initial roughness and the subsequent albedo changes due to vegetation feedback (Fig. 2). We found that for the temperature change, roughness and vegetation feedback contribute almost equally (+1.00 versus +1.16 K). The roughness-induced warming occurs because wind reduction weakens the near-surface vertical turbulence transport [Wang and Prinn, 2010]. In contrast, for precipitation change, 80% of the increase (+0.20 mm/day) comes from vegetation feedback, whereas roughness plays only a secondary role, except as an initial trigger. These results suggest that the absence of vegetation feedback in the model [Wang and Eltahir, 2000a,b] would considerably underestimate the temperature and precipitation impacts of the large-scale wind farms in the Sahara.

Although wind and solar farms both enhance precipitation in our experiments,

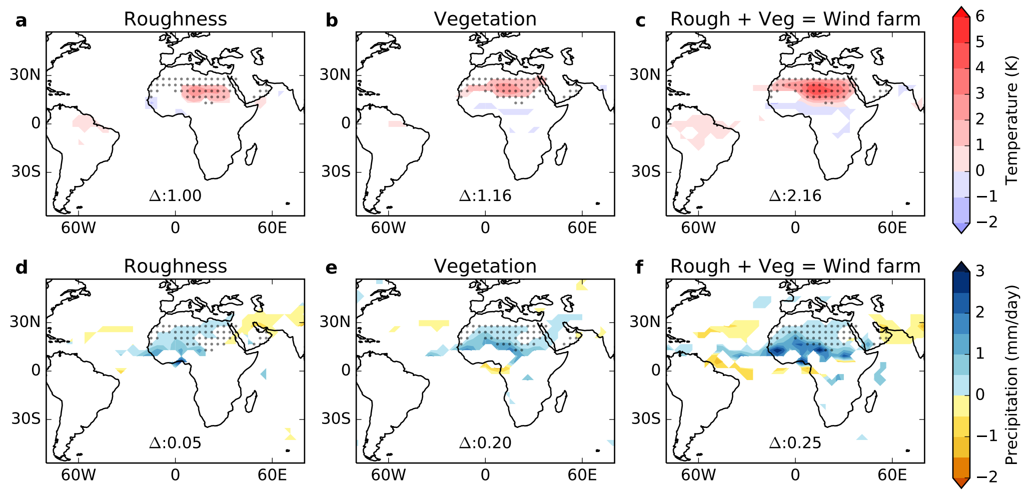

Figure 5.2: Relative contributions of roughness change (Rough) and vegetation feedback (Veg) in the climate impacts of wind farms in the Sahara. Contributions in the temperature (A, C, and E) and the precipitation (B, D, and F) impacts are shown. The wind farm impact is produced by the initial roughness of wind turbines and the subsequent albedo changes due to vegetation feedback. At the bottom of each plot, the number after Δ represents the changes in climate (in either kelvin or millimeters of precipitation per day) averaged over areas covered by wind farms.

solar farms will not necessarily always increase precipitation through albedo changes. The direction of precipitation change is largely determined by the sign of the albedo change before and after a solar farm is installed. More specifically, it depends on the conversion efficiency of the solar panel and the background environment albedo. The precipitation increase in our solar farm experiments is due to the relatively low conversion efficiency of the panels (15%, typical current conversion efficiency for photovoltaic panels), which results in albedo decrease (See Supplementary Materials). However, if solar panel efficiency and the associated effective albedo are high enough to lead to an albedo increase relative to the background environment (as, for example, a 45% efficiency would), the climate impact would be surface cooling with precipitation suppression (fig. S6), similar to the impact of overgrazing in the desert [Charney, 1975]. Assuming an intermediate conversion efficiency higher than 15% for solar panels (e.g., 30% efficiency) results in negligible albedo change and, thus, insignificant climate impacts (fig. S6).

In this study, we used a model running at a relatively coarse spatial resolution to simulate the impact of wind and solar farms. However, the model has been shown to be capable of capturing the large-scale impacts from changing albedo, roughness, and vegetation responses [Zeng et al., 1999; Kucharski et al., 2013; Zeng and Yoon, 2009; Li et al., 2016a] and has skills comparable to those of other higher-resolution models in simulating modern climate and multidecadal variability in this region in multiple model intercomparison projects [Scaife et al., 2009; Xue et al., 2016]. Still, uncertainties remain in the magnitude of climate response and the strength of vegetation feedbacks. The complexity of a global model also limits its ability in capturing the impacts on synoptic and mesoscale weather processes. It is not clear if all of our findings are directly applicable to wind and solar farms with a size much smaller than the model grid. Nevertheless, the temperature impacts of wind and solar farms in our study (i.e., the warming effect of wind farms and the albedo-dependent impact of solar panels) are consistent with those reported in studies conducted at the local scale [Millstein and Menon, 2011; Taha, 2013]. For the precipitation change, the impact is more uncertain due to its region-specific and scale-dependent nature. We addressed these uncertainties by designing additional experiments (see Supplementary Materials). We found that expanding the wind and solar farms from the Sahara to the world's other deserts does not significantly increase the climate impact (fig. S7). The most significant impact is still concentrated in the Sahara and the surrounding regions, whereas the impact is not significant in many other deserts, due to their scattered geographical distributions, smaller sizes, and weaker changes in albedo (fig. S8). Even in the Sahara, the wind and solar farms impacts also depend on their specific location and spatial distribution, with uneven impacts when deployed with different spatial configurations (i.e., the "checkerboard" and "quarter" wind farm experiments represented in fig. S9). Therefore, to assess the impacts of smaller-scale wind and solar farms installed at specific locations, further studies are required, especially those using more advanced global and regional climate models with higher spatial resolutions [Vautard et al., 2014].

Our results obtained from experiments performed with a climate model suggest that, for installations of wind and solar farms with current conversion efficiency in the desert at a scale large enough to power the entire world, the impacts on regional climate would be beneficial rather than detrimental, and the impacts on global mean temperature are still small compared with those induced by CO_2 emission from fossil fuels [Seneviratne et al., 2016; Hu et al., 2016]. If carefully planned, these farms could also trigger more precipitation, largely because of a previously overlooked vegetation feedback. This highlights that, in addition to avoiding anthropogenic greenhouse gas emissions from fossil fuels and the resulting warming, wind and solar energy could have other unexpected beneficial climate impacts when deployed at a large scale in the Sahara, where conditions are especially favorable for these impacts. Efforts to build such large-scale wind and solar farms for electricity generation may still face many technological (e.g., transmission, efficiency), socioeconomic (e.g., cost, politics), and environmental challenges, but this goal has become increasingly achievable and cost-effective [Wu et al., 2017] (supplementary text). These results indicate that renewable energy can have multiple benefits for climate and sustainable development and thus could be widely adopted as a primary solution to the challenges of global energy, climate change, and environmental and societal sustainability [Motesharrei et al., 2016].

Acknowledgments

We thank the University of Maryland and the Univ. of Illinois for supercomputing resources—in particular, the Deepthought2 (http://hpcc.umd.edu) and Bluewaters (www.ncsa.illinois.edu/enabling/bluewaters) supercomputers—made available for conducting the research reported in this paper. We also thank three anonymous reviewers for constructive comments.

Funding

Y.L. acknowledges support from the National Key R&D Program of China (no. 2017YFA0604701). E.K. and S.M. acknowledge Lev Gandin funding (grant 2956713) provided by G. Brin.

Authors contributions

E.K., Y.L., and S.M. conceptualized the study; Y.L., E.K., S.M., F.K., and J.R. designed the experiments; Y.L. and E.B. performed the model simulations; F.K., N.Z., and Y.L. developed the UMD–ICTP model version used in this study; Y.L., E.K., S.M., and F.K. analyzed the data, with contributions from other co-authors; and Y.L., S.M., E.K., F.K., and J.R. wrote the manuscript, with discussions and contributions from other co-authors.

Competing interests

D.K.-D. is a lead research scientist at AWS Truepower, whose work involves forecasting renewable generation for grid operators.

Data and materials availability

The model simulation data are available at Figshare [Li, 2018].

Chapter 6: Conclusion and Future Directions

In this dissertation, I presented a suite of mainly published research papers that employ methods from various fields of science, including Systems Science and Dynamic Modeling, to investigate the effects of feedbacks in coupled systems. The problems we investigated aim to address the sustainability challenges of the environment and society, especially the grand challenges of the Energy–Water–Food Nexus [Biggs et al., 2015; Bazilian et al., 2011; Conway et al., 2015].

Chapter 5 showed extremely beneficial precipitation and vegetation impacts of large-scale wind and solar farms in the Sahara. Their beneficial impacts on rainfall are summarized below in Figures 6.1 and 6.2. Such innovative solutions offer promising directions for addressing sustainability and climate challenges that our planet and society are facing.

Potential future directions for the work presented in this dissertation could be to:

1. develop the Energy Model, based on the framework established in HANDY2 (see Appendix C;
2. include the aerosol feedback in the coupled Climate–Vegetation model to investigate the effect of this feedback on the Sahara wind and solar farms results;

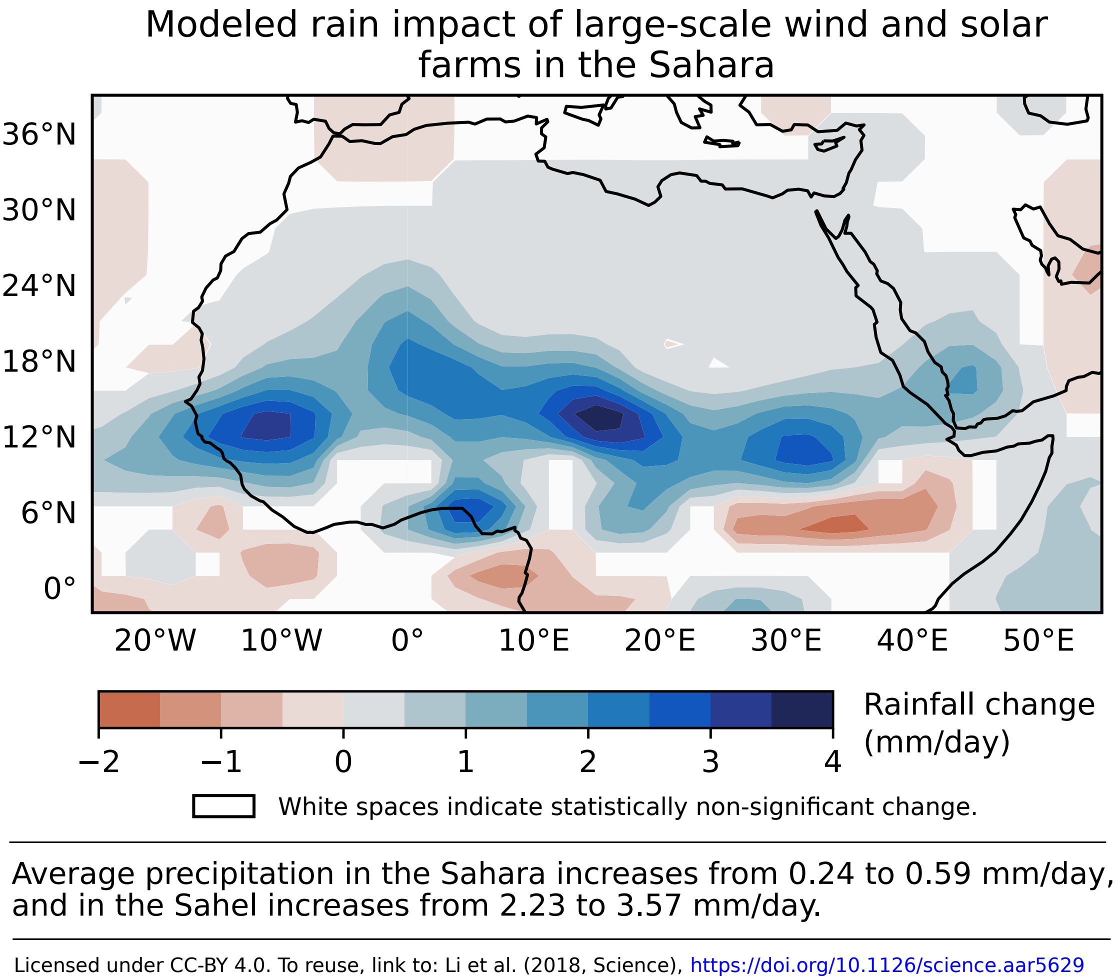

Figure 6.1: Summary of beneficial rain impacts of large-scale wind and solar farms in the Sahara. Average precipitation in the Sahara increases from 0.24 to 0.59 mm/day, and in the Sahel increases from 2.23 to 3.57 mm/day [Li et al., 2018].

3. include the effect of additional vegetation cover on land surface friction;

4. continue the Sahara simulations to find whether these wind and solar farms might be able to trigger the return of the Sahara to its "Green Sahara" state [Brovkin et al., 1998];

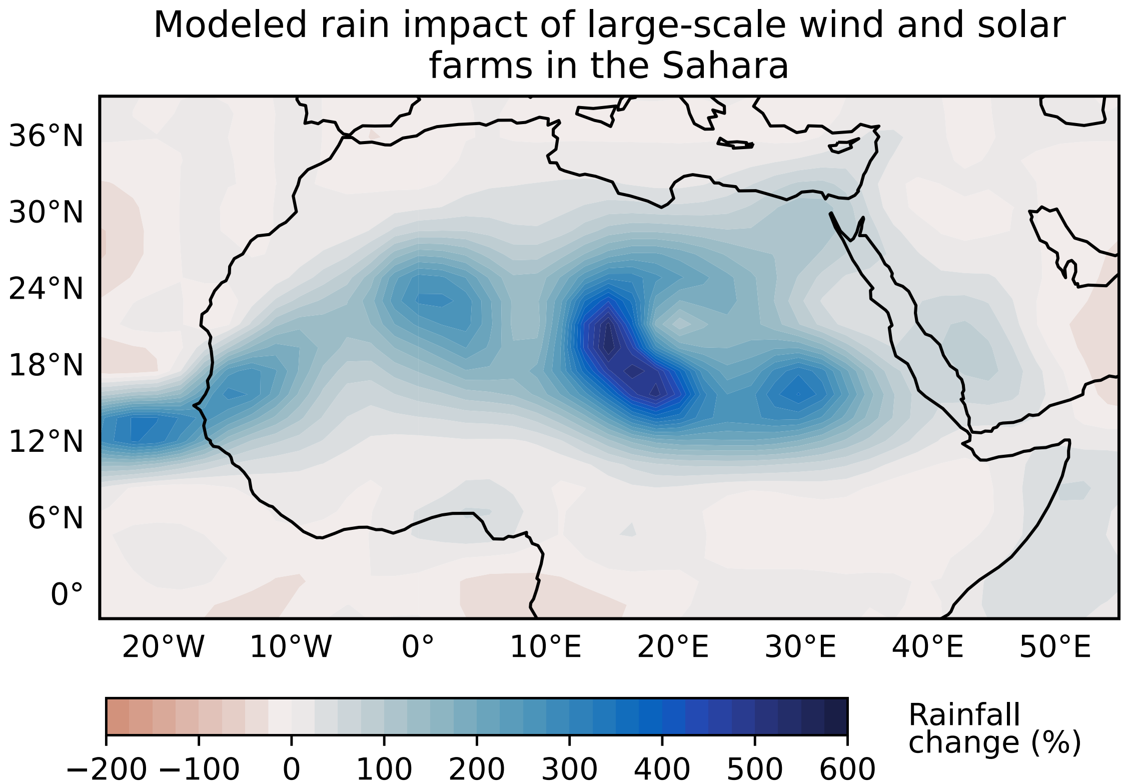

Figure 6.2: Summary of relative change in precipitation as a result of large-scale wind and solar farms in the Sahara. In the tropical region to the southeast of Sahel where absolute decreases in precipitation can be up to 2 mm/day (see Fig. 6.1), the relative precipitation change is negligible [Li et al., 2018].

5. develop a dynamic model for Agriculture and Food production, distribution, and consumption;

6. develop a macroeconomic model for each of these sectors;

7. couple UMD–ICTP climate–vegetation model, COWA (Water), Energy, and Agriculture models, together with macroeconomic model, initially for one re-

gion;

8. eventually couple the full model for multiple regions to include trade (and virtual trade) and investigate the sustainability of each sector, and the full Earth–Human System, in each region, country, and globally.

Recent research has integrated biodiversity into a coupled human population and natural resource model with feedbacks, highlighting the dangers of delayed action to preserve the ecosystems [Lafuite and Loreau, 2017; Lafuite et al., 2017, 2018]. Henderson and Loreau [2018] developed a minimal dynamic model to investigate the effects of feedbacks among agricultural land use, human population, and biodiversity. Another group of researchers have, for the first time, developed a dynamic human population model for an advanced ESM, Community Earth System Model (CESM) [Navarro et al., 2017, 2018].

A key goal of such scientific and modeling effort is to detect signals about the health and stability of these systems years and decades before potential catastrophes endanger their survival. Work presented in this dissertation aims to show possible explorations in that direction. Naturally, it is just a beginning of a long, curvy path to understand and address a wide range of global environmental and social problems, and to explore possible innovative solutions, such as massive wind and solar farms. These models will allow us to propose, design, test, and improve science-based policies that direct the system onto a sustainable path — to ensure a healthy environment and a prosperous, productive life for current and future generations.

Appendix A: Supplementary Information for COWA: a Two-way Coupled Human–Climate–Water Model to explore water management options

A.1 Further thoughts and notes by Jorge Rivas and Safa Motesharrei

Another major finding emphasized in this paper is that our model shows that public policies are fundamental to water resource management and furthermore that these policies can be very successful. [See notes about Somalia. The Somalia case shows that the lack of policies can be disastrous.]

Draft of Brief paragraph on Arizona water policies and the sources of success:

In contrast to other basins, such as California's Central Valley list others where groundwater stocks have declined substantially, groundwater stocks in the Phoenix AMA have not been declining. The fundamental reasons for the success of groundwater management in the Phoenix AMA are the public water management policies explicitly designed to reduce groundwater withdrawals and artificially recharge groundwater stocks. Artificial recharge is a means of storing currently available excess water supplies to be used in the future. Artificial recharge has become a critical component of Arizona's water supply management, driven by the need to meet the targets of the 1980 Groundwater Management Code and many other state and local statutes and policies, including the Underground Water Storage and Recovery program established in 1986 and the Underground Water Storage, Savings, and Replenishment Act (UWS), enacted in 1994 by the Arizona Legislature. The recharge management policies and programs are administered by Arizona Department of Water Resources.

These policies are designed to store current excess flows of water underground through artificial recharge in order to replenish over-withdrawal and ensure an adequate supply for the future. Both the geology and desert environment of Arizona makes artificial recharge of water underground both practical and cost-effective. The current excess flows that are used for this artificial recharge themselves are also a product of other policies and programs. Arizona is allotted X quantity of water, through the CAP, which is diverted from the Colorado river system located outside the basin and channeled to the basin by X kilometers of artificial canal.

Brief overview Paragraph of the policies:

Without these past policies, Arizona would not be have been able to sustain even the population it currently has, much less an expanded population in the future. For decades in Arizona groundwater was pumped from aquifers at higher rates than naturally recharged back into the underground stocks, significantly depleting many of the aquifers. As early as the 1950s groundwater depressions had developed due to well extraction exceeding natural recharge depleting groundwater stocks. In order to meet the challenges of this imbalance, state and local governments responded with policies to artificially recharge groundwater stocks using both artificial flows from outside the region as well as diversion of treated wastewater back to into the aquifers using artificial recharge. The water is artificially recharged using Percolation Basins (depressed areas of land specifically designed to hold water over a permeable substrate causing the water to percolate back into the ground to recharge groundwater stocks) and Injection Wells(wells constructed specifically for the purpose of injecting water back into the aquifer). Water use policies have also been designed to encourage the use of renewable flows for direct usage rather than rely on non-renewable stocks for direct usage. These recharge and usage policies are combined with policies to encourage higher efficiency in water use, reduced leakage and waste, and a transition away from higher-water intensity to lower-water uses in economic activities and in residential design. The Phoenix AMA is mandated by these policies to combine efficient water uses with decreased groundwater withdrawals to be replaced by the increased use of renewable water supplies in order to reach safe-yield levels by the year 2025.

Compare with the San Joaquin valley per capita water usage rates (and maybe compare with average for the US).

Another example of how important policies are: Explain in the text of the paper that governments have created the infrastructure and policies that divert a certain amount of water from other regions to Arizona ("CAP" and "incidental") and that furthermore Arizona has enacted policies and infrastructure that use this excess water to recharge GW levels. This is a very successful policy that is the opposite of what is happening most elsewhere in the world where GW levels are being rapidly depleted (citations to literature).

Compare California's rapidly declining GW levels with Arizona's increasing GW levels. This emphasizes how different policies can produce such different results in two neighboring states, and also that the California water situation is unsustainable.

Also, if possible, it would help to show a comparison of % of California water obtained from GW vs. from SW, and compare this with the Arizona %s. This would also address whether the recent return of precip to Calif "solves" the water crisis or whether California is essentially living off of GW depletion, which cannot go on for ever.

If the California Central Valley per capita usage rates are significantly higher than Arizona, then it would be really interesting to run the Arizona COWA model with California Central Valley per capita usage rates to show how important reducing per capita rates has been for Arizona and also how important this is for the effects in the future if they used as much per capita as Calif (i.e., GW depletion and population decline much sooner). In fact, it might be interesting to try to obtain California Central Valley water usage rates (where Ag-water usage is very high), and also run the Arizona model using those. This would show how much sooner the limits would be reached if per capita rates in Arizona were those of a high-Ag region. Also, Ariz and Calif are right next to each other, and both are relatively water-scarce regions, so they are meaningful comparisons (i.e., it's not as if we were comparing Arizona with Bangladesh or the Amazon).

This shows that water is a local spatial scale issue. Looking at averaged data for a larger region could be misleading, and becomes almost meaningless at large scales, such as the whole US.

Including all these California comparisons will dramatically increase the importance, relevance and urgency of the implications of the model and will also make the paper a natural step towards doing the California model. It will also point out that although the precipitation returned to California, the water crisis is not over.

If Arizona is not a high Agricultural producing state, then we are essentially modeling a human consumption water model, whereas in most places Ag is the main consumer of water. Compare with Calif.

Also: Is it the case that Arizona used to produce more high-water using Ag but that it has shifted away from that and this has played a role in reducing per capita consumption? [we should find out]. If so, we should point this out too.

The important implication of this is to point out that Arizona is importing part of its water usage through its imports of Ag products (i.e., they are exporting their water footprint). This is not possible everywhere because food has to be produced somewhere.

Storing excess flow in reservoirs (above or below ground) does not increase the long-term Water Carrying Capacity of the region. But In cases like Somalia, it does significantly increase the resilience of the region to severe short- to medium-term droughts.

In conflict-ridden regions such as Somalia, underground reservoirs would be less susceptible to destruction.

(These last two points will go into the short Nature/Science paper for Somalia.)

Add that Phoenix AMA does not have a large Ag sector, as opposed to Central Valley. This means it receives virtual water imports via its food imports.

Going deeper in the ground for water becomes more expensive with depth, hence many of the farms in CA, and even a whole town, went bankrupt due to the expense of reaching the lower GW depths.

In the Phoenix AMA, Ag water consumption has gone down despite growing population. But that means the water is being virtually imported through food products.

This reduction in per capita consumption is not reproducible in other areas because the reduction is dependent on the fact that urbanization in the Phoenix AMA has displaced the most water intensive economic activity, i.e., Ag activity.

Other points raised by Lenny Konikow: Higher costs and lower withdrawal rates as the wells go deeper. As GW goes lower, the withdrawals are automatically curtailed due to the increased difficulty.

Tragedy of the Commons (or Prisoner's Dilemma) explains the lack of incentives for the farmers to conserve GW, since neighboring farms will take the GW regardless.

Fights between states, e.g., Mississippi and Alabama, Colorado and Arkansas, over water rights.

A.2 Introduction

Over the last two centuries, the impact of the Human System has grown dramatically, becoming strongly dominant within the Earth System in many different ways. Both population and per capita consumption have grown rapidly, especially since about 1950, putting tremendous pressure on natural resources. The changes in the Earth System have important feedback effects on the Human System. However, current models that project the future of resources and humanity do not include such feedbacks, even though they exist in reality. Following the framework proposed in Motesharrei et al. [2016], we have developed a model by coupling Freshwater and Human Systems with bidirectional feedbacks.

The Earth's natural freshwater resources are expected to meet the supply needs of the natural environments and human societies surrounding them. The perceived value of water by its users is much higher in rain-fed, water-scarce or undeveloped regions, where readily accessible potable water is limited, while the perceived value is much lower in water-rich or developed regions, where water accessibility is less difficult. Regardless of its perceived value, water resources are intrinsically valuable as water is a fundamental necessity for many important natural functions (e.g., climate, weather, soil dynamics, photosynthesis, etc.), basic human needs (e.g., hygiene, sanitation, hydration, etc.), and societal development needs (e.g., energy production and cooling, irrigation, manufactured goods production, recreational uses, etc.). Sustained access to freshwater can dictate the success or collapse of a natural environment or human society. Therefore, the sustainable management of the regional water supply has huge implications on human well being and productivity.

In order to efficiently, effectively and responsibly control water supply, it is necessary to understand paths and flows of the supply/demand system which straddles both natural and human elements. However, the natural-human water system is a very complex system and therefore, simplified models can help assess applied experiments with such complex systems which would otherwise be unimplementable.A simplification of complex systems may lessen the model's ability to capture point-by-point precision, allows for the ability to realistically capture long-term behavioral trends. Further, model experimentations provide insight towards the system's reactions to hypothetical scenarios of changes in policy or climate. The bidirectionally coupled natural-human modeling structure shows significantly different projections for population growth than uncoupled model projections, suggesting further analysis of current modeling practices.

A.2.1 Problem Statement

Over the past few decades, an increase in global water resource awareness [United Nations, 1992, 2003; Food and Agriculture Organization, 2007; World Bank, 2008a,b; United Nations, 2009; UNEP, 2012; Food and Agriculture Organization, 2013; United Nations, 2013a, 2015a] has driven national concern (cite GAO, EPA, DOE, ACE) for regional freshwater sustainability and sparked a wave of studies at the local level as well (cite 1, 2, 3, 4). However, there has been no clear consensus over how to move forward, only that collaboration and communication among sectors will be necessary. This recent push to further understand complexities of the hydrological system has made it increasingly apparent that sustaining the quality and quantity of our freshwater resources, in the midst of increasing human population and climate uncertainties, has become a complex and challenging management problem.

As a result of the basic need of freshwater for survival, water resources are typically considered a common good, and its use, a human right. However, the sustainability of this good and therefore the future exercising of this right, has been called into question. It has been suggested that the issue of available freshwater for human use has been underestimated in previous research. And further that water scarcity is a widespread problem, already impacting two-thirds of the global population and likely to be exacerbated with the uncertainties associated with climate change [Mekonnen and Hoekstra, 2016].

A system perspective of vital human resources (i.e., food, energy, water) has shed some light on the interconnectedness of both our natural earth system and our built human systems, bringing issues like the Food-Water-Energy Nexus and Integrated Water Resource Management (IWRM) to the forefront of local, national and international discussion.

We need to develop an understanding of the integrated dynamics of the major components influencing the coupled natural-human water system within water management, policy, and society in general.

A.2.2 Scientific contribution

Water-efficient technologies [Water, 2009; Inman and Jeffrey, 2006; Deng et al., 2006], better pipe quality [EPA, 2010; Colombo and Karney, 2002], water recycling and reuse [Bryck et al., 2008; Toze, 2006; Sala and Serra, 2004; Anderson, 2003], and rooftop rainwater collection [Steffen et al., 2013; Li et al., 2010] should all be very useful for sustaining the water supply [EPA, 2013]. However, full adoption and responsible implementation of these solutions requires significant investment unlikely to be available under current economic pressures. Also, the solutions may have different cost-to-benefit ratios in different regions. For example, if in a certain region the pipelines are in good condition, so that leakage is not a major concern, available funding might be better invested in building water recycling facilities. One goal of this research is to find the efficiencies of different water-saving strategies under different policy scenarios in order to determine the most sustainable water management decisions.

Computer models provide us with a powerful tool to simulate the outcomes under different sets of conditions. So far, few studies have used computer models to test the efficiency of different water policies. One example is a recent research on water use in South Florida, in which Ahmad and Prashar [2010] applied a complex system dynamics model to study certain factors in the regional water management. Ahmad and Prashar used only the water levels in one lake from 1980-2005, so their results may not hold if the precipitation regime changes in future. Furthermore, a highly complex model with quite a few parameters requires a huge body of data for tuning that may not be available. Consequently, it may be difficult to replicate such work for another region. These potential shortcomings motivate us to establish a framework applicable to different regions, using a minimal, efficient model. Such a model provides an opportunity to carry out many experiments that can help to understand more efficient ways of conserving water resources.

We have built our coupled water model with the following components: The University of Maryland (UMD) Earth System Model (ESM), is used to conduct an offline run for the region of interest with the monthly observational datasets from the Climate Research Unit (CRU). A River-Routing Module (RRM) is developed and coupled with the UMD ESM. From the runoff output information for each model grid, total river inflow and outflow for the region of interest is calculated. Then the simulated precipitation, evaporation and river inflow and outflow rates are fed into COWA. By doing so, natural water resource stock can be approximated and the efficiency of different water-conserving options can be evaluated. Some of these options include implementing water-efficient technologies, fixing pipeline leaks, increasing the water recycling capacity, and introducing long-term water withdrawal policies.

The Coupled Human-Water-Climate (COWA) model is verified with the available historic data for the Phoenix Region from several sources, including US Census Bureau, USGS National Water Information System, USGS Instantaneous Data Archive, and ADWR Groundwater Site Inventory and extracted data from the records available at the US National Archives.

The results can help policymakers to choose priorities for adaptation/mitigation water policies that can lead to effective investment of limited funds. In our future works, we will explore the possibility of applying the model to other regions, such as the State of California, the Potomac River Basin, the Fertile Crescent (e.g., Iraq, Syria, Lebanon, Jordan and Israel/Palestine) and eastern Africa (e.g., Somalia) where water problems are crucial and there is little data available.

The goal of this research is to model and then analyze the impacts of different policy factors on both the human system, through changes in population stocks, and the natural system, through changes in ground and surface water stocks, when they are considered to be coupled and endogenously linked.

A.3 Modeling Approach

COWA was developed by a group of interdisciplinary academics (i.e., atmospheric, hydrologic, geographical, and public policy sciences). The goal of the model was to explore the dynamics of the human system when freshwater resources are treated as a required, yet, restricted driver of growth and, likewise, to explore the dynamics of the natural system when total water demands are a function of population. Therefore, both natural and human water systems are represented and integrated with bi-directional feedbacks between them to simulate the duality of the real system's dynamics.

Section A.3.1 provides a general description of modeling techniques used in this research as well as discussion of strengths and weaknesses associated with these choices. The Section A.3.2 provides an overview of the model's purpose through a brief account of the model conceptualization process.

A.3.1 Technique

To conduct this research, we utilized the UMD Earth System Model (ESM) and a River Routing Module (RRM) as exogenous inputs into the Coupled Human-Climate-Water (COWA) model to provide certain climatic (i.e., precipitation and evapotranspiration) and hydrologic (i.e., river inflow and river outflow) flows. The model framework is illustrated in Fig. 3.2. Detailed information regarding the ESM and RRM used in this research can be found in the Appendix. COWA is a system dynamics (SD) model used to study various effects of the human system on the water resources and water supplies over time. COWA includes demographic characteristics of the human system, such as population, growth rate, regional net migration, and water demand per capita, as well as the influence of human decision on the management of water systems. By coupling the ESM and RRM to COWA, we can simulate future availability of water supplies under changing climate and water policies.

The system dynamics (SD, ref) approach to modeling allows users to simulate changes to stocks and flows over time given certain inter-relationships and potential feedbacks or delays, inherent or hypothetical, within the real system. With its initial intent to assist in the optimization of industrial flows, then finding applications in urban planning, most recently, SD modeling has become very popular for the purpose of socioeconomic and natural resource sustainability modeling. The SD approach to modeling is a powerful tool for analyzing complex and dynamic systems with many changing parts, allowing for better understanding of these systems by its users. Vensim ®is a SD modeling and simulation software created by Ventana Systems. The Vensim Professional version 5.10x3 is the system dynamics tool used in this research. It was chosen on the basis of its ability to detect inconsistencies, its flexibility with data modification and its relatively simple graphical user interface (GUI). Vensim facilitates identifying errors by highlighting variables with conflicting units or illogical governing equations and allows for on-the-fly changes to variables quantities with the use of the SyntheSim instrument. The SyntheSim tool provides a slide bar below each parameter, allowing the user to adjust selected values while simultaneously viewing the changes to the system through interactive graphs. Vensim also provides the option for various graphical outputs including bar, line, and sensitivity graphs, as well as a table of the simulated time series data output for each variable, a catalog of all variables/parameters, their explanations, defining equations and calibration values in document format. Unfortunately, Vensim does have some inconvenient limitations such as its restricted ability to customize graphical output and its inability to model spatial variation. However, these limitations can be resolved through supplemental use of the other modeling tools and programming languages (e.g., R, Python/GIS, AnyLogic, etc.).

A.3.2 Conceptualization

COWA (The COupled human-climate-WAter model) is a minimal model for the natural-human water system. COWA is coupled to an Earth System Model (ESM) and a River Routing Module (RRM). Other than ESM and RRM, the model has only four primary stocks: Population, Surface Water Sources, Groundwater Sources, and Freshwater Supply.

The purpose of this model was to simulate the feedbacks between the natural environment's regeneration and use of freshwater resources and the human interferences of those natural processes. This model was designed to help gain insight into which human actions would have most significant impacts on sustaining our natural freshwater resources for both human and natural demands and, ideally, to help determine what is the best course of action for responsibly managing our water supplies for generations to come.

A.4 Model Description

In this version of COWA, consumption of water by different sectors of the economy and society is combined into a single flow, *Consumption.* A main feature of COWA is that Population is endogenously coupled to the water system through bi-directional feedbacks. This coupling can produce results that would be otherwise be impossible to obtain if population is treated as an exogenous variable.

One can use COWA to run *"thought experiments"* on the lifetime of Sources / Supply under various assumptions for climatic and human behavior, including changes to recycling capacity, pipeline leakage, and dispensing technology. There are certain parameters in the model that are determined through policies. Therefore, effects of various policies can be studied with COWA.

The four key state variables in COWA are Population, x, Surface Water Sources, y_S, Groundwater Sources, y_G and (stored) Freshwater Supply, z. (These four variables do not account for the state variables in the Earth System Model and the River Routing Model.) Population is controlled by the death rate, α, birth rate, β, and immigration rate, I. Death rate is not a constant but increases as consumption per capita decreases below a threshold value. Immigration rate is proportional to the consumption per capita, and becomes negative if consumption drops below a certain threshold. Surface water stock, y_S, is controlled by several flows: river inflow, Φ, river outflow, Ψ, precipitation, P, evapotranspiration, E, withdrawal of water from surface water sources into the supply, W_S, groundwater recharge, G, reservoir overflow, O, leak to sources, Λ, flow of non-recycled water to sources, N, and runoff to sources, Ω. Groundwater stock, y_G, receives three incoming flows, groundwater recharge, G, reservoir overflow, O, and artificial recharge, A, and has two outgoing flows, withdrawal of groundwater into the supply, W_G, and groundwater contamination, G_C. Freshwater supply, z, is controlled by three inflows, withdrawals, $W_S + W_G$, and recycling, R, and two outflows, supply collection, K, and leakage, L. Rooftop collection rate, Γ, is directly available for consumption and therefore, is deducted from the total precipitation when calculating net inflow of water to (surface water) sources.

While P, E, Γ, Φ, and Ψ are exogenous variables (or time series) for COWA,

W_G, W_S, K, R, L, Λ, Ω, N, and Σ are all functions of other model parameters and variables. Model parameters are demand per capita, δ, technology factor, τ, transfer efficiency, η, assurance factor, θ, maximum withdrawal capacity, W_M, maximum groundwater withdrawal rate, W_{GM}, maximum recycling capacity, R_M, maximum surface water, y_{SM}, and maximum capacity of supply, z_M. There are also four coefficients which are bounded between 0 and 1: consumptive to sewer, σ, leak to sources, λ, runoff to sources, ω, and non-recycled to sources, ν. It is assumed that a portion λ of the leaked water returns to sources with a time delay T_L.

Total demand, $\Delta(t)$ is given by:

$$\Delta(t) = \delta x(t). \tag{A.1}$$

Effective demand is given by the total demand divided by the technology factor:

$$D(t) = \frac{\Delta(t)}{\tau} = \frac{\delta}{\tau} x(t). \tag{A.2}$$

It can be seen that $\tau = 1$ represents the base technology, $\tau > 1$ indicates a water saving technology, and $\tau < 1$ refers to an inefficient water dispensing technology. Transfer efficiency, η, is defined through the equation:

$$K(t) = \eta\big(K(t) + L(t)\big). \tag{A.3}$$

This equation essentially shows that only a factor η of the total water withdrawn from the freshwater *supply*, $K+L$, is consumed and the rest is wasted through leaks. Therefore, leakage rate and consumption rate are directly related through η:

$$L(t) = \frac{1-\eta}{\eta} K(t). \tag{A.4}$$

Net water that is available for recycling is the sum of the consumption to sewer rate, $\Sigma(t) = \sigma(K(t)+\Gamma(t))$. Flows that determine the Supply level, i.e., (two) withdrawals, consumption, leakage, and recycling can then be expressed as follows:

$$\begin{cases} W_S(t) &= \min\left(\theta_S \dfrac{y_S}{\Delta t}, \theta_O \dfrac{z_M - z}{\Delta t}, W_{SM}\right) \times \min\left(1, \dfrac{y_S}{n_S D}\right) \\ W_G(t) &= \min\left(\theta_G \dfrac{y_G}{\Delta t}, \theta_O \dfrac{z_M - z}{\Delta t}, W_{GM}\right) \times \min\left(1, \dfrac{y_G}{n_G D}\right) \\ K(t) &= \max\left(0, \min\left(D(t), \theta_K \eta \dfrac{z(t)}{\Delta t}\right) - \Gamma\right) \\ L(t) &= \dfrac{1-\eta}{\eta} K(t) \\ R(t) &= \min\left(\theta_O \dfrac{z_M - z}{\Delta t}, \Sigma(t), R_M\right) \end{cases} \tag{A.5}$$

The consumed water that does not go to sewer, $(1-\sigma)(K+\Gamma)$, flows to runoff and a portion of it, Ω, goes to sources. Moreover, a portion of the water that has gone into the sewer but has not been recycled, N, goes back to the sources. These three flows are therefore defined by:

$$
\begin{cases}
\Lambda(t) & = & \lambda \cdot L(t - T_L) \\
\Omega(t) & = & \omega(1-\sigma)(K(t)+\Gamma(t)) \\
N(t) & = & \nu\left(\Sigma(t) - R(t)\right) \\
\Sigma(t) & = & \sigma\left(K(t)+\Gamma(t)\right)
\end{cases}
\tag{A.6}
$$

In addition to the withdrawal from groundwater, $W_G(t)$, defined in (A.5), the following flows determine the changes in Groundwater:

$$
\begin{cases}
G(t) & = & f \cdot (P(t) - E(t)) \\
O(t) & = & \max\left(\dfrac{y_S - y_{SM}}{\Delta t}, 0\right) \\
G_C(t) & = & r_{GC}\dfrac{y_G}{\Delta t} \text{ at } t = T_{GWC}, \text{else } 0 \\
A(t) & = & A_{CAP} + A_{Incidental} + A_{Additional}
\end{cases}
\tag{A.7}
$$

Now that we have defined all the components, we can write the equations governing COWA:

$$
\begin{cases}
\dot{x} &= \beta x - \alpha x + I(t) \\
\dot{y}_S &= \Phi(t) + P(t) - \Psi(t) - E(t) - W_S(t) + \Omega(t) + \Lambda(t) + N(t) - G(t) - O(t) \\
\dot{y}_G &= G(t) - W_G(t) - G_C(t) + O(t) + A(t) \\
\dot{z} &= W_S(t) + W_G(t) + R(t) - K(t) - L(t)
\end{cases}
\tag{A.8}
$$

A schematic of the variables of COWA and their connections to the ESM and RRM is shown in Fig. A.1.

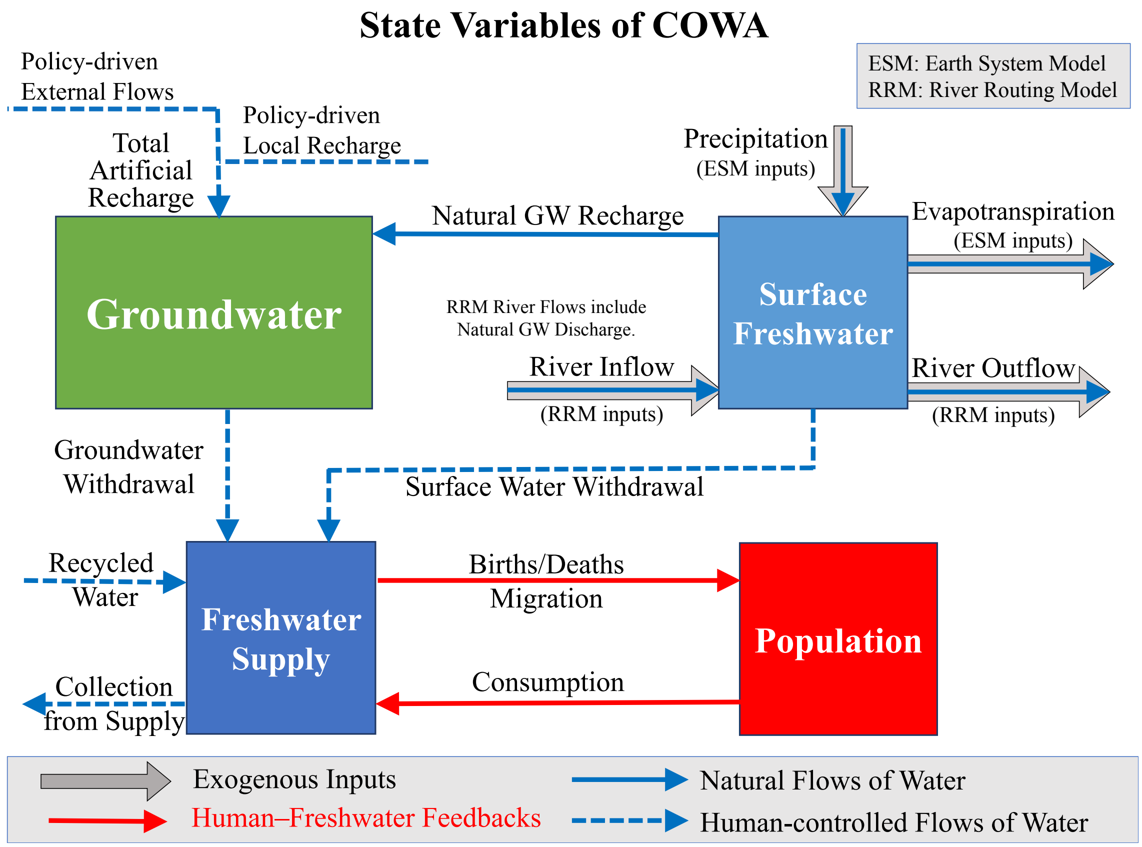

Figure A.1: A schematic of the state variables of COWA, including the flows among them as well as the linkages to ESM and RRM. Red arrows show feedbacks while black arrows show flow of water.

Below we will present definitions for variables, parameters, and functions used in COWA in three tables:

Table A.1: State Variables (Stocks) used in COWA

Variable Symbol	Variable Name	Governing Equation
x	Population	$\dot{x} = \beta x - \alpha x + I$
y_S	Surface Water Sources	$\dot{y}_S = P - E + \Phi - \Psi - W_S + \Lambda + \Omega + N - G - O$
y_G	Groundwater Sources	$\dot{y}_G = G - W_G - G_C + O + A$
z	Freshwater Supply	$\dot{z} = W_S + W_G + R - K - L$

Table A.2: Definition of Functions used in COWA Equations

Function Symbol	Function Name	Describing Equation
P	Precipitation rate	Exogenous
E	Evapotranspiration rate	Exogenous
Φ	Net River Inflow rate	Exogenous
Ψ	Net River Outflow rate	Exogenous
Γ	Rooftop Collection rate	Exogenous
I	Immigration rate	$= I_b(x)\Big(\frac{C}{C_{th}} - 1\Big)$
I_b	Base Immigration	$= I_{br}x$ for $t \geq 1925$ else $= 100$
G	Groundwater Recharge rate	$= \max\big(0, f(P-E)\big)$
W_S	Surface Water Withdrawal rate	$= \min\Big(\theta_S\frac{y_S}{\Delta t}, \theta_O\frac{z_M - z}{\Delta t}, W_{SM}\Big) \times \min\Big(1, \frac{y_S}{n_S D}\Big)$
W_G	Groundwater Withdrawal rate	$= \min\Big(\theta_G\frac{y_G}{\Delta t}, \theta_O\frac{z_M - z}{\Delta t}, W_{GM}\Big) \times \min\Big(1, \frac{y_G}{n_G D}\Big)$
K	Rate of Collection from Supply	$= \max\Big(0, \min\big(D, \theta_K\eta\frac{z}{\Delta t}\big) - \Gamma\Big)$
L	Leakage rate	$= \frac{1-\eta}{\eta}K$
R	Recycled Water rate	$= \min\Big(\theta_O\frac{z_M - z}{\Delta t}, \Sigma, R_M\Big)$
Δ	Total Demand	$= \delta x$
D	Effective Demand	$= \Delta/\tau$
C	Consumption per Capita	$= (K+\Gamma)/x$
C_{th}	Threshold Consumption per Capita	$= \mu(\delta/\tau)$
α	Death rate	$= \max\Big(\alpha_M - (\alpha_M - \alpha_m)\frac{C}{C_{th}}, \alpha_M\Big)$
Λ	Leak to Sources	$= \lambda L(t - T_L)$
Ω	Runoff to Sources rate	$= \omega(1-\sigma)(K+\Gamma)$
N	Nonrecycled to Sources rate	$= \nu(\Sigma - R)$
Σ	Consumptive to Sewer rate	$= \sigma(K+\Gamma)$
A	Artificial Recharge	$= A_{CAP} + A_{incidental} + A_{additional}$
O	Reservoir Overflow	$\max\Big(0, \frac{y_S - y_{SM}}{\Delta t}\Big)$
G_C	Groundwater Contamination	$r_{GC}y_G/\Delta t$ at $t = T_{GWC}$, 0 otherwise
d	Drought Factor	$e^{-r_d(t-T_d)}$ for $t > T_d$, 1 otherwise

Table A.3: Description of Parameters used in COWA

Parameter Symbol	Parameter Name
α_m	Normal (Minimum) Death rate
α_M	Famine (Maximum) Death rate
β	Birth rate
I_{br}	Base Immigration rate
δ	Demand per Capita
μ	Threshold Consumption per Capita ratio
η	Transfer Efficiency
τ	Technology factor
z_M	Maximum Capacity of Freshwater Supply
y_{SM}	Maximum Surface Water Capacity
W_{SM}	Maximum Surface Water Withdrawal rate
W_{GM}	Maximum Groundwater Withdrawal rate
R_M	Maximum Recycling Capacity
$n_{S,G}$	Number of Reserve Months (Long-term Policy) for Surface Water and Groundwater
f	Infiltration rate
$\theta_{S,G,K,O}$	Assurance factor (Short-term Policy) for Surface/Ground Water Withdrawal, Collection from Supply, and Supply Overflow
λ	Leak to Sources ratio
T_L	Leak to Sources Time Delay
ω	Runoff to Sources ratio
ν	Nonrecycled to Sources ratio
σ	Consumptive to Sewer ratio
r_d	Drought coefficient
T_d	Drought onset time
T_{GCW}	Groundwater Contamination time
T_p	Policy start year

A.4.1 The Natural System

This section should mention (again briefly) the exogenous natural, hydrological variables (precip., evap., river IN/OUT flow), Surface Water sources and Groundwater sources - with mention of other natural elements included in the model's structure (i.e., overflow, and natural recharge).

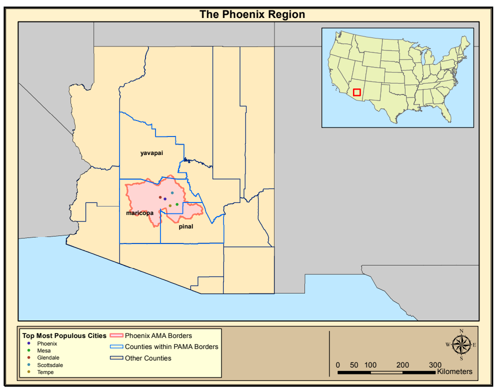

(a) Administrative borders and major cities of the Phoenix region in south-central Arizona,USA

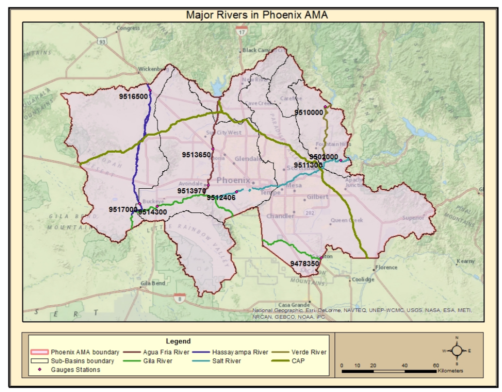

(b) Counties, sub-watersheds and well sites used in study Phoenix region

Figure A.2: Case study site: Phoenix Active Management Area

Exogenous inputs for the COWA model are listed and labeled in Table X. Most of the exogenous variables included in this model [1] represent the natural hydrological flows that largely define a region's available water supply (i.e. precipitation, river inflow, evapotranspiration, and river outflow). Although, the COWA model structure is intended to assess coupled natural-human water flows, it is not suited to

[1]with the exception of *birth rate* and *artificial recharge* rates

forecast physical, natural hydrological at a monthly resolution and therefore accepts these flows as input from other, better-suited General Climate Model (GCM), Earth Systems Model (ESM) and River-Routing Module (RRM) . Below is a list and of all imported datasets used as exogenous input to force the COWA model to date:

1. **Climate Import:**
   - A time-series dataset consisting of volume/time units of total monthly precipitation and evaporatranspiration from 1900-2100 was generated by a GCM called SPEEDY developed by the UMD-ICTP.
2. **River Import:**
   - A second time-series dataset of volume/time units of total monthly river inflow to and river outflow from the region from 1900-2100 was generated by a River -routing module (RRM) coupled to the UMD-ICTP's ESM, developed by a collaborating researcher.
3. **Births Import:**
   - A third time-series dataset was compiled from 15-year averages of annual crude birth rates form 1900-2015 for Maricopa and Pinal counties [2].
4. **Artificial Recharge Imports:**
   - A fourth time-series dataset was compiled from total annual estimations

[2] when estimates were not available at county-level, state-level estimates were used as proxy values; when state-level estimates were not available, national estimates were used

of incidental recharge from 1985-2009, summed across all water-use sectors.

- A fifth time-series dataset was compiled from total volume of annual CAP water-deliveries to direct (e.g USFs) and indirect (e.g GSFs) groundwater recharge efforts from 1985-2009.

A.4.2 The UMD Earth System Model: Land and vegetation models

The UMD ESM includes a dynamic vegetation model (VEGAS), a simple land model (SLAND), and several other components. COWA requires as inputs precipitation, evaporation and river inflow and outflow rates in the region of study (in this case, PAMAWR). The river inflow and outflow rates are computed from the coupled River Routing Module, driven by runoff.

The land surface parameterization scheme is called Simple-Land (SLand). It has been built at an intermediate level of complexity to simulate the first-order effects of vegetation on climate variables. For simplicity, there is no diurnal cycle, and no environmental control on photosynthesis. Therefore, the soil moisture and seasonal variation of radiation are the main controlling factors. A single soil layer with different depth for the energy and the water balance is assumed. More information on energy balance and water budget equations can be found in Zeng et al. [2000]

The terrestrial carbon model VEgetation-Global-Atmosphere-Soil (VEGAS) simulates the dynamics of vegetation growth and competition among four different plant functional types (PFTs): broadleaf tree, needleleaf tree, cold grass, and warm grass. The different photosynthetic pathways are distinguished for C4 (warm grass) and C3 (the other three PFTs) plants. Phenology is dynamically simulated as the balance between growth and respiration/turnover. Competition is determined by climatic constraints as well as resource allocation strategies such as temperature tolerance and height-dependent shading. The relative competitive advantage then determines fractional coverage of each PFT with possibility of coexistence [Zeng, 2003; Zeng et al., 2005].

A.4.3 Environmental Drivers: Bias Correction and Summary

General Circulation Models (GCMs) are important tools in assessing climate change and in helping decision making to mitigate and adapt to future availability of water. However, there are inevitable model biases due to inadequate knowledge of key physical processes (e.g., cloud physics) and simplification of the natural heterogeneity of the climate system that exist at finer spatial scales. For example, substantial precipitation biases, especially in the tropics, are common in many models [Randall et al., 2007].

Traditionally, additive correction is often applied to correct the biases of model means, that is, to simply add the delta difference between a reference observation period and the model simulated mean future climatology:

$$\bar{C} = \bar{O} + M - \bar{M}, \tag{A.9}$$

where C is the corrected value, $\bar{O}$ is the observed climatology for the reference period, M is the simulated value, and $\bar{M}$ is the simulated climatology. For wet biases (model simulates higher precipitation climatology than observation), this method may result in negative rainfall, which is unphysical.

An alternative method is multiplicative correction [Sheffield et al., 2006]:

$$\bar{C} = \bar{O} + \frac{\bar{O}}{\bar{M}} \times (M - \bar{M}) \tag{A.10}$$

This method scales the perturbation with the ratio of observed to modeled climatology. A drawback for this method is when model has large dry bias, this correction could lead to unrealistically high rainfall.

To avoid the limitations of the two methods above, we implemented a Mixed Additive-Multiplicative (MAM) correction method to perform bias correction using rainfall observation from the latest global gridded Climate Research Unit (CRU) TS3.21 dataset. We chose 1961-1990 as the reference period for climatology:

$$\bar{C} = \begin{cases} \bar{O} + M - \bar{M}, & \text{when} \quad \dfrac{\bar{O}}{\bar{M}} \geq 1 \\ \\ \bar{O} + \dfrac{\bar{O}}{\bar{M}} \times (M - \bar{M}), & \text{when} \quad \dfrac{\bar{O}}{\bar{M}} < 1 \end{cases} \tag{A.11}$$

As a simple combination of two popular methods, we believe MAM correction is a conceptually intuitive, easy to implement, yet effective bias correction method.

To create the monthly rainfall scenario for PAMAWR, we chose a representative ensemble member of the National Center for Atmospheric Research (NCAR) Community Climate System Model (CCSM) RCP4.5 output. This model is a participant in the Intergovernmental Panel on Climate Change (IPCC) Coupled Model

Intercomparison Project Phase 5 (CMIP5). We retrieved the simulated rainfall from the Earth System Grid Federation (ESGF), an international network of distributed climate data servers [Williams et al., 2011]. Then we applied the MAM method to create a combined (1901-2012 CRU and 2013-2100 CCSM) rainfall monthly time series for the AMA watershed from 1901-2100.

Similarly, for monthly evaporation losses, we combined the simulated results from the UMD ESM and the CCSM output for PAMAWR with the MAM method.

A.4.4 River-Routing Module (RRM)

Based on the principles in Miller et al. [1994], similar to the concept of the Total Runoff Integrating Pathways (TRIP) developed by Oki and Sud [1998], we developed a river routing module (RRM) that routes runoff based on river channel characteristics in the Global Dominant River Tracing (DRT) based Hydrography Datasets. The recently developed DRT algorithms utilize information on global and local drainage patterns from baseline fine scale hydrography inputs to determine upscaled flow directions and other critical variables including upscaled basin area, basin shape and river lengths. It preserves the original baseline hierarchical drainage structure by tracing each entire flow path from headwater to river mouth at fine scale while prioritizing successively higher order basins and rivers for tracing [Wu et al., 2011, 2012]. We use the 0.5 degree version of flow direction, flow and river channel slope from the DRT dataset as input to the River Routing Module. We followed the equations in Miller et al. [1994] for computing river flows, specifically, the equations are as below.

The rate at which water leaves a grid box, F, mainly depends on the water storage above the sill depth, S, the flow distance between the grid boxes, d, and topography gradient.

$$F = S \cdot \frac{u}{d} \tag{A.12}$$

In Eq. (A.12), F (Kg·m^{-2}·s^{-1}) is the river flow flux to the downstream grid; S (kg·m^{-2}) represents the free-flowing mass of water (lakes, rivers, and groundwater) above the sill depth in each grid; d (m) is the meandering flow distance from the DRT dataset distance (we use the minimum of the meandering flow distance from DRT dataset and the shortest distance between current and its downstream grid); and u (m·s^{-1}) is an effective flow speed of water from a grid box to its downstream neighbor.

The value of u depends on local characteristics of the river basin, such as its morphology and topography gradient:

$$u = 0.35\,(i/i_0)^{1/2}, \tag{A.13}$$

where i is the river channel slope from the DRT dataset and $i_0 = 0.004$ (median value of the DRT dataset) is the reference topography gradient we use. We limit u within a realistic range of 0.15 – 5 m/s. An upper limit on u is necessary to prevent numerical instabilities in the river routing model. Minimum u is used when the downstream grid is at a higher elevation than upstream.

Changes in water storage at each grid box is given by:

$$\frac{dS}{dt} = R + \sum F_{IN} - F_{OUT}, \tag{A.14}$$

where F_{OUT} is the rate at which river mass leaves a grid box, $\sum F_{IN}$ is the sum of the water flux entering a grid from all of its neighbors, and R represents the runoff from the UMD model. At each time step, after computing the river outflow at grid X, we add it to the inflow of its downstream grid, Y (if Y is also a land grid). Thus river inflow at every grid is calculated after looping through all grids.

We found this simple river routing scheme captures a realistic global river flow pattern, and we believe it is suitable for the purpose of this study, where we simply sum up river flow entering and exiting PAMAWR each month from 1900-2010.

We assume river inflow and outflow in future shows similar characteristics as the historical period, and we simply repeat the river inflow and outflow time series from our River Routing Model as the future river flows for AMA watershed. Admittedly this is a simple treatment, however, given the purpose of this conceptual study, and the large uncertainty in evaporation and river flow simulations, we believe the scenario we used in our study is plausible.

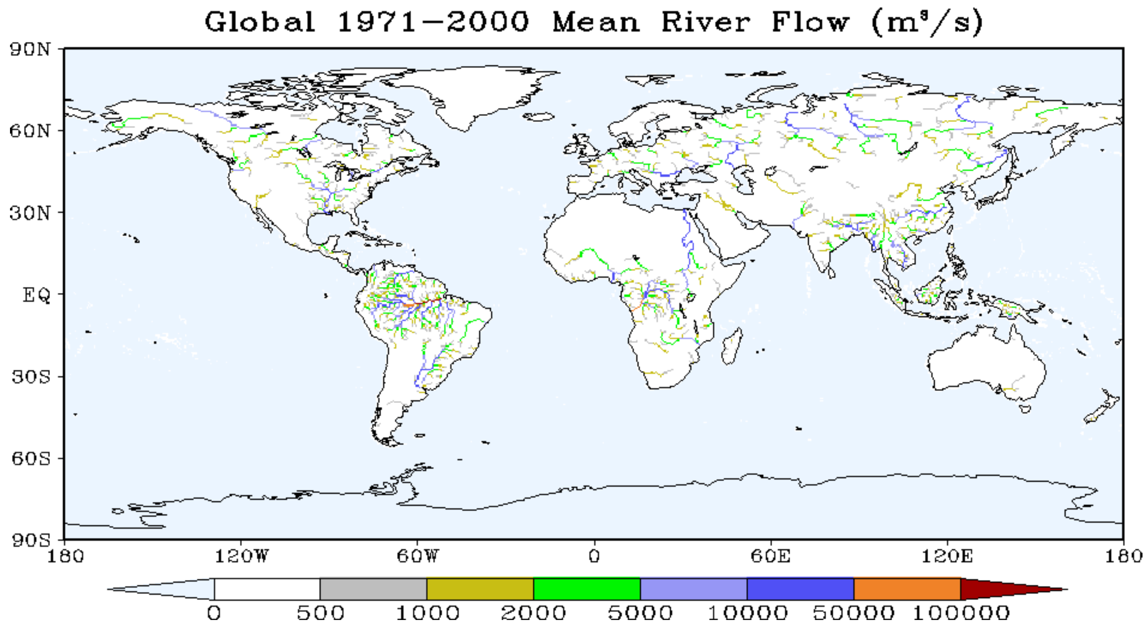

Figure A.3: Global mean river flow from 1971 to 2000.

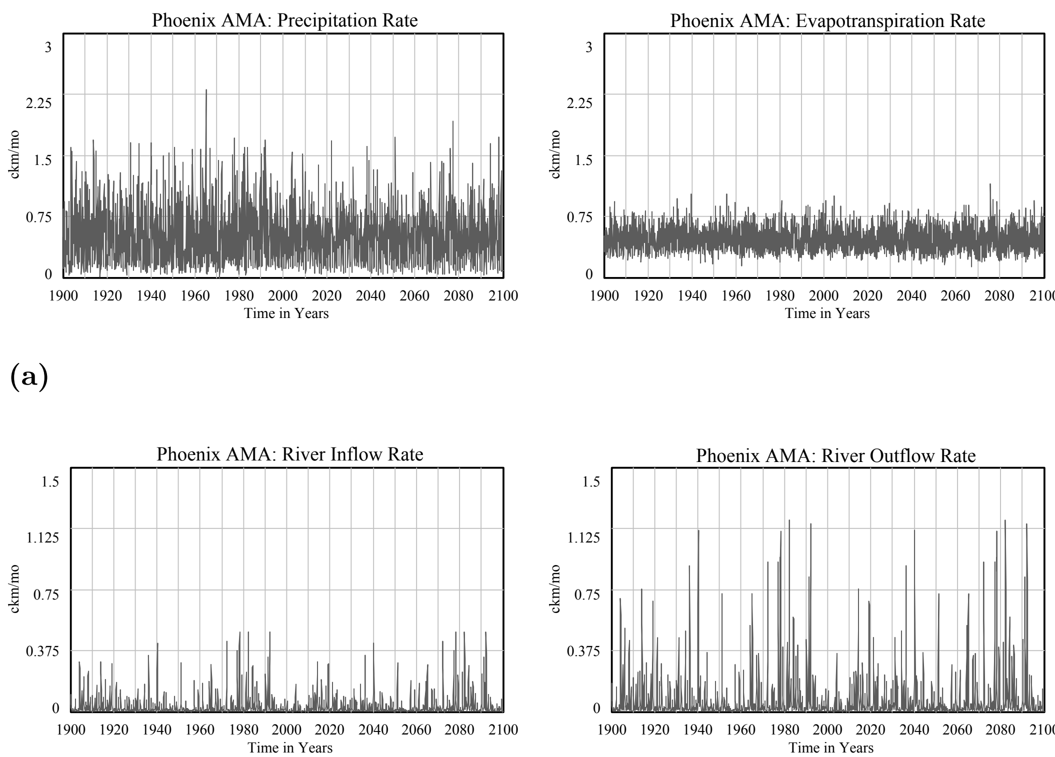

Figure A.4: Time Series of monthly precipitation, evaporation, and river inflow and outflow for PAMAWR from 1900 to 2100.

A.5 Calculating the Water Carrying Capacity

To calculate the Water Carrying Capacity in each scenario, we run the model until the state variables reach an equilibrium state, which typically requires several centuries of model time. Then we average the population over 100 years of model time.

Appendix B: Supplementary Materials: Climate model shows large-scale wind and solar farms in the Sahara increase rain and vegetation

B.1 Materials and Methods

B.1.1 Model description

The UMD–ICTP (University of Maryland–International Centre for Theoretical Physics) Earth System Model is used to conduct the experiments. The model consists of an Atmospheric General Circulation Model (AGCM), SPEEDY (Simplified Parameterizations, primitivE-Equation DYnamics) [Kucharski et al., 2012], a physical land surface model, Sland (Simple land) [Zeng et al., 2000], and a dynamic vegetation and carbon model, VEGAS (VEgetation–Global–Atmosphere–Soil) [Zeng, 2003; Zeng et al., 2005]. The model setup for the experiments of this study uses prescribed sea surface temperatures (SSTs) and is therefore considered to be a climate model. The atmospheric model, SPEEDY, is based on a hydrostatic spectral dynamical core [Kucharski et al., 2012; Molteni, 2003]. The parameterized processes include short- and long-wave radiation, large-scale condensation, convection, vertical diffusion, and surface fluxes of momentum, heat, and moisture. In this study, the AGCM model SPEEDY is configured with 8 vertical (sigma) levels and with a spectral resolution of T30 (48×96), equivalent to a spatial resolution of 3.75 × 3.75 degrees. The dynamic vegetation model VEGAS simulates the dynamics of vegetation growth and competition among different plant functional types (PFTs), including broadleaf trees, needleleaf trees, cold grass, and warm grass. The dynamic vegetation model is coupled with the AGCM, allowing for the representation of the two-way interactions between vegetation and climate, which have rarely been taken into account in previous studies regarding wind and solar farm impacts. The model has participated in multiple model intercomparison projects [Scaife et al., 2009; Xue et al., 2016], and was shown to have skills comparable to other higher resolution models in simulating modern climate and multi-decadal variability in this region. In addition, the model setup used in this study has been validated against observational data for the Sahara region from the Climate Research Unit [Kucharski et al., 2013].

B.1.2 Parameterization of wind and solar farms

The large-scale wind and solar farms can directly modify land surface properties. Wind turbines can increase surface friction (roughness) and solar panels can decrease albedo (for typical low-efficiency photovoltaic cells installed in the desert). Therefore, in the model, their impacts can be parameterized by changing the model parameters representing surface friction and albedo, respectively. Whereas more sophisticated schemes exist for wind turbines such as TKE (turbulent kinetic energy)

[Roy et al., 2004; Fitch, 2015], the advantage of such a simple parameterization is the simplicity of its implementation in the Earth System Model framework and the ability to capture the first order impacts. The impact of wind farms is parameterized by an increase of the drag coefficient (C_D value), which is directly linked to surface friction in the atmospheric model. The default C_D value (0.0024) in the model is multiplied by 4, so that the resulting amplified C_D value (0.0096) falls in the range of 0.005–0.013. This range represents a realistic wind farm scenario with an average turbine spacing of five to eight rotor diameters and a 100 m turbine hub height [Keith et al., 2004]. Solar panels are parameterized based on the "effective albedo" concept [Taha, 2013]. Effective albedo is used to describe how much incoming shortwave radiation is not absorbed by the land surface in the presence of a PV panel. It is defined as the sum of the reflectivity of the PV panel and of the percentage of harvested energy, divided by incoming shortwave radiation. Effective albedo enables the model to emulate the solar panel impact through a surface albedo change. Assuming PV panels have a reflectivity of $\alpha_p = 0.1$ and a conversion efficiency of $\eta = 0.15$, the available shortwave radiation that a PV panel receives after reflection, $1 - \alpha_p = 1 - 0.1 = 0.90$, multiplied by 0.15 conversion efficiency gives the portion of the solar energy converted to electricity as $\eta(1 - \alpha_p) = 0.15 \times (1 - 0.1) = 0.135$. This ratio, $\eta(1 - \alpha_p)$, plus the reflectivity of the PV panel, α_p, gives the effective albedo $\alpha_e = \alpha_p + \eta(1 - \alpha_p) = 0.235$. The solar panel from the example above will reduce the land surface albedo for sand from ~0.4 to 0.235 when installed in the Sahara, and thus affect the local climate.

B.1.3 Experimental setup

The large-scale wind and solar farms in this study cover either just the Sahara desert or all the deserts of the world. The Sahara desert is defined in the model as the region within latitudes of 3.75N–30N and longitudes of 0–60E and with an annual mean precipitation from the control run less than 250 mm. The world deserts in the model are defined based on different conditions: (1) leaf area < 2 m^2/m^2; (2) annual near-surface air temperature > 5°C; and (3) annual precipitation < 500 mm. The resulting model desert locations match fairly well with those in the real world. For experiments involving a wind farm in the Sahara or the world's deserts, we increased the surface drag (CD value) four-fold to simulate the wind farm effect. For experiments involving a solar farm in the Sahara or the world's deserts, we set the surface albedo to 0.235 for 20% of the area of a model grid, assuming solar panels cover 20% of the land. This albedo of 0.235 corresponds to the effective albedo of a 15% conversion efficiency PV panel with a reflectivity of 0.1. The 15% efficiency chosen here represents the medium range of conversion efficiency of solar panels that are commercially available (44). A greater coverage of solar panels than the assumed 20% here would result in larger albedo change and thus stronger climate response. For experiments in which wind and solar farms are deployed together, both surface drag and albedo are modified accordingly. To better understand how roughness and vegetation feedback produce climate changes, we carried out an additional factorial wind farm experiment in the Sahara, since wind farm impacts arise from changes in both roughness and albedo (albedo changes due to vegetation feedback). To separate the contributions from roughness and albedo, we compare the results of the standard wind farm simulation, which includes the effects of both roughness change and vegetation feedback, with the experiment that only includes the effect of roughness change in which vegetation feedback is disabled and the albedo is the same as the control run. To investigate how impacts of solar farms depend on different conversion efficiency rates of the solar panel, we run solar farm experiments with alternative efficiency of 30% and 45%, representing a much higher efficiency than commercially available panels at present. The 30% and 45% efficiency solar panels correspond to effective albedos of 0.37 and 0.505, respectively. The results of these experiments are shown in Fig S6. To investigate how climate impacts of wind farm would differ when installed with different spatial configurations (spatial extent, density, and location), we designed two pairs of wind farm experiments in the Sahara, referred to as the "checkerboard" and "quarter surface" types (Fig. S9). The two checkerboard wind farm layouts — which still cover the Sahara but whose coverage is half of the coverage of the original wind farm, i.e., every other grid box — are expected to have smaller impacts. The four quarter-type wind farms, each of similar size, are located in different quadrants (northeast, southeast, southwest, and northwest) of the Sahara. The northwest quadrant farms produce significantly more precipitation than the other three quadrants, presumably due to the closeness to the Atlantic ocean and the Mediterranean sea. This suggests that the actual climate impacts of wind farms are determined not only by the imposed perturbation but also by the environmental conditions at a given location, such as the distance to the ocean, which provides the moisture source for the additional precipitation. All experiments described above were run in the model for 100 years with a 100-year spin-up, driven by the observed SST data from 1901 to 2000. The averaged climate of the last 50 years of simulation in each experiment was used for the analysis.

B.2 Supplementary Text

B.2.1 Estimate of electrical power generated by wind and solar farms in the Sahara

To roughly estimate the power generated by the modeled wind infrastructure, we note that studies of the limits of wind generation suggest that an installed capacity of 1.0 W/m^2 is a safe limit to avoid substantial reductions in generation due to wind turbine wakes [Miller et al., 2015]. The area of the Sahara desert is approximately A = 9.2 million km^2, which yields an installed capacity of 9.2 TW. Typical Capacity Factors for new wind farms in locations with a good resource (such as the Sahara) are around 0.35 [US EIA, 2018b], yielding an expected generation of about 3.2 TW. For solar infrastructure, we assume an annual average insolation of $S = 320$ W/m^2 for the Sahara [Labed, 2008]. Assuming $\eta = 15\%$ conversion efficiency, $\alpha_p = 0.1$ panel reflectivity, and $\rho = 20\%$ area coverage by the panels, yields $S \times [\eta \times (1 - \alpha_p)] \times [\rho \times A] = 79$ TW of electrical power generation, averaged over a typical year. In comparison, the average rate of global consumption of energy is about 18 TW [IEA, 2017].

B.2.2 Feasibility of the transmission of electricity generated in the Sahara by wind and solar farms to other regions

The export of electricity from the Sahara would require the use of long-distance electricity transmission systems such as High Voltage Direct Current (HVDC). HVDC can dramatically reduce the line losses in the transmission of electricity over long distances, and also has lower construction costs compared to Alternating Current (AC) lines [US EIA, 2018a]. For example, according to Siemens [1], their Ultra High Voltage Direct Current (UHVDC) system at 800 kV has less than 3% line losses for every 1,000 kilometers with a transmission capacity of 10 GW over a single UHVDC link across transmission lengths of over 2,000 km. Their converter stations at the end of the line to convert to local AC systems have losses of approximately 0.7% of rated power. As to the feasibility of the required long distance transmission systems, we compare already existing long-distance HVDC transmission distances in developing countries with those required for the export of renewable power from the Sahara. We first estimate the approximate distances that would be required to export energy from North Africa to Europe: the distance from Tunis, Tunisia to Rome, Italy is 601 km, Rabat, Morocco to Madrid, Spain is 770 km, and Algiers, Algeria to Paris, France is 1,347 km. With regards to supplying energy to Sub-Saharan Africa, the distance from Niamey, Niger to Lagos, Nigeria is 790 km, Agadez, Niger to Abuja, Nigeria is 881 km, Timbuktu, Mali to Abidjan, Côte d'Ivoire is 1,275 km,

[1] Benefits of HVDC Classic. Available at https://www.energy.siemens.com/hq/en/power-transmission/hvdc/hvdc-classic.htm. Accessed June 28, 2018

Khartoum, Sudan to Addis Ababa, Ethiopia is 990 km, and from Khartoum all the way to Nairobi, Kenya is 1,927 km. For comparison, the following existing long distance HVDC projects were compiled from various sources [2]. China alone already has over 20 HVDC lines, each over ~900 km in length, with a total length of over 28,000 km. The Jinping–Sunan and the Xiangjiaba—-Shanghai HVDC transmission lines are each over 2,000 km. India has 9 HVDC lines each over 700 km long, including the 1,830 km Tamil Nadu line and the 1,728 km North- East Agra line. In Brazil, the Rio Madeira HVDC link, connecting Rondnia to So Paulo is composed of two sets of 600 kV DC lines of 3 GW capacity each over 2,375 km. Brazil completed two other 600 kV Itaipu HVDC lines each with a rated power of 3 GW and a total distance of 1,650 km as early as 1987, and Brazil began construction of the ~2,100 km Xingu–Estreito HVDC transmission line in 2017. As with other infrastructure, it is expected that as the scale of construction continues to grow, voltage and distance capacities will also increase. For example, in 2017 China began construction of the record-breaking 1100 kV ~3,300 km UHVDC Xinjiang–Anhui link, which will transmit 10–12 GW. At 1100 kV, this UHVDC link will significantly reduce line losses even further. Furthermore, long-distance HVDC transmission lines have already

[2](a)SIEMENS HVDC reference projects. Available at https://www.energy.siemens.com/us/en/power-transmission/hvdc/references.htm. Accessed June 28, 2018. (b) ABB HVDC reference projects. Available at https://new.abb.com/systems/hvdc/references/. Accessed June 28, 2018. (c) HVDC PROJECTS LISTING Prepared for the HVDC and Flexible AC Transmission Subcommittee of the IEEE Transmission and Distribution Committee. Available at http://www.ece.uidaho.edu/hvdcfacts/Projects/HVDCProjectsListingMarch2012-existing.pdf. Accessed June 28, 2018.

existed in Africa for decades. For example, the 1,700 km Inga–Shaba Extra High Voltage (EHVDC) Intertie transmission line in the Democratic Republic of Congo was completed in 1982. The 1,420 km Cahora–Bassa HVDC transmission line from Mozambique to South Africa was completed in 1979. Other kinds of development projects on this scale of distance also already exist deep within the Sahara itself. Starting in the 1980s, Libya built ~2,800 km of underground pipes to supply the cities on the coast with ~6,500,000 m3 of freshwater per day from over 1,300 wells in the Nubian Sandstone Aquifer System located deep in the Sahara (50). These examples demonstrate that the long distance transmission required is technologically feasible and already in use, which allows the long distance transmission of renewable power to be economically viable. Solar power projects in North Africa and the Middle East are already underway. Examples include: Dubai's Al Maktoum Solar Park (Phase 1 (13MW) completed 2013, Phase 2 (200 MW) completed 2017, and Phase 3 (800 MW) due 2020; Abu Dhabi's Shams solar plant, Phase 1 (100 MW) completed 2014; Saudi Arabia's Al-Aflaj 50 MW solar plant; Kuwait's Shagaya solar project (50 MW); and Morocco's Noor solar plant (580 MW), phase 1 (160 MW) completed 2016 (Morocco already has a transmission link to Europe) (51, 52). Saudi Arabia recently announced a plan to install 200 GW of solar power by 2030, at a projected cost of 200 billion USD (i.e., at an average cost of $1 per Watt) [3]. Investments on this scale would likely lead to further reductions in the costs of both photovoltaics

[3] Saudi Arabia To Build Massive Solar Power Installation. Available at https://www.forbes.com/sites/ellenrwald/2018/03/29/saudi-arabia-to-build-massive-solar-power-installation/. Accessed June 28, 2018.

and transmission infrastructure. In assessing the comparative costs, one also has to take into account that with renewables, there is the one-time cost of transporting the generation infrastructure to the location of generation, whereas with the current system of fossil fuel-based generation, in addition to the one-time cost of transporting the generation infrastructure to the location of generation, there is the continuous cost of transporting the stream of fuels (coal, oil, and gas) to the generation plants. For coal and nuclear, there is also the additional cost of transporting the waste for disposal, and the energy required for processing and disposing of the waste. Costs should also be compared to benefits. Today, the Sahel region is the poorest region on the planet. It is also the region with the fastest rate of population growth, and with the highest forecast for its future absolute population growth [United Nations, 2017; van Ittersum et al., 2016]. With massive investment in solar and wind generation, the region could not only meet its own rapidly growing electricity needs, but it could also become a major electricity exporter to other regions in Sub-Saharan Africa, providing needed earnings to fund the internal economic development of this very poor region. If these investments in wind and solar power production were to also increase local precipitation and vegetation growth through similar vegetation feedback mechanisms involved in the Green Sahara [Brovkin et al., 1998], this could provide these regions with increased agricultural production. Moreover, the availability of massive amounts of clean, renewable energies could help greatly with desalination and transport of seawater, as well as recycling and reuse of consumed freshwater. These processes, which can alleviate the problems associated with water scarcity (such as famines), are currently employed only in few places around the

Unit:	Control		Wind farm		Solar farm		Wind + Solar	
mm/day	Sahara	Sahel	Sahara	Sahel	Sahara	Sahel	Sahara	Sahel
Precipitation	0.24	2.23	+0.29	+1.12	+0.13	+0.57	+0.35	+1.34

Table B.1: Precipitation changes averaged over the Sahara wind farm locations and averaged over the whole Sahel region. Sahel region is defined as the rectangular land area with latitudes from 10N to 20N and longitudes from 20W to 30E.

world because they are energy intensive, and therefore expensive. Improved availability of freshwater, in turn, will bring positive societal, economic, environmental, ecological, and health impacts. The interconnected nature of these factors renders the Sahara as an ideal testbed for research on the Human–Climate System and Food–Energy–Water Nexus.

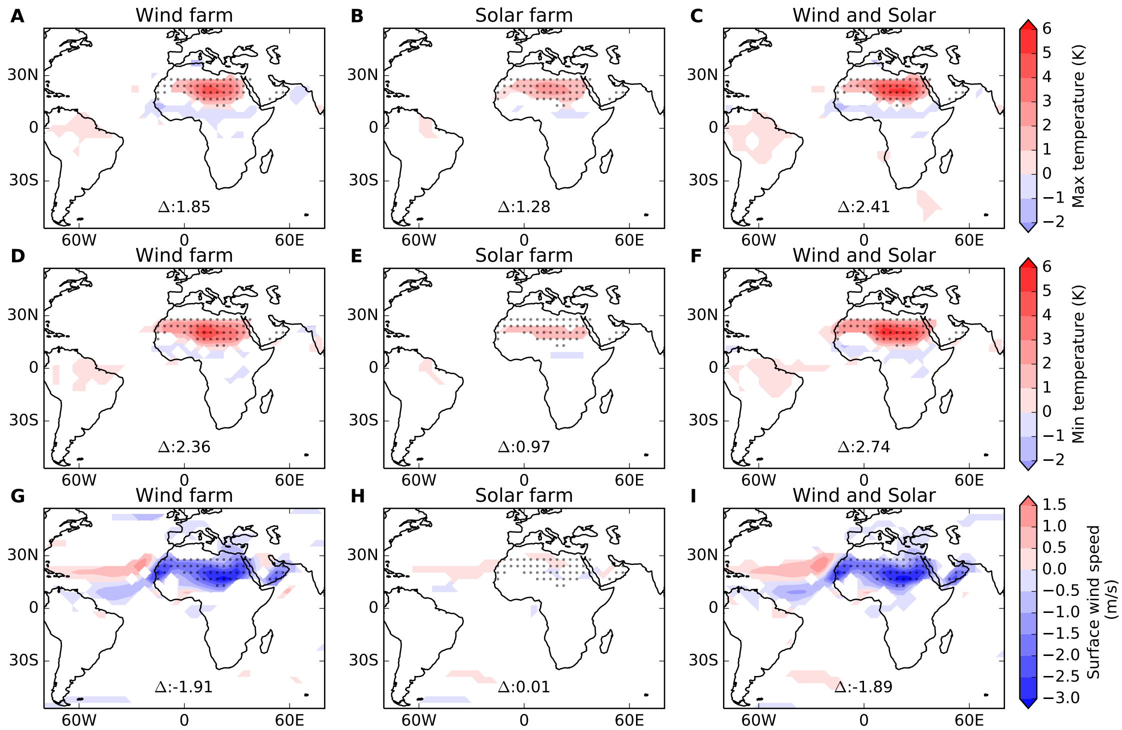

Figure B.1: Impacts of wind and solar farms in the Sahara on (A–C) maximum near-surface air temperature, (D–F) minimum near-surface air temperature, and (G–I) surface wind speed. Columns 1 to 3 show the impacts of wind farms, solar farms, and wind and solar farms together, respectively. Only areas with changes significant at 95% by the *t*-test are displayed on the map. Black dots on the map denote the location of wind/solar farms. The number after Δ shows the change in climate averaged over areas covered by wind farms. The average values from the control run (i.e., baseline) over the Sahara wind/solar farms locations are 299.46K for mean temperature (Fig. 1), 303.49 K for max temperature, 295.56 K for min temperature, and 5.09 m/s for surface wind speed.

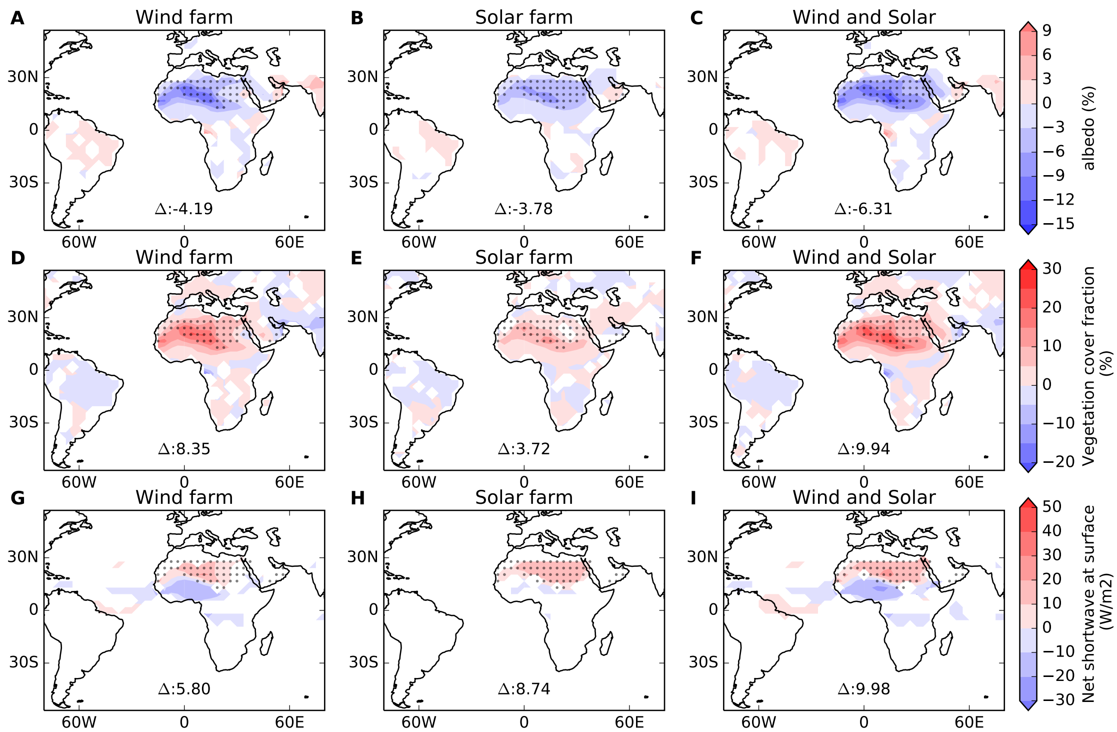

Figure B.2: Impacts of wind and solar farms in the Sahara on (A–C) albedo, (D–F) vegetation cover fraction, and (G–I) net shortwave radiation at surface. The average values from the control run (i.e., baseline) over the Sahara wind/solar farms locations are 0.34 for albedo, 0.35 for vegetation cover fraction, and 194.52 W/m^2 for net shortwave at surface.

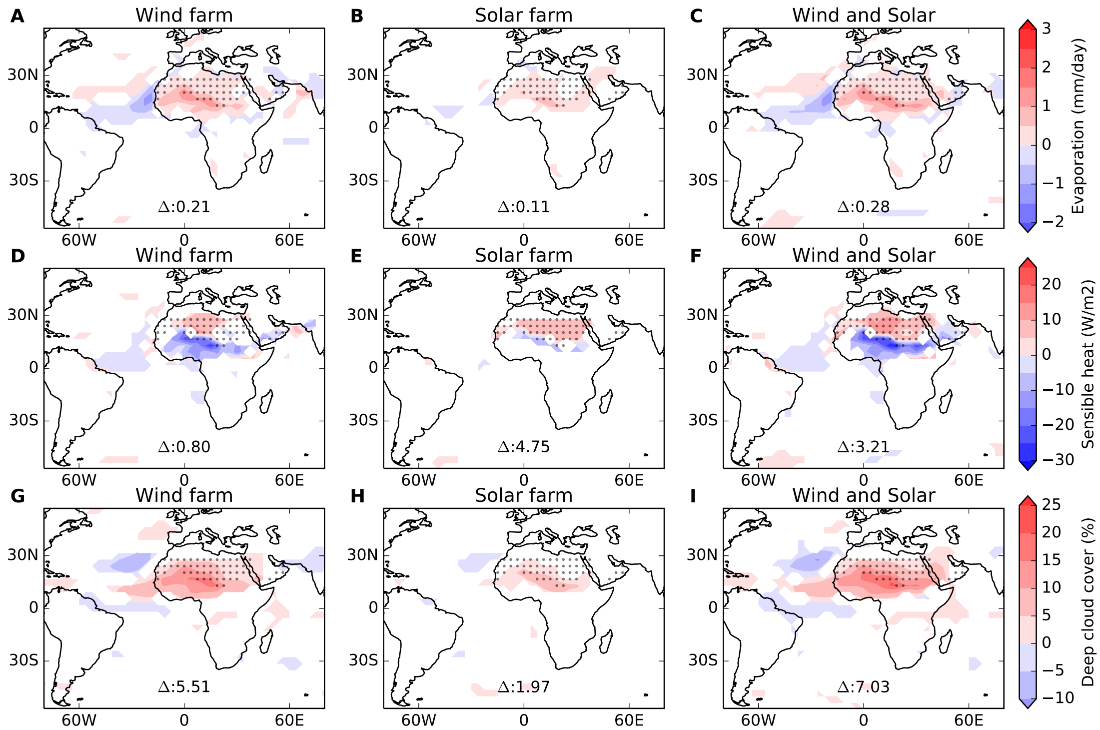

Figure B.3: Impacts of wind and solar farms in the Sahara on (A–C) evaporation, (D–F) sensible heat, and (G–I) deep cloud cover. The average values from the control run (i.e., baseline) over the Sahara wind/solar farms locations are 0.23 mm/day for evaporation, 49.89 W/m^2 for sensible heat, and 16.01% for deep cloud cover.

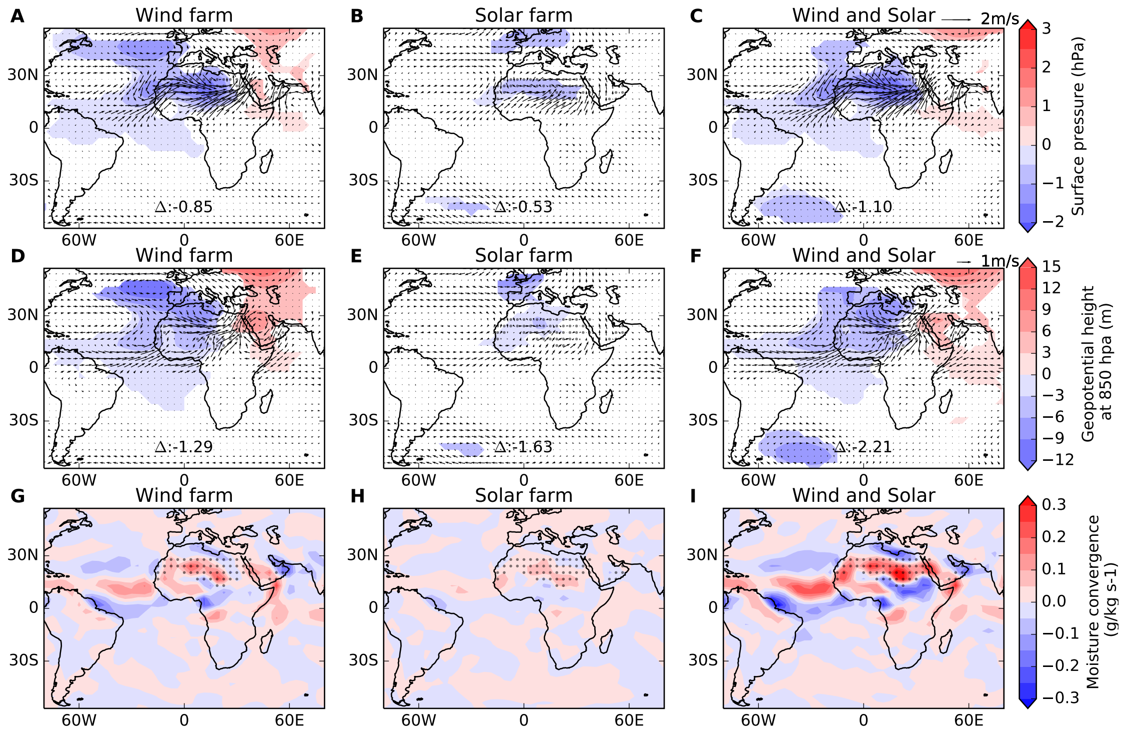

Figure B.4: Impacts of wind and solar farms in the Sahara on (A–C) surface pressure and surface wind field, (D–F) geopotential height and wind field at 850 hpa, and (G–I) moisture convergence. Note all changes for moisture convergence are shown on the map, including both significant and non-significant changes. The average values from the control run (i.e., baseline) over the Sahara wind/solar farms locations are 961.58 hPa for surface pressure, and 1517.81 m for geopotential height at 850 hPa.

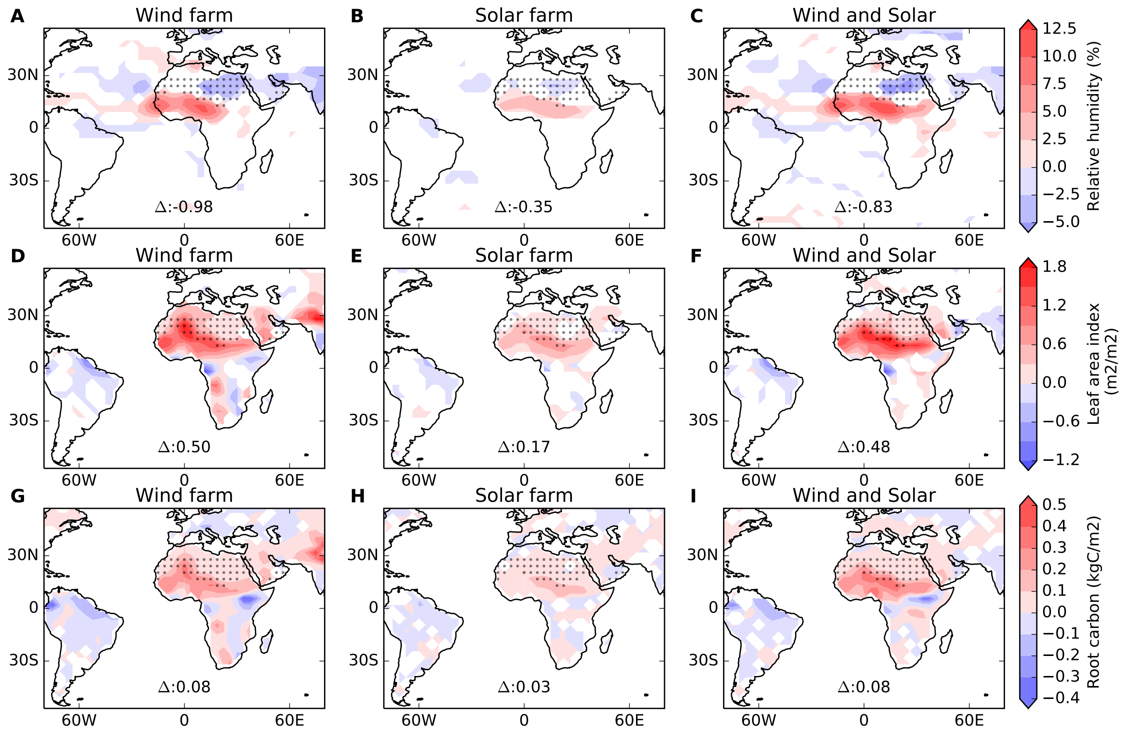

Figure B.5: Impacts of wind and solar farms in the Sahara on (A–C) relative humidity, (D–F) leaf area index (LAI), and (G–I) root carbon. The average values from the control run (i.e., baseline) over the Sahara wind/solar farms locations are 29.92% for relative humidity, 0.64 m^2/m^2 for leaf area index, and 0.095 kgC/m^2 for root carbon.

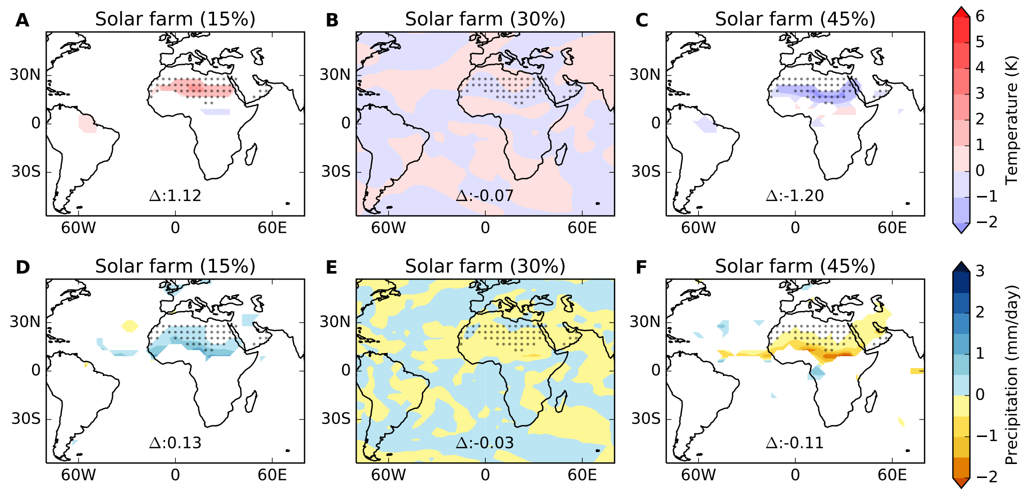

Figure B.6: Impacts of solar farms of varying PV panel solar conversion efficiencies (15% (A,D), 30% (B,E), and 45% (C,F)) in the Sahara on temperature and precipitation. Note that the impacts on regional climate from the 30% efficiency solar farms (B,E) are not significant (at the 95% level) but are shown here for display purposes. For 15% (A,D) and 45% (C,F) PV efficiencies, only significant changes are plotted, while white blank areas represent non-significant changes (at the 95% level).

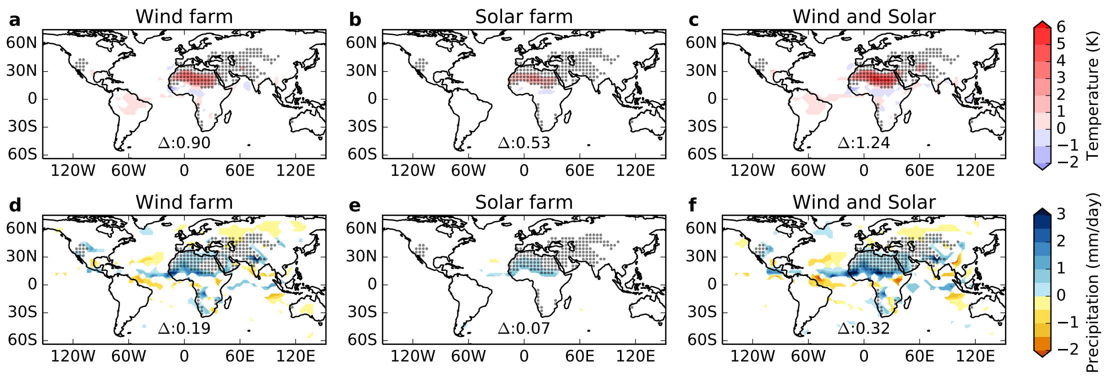

Figure B.7: Impacts of wind and solar farms in the world's deserts on near-surface mean temperature and precipitation. Rows 1 to 3 show the impacts of wind farms (A, B), solar farms (C, D), and wind and solar farms together (E, F). Only areas where changes are significant at 95% by the t-test are displayed on the map. Black dots on the map denote locations of wind farms/solar farms. The number after Δ at the bottom shows the changes in climate averaged over areas covered by wind/solar farms. The average values from the control run (i.e., baseline) over the global wind/solar farms locations are 249.64 K for mean temperature, and 0.55 mm/day for precipitation.

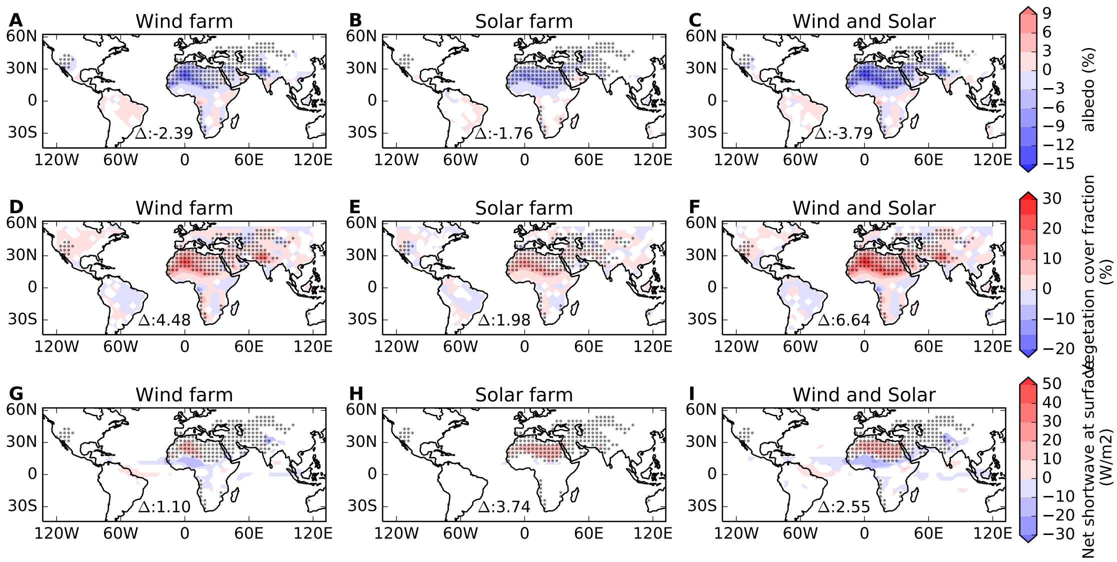

Figure B.8: Impacts of wind and solar farms in the world's deserts on (A–C) albedo, (D–F) vegetation cover fraction, and (G–I) net shortwave radiation at surface. The average values from the control run (i.e., baseline) over the global wind/solar farms locations are 0.29 for albedo, 0.46 for vegetation cover fraction, and 188.99 W/m^2 for net shortwave at surface.

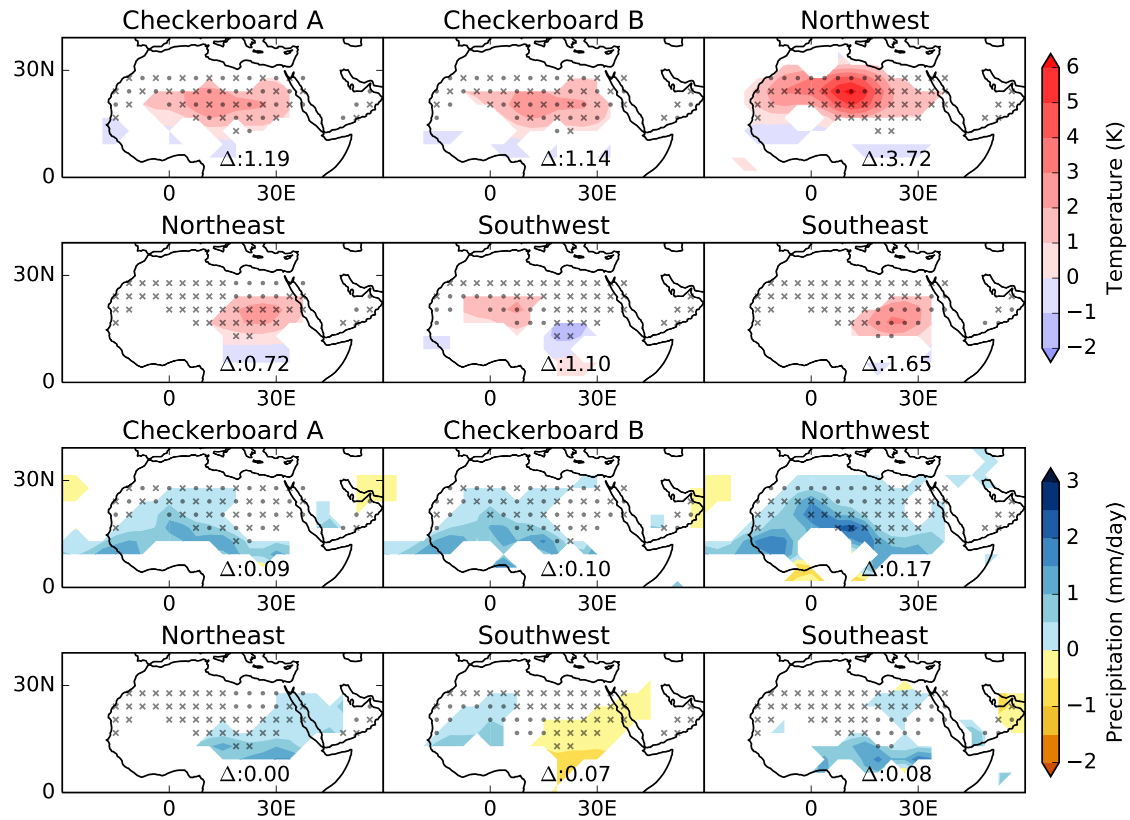

Figure B.9: Impacts of checkerboard (A, B) and quarter (northwest, northeast, southwest, southeast) layouts for wind farms in the Sahara. Wind farm locations are denoted by a "dot" and non-wind farm grid boxes by a "cross". The two checkerboard wind farm layouts cover the Sahara but with half the density of the full wind farm. The four quarter type wind farms are each of similar size but located in different quadrants of the Sahara (northeast, southeast, southwest, and northwest). The number after Δ shows the change in climate averaged over areas covered by wind farms. The results show that the northwest wind farm induces the largest precipitation and temperature changes.

Appendix C: Human and Nature Dynamics: Generation 2 (HANDY2)

Appendix C presents a proposed formulation for the second generation of the HANDY model [Motesharrei et al., 2014], HANDY2. HANDY2 introduces a novel categorization of natural resources: the stock of Nonrenewable resources (e.g., fossil energy, fossil water); the stock of Regenerating energy (e.g., crops, forest, biofuel, livestock), which is currently often categorized as renewable resources; and the Flows of Renewables (e.g., solar, wind, rain). From a systems point of view, Regenerating resources and Flows of Renewables are governed by very different laws, and distinguishing the two provides a fresh insight into sustainability studies of the natural systems, especially the energy systems, with results that could not be predicted and explained otherwise.

HANDY2 introduces endogenous mechanisms for distribution of labor into various sectors of the economy. This formulation with bidirectional interactions allows capturing real mechanisms that influence the variations in different sectors of the labor market due to availability level of different types of natural resources. Moreover, we model capital investments for extraction and production of various types of natural resources. This allows the model to capture the impacts of increased interest and investment in a particular type of resource on the long-term sustainability of natural resources as well as the stability prospects of the human system that depends on that natural system. Because HANDY2 includes all the three fundamental types of natural resources (Regenerating, Non-renewable, Flows of Renewables), it could provide a general formulation for Carrying Capacity of a coupled Earth–Human System.

HANDY2 provides the foundation upon which we will develop an Energy Model to couple with COWA, and later to the Agriculture Model. The coupled system will allow understanding fundamental interactions that challenge viability of the Food–Energy–Water Nexus Systems, and help us to propose, design, and test policies that can steer this interconnected system onto a sustainable path. Most importantly, the vision offered by our proposed coupled model helps to understand the dynamics of the whole system in the long term, which is the time scale of change in these human system. This vision paves the way for transitioning into a new paradigm of thinking about, and modeling of, human and natural systems.

C.1 Formulation of HANDY2

HANDY2 equations are given by:

$$
\begin{cases}
\dot{x}_C &= \beta_C x_C - \alpha_C x_C + \mu x_E \\
\dot{x}_E &= \beta_E x_E - \alpha_E x_E - \mu x_E \\
\dot{y}_R &= \gamma y_R(\lambda - y_R) - \delta_R(L_R x_C)(\eta_R y_R) \\
\dot{y}_N &= \qquad\qquad -\delta_N(L_N x_C)(\eta_N y_N) \\
\dot{w} &= \delta_R(L_R x_C)(\eta_R y_R) + \delta_N(L_N x_C)(\eta_N y_N) + \delta_F(L_F x_C)(\eta_F F) \\
 & \quad -C_C - C_E - I_R - I_N - I_F \\
\dot{A}_{R,N,F} &= I_{R,N,F} - \sigma_{R,N,F} A_{R,N,F}
\end{cases}
\tag{C.1}
$$

In this generation of HANDY, Nature is divided into three stocks: Regenerating (R), Nonrenewable (N), and Renewable Flows (F). Labor (x_C) is assigned to production from different types of Nature according to the labor assignment ratio, L given by the following set of equations

$$
\begin{cases}
L_R &= \dfrac{\delta_R x_C(\eta_R y_R)}{\delta_R x_C(\eta_R y_R) + \delta_N x_C(\eta_N y_N)}(1 - L_F) \\
L_N &= \dfrac{\delta_N x_C(\eta_N y_N)}{\delta_R x_C(\eta_R y_R) + \delta_N x_C(\eta_N y_N)}(1 - L_F) \\
L_F &= \min\left(\phi, \dfrac{1}{\delta_F x_C}\right)
\end{cases}
\tag{C.2}
$$

This definition for L_F ensures that the total production from flows of renewables is capped by the total accessible flow, $\eta_F F$. Here, ϕ denotes the ratio of the total investment in accessibility that is assigned to renewable flows (see (C.11)). An automatic constraint would be therefore $L_R + L_N + L_F = 1$.

As before, wealth threshold, w_{th}, is defined by:

$$w_{th} = \rho x_C + \kappa \rho x_E. \tag{C.3}$$

w_{th} can be used to define a dimensionless variable, ω:

$$\omega := \frac{w}{w_{th}}. \tag{C.4}$$

C_C and C_E, the consumption rates for the Commoner and the Elite respectively, are given by the same equations as in HANDY1:

$$\begin{cases} C_C &= \min(1, \omega) s x_C \\ C_E &= \min(1, \omega) \kappa s x_E \end{cases} \tag{C.5}$$

A graphical representation of the consumption rates are given in the figure below.

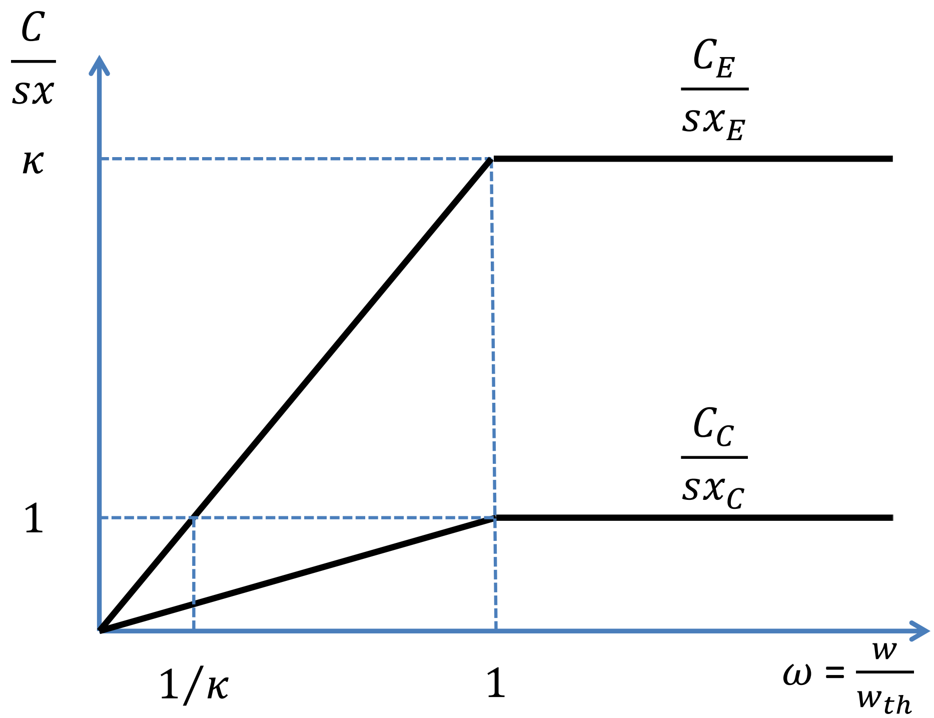

Figure C.1: Consumption rates for Elites and Commoners as a function of Wealth. Famine starts when $\frac{C}{sx} \leq 1$. Therefore, Commoners start experiencing famine when $\omega \leq 1$, while Elites do not experience famine until $\omega \leq \frac{1}{\kappa}$.

The death rates for the Commoner and the Elite, α_C and α_E, are the same functions (as in HANDY1) of the consumption rates:

$$\begin{cases} \alpha_C = \alpha_m + \max\left(0, 1 - \dfrac{C_C}{sx_C}\right)(\alpha_M - \alpha_m) \\ \\ \alpha_E = \alpha_m + \max\left(0, 1 - \dfrac{C_E}{sx_E}\right)(\alpha_M - \alpha_m) \end{cases} \tag{C.6}$$

The death rates can be graphically represented as a function of ω:

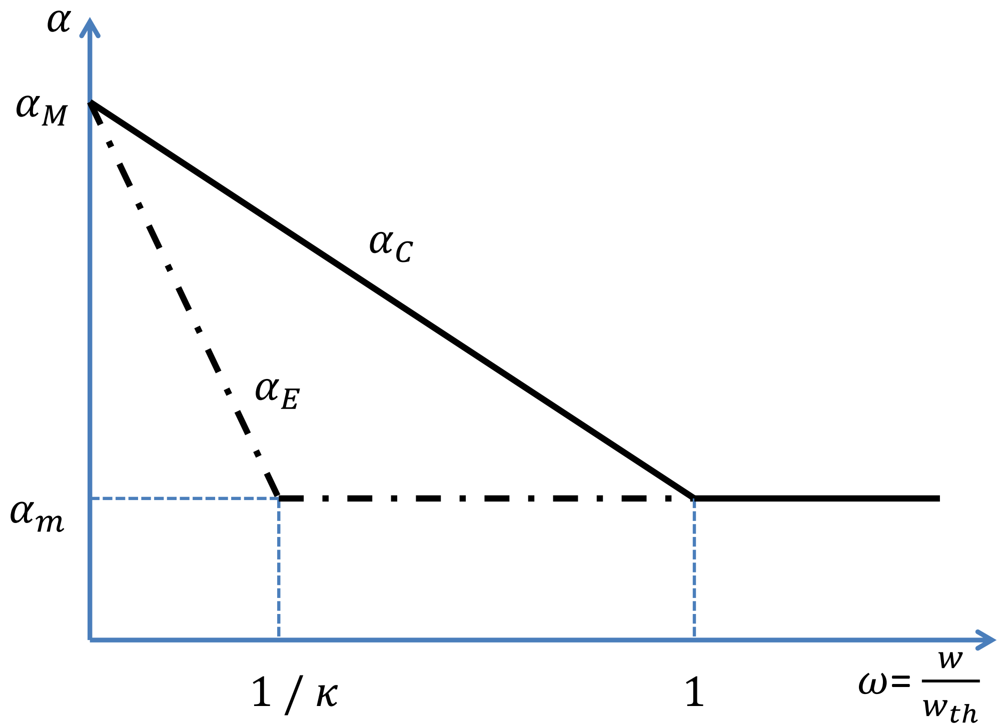

Figure C.2: Death rates for Elites and Commoners as a function of Wealth. Elites experience famine with a delay due to their unequal access to Wealth.

A new mechanism for *downward mobility* is introduced in HANDY2. As ω falls below a certain value, ω_o, which determines the onset of the mobility process, Elites start joining the Commoners at a per capita rate of μ, which is given as the following in terms of the maximum mobility rate, μ_M:

$$\mu(\omega) = \mu_M \left(1 - \frac{\omega}{\omega_o}\right). \tag{C.7}$$

See figure C.3 for a graphical representation of the mobility rate μ.

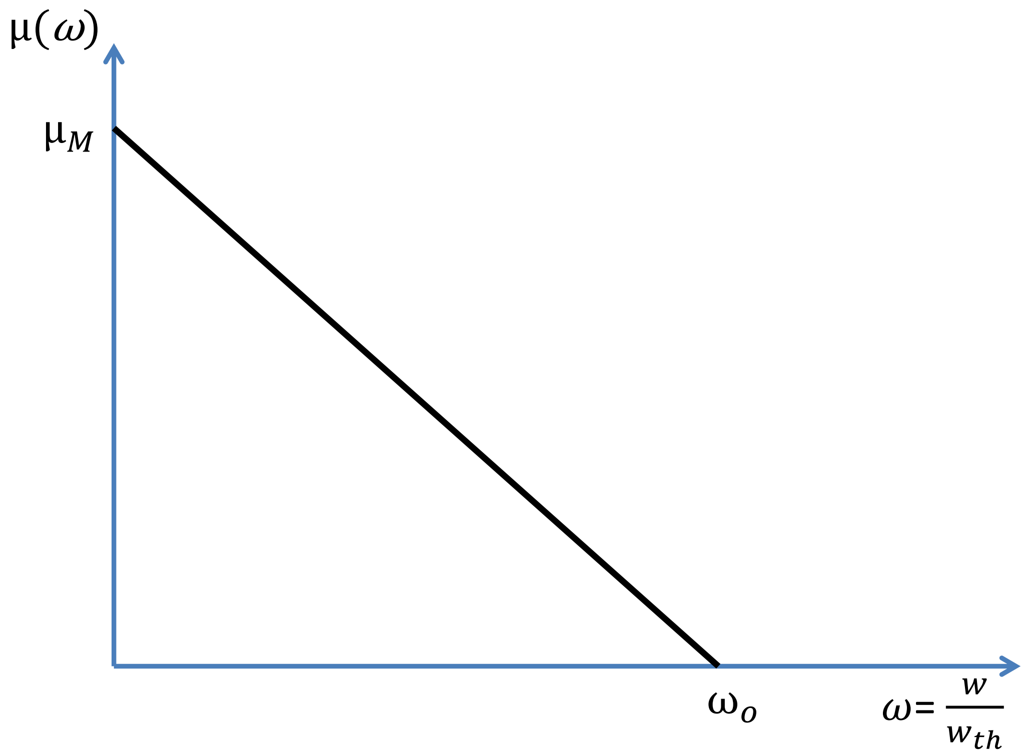

Figure C.3: Mobility rate in HANDY2 as a function of Wealth. Elites start becoming Commoners as Wealth drops below a certain threshold determined by ω_o.

A is the Accumulated investment in accessibility for different types of Nature. It can be normalized by defining a "threshold" value for it, A_{th}. Normalized accessibility investment, a, is thus defined by:

$$a := \frac{A}{A_{th}}. \tag{C.8}$$

The *accessibility factor*, η, is assumed to be a function of a:

$$\eta(a) = \frac{1}{1 + (\eta_m^{-1} - 1)e^{-a}}. \tag{C.9}$$

Its graphical representation is:

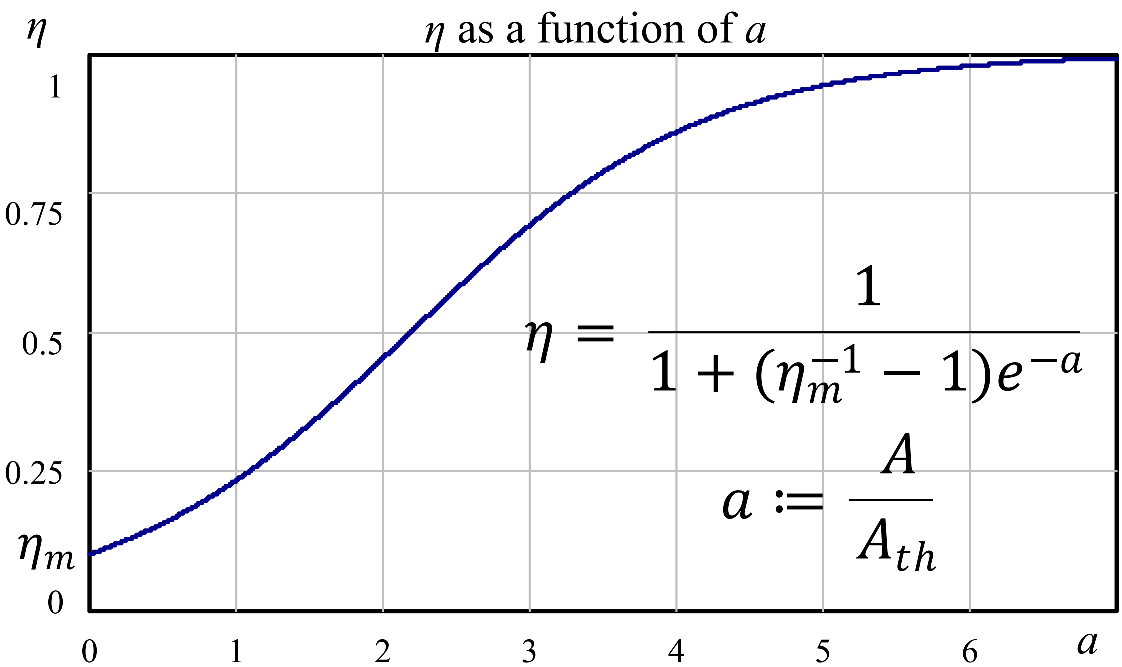

Figure C.4: Accessibility factor, η, as a function of accumulated investment in accessibility, A.

I is the total *Investment in accessibility*. We choose a *base investment in accessibility*, J, in order to normalize I. Normalized I is assumed to be a function of ω:

$$\frac{I}{J} = \begin{cases} \theta(\omega - 1) & \text{if } \omega \geq 1 \\ 0 & \text{if } \omega < 1 \end{cases} \tag{C.10}$$

θ is a dimensionless parameter that can be tweaked in order to vary the rate of investment as ω increases. A graphical representation of the above equation is given below.

From the total investment, a portion ϕ is invested in accessing renewable flows, and the rest is divided between regenerating and nonrenewable sectors:

$$\begin{cases} I_R = \frac{y_R}{y_R+y_N}(1-\phi)I \\ I_N = \frac{y_N}{y_R+y_N}(1-\phi)I \\ I_F = \phi I \end{cases} \tag{C.11}$$

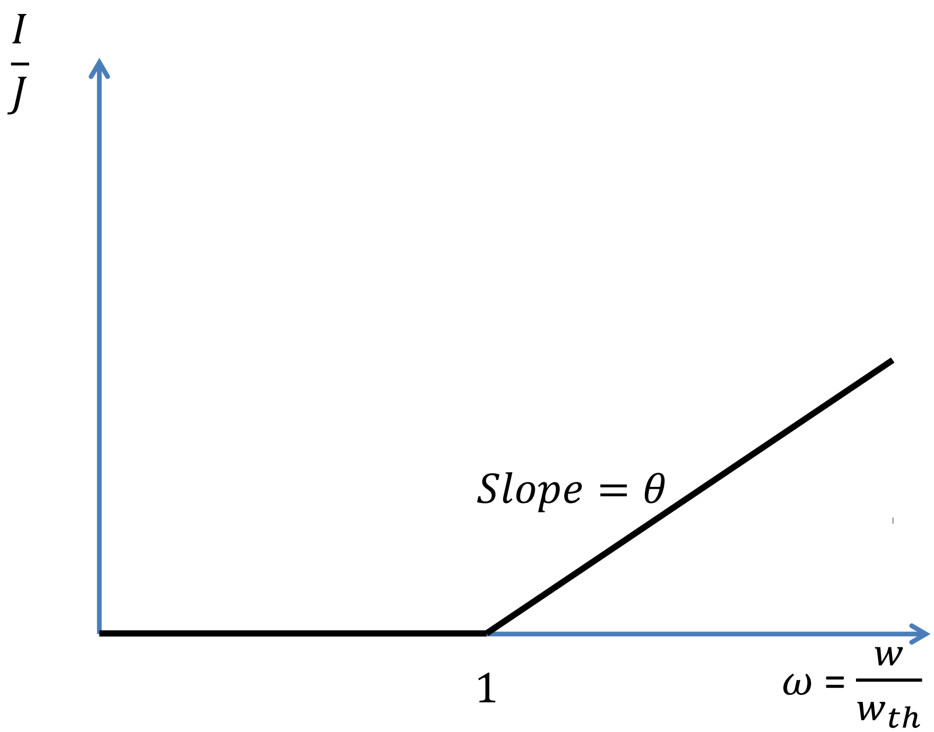

Figure C.5: Investment in accessibility, I, as a function of wealth, w.

Table C.1: Description of Parameters used in HANDY2

Parameter Symbol	Parameter Name	Typical Value(s)
α_m	Normal (Minimum) Death rate	1.0×10^{-2}
α_M	Famine (Maximum) Death rate	7.0×10^{-2}
β_C	Commoner Birth rate	3.0×10^{-2}
β_E	Elite Birth rate	3.0×10^{-2}
s	Subsistence Salary per Capita	5.0×10^{-4}
ρ	Threshold Wealth per Capita	5.0×10^{-3}
γ	Regeneration rate of Nature	1.0×10^{-2}
λ	(Regenerating) Nature Carrying Capacity	$1.0 \times 10^{+2}$
F	Rate of Flow of Renewables	
κ	Inequality factor	$1, 10, 100$
μ_M	Maximum Mobility rate	
ω_o	Mobility Onset	
δ_R	Production Factor for Regenerating Nature	
δ_N	Production Factor for Nonrenewables	
δ_F	Production Factor for Renewable Flows	
J	Base Investment in Accessibility	
θ	rate of Investment in Accessibility	
ϕ	ratio of investment in accessibility of renewable flows	
A_{th}	(array of) Threshold of Accumulated Accessibility Investment	
σ	(array of) Accessibility Investment Depreciation rate	

Variable Symbol	Variable Name	Typical Initial Value(s)
x_C	Commoner Population	$1.0 \times 10^{+2}$
x_E	Elite Population	$0, 1, 25$
y_R	Regenerating Nature	λ
y_N	Nonrenewable Nature	
w	Accumulated Wealth	0
A	(array of) Accumulated Investment in Accessibility	

Table C.2: List of state variables in HANDY2. $x_E(0)$ takes different values for different scenarios.

Variable Symbol	Variable Name	Defining Equation
w_{th}	Threshold Wealth	(C.3)
ω	Normalized Wealth	w/w_{th}
C_C	Commoner Consumption	(C.5) (figure C.1)
C_E	Elite Consumption	(C.5) (figure C.1)
α_C	Commoner Death Rate	(C.6) (figure C.2)
α_E	Elite Death Rate	(C.6) (figure C.2)
μ	Downward Mobility	(C.7) (figure C.3)
L	(array of) Labor Assignment ratio	(C.2)
I	Investment in Accessibility	(C.11)
a	(array of) Normalized Accumulated Investment in Accessibility	(C.8)
η	(array of) Accessibility Factor	(C.9) (figure C.4)

Table C.3: As a reference, all auxiliary variables and functions in HANDY2 are listed in this table. Subscript e denotes *equilibrium* value everywhere in this paper.

Bibliography

Henry Abarbanel. *Analysis of observed chaotic data*. Springer, 1996.

Mohammad Jalal Abbasi-Shavazi, Peter McDonald, and Meimanat Hosseini-Chavoshi. *The Fertility Transition in Iran: Revolution and Reproduction*. Springer Netherlands, Dordrecht, 2009. ISBN 978-90-481-3197-6 978-90-481-3198-3. URL http://link.springer.com/10.1007/978-90-481-3198-3.

Guy J. Abel and Nikola Sander. Quantifying Global International Migration Flows. *Science*, 343(6178):1520–1522, March 2014. ISSN 0036-8075, 1095-9203. doi: 10.1126/science.1248676. URL http://www.sciencemag.org/content/343/6178/1520.

ACE. 2016 Report to Congress on Future Water Resources Development. Technical report, The United States Army Corps of Engineers, February 2016. URL http://www.usace.army.mil/Portals/2/docs/civilworks/Project%20Planning/wrda/2014/2016Report_FutureWaterResources.pdf.

ADWR. Arizona Water Atlas Vol. 8 Active Managament Areas. Technical report, Arizona Department of Water Resources, 2010. URL http://www.azwater.gov/AzDWR/StatewidePlanning/WaterAtlas/Volume1ExecutiveSummary.htm.

Werner Aeschbach-Hertig and Tom Gleeson. Regional strategies for the accelerating global problem of groundwater depletion. *Nature Geoscience*, 5(12):853–861, December 2012. ISSN 1752-0894. doi: 10.1038/ngeo1617. URL http://www.nature.com/ngeo/journal/v5/n12/abs/ngeo1617.html.

Sajjad Ahmad and Dinesh Prashar. Evaluating municipal water conservation policies using a dynamic simulation model. *Water resources management*, 24(13):3371–3395, 2010. URL http://link.springer.com/article/10.1007/s11269-010-9611-2.

Sudhir Anand and Amartya Sen. Human development Index: Methodology and Measurement. Human Development Occasional Papers (1992-2007) HDOCPA-1994-02, Human Development Report Office (HDRO), United Nations Development Programme (UNDP), 1994. URL https://ideas.repec.org/p/hdr/hdocpa/hdocpa-1994-02.html.

J. Anderson. The environmental benefits of water recycling and reuse. *Water Science and Technology: Water Supply*, 3(4):1–10, August 2003. ISSN 1606-9749. doi: 10.2166/ws.2003.0041. URL /ws/article/3/4/1/25794/The-environmental-benefits-of-water-recycling-and.

Jeffrey L. Anderson. An Ensemble Adjustment Kalman Filter for Data Assimilation. *Monthly Weather Review*, 129(12):2884–2903, December 2001. ISSN 0027-0644. doi: 10.1175/1520-0493(2001)129⟨2884:AEAKFF⟩2.0.CO;2. URL http://journals.ametsoc.org/doi/abs/10.1175/1520-0493(2001)129%3C2884:AEAKFF%3E2.0.CO;2.

J. D. Annan and J. C. Hargreaves. Efficient parameter estimation for a highly chaotic system. *Tellus A*, 56(5):520–526, October 2004. ISSN 1600-0870. doi: 10.1111/j.1600-0870.2004.00073.x. URL http://onlinelibrary.wiley.com/doi/10.1111/j.1600-0870.2004.00073.x/abstract.

J. D. Annan, D. J. Lunt, J. C. Hargreaves, and P. J. Valdes. Parameter estimation in an atmospheric GCM using the Ensemble Kalman Filter. *Nonlinear Processes in Geophysics*, 12(3):363–371, February 2005. URL https://hal.archives-ouvertes.fr/hal-00302567.

Alona Armstrong, Ralph R. Burton, Susan E. Lee, Stephen Mobbs, Nicholas Ostle, Victoria Smith, Susan Waldron, and Jeanette Whitaker. Ground-level climate at a peatland wind farm in Scotland is affected by wind turbine operation. *Environmental Research Letters*, 11(4):044024, 2016. ISSN 1748-9326. doi: 10.1088/1748-9326/11/4/044024. URL http://stacks.iop.org/1748-9326/11/i=4/a=044024.

Chester L. Arnold and C. James Gibbons. Impervious Surface Coverage: The Emergence of a Key Environmental Indicator. *Journal of the American Planning Association*, 62(2):243–258, June 1996. ISSN 0194-4363. doi: 10.1080/01944369608975688. URL http://dx.doi.org/10.1080/01944369608975688.

Millennium Ecosystem Assessment. *Ecosystems and human well-being: Synthesis*, volume 5. Island Press, Washington, DC, 2005. URL http://www.millenniumassessment.org/documents/document.356.aspx.pdf.

Nihat Ay and Daniel Polani. Information flows in causal networks. *Advances in Complex Systems*, 11(01):17–41, 2008. doi: 10.1142/S0219525908001465. URL http://www.worldscientific.com/doi/abs/10.1142/S0219525908001465.

Giovanni Baiocchi, Jan Minx, and Klaus Hubacek. The Impact of Social Factors and Consumer Behavior on Carbon Dioxide Emissions in the United Kingdom. *Journal of Industrial Ecology*, 14(1):50–72, January 2010. ISSN 1530-9290. doi: 10.1111/j.1530-9290.2009.00216.x. URL http://onlinelibrary.wiley.com/doi/10.1111/j.1530-9290.2009.00216.x/abstract.

Alexander V. Balatsky, Galina I. Balatsky, and Stanislav S. Borysov. Resource Demand Growth and Sustainability Due to Increased World Consumption. *Sustainability*, 7(3):3430–3440, March 2015. doi: 10.3390/su7033430. URL http://www.mdpi.com/2071-1050/7/3/3430.

Ki-moon Ban. A Climate Culprit In Darfur. *The Washington Post*, June 2007. ISSN 0190-8286. URL http://www.washingtonpost.com/wp-dyn/content/article/2007/06/15/AR2007061501857.html.

World Bank. World Development Indicators 2014. Technical report, World Bank, 2014a. URL http://wdi.worldbank.org/table/3.8.

World Bank. World Development Indicators 2014: Table 3.8: Energy dependency, efficiency and carbon dioxide emissions. Technical report, World Bank, 2014b. URL http://wdi.worldbank.org/table/3.8.

Alisson F. Barbieri, Edson Domingues, Bernardo L. Queiroz, Ricardo M. Ruiz, José I. Rigotti, José A. M. Carvalho, and Marco F. Resende. Climate change and population migration in Brazil's Northeast: scenarios for 2025–2050. *Population and Environment*, 31(5):344–370, March 2010. ISSN 0199-0039, 1573-7810. doi: 10.1007/s11111-010-0105-1. URL http://link.springer.com/article/10.1007/s11111-010-0105-1.

Jon Barnett. Security and climate change. *Global Environmental Change*, 13 (1):7–17, April 2003. doi: 10.1016/S0959-3780(02)00080-8. URL http://www.sciencedirect.com/science/article/pii/S0959378002000808.

Lionel Barnett and Anil K. Seth. The MVGC multivariate granger causality toolbox: A new approach to granger-causal inference. *Journal of Neuroscience Methods*, 223(0):50 – 68, 2014. ISSN 0165-0270. doi: http://dx.doi.org/10.1016/j.jneumeth.2013.10.018. URL http://www.sciencedirect.com/science/article/pii/S0165027013003701.

Lionel Barnett, Adam B. Barrett, and Anil K. Seth. Granger causality and transfer entropy are equivalent for gaussian variables. *Phys. Rev. Lett.*, 103:238701, Dec 2009. doi: 10.1103/PhysRevLett.103.238701. URL http://link.aps.org/doi/10.1103/PhysRevLett.103.238701.

Tim P. Barnett, David W. Pierce, Hugo G. Hidalgo, Celine Bonfils, Benjamin D. Santer, Tapash Das, Govindasamy Bala, Andrew W. Wood, Toru Nozawa, Arthur A. Mirin, Daniel R. Cayan, and Michael D. Dettinger. Human-Induced Changes in the Hydrology of the Western United States. *Science*, 319(5866):1080–1083, February 2008. ISSN 0036-8075, 1095-9203. doi: 10.1126/science.1152538. URL http://science.sciencemag.org/content/319/5866/1080.

Anthony D. Barnosky, Elizabeth A. Hadly, Jordi Bascompte, Eric L. Berlow, James H. Brown, Mikael Fortelius, Wayne M. Getz, John Harte, Alan Hastings, Pablo A. Marquet, Neo D. Martinez, Arne Mooers, Peter Roopnarine, Geerat

Vermeij, John W. Williams, Rosemary Gillespie, Justin Kitzes, Charles Marshall, Nicholas Matzke, David P. Mindell, Eloy Revilla, and Adam B. Smith. Approaching a state shift in Earth's biosphere. *Nature*, 486(7401):52–58, June 2012. ISSN 0028-0836. doi: 10.1038/nature11018. URL http://www.nature.com/nature/journal/v486/n7401/full/nature11018.html.

John Barrett, Glen Peters, Thomas Wiedmann, Kate Scott, Manfred Lenzen, Katy Roelich, and Corinne Le Quéré. Consumption-based GHG emission accounting: a UK case study. *Climate Policy*, 13(4):451–470, July 2013. ISSN 1469-3062. doi: 10.1080/14693062.2013.788858. URL http://dx.doi.org/10.1080/14693062.2013.788858.

R. J. Barthelmie and S. C. Pryor. Potential contribution of wind energy to climate change mitigation. *Nature Climate Change*, 4(8):684–688, August 2014. ISSN 1758-6798. doi: 10.1038/nclimate2269. URL https://www.nature.com/articles/nclimate2269.

David S. Battisti and Rosamond L. Naylor. Historical Warnings of Future Food Insecurity with Unprecedented Seasonal Heat. *Science*, 323(5911):240–244, January 2009. ISSN 0036-8075, 1095-9203. doi: 10.1126/science.1164363. URL http://science.sciencemag.org/content/323/5911/240.

M. Bauer, J.W. Cox, M.H. Caveness, James J. Downs, and N.F. Thornhill. Finding the direction of disturbance propagation in a chemical process using transfer entropy. *Control Systems Technology, IEEE Transactions on*, 15(1):12–21, Jan 2007. ISSN 1063-6536. doi: 10.1109/TCST.2006.883234.

Kevin A. Baumert, Timothy Herzog, and Jonathan Pershing. *Navigating the numbers: Greenhouse gas data and international climate policy*. World Resources Institute, 2005. ISBN 1-56973-599-9. URL http://pdf.wri.org/navigating_numbers.pdf.

Morgan Bazilian, Holger Rogner, Mark Howells, Sebastian Hermann, Douglas Arent, Dolf Gielen, Pasquale Steduto, Alexander Mueller, Paul Komor, Richard S. J. Tol, and Kandeh K. Yumkella. Considering the energy, water and food nexus: Towards an integrated modelling approach. *Energy Policy*, 39(12):7896–7906, December 2011. doi: 10.1016/j.enpol.2011.09.039. URL http://www.sciencedirect.com/science/article/pii/S0301421511007282.

Richard O. Bierregaard, Thomas E. Lovejoy, Valerie Kapos, Angelo Augusto dos Santos, and Roger W. Hutchings. The Biological Dynamics of Tropical Rainforest Fragments. *BioScience*, 42(11):859–866, 1992. doi: 10.2307/1312085. URL http://www.jstor.org/stable/1312085.

Eloise M. Biggs, Eleanor Bruce, Bryan Boruff, John M. A. Duncan, Julia Horsley, Natasha Pauli, Kellie McNeill, Andreas Neef, Floris Van Ogtrop, Jayne Curnow, Billy Haworth, Stephanie Duce, and Yukihiro Imanari. Sustainable development and the water–energy–food nexus: A perspective on livelihoods. *Environmental Science & Policy*, 54:389–397, December 2015. ISSN 1462-9011. doi: 10.1016/j.envsci.2015.08.002. URL http://www.sciencedirect.com/science/article/pii/S1462901115300563.

Tom A. Boden, Gregg Marland, and Robert J. Andres. Global, regional, and national fossil fuel CO2 emissions. Technical report, Carbon Dioxide Information Analysis Center, Oak Ridge National Laboratory, U.S. Department of Energy, Oak Ridge, Tenn., U.S.A., 2013.

Jutta Bolt and Jan Luiten van Zanden. The Maddison Project: collaborative research on historical national accounts. *The Economic History Review*, 67(3):627–651, August 2014. ISSN 1468-0289. doi: 10.1111/1468-0289.12032. URL http://onlinelibrary.wiley.com/doi/10.1111/1468-0289.12032/abstract.

John Bongaarts. Development: Slow down population growth. *Nature*, 530(7591):409–412, February 2016. ISSN 0028-0836, 1476-4687. doi: 10.1038/530409a. URL http://www.nature.com/doifinder/10.1038/530409a.

Alexander F. Bouwman, Tom Kram, and Kees Klein Goldewijk. Integrated Modelling of Global Environmental Change, An Overview of IMAGE 2.4, Netherlands Environmental Assessment Agency. *MNP, Bilthoven, The Netherlands*, 2006.

Amir E. BozorgMagham, Safa Motesharrei, Stephen G. Penny, and Eugenia Kalnay. Causality Analysis: Identifying the Leading Element in a Coupled Dynamical System. *PLoS ONE*, 10(6):e0131226, June 2015. doi: 10.1371/journal.pone.0131226. URL http://dx.doi.org/10.1371/journal.pone.0131226.

Steven L. Bressler and Anil K. Seth. Wienergranger causality: A well established methodology. *NeuroImage*, 58(2):323 – 329, 2011. ISSN 1053-8119. doi: http://dx.doi.org/10.1016/j.neuroimage.2010.02.059. URL http://www.sciencedirect.com/science/article/pii/S1053811910002272.

Victor Brovkin, Martin Claussen, Vladimir Petoukhov, and Andrey Ganopolski. On the stability of the atmosphere-vegetation system in the Sahara/Sahel region. *Journal of Geophysical Research: Atmospheres*, 103(D24):31613–31624, December 1998. ISSN 2156-2202. doi: 10.1029/1998JD200006. URL https://agupubs.onlinelibrary.wiley.com/doi/abs/10.1029/1998JD200006.

Neville Brown. Climate, ecology and international security. *Survival*, 31(6):519–532, November 1989. ISSN 0039-6338. doi: 10.1080/00396338908442497. URL http://dx.doi.org/10.1080/00396338908442497.

Martin Bruckner, Stefan Giljum, Christian Lutz, and Kirsten Svenja Wiebe. Materials embodied in international trade – Global material extraction and consumption between 1995 and 2005. *Global Environmental Change*, 22(3):568–576, August 2012. ISSN 0959-3780. doi: 10.1016/j.gloenvcha.2012.03.011. URL http://www.sciencedirect.com/science/article/pii/S0959378012000350.

Gro Harlem Brundtland, Paul Ehrlich, Jose Goldemberg, James Hansen, Amory Lovins, Gene Likens, Syukuro Manabe, Robert May, Harold A. Mooney, Karl-Henrik Robert, Emil Salim, Gordon Sato, Susan Solomon, Nicholas Stern, MS Swaminathan, and Robert Watson. Environment and Development Challenges: The Imperative to Act. Technical report, Barefoot College, Conservation International, International institute for Environment and Development, and International Union for the Conservation of Nature, 2012. URL http://www.conservation.org/publications/Documents/CI_RIOplus20_Blue-Planet-Prize_Environment-and-Development-Challenges.pdf.

Jack Bryck, Rajesh Prasad, Trevor Lindley, Steve Davis, and Guy Carpenter. *National Database of Water Reuse Facilities Summary Report*. Number 02-004-01 in WRF-004-01. WateReuse Foundation, Alexandria, VA, 2008. ISBN 978-1-934183-01-4. URL https://www.watereuse.org/files/s/docs/02-004-01.pdf.

M. I. Budyko. The Heat Balance of the Earth's Surface. *Soviet Geography*, 2(4):3–13, January 1961. ISSN 0038-5417. doi: 10.1080/00385417.1961.10770761. URL http://dx.doi.org/10.1080/00385417.1961.10770761.

R. Buizza, J. Tribbia, F. Molteni, and T. Palmer. Computation of optimal unstable structures for a numerical weather prediction model. *Tellus A*, 45(5): 388–407, October 1993. ISSN 1600-0870. doi: 10.1034/j.1600-0870.1993.t01-4-00005.x. URL http://onlinelibrary.wiley.com/doi/10.1034/j.1600-0870.1993.t01-4-00005.x/abstract.

R. Buizza, M. Milleer, and T. N. Palmer. Stochastic representation of model uncertainties in the ECMWF ensemble prediction system. *Quarterly Journal of the Royal Meteorological Society*, 125(560):2887–2908, October 1999. ISSN 1477-870X. doi: 10.1002/qj.49712556006. URL http://onlinelibrary.wiley.com/doi/10.1002/qj.49712556006/abstract.

Marshall B. Burke, Edward Miguel, Shanker Satyanath, John A. Dykema, and David B. Lobell. Warming increases the risk of civil war in Africa. *Proceedings of the National Academy of Sciences*, 106(49):20670–20674, December 2009. ISSN 0027-8424, 1091-6490. doi: 10.1073/pnas.0907998106. URL http://www.pnas.org/content/106/49/20670.

Wei-Jun Cai, Xinping Hu, Wei-Jen Huang, Michael C. Murrell, John C. Lehrter, Steven E. Lohrenz, Wen-Chen Chou, Weidong Zhai, James T. Hollibaugh, Yongchen Wang, Pingsan Zhao, Xianghui Guo, Kjell Gundersen, Minhan Dai, and Gwo-Ching Gong. Acidification of subsurface coastal waters enhanced by eutrophication. *Nature Geoscience*, 4(11):766–770, November 2011. ISSN 1752-0894. doi: 10.1038/ngeo1297. URL http://www.nature.com/ngeo/journal/v4/n11/full/ngeo1297.html.

Wenju Cai, Simon Borlace, Matthieu Lengaigne, Peter van Rensch, Mat Collins, Gabriel Vecchi, Axel Timmermann, Agus Santoso, Michael J. McPhaden, Lixin

Wu, Matthew H. England, Guojian Wang, Eric Guilyardi, and Fei-Fei Jin. Increasing frequency of extreme El Niño events due to greenhouse warming. *Nature Climate Change*, 4(2):111–116, February 2014. ISSN 1758-678X. doi: 10.1038/nclimate2100. URL http://www.nature.com/nclimate/journal/v4/n2/full/nclimate2100.html#affil-auth.

Wenju Cai, Guojian Wang, Agus Santoso, Michael J. McPhaden, Lixin Wu, Fei-Fei Jin, Axel Timmermann, Mat Collins, Gabriel Vecchi, Matthieu Lengaigne, Matthew H. England, Dietmar Dommenget, Ken Takahashi, and Eric Guilyardi. Increased frequency of extreme La Niña events under greenhouse warming. *Nature Climate Change*, 5(2):132–137, February 2015. ISSN 1758-678X. doi: 10.1038/nclimate2492. URL http://www.nature.com/nclimate/journal/v5/n2/abs/nclimate2492.html.

Nicolas Caillon, Jeffrey P. Severinghaus, Jean Jouzel, Jean-Marc Barnola, Jiancheng Kang, and Volodya Y. Lipenkov. Timing of atmospheric co2 and antarctic temperature changes across termination iii. *Science*, 299(5613):1728–1731, 2003. doi: 10.1126/science.1078758. URL http://www.sciencemag.org/content/299/5613/1728.abstract.

Katherine Calvin, Marshall Wise, Leon Clarke, Jae Edmonds, Page Kyle, Patrick Luckow, and Allison Thomson. Implications of simultaneously mitigating and adapting to climate change: initial experiments using GCAM. *Climatic Change*, 117(3):545–560, April 2013. ISSN 0165-0009, 1573-1480. doi: 10.1007/s10584-012-0650-y. URL http://link.springer.com/article/10.1007/s10584-012-0650-y.

Martha Campbell, Nuriye Nalan Sahin-Hodoglugil, and Malcolm Potts. Barriers to Fertility Regulation: A Review of the Literature. *Studies in Family Planning*, 37(2):87–98, June 2006. ISSN 1728-4465. doi: 10.1111/j.1728-4465.2006.00088.x. URL http://onlinelibrary.wiley.com/doi/10.1111/j.1728-4465.2006.00088.x/abstract.

Martha M. Campbell, Ndola Prata, and Malcolm Potts. The impact of freedom on fertility decline. *Journal of Family Planning and Reproductive Health Care*, 39(1):44–50, January 2013. ISSN 1471-1893, 2045-2098. doi: 10.1136/jfprhc-2012-100405. URL http://jfprhc.bmj.com/content/39/1/44.

Mark A. Cane, Stephen E. Zebiak, and Sean C. Dolan. Experimental forecasts of El Niño. *Nature*, 321(6073):827–832, June 1986. ISSN 0028-0836. doi: 10.1038/321827a0. URL http://www.nature.com/nature/journal/v321/n6073/abs/321827a0.html.

Donald E. Canfield, Alexander N. Glazer, and Paul G. Falkowski. The Evolution and Future of Earth's Nitrogen Cycle. *Science*, 330(6001):192–196, October 2010. ISSN 0036-8075, 1095-9203. doi: 10.1126/science.1186120. URL http://science.sciencemag.org/content/330/6001/192.

Liangyue Cao. Practical method for determining the minimum embedding dimension of a scalar time series. *Physica D: Nonlinear Phenomena*, 110(12): 43 – 50, 1997. ISSN 0167-2789. doi: http://dx.doi.org/10.1016/S0167-2789(97)00118-8. URL http://www.sciencedirect.com/science/article/pii/S0167278997001188.

Jacob Carstensen, Jesper H. Andersen, Bo G. Gustafsson, and Daniel J. Conley. Deoxygenation of the Baltic Sea during the last century. *Proceedings of the National Academy of Sciences*, 111(15):5628–5633, April 2014. ISSN 0027-8424, 1091-6490. doi: 10.1073/pnas.1323156111. URL http://www.pnas.org/content/111/15/5628.

Stephanie L. Castle, Brian F. Thomas, John T. Reager, Matthew Rodell, Sean C. Swenson, and James S. Famiglietti. Groundwater depletion during drought threatens future water security of the Colorado River Basin. *Geophysical Research Letters*, 41(16):2014GL061055, August 2014. ISSN 1944-8007. doi: 10.1002/2014GL061055. URL http://onlinelibrary.wiley.com/doi/10.1002/2014GL061055/abstract.

William R. Catton. *Overshoot: The Ecological Basis of Revolutionary Change*. University of Illinois Press, 1980.

Gerardo Ceballos, Paul R. Ehrlich, and Rodolfo Dirzo. Biological annihilation via the ongoing sixth mass extinction signaled by vertebrate population losses and declines. *Proceedings of the National Academy of Sciences*, page 201704949, July 2017. ISSN 0027-8424, 1091-6490. doi: 10.1073/pnas.1704949114. URL http://www.pnas.org/content/early/2017/07/05/1704949114.

J. G. Charney. Dynamics of deserts and drought in the Sahel. *Quarterly Journal of the Royal Meteorological Society*, 101(428):193–202, April 1975. ISSN 1477-870X. doi: 10.1002/qj.49710142802. URL https://rmets.onlinelibrary.wiley.com/doi/abs/10.1002/qj.49710142802.

Jule Charney, William J. Quirk, Shu–hsien Chow, and Jack Kornfield. A Comparative Study of the Effects of Albedo Change on Drought in Semi–Arid Regions. *Journal of the Atmospheric Sciences*, 34(9):1366–1385, September 1977. ISSN 0022-4928. doi: 10.1175/1520-0469(1977)034⟨1366:ACSOTE⟩2.0.CO;2. URL https://journals.ametsoc.org/doi/abs/10.1175/1520-0469(1977)034%3C1366:ACSOTE%3E2.0.CO;2.

Jule G. Charney, Akio Arakawa, D. James Baker, Bert Bolin, Robert E. Dickinson, Richard M. Goody, Cecil E. Leith, Henry M. Stommel, and Carl I. Wunsch. *Carbon Dioxide and Climate: A Scientific Assessment*. National Academy of Sciences, Washington, DC, 1979. Report of an Ad Hoc Study Group on Carbon Dioxide and Climate, Woods Hole, Massachusetts, July 23-27, 1979 to the Climate Research Board, Assembly of Mathematical and Physical Sciences, National Research Council.

Chris Chatfield. *The analysis of time series: an introduction*. CRC press, 2013.

Yonghong Chen, Govindan Rangarajan, Jianfeng Feng, and Mingzhou Ding. Analyzing multiple nonlinear time series with extended granger causality. *Physics Letters A*, 324(1):26 – 35, 2004. ISSN 0375-9601. doi: http://dx.doi.org/10.1016/j.physleta.2004.02.032. URL http://www.sciencedirect.com/science/article/pii/S0375960104002403.

Matthew Christenson. Global Population Growth. Technical report, U.S. Census Bureau, 2002. URL http://www.census.gov/population/international/files/wp02/wp-02003.pdf.

Philippe Ciais, Christopher Sabine, Govindasamy Bala, Laurent Bopp, Victor Brovkin, Josep Canadell, Abha Chhabra, Ruth DeFries, James Galloway, Martin Heimann, Christopher Jones, Corinne Le Quéré, Ranga B. Myneni, Shilong Piao, and Peter Thornton. Carbon and other biogeochemical cycles. In *Climate Change 2013: The Physical Science Basis. Contribution of Working Group I to the Fifth Assessment Report of the Intergovernmental Panel on Climate Change*, pages 465–570. Cambridge University Press, Cambridge, United Kingdom and New York, NY, USA, 2013. URL http://pubman.mpdl.mpg.de/pubman/item/escidoc:2058766/component/escidoc:2058768/WG1AR5_Chapter06_FINAL.pdf.

Cutler J Cleveland and Matthias Ruth. When, where, and by how much do biophysical limits constrain the economic process?: A survey of Nicholas Georgescu-Roegen's contribution to ecological economics. *Ecological Economics*, 22(3):203–223, September 1997. ISSN 0921-8009. doi: 10.1016/S0921-8009(97)00079-7. URL http://www.sciencedirect.com/science/article/pii/S0921800997000797.

Cutler J. Cleveland and Matthias Ruth. Indicators of Dematerialization and the Materials Intensity of Use. *Journal of Industrial Ecology*, 2(3):15–50, July 1998. ISSN 1530-9290. doi: 10.1162/jiec.1998.2.3.15. URL http://onlinelibrary.wiley.com/doi/10.1162/jiec.1998.2.3.15/abstract.

Joel E. Cohen. *How Many People Can the Earth Support?* W. W. Norton & Company, 1995.

Joel E. Cohen. Make secondary education universal. *Nature*, 456(7222):572–573, December 2008. ISSN 0028-0836. doi: 10.1038/456572a. URL http://www.nature.com/nature/journal/v456/n7222/full/456572a.html.

Andrew F. Colombo and Bryan W. Karney. Energy and Costs of Leaky Pipes: Toward Comprehensive Picture. *Journal of Water Resources Planning and Management*, 128(6):441–450, November 2002. doi: 10.1061/(ASCE)0733-9496(2002)128:6(441). URL https://ascelibrary.org/doi/abs/10.1061/(ASCE)0733-9496(2002)128:6(441).

Rita R. Colwell. Global Climate and Infectious Disease: The Cholera Paradigm. *Science*, 274(5295):2025–2031, December 1996. ISSN 0036-8075, 1095-9203. doi:

10.1126/science.274.5295.2025. URL http://www.sciencemag.org/content/274/5295/2025.

Declan Conway, Emma Archer van Garderen, Delphine Deryng, Steve Dorling, Tobias Krueger, Willem Landman, Bruce Lankford, Karen Lebek, Tim Osborn, Claudia Ringler, James Thurlow, Tingju Zhu, and Carole Dalin. Climate and southern Africa's water–energy–food nexus. *Nature Climate Change*, 5(9):837–846, September 2015. ISSN 1758-6798. doi: 10.1038/nclimate2735. URL https://www.nature.com/articles/nclimate2735.

Robert Costanza and Matthias Ruth. Using Dynamic Modeling to Scope Environmental Problems and Build Consensus. *Environmental Management*, 22(2): 183–195, March 1998. ISSN 0364-152X, 1432-1009. doi: 10.1007/s002679900095. URL http://link.springer.com/article/10.1007/s002679900095.

Robert Costanza, Ida Kubiszewski, Enrico Giovannini, Hunter Lovins, Jacqueline McGlade, Kate E. Pickett, Kristín Vala Ragnarsdóttir, Debra Roberts, Roberto De Vogli, and Richard Wilkinson. Development: Time to leave GDP behind. *Nature*, 505(7483):283–285, January 2014. ISSN 0028-0836, 1476-4687. doi: 10.1038/505283a. URL http://www.nature.com/doifinder/10.1038/505283a.

Thomas M Cover and Joy A Thomas. *Elements of information theory*. John Wiley & Sons, 2012.

Andrés Cózar, Fidel Echevarría, J. Ignacio González-Gordillo, Xabier Irigoien, Bárbara Úbeda, Santiago Hernández-León, Álvaro T. Palma, Sandra Navarro, Juan García-de Lomas, Andrea Ruiz, María L. Fernández-de Puelles, and Carlos M. Duarte. Plastic debris in the open ocean. *Proceedings of the National Academy of Sciences*, 111(28):10239–10244, July 2014. ISSN 0027-8424, 1091-6490. doi: 10.1073/pnas.1314705111. URL http://www.pnas.org/content/111/28/10239.

A. Crimmins, J. Balbus, J. L. Gamble, C.B. Beard, J.E. Bell, D. Dodgen, R.J. Eisen, N. Fann, M.D. Hawkins, S.C. Herring, L. Jantarasami, D.M. Mills, S. Saha, M.C. Sarofim, J. Trtanj, and L. Ziska. *The Impacts of Climate Change on Human Health in the United States: A Scientific Assessment*. United States Global Change Research Program, Washington, DC, April 2016. URL http://dx.doi.org/10.7930/J0R49NQX.

Paul J. Crutzen. Geology of mankind. *Nature*, 415(6867):23–23, January 2002. ISSN 0028-0836. doi: 10.1038/415023a. URL http://www.nature.com/nature/journal/v415/n6867/full/415023a.html.

Paul J. Crutzen. The "Anthropocene". In Professor Dr Eckart Ehlers and Dr Thomas Krafft, editors, *Earth System Science in the Anthropocene*, pages 13–18. Springer Berlin Heidelberg, January 2006. ISBN 978-3-540-26588-7 978-3-540-26590-0. URL http://link.springer.com/chapter/10.1007/3-540-26590-2_3.

Gretchen Daily. *Nature's Services: Societal Dependence On Natural Ecosystems*. Island Press, Washington, DC, February 1997. ISBN 978-1-55963-476-2.

Gretchen C Daily, Stephen Polasky, Joshua Goldstein, Peter M Kareiva, Harold A Mooney, Liba Pejchar, Taylor H Ricketts, James Salzman, and Robert Shallenberger. Ecosystem services in decision making: time to deliver. *Frontiers in Ecology and the Environment*, 7(1):21–28, February 2009. ISSN 1540-9295. doi: 10.1890/080025. URL http://www.esajournals.org/doi/abs/10.1890/080025.

Virginia H. Dale, Rebecca A. Efroymson, and Keith L. Kline. The land use–climate change–energy nexus. *Landscape Ecology*, 26(6):755–773, May 2011. ISSN 0921-2973, 1572-9761. doi: 10.1007/s10980-011-9606-2. URL http://link.springer.com/article/10.1007/s10980-011-9606-2.

Herman E. Daly. *Beyond growth: the economics of sustainable development*. Beacon Press, 1996.

Herman E. Daly and Joshua Farley. *Ecological Economics: Principles And Applications*. Island Press, 1st edition, November 2003. ISBN 1-55963-312-3.

Steven J. Davis and Ken Caldeira. Consumption-based accounting of CO2 emissions. *Proceedings of the National Academy of Sciences*, 107(12):5687–5692, March 2010. ISSN 0027-8424, 1091-6490. doi: 10.1073/pnas.0906974107. URL http://www.pnas.org/content/107/12/5687.

Xi-Ping Deng, Lun Shan, Heping Zhang, and Neil C. Turner. Improving agricultural water use efficiency in arid and semiarid areas of China. *Agricultural Water Management*, 80(1):23–40, February 2006. ISSN 0378-3774. doi: 10.1016/j.agwat.2005.07.021. URL http://www.sciencedirect.com/science/article/pii/S0378377405002866.

DESTATIS. Annual Report 2015. Technical report, Federal Statistical Office of Germany, Wiesbaden, Germany, July 2016. URL https://www.destatis.de/EN/AboutUs/OurMission/AnnualReport/AnnualReport2015.pdf.

Ethan R. Deyle and George Sugihara. Generalized theorems for nonlinear state space reconstruction. *PLoS ONE*, 6(3):e18295, 03 2011. doi: 10.1371/journal.pone.0018295. URL http://dx.doi.org/10.1371%2Fjournal.pone.0018295.

Ethan R. Deyle, Michael Fogarty, Chih-hao Hsieh, Les Kaufman, Alec D. MacCall, Stephan B. Munch, Charles T. Perretti, Hao Ye, and George Sugihara. Predicting climate effects on pacific sardine. *Proceedings of the National Academy of Sciences*, 110(16):6430–6435, 2013. doi: 10.1073/pnas.1215506110. URL http://www.pnas.org/content/110/16/6430.abstract.

G. Di Baldassarre, A. Castellarin, and A. Brath. Analysis of the effects of levee heightening on flood propagation: example of the River Po, Italy. *Hydrological Sciences Journal*, 54(6):1007–1017, December 2009. ISSN 0262-6667.

doi: 10.1623/hysj.54.6.1007. URL http://www.tandfonline.com/doi/abs/10.1623/hysj.54.6.1007.

Dominic C. DiGiulio and Robert B. Jackson. Impact to Underground Sources of Drinking Water and Domestic Wells from Production Well Stimulation and Completion Practices in the Pavillion, Wyoming, Field. *Environmental Science & Technology*, 50(8):4524–4536, April 2016. ISSN 0013-936X. doi: 10.1021/acs.est.5b04970. URL http://dx.doi.org/10.1021/acs.est.5b04970.

Mingzhou Ding, Yonghong Chen, and Steven L Bressler. 17 granger causality: basic theory and application to neuroscience. *Handbook of time series analysis: recent theoretical developments and applications*, page 437, 2006.

DOE. FY 2017 Congressional Budget Request: Budget in Brief. Technical Report DOE/CF-0125, US Department of Energy, February 2016. URL http://energy.gov/cfo/downloads/fy-2017-budget-justification.

Petra Döll, Hannes Müller Schmied, Carina Schuh, Felix T. Portmann, and Annette Eicker. Global-scale assessment of groundwater depletion and related groundwater abstractions: Combining hydrological modeling with information from well observations and GRACE satellites. *Water Resources Research*, 50 (7):5698–5720, July 2014. ISSN 1944-7973. doi: 10.1002/2014WR015595. URL http://onlinelibrary.wiley.com/doi/10.1002/2014WR015595/abstract.

Sean S. Downey, W. Randall Haas, and Stephen J. Shennan. European Neolithic societies showed early warning signals of population collapse. *Proceedings of the National Academy of Sciences*, 113(35):9751–9756, August 2016. ISSN 0027-8424, 1091-6490. doi: 10.1073/pnas.1602504113. URL http://www.pnas.org/content/113/35/9751.

Faye Duchin. *The Future of the Environment: Ecological Economics and Technological Change*. Oxford University Press, New York, NY, 1994. ISBN 978-0-19-508574-7.

David R. Easterling, Gerald A. Meehl, Camille Parmesan, Stanley A. Changnon, Thomas R. Karl, and Linda O. Mearns. Climate Extremes: Observations, Modeling, and Impacts. *Science*, 289(5487):2068–2074, September 2000. ISSN 0036-8075, 1095-9203. doi: 10.1126/science.289.5487.2068. URL http://science.sciencemag.org/content/289/5487/2068.

J. E. Edmonds, M. A. Wise, and C. N. MacCracken. *Advanced energy technologies and climate change: An analysis using the global change assessment model (GCAM)*. Fondazione ENI Enrico Mattei, 1994. URL http://sedac.ciesin.org/mva/MCPAPER/mcpaper.html.

Julia A. Ekstrom, Lisa Suatoni, Sarah R. Cooley, Linwood H. Pendleton, George G. Waldbusser, Josh E. Cinner, Jessica Ritter, Chris Langdon, Ruben van Hooidonk, Dwight Gledhill, Katharine Wellman, Michael W. Beck, Luke M. Brander, Dan

Rittschof, Carolyn Doherty, Peter E. T. Edwards, and Rosimeiry Portela. Vulnerability and adaptation of US shellfisheries to ocean acidification. *Nature Climate Change*, 5(3):207–214, March 2015. ISSN 1758-678X. doi: 10.1038/nclimate2508. URL http://www.nature.com/nclimate/journal/v5/n3/full/nclimate2508.html.

EPA. Control and Mitigation of Drinking Water Losses in Distribution System. Technical Report EPA 816-R-10-019, US Environmental Protection Agency, November 2010. URL http://www.allianceforwaterefficiency.org/uploadedFiles/Resource_Center/Library/water_loss/EPA-Water-Loss-Control-November-2010.pdf.

EPA. Providing Safe Drinking Water in America. National Public Water Systems Compliance Report EPA Document 305R15001, The United States (U.S.) Environmental Protection Agency (EPA), Office of Enforcement and Compliance Assurance, Washington, DC, USA, 2013.

Jan Willem Erisman, Mark A. Sutton, James Galloway, Zbigniew Klimont, and Wilfried Winiwarter. How a century of ammonia synthesis changed the world. *Nature Geoscience*, 1(10):636–639, October 2008. ISSN 1752-0894. doi: 10.1038/ngeo325. URL http://www.nature.com/ngeo/journal/v1/n10/abs/ngeo325.html.

G. Evensen. The ensemble Kalman filter for combined state and parameter estimation. *IEEE Control Systems*, 29(3):83–104, June 2009. ISSN 1066-033X. doi: 10.1109/MCS.2009.932223.

J. S. Famiglietti. The global groundwater crisis. *Nature Climate Change*, 4(11):945–948, November 2014. ISSN 1758-678X. doi: 10.1038/nclimate2425. URL http://www.nature.com/nclimate/journal/v4/n11/full/nclimate2425.html.

J. S. Famiglietti, M. Lo, S. L. Ho, J. Bethune, K. J. Anderson, T. H. Syed, S. C. Swenson, C. R. de Linage, and M. Rodell. Satellites measure recent rates of groundwater depletion in California's Central Valley. *Geophysical Research Letters*, 38(3):L03403, February 2011. ISSN 1944-8007. doi: 10.1029/2010GL046442. URL http://onlinelibrary.wiley.com/doi/10.1029/2010GL046442/abstract.

James S. Famiglietti and Matthew Rodell. Water in the Balance. *Science*, 340(6138):1300–1301, June 2013. ISSN 0036-8075, 1095-9203. doi: 10.1126/science.1236460. URL http://www.sciencemag.org/content/340/6138/1300.

J. Doyne Farmer and John J. Sidorowich. Predicting chaotic time series. *Phys. Rev. Lett.*, 59:845–848, Aug 1987. doi: 10.1103/PhysRevLett.59.845. URL http://link.aps.org/doi/10.1103/PhysRevLett.59.845.

Allen A. Fawcett, Gokul C. Iyer, Leon E. Clarke, James A. Edmonds, Nathan E. Hultman, Haewon C. McJeon, Joeri Rogelj, Reed Schuler, Jameel Alsalam, Ghassem R. Asrar, Jared Creason, Minji Jeong, James McFarland, Anupriya Mundra, and Wenjing Shi. Can Paris pledges avert severe climate change? *Science*, 350(6265):1168–1169, December 2015. ISSN 0036-8075, 1095-9203. doi: 10.1126/science.aad5761. URL http://www.sciencemag.org.proxy-um.researchport.umd.edu/content/350/6265/1168.

Kuishuang Feng, Klaus Hubacek, Dabo Guan, Monica Contestabile, Jan Minx, and John Barrett. Distributional Effects of Climate Change Taxation: The Case of the UK. *Environmental Science & Technology*, 44(10):3670–3676, May 2010a. ISSN 0013-936X. doi: 10.1021/es902974g. URL http://dx.doi.org/10.1021/es902974g.

Kuishuang Feng, Ashok Chapagain, Sangwon Suh, Stephan Pfister, and Klaus Hubacek. Comparison of Bottom-up and Top-down Approaches to Calculating the Water Footprints of Nations. *Economic Systems Research*, 23(4):371–385, December 2011a. ISSN 0953-5314. doi: 10.1080/09535314.2011.638276. URL http://dx.doi.org/10.1080/09535314.2011.638276.

Kuishuang Feng, Klaus Hubacek, Jan Minx, Yim Ling Siu, Ashok Chapagain, Yang Yu, Dabo Guan, and John Barrett. Spatially Explicit Analysis of Water Footprints in the UK. *Water*, 3(1):47–63, 2011b. doi: 10.3390/w3010047. URL http://www.mdpi.com/2073-4441/3/1/47.

Kuishuang Feng, Yim Ling Siu, Dabo Guan, and Klaus Hubacek. Analyzing Drivers of Regional Carbon Dioxide Emissions for China. *Journal of Industrial Ecology*, 16(4):600–611, August 2012. ISSN 1530-9290. doi: 10.1111/j.1530-9290.2012.00494.x. URL http://onlinelibrary.wiley.com/doi/10.1111/j.1530-9290.2012.00494.x/abstract.

Shuaizhang Feng, Alan B. Krueger, and Michael Oppenheimer. Linkages among climate change, crop yields and Mexico–US cross-border migration. *Proceedings of the National Academy of Sciences*, 107(32):14257–14262, August 2010b. ISSN 0027-8424, 1091-6490. doi: 10.1073/pnas.1002632107. URL http://www.pnas.org/content/107/32/14257.

Gonçalo Ferraz, Gareth J. Russell, Philip C. Stouffer, Richard O. Bierregaard, Stuart L. Pimm, and Thomas E. Lovejoy. Rates of species loss from Amazonian forest fragments. *Proceedings of the National Academy of Sciences*, 100(24):14069–14073, November 2003. ISSN 0027-8424, 1091-6490. doi: 10.1073/pnas.2336195100. URL http://www.pnas.org/content/100/24/14069.

Anna C. Fitch. Climate Impacts of Large-Scale Wind Farms as Parameterized in a Global Climate Model. *Journal of Climate*, 28(15):6160–6180, May 2015. ISSN 0894-8755. doi: 10.1175/JCLI-D-14-00245.1. URL https://journals.ametsoc.org/doi/10.1175/JCLI-D-14-00245.1.

Jonathan A. Foley, Ruth DeFries, Gregory P. Asner, Carol Barford, Gordon Bonan, Stephen R. Carpenter, F. Stuart Chapin, Michael T. Coe, Gretchen C. Daily, Holly K. Gibbs, Joseph H. Helkowski, Tracey Holloway, Erica A. Howard, Christopher J. Kucharik, Chad Monfreda, Jonathan A. Patz, I. Colin Prentice, Navin Ramankutty, and Peter K. Snyder. Global Consequences of Land Use. *Science*, 309(5734):570–574, July 2005. ISSN 0036-8075, 1095-9203. doi: 10.1126/science.1111772. URL http://www.sciencemag.org/content/309/5734/570.

Food and Agriculture Organization. Coping with Water Scarcity: Challenge of the 21st Century, 2007. URL http://www.fao.org/publications/card/en/c/c89f03ee-e785-5c76-a2a5-72b3b4bc955e.

Food and Agriculture Organization. Water Security & the Global Water Agenda, 2013. URL http://www.fao.org/publications/card/en/c/cb78270e-198a-50b5-b1a3-95eb8e6bf56d.

Andrew M. Fraser and Harry L. Swinney. Independent coordinates for strange attractors from mutual information. *Phys. Rev. A*, 33:1134–1140, Feb 1986. doi: 10.1103/PhysRevA.33.1134. URL http://link.aps.org/doi/10.1103/PhysRevA.33.1134.

P. Friedlingstein, R. M. Andrew, J. Rogelj, G. P. Peters, J. G. Canadell, R. Knutti, G. Luderer, M. R. Raupach, M. Schaeffer, D. P. van Vuuren, and C. Le Quéré. Persistent growth of CO2 emissions and implications for reaching climate targets. *Nature Geoscience*, 7(10):709–715, October 2014. ISSN 1752-0894. doi: 10.1038/ngeo2248. URL http://www.nature.com/ngeo/journal/v7/n10/full/ngeo2248.html.

Bojie Fu and Yan Li. Bidirectional coupling between the Earth and human systems is essential for modeling sustainability. *National Science Review*, 3(4):397–398, December 2016. ISSN 2095-5138. doi: 10.1093/nsr/nww094. URL https://academic.oup.com/nsr/article/3/4/397/2669336/Bidirectional-coupling-between-the-Earth-and-human.

J. N. Galloway, F. J. Dentener, D. G. Capone, E. W. Boyer, R. W. Howarth, S. P. Seitzinger, G. P. Asner, C. C. Cleveland, P. A. Green, E. A. Holland, D. M. Karl, A. F. Michaels, J. H. Porter, A. R. Townsend, and C. J. Vöosmarty. Nitrogen Cycles: Past, Present, and Future. *Biogeochemistry*, 70(2):153–226, 2004. ISSN 0168-2563, 1573-515X. doi: 10.1007/s10533-004-0370-0. URL http://link.springer.com/article/10.1007/s10533-004-0370-0.

GAO. Energy-Water Nexus: Coordinated Federal Approach Needed to Better Manage Energy and Water Tradeoffs. Technical Report GAO-12-880, US Government Accountability Office, September 2012. URL http://www.gao.gov/assets/650/648306.pdf.

Nicholas Georgescu-Roegen. *The entropy law and the economic process*. Harvard University Press, Cambridge, Mass., 1971.

Patrick Gerland, Adrian E. Raftery, Hana Ševčíková, Nan Li, Danan Gu, Thomas Spoorenberg, Leontine Alkema, Bailey K. Fosdick, Jennifer Chunn, Nevena Lalic, Guiomar Bay, Thomas Buettner, Gerhard K. Heilig, and John Wilmoth. World population stabilization unlikely this century. *Science*, 346(6206):234–237, October 2014. ISSN 0036-8075, 1095-9203. doi: 10.1126/science.1257469. URL http://www.sciencemag.org/content/346/6206/234.

Luke Gibson, Antony J. Lynam, Corey J. A. Bradshaw, Fangliang He, David P. Bickford, David S. Woodruff, Sara Bumrungsri, and William F. Laurance. Near-Complete Extinction of Native Small Mammal Fauna 25 Years After Forest Fragmentation. *Science*, 341(6153):1508–1510, September 2013. ISSN 0036-8075, 1095-9203. doi: 10.1126/science.1240495. URL http://www.sciencemag.org/content/341/6153/1508.

Line J. Gordon, Garry D. Peterson, and Elena M. Bennett. Agricultural modifications of hydrological flows create ecological surprises. *Trends in Ecology & Evolution*, 23(4):211–219, April 2008. ISSN 0169-5347. doi: 10.1016/j.tree.2007.11.011. URL http://www.sciencedirect.com/science/article/pii/S016953470800058X.

C. W. J. Granger. Investigating causal relations by econometric models and cross-spectral methods. *Econometrica*, 37(3):pp. 424–438, 1969. ISSN 00129682. URL http://www.jstor.org/stable/1912791.

C.W.J. Granger. Testing for causality: A personal viewpoint. *Journal of Economic Dynamics and Control*, 2(0):329 – 352, 1980. ISSN 0165-1889. doi: http://dx.doi.org/10.1016/0165-1889(80)90069-X. URL http://www.sciencedirect.com/science/article/pii/016518898090069X.

Stephen Grasby. World Water Resources at the Beginning of the 21st Century. *Geoscience Canada*, 31(3), September 2004. ISSN 1911-4850. URL http://journals.hil.unb.ca/index.php/GC/article/view/2765.

Lorna A. Greening, David L. Greene, and Carmen Difiglio. Energy efficiency and consumption — the rebound effect — a survey. *Energy Policy*, 28(6–7):389–401, June 2000. ISSN 0301-4215. doi: 10.1016/S0301-4215(00)00021-5. URL http://www.sciencedirect.com/science/article/pii/S0301421500000215.

World Bank Group. Turn down the heat: confronting the new climate normal. Technical report, World Bank, Washington, DC, 2014. URL https://openknowledge.worldbank.org/handle/10986/20595.

Nicolas Gruber and James N. Galloway. An Earth-system perspective of the global nitrogen cycle. *Nature*, 451(7176):293–296, January 2008. ISSN 0028-0836. doi: 10.1038/nature06592. URL http://www.nature.com/nature/journal/v451/n7176/full/nature06592.html.

Dabo Guan and Klaus Hubacek. Assessment of regional trade and virtual water flows in China. *Ecological Economics*, 61(1):159–170, February 2007. doi: 10.1016/j.ecolecon.2006.02.022. URL http://www.sciencedirect.com/science/article/pii/S0921800906000930.

Dabo Guan and Klaus Hubacek. A new and integrated hydro-economic accounting and analytical framework for water resources: A case study for North China. *Journal of Environmental Management*, 88(4):1300–1313, September 2008. doi: 10.1016/j.jenvman.2007.07.010. URL http://www.sciencedirect.com/science/article/pii/S0301479707002253.

Dabo Guan, Klaus Hubacek, Christopher L. Weber, Glen P. Peters, and David M. Reiner. The drivers of Chinese CO2 emissions from 1980 to 2030. *Global Environmental Change*, 18(4):626–634, October 2008. doi: 10.1016/j.gloenvcha.2008.08.001. URL http://www.sciencedirect.com/science/article/pii/S095937800800068X.

Dabo Guan, Glen P. Peters, Christopher L. Weber, and Klaus Hubacek. Journey to world top emitter: An analysis of the driving forces of China's recent CO2 emissions surge. *Geophysical Research Letters*, 36(4):L04709, February 2009. ISSN 1944-8007. doi: 10.1029/2008GL036540. URL http://onlinelibrary.wiley.com/doi/10.1029/2008GL036540/abstract.

José Miguel Guzmán, George Martine, Gordon McGranahan, Daniel Schensul, and Cecilia Tacoli. *Population Dynamics and Climate Change*. UNFPA and IIEE, New York, NY, USA; London, England, 2009. ISBN 978-0-89714-919-8.

Helmut Haberl, K. Heinz Erb, Fridolin Krausmann, Veronika Gaube, Alberte Bondeau, Christoph Plutzar, Simone Gingrich, Wolfgang Lucht, and Marina Fischer-Kowalski. Quantifying and mapping the human appropriation of net primary production in earth's terrestrial ecosystems. *Proceedings of the National Academy of Sciences*, 104(31):12942–12947, July 2007. ISSN 0027-8424, 1091-6490. doi: 10.1073/pnas.0704243104. URL http://www.pnas.org/content/104/31/12942.

Helmut Haberl, Karl-Heinz Erb, Fridolin Krausmann, Alberte Bondeau, Christian Lauk, Christoph Müller, Christoph Plutzar, and Julia K. Steinberger. Global bioenergy potentials from agricultural land in 2050: Sensitivity to climate change, diets and yields. *Biomass & Bioenergy*, 35(12):4753–4769, December 2011. ISSN 0961-9534. doi: 10.1016/j.biombioe.2011.04.035. URL http://www.ncbi.nlm.nih.gov/pmc/articles/PMC3236288/.

Bruce Hannon and Matthias Ruth. *Dynamic modeling of diseases and pests*. Springer, 2009. URL http://link.springer.com/content/pdf/10.1007/978-0-387-09560-8.pdf.

Bruce Hannon and Matthias Ruth. *Modeling Dynamic Biological Systems*. Springer, 2014. URL http://link.springer.com/chapter/10.1007/978-3-319-05615-9_1.

Bruce M. Hannon and Matthias Ruth. *Dynamic modeling*. Springer-Verlag, Berlin, New York, 1 edition, 1994. ISBN 978-0-387-94287-2. URL http://adsabs.harvard.edu/abs/1994dymo.book.....H.

James Hansen, Pushker Kharecha, Makiko Sato, Valerie Masson-Delmotte, Frank Ackerman, David J. Beerling, Paul J. Hearty, Ove Hoegh-Guldberg, Shi-Ling Hsu, Camille Parmesan, Johan Rockstrom, Eelco J. Rohling, Jeffrey Sachs, Pete Smith, Konrad Steffen, Lise Van Susteren, Karina von Schuckmann, and James C. Zachos. Assessing "Dangerous Climate Change": Required Reduction of Carbon Emissions to Protect Young People, Future Generations and Nature. *PLoS ONE*, 8(12):e81648, December 2013. doi: 10.1371/journal.pone.0081648. URL http://dx.doi.org/10.1371/journal.pone.0081648.

Ilkka Hanski, Gustavo A. Zurita, M. Isabel Bellocq, and Joel Rybicki. Species–fragmented area relationship. *Proceedings of the National Academy of Sciences*, 110(31):12715–12720, July 2013. ISSN 0027-8424, 1091-6490. doi: 10.1073/pnas.1311491110. URL http://www.pnas.org/content/110/31/12715.

Hao He, Konstantin Y. Vinnikov, Can Li, Nickolay A. Krotkov, Andrew R. Jongeward, Zhanqing Li, Jeffrey W. Stehr, Jennifer C. Hains, and Russell R. Dickerson. Response of SO2 and particulate air pollution to local and regional emission controls: A case study in Maryland. *Earth's Future*, 4(4): 2015EF000330, April 2016. ISSN 2328-4277. doi: 10.1002/2015EF000330. URL http://onlinelibrary.wiley.com/doi/10.1002/2015EF000330/abstract.

Gerhard K. Heilig, Thomas Buettner, Nan Li, Patrick Gerland, Leontine Alkema, Jennifer Chunn, and Adrian E. Raftery. Future population trends found to be highly uncertain in Least Developed Countries. 2010. URL http://esa.un.org/Unpd/Wpp/Publications/Files/Heilig_2010_Future%20population%20trends%20found%20to%20be%20highly%20uncertain%20in%20Least%20Developed%20Countries.pdf.

Kirsten Henderson and Michel Loreau. How ecological feedbacks between human population and land cover influence sustainability. *PLOS Computational Biology*, 14(8):e1006389, August 2018. ISSN 1553-7358. doi: 10.1371/journal.pcbi.1006389. URL https://journals.plos.org/ploscompbiol/article?id=10.1371/journal.pcbi.1006389.

Chris Hendrickson, Arpad Horvath, Satish Joshi, and Lester Lave. Peer Reviewed: Economic Input–Output Models for Environmental Life-Cycle Assessment. *Environmental Science & Technology*, 32(7):184A–191A, April 1998. ISSN 0013-936X. doi: 10.1021/es983471i. URL http://dx.doi.org/10.1021/es983471i.

R. R. Hernandez, S. B. Easter, M. L. Murphy-Mariscal, F. T. Maestre, M. Tavassoli, E. B. Allen, C. W. Barrows, J. Belnap, R. Ochoa-Hueso, S. Ravi, and

M. F. Allen. Environmental impacts of utility-scale solar energy. *Renewable and Sustainable Energy Reviews*, 29:766–779, January 2014. ISSN 1364-0321. doi: 10.1016/j.rser.2013.08.041. URL http://www.sciencedirect.com/science/article/pii/S1364032113005819.

Edgar G. Hertwich and Glen P. Peters. Carbon Footprint of Nations: A Global, Trade-Linked Analysis. *Environmental Science & Technology*, 43(16):6414–6420, August 2009. ISSN 0013-936X. doi: 10.1021/es803496a. URL http://dx.doi.org/10.1021/es803496a.

Craig Hiemstra and Jonathan D. Jones. Testing for linear and nonlinear granger causality in the stock price-volume relation. *The Journal of Finance*, 49(5):1639–1664, 1994. ISSN 1540-6261. doi: 10.1111/j.1540-6261.1994.tb04776.x. URL http://dx.doi.org/10.1111/j.1540-6261.1994.tb04776.x.

A. Hilboll, A. Richter, and J. P. Burrows. Long-term changes of tropospheric NO2 over megacities derived from multiple satellite instruments. *Atmos. Chem. Phys.*, 13(8):4145–4169, April 2013. ISSN 1680-7324. doi: 10.5194/acp-13-4145-2013. URL http://www.atmos-chem-phys.net/13/4145/2013/.

Katerina Hlavkov-Schindler, Milan Palu, Martin Vejmelka, and Joydeep Bhattacharya. Causality detection based on information-theoretic approaches in time series analysis. *Physics Reports*, 441(1):1 – 46, 2007. ISSN 0370-1573. doi: http://dx.doi.org/10.1016/j.physrep.2006.12.004. URL http://www.sciencedirect.com/science/article/pii/S0370157307000403.

Gordon W. Holtgrieve, Daniel E. Schindler, William O. Hobbs, Peter R. Leavitt, Eric J. Ward, Lynda Bunting, Guangjie Chen, Bruce P. Finney, Irene Gregory-Eaves, Sofia Holmgren, Mark J. Lisac, Peter J. Lisi, Koren Nydick, Lauren A. Rogers, Jasmine E. Saros, Daniel T. Selbie, Mark D. Shapley, Patrick B. Walsh, and Alexander P. Wolfe. A Coherent Signature of Anthropogenic Nitrogen Deposition to Remote Watersheds of the Northern Hemisphere. *Science*, 334(6062):1545–1548, December 2011. ISSN 0036-8075, 1095-9203. doi: 10.1126/science.1212267. URL http://science.sciencemag.org/content/334/6062/1545.

J. T. Houghton, B. A. Callander, and S. K. Varney. *Climate change 1992: the supplementary report to the IPCC scientific assessment*. Cambridge University Press, 1992. ISBN 0-521-43829-2. URL http://bases.bireme.br/cgi-bin/wxislind.exe/iah/online/?IsisScript=iah/iah.xis&src=google&base=REPIDISCA&lang=p&nextAction=lnk&exprSearch=70547&indexSearch=ID.

Robert Howarth, Dennis Swaney, Gilles Billen, Josette Garnier, Bongghi Hong, Christoph Humborg, Penny Johnes, Carl-Magnus Mörth, and Roxanne Marino. Nitrogen fluxes from the landscape are controlled by net anthropogenic nitrogen inputs and by climate. *Frontiers in Ecology and the Environment*, 10(1):37–43, February 2012. ISSN 1540-9309. doi: 10.1890/100178. URL http://onlinelibrary.wiley.com/doi/10.1890/100178/abstract.

Solomon M. Hsiang. Temperatures and cyclones strongly associated with economic production in the Caribbean and Central America. *Proceedings of the National Academy of Sciences*, 107(35):15367–15372, August 2010. ISSN 0027-8424, 1091-6490. doi: 10.1073/pnas.1009510107. URL http://www.pnas.org/content/107/35/15367.

Solomon M. Hsiang and Amir S. Jina. The Causal Effect of Environmental Catastrophe on Long-Run Economic Growth: Evidence From 6,700 Cyclones. Working Paper 20352, National Bureau of Economic Research, July 2014. URL http://www.nber.org/papers/w20352.

Solomon M. Hsiang, Kyle C. Meng, and Mark A. Cane. Civil conflicts are associated with the global climate. *Nature*, 476(7361):438–441, August 2011. ISSN 0028-0836. doi: 10.1038/nature10311. URL http://www.nature.com/nature/journal/v476/n7361/full/nature10311.html%3FWT.ec_id=NATURE-20110825.

Solomon M. Hsiang, Marshall Burke, and Edward Miguel. Quantifying the Influence of Climate on Human Conflict. *Science*, 341(6151):1235367, September 2013. ISSN 0036-8075, 1095-9203. doi: 10.1126/science.1235367. URL http://www.sciencemag.org/content/341/6151/1235367.

Aixue Hu, Samuel Levis, Gerald A. Meehl, Weiqing Han, Warren M. Washington, Keith W. Oleson, Bas J. van Ruijven, Mingqiong He, and Warren G. Strand. Impact of solar panels on global climate. *Nature Climate Change*, 6(3):290–294, March 2016. ISSN 1758-6798. doi: 10.1038/nclimate2843. URL https://www.nature.com/articles/nclimate2843.

Klaus Hubacek and Laixiang Sun. A scenario analysis of China's land use and land cover change: incorporating biophysical information into input–output modeling. *Structural Change and Economic Dynamics*, 12(4):367–397, December 2001. doi: 10.1016/S0954-349X(01)00029-7. URL http://www.sciencedirect.com/science/article/pii/S0954349X01000297.

Klaus Hubacek, Kuishuang Feng, Jan C. Minx, Stephan Pfister, and Naijun Zhou. Teleconnecting Consumption to Environmental Impacts at Multiple Spatial Scales. *Journal of Industrial Ecology*, 18(1):7–9, February 2014. ISSN 1530-9290. doi: 10.1111/jiec.12082. URL http://onlinelibrary.wiley.com/doi/10.1111/jiec.12082/abstract.

Klaus Hubacek, Giovanni Baiocchi, Kuishuang Feng, and Anand Patwardhan. Poverty eradication in a carbon constrained world. *Nature Communications*, 2016. Under review.

Brian R. Hunt, Edward Ott, and James A. Yorke. Differentiable generalized synchronization of chaos. *Phys. Rev. E*, 55:4029–4034, Apr 1997. doi: 10.1103/PhysRevE.55.4029. URL https://link.aps.org/doi/10.1103/PhysRevE.55.4029.

Brian R. Hunt, Eric J. Kostelich, and Istvan Szunyogh. Efficient data assimilation for spatiotemporal chaos: A local ensemble transform Kalman filter. *Physica D: Nonlinear Phenomena*, 230(1–2):112–126, June 2007. ISSN 0167-2789. doi: 10.1016/j.physd.2006.11.008. URL http://www.sciencedirect.com/science/article/pii/S0167278906004647.

Karen Hussey and Jamie Pittock. The Energy-Water Nexus: Managing the Links between Energy and Water for a Sustainable Future. *Ecology and Society*, 17 (1), 2012. ISSN 1708-3087. doi: 10.5751/ES-04641-170131. URL http://www.ecologyandsociety.org/vol17/iss1/art31/.

IEA. Key World Energy Statistics 2017. Technical report, International Energy Agency, 2017. URL https://www.iea.org/publications/freepublications/publication/KeyWorld2017.pdf.

Marc L. Imhoff, Lahouari Bounoua, Taylor Ricketts, Colby Loucks, Robert Harriss, and William T. Lawrence. Global patterns in human consumption of net primary production. *Nature*, 429(6994):870–873, June 2004. doi: 10.1038/nature02619. URL http://www.nature.com/nature/journal/v429/n6994/full/nature02619.html.

M.L. Imhoff, C.J. Tucker, W.T. Lawrence, and D.C. Stutzer. The use of multisource satellite and geospatial data to study the effect of urbanization on primary productivity in the United States. *IEEE Transactions on Geoscience and Remote Sensing*, 38(6):2549–2556, November 2000. ISSN 0196-2892. doi: 10.1109/36.885202. URL http://ieeexplore.ieee.org/document/885202/.

David Inman and Paul Jeffrey. A review of residential water conservation tool performance and influences on implementation effectiveness. *Urban Water Journal*, 3 (3):127–143, September 2006. ISSN 1573-062X. doi: 10.1080/15730620600961288. URL https://doi.org/10.1080/15730620600961288.

IPCC. *Climate Change 2001: The Scientific Basis. Contribution of Working Group I to the Third Assessment Report of the Intergovernmental Panel on Climate Change*. Cambridge University Press, Cambridge, United Kingdom and New York, NY, USA,, 2001.

IPCC. *Climate change 2007: Synthesis Report. Contribution of Working Groups I, II and III to the Fourth Assessment Report of the Intergovernmental Panel on Climate Change*. IPCC, Geneva, Switzerland, 2007.

IPCC. *Climate Change 2014: Synthesis Report. Contribution of Working Groups I, II and III to the Fifth Assessment Report of the Intergovernmental Panel on Climate Change [Core Writing Team, R.K. Pachauri and L.A. Meyer (eds.)]*. IPCC, Geneva, Switzerland, 2014.

Gokul C. Iyer, James A. Edmonds, Allen A. Fawcett, Nathan E. Hultman, Jameel Alsalam, Ghassem R. Asrar, Katherine V. Calvin, Leon E. Clarke, Jared Creason, Minji Jeong, Page Kyle, James McFarland, Anupriya Mundra, Pralit Patel, Wenjing Shi, and Haewon C. McJeon. The contribution of Paris to limit global warming to 2 °C. *Environmental Research Letters*, 10(12):125002, 2015. ISSN 1748-9326. doi: 10.1088/1748-9326/10/12/125002. URL http://stacks.iop.org/1748-9326/10/i=12/a=125002.

Andrea E. Izquierdo, Carlos D. De Angelo, and T. Mitchell Aide. Thirty Years of Human Demography and Land-Use Change in the Atlantic Forest of Misiones, Argentina: an Evaluation of the Forest Transition Model. *Ecology & Society*, 13 (2), 2008. URL http://www.ecologyandsociety.org/vol13/iss2/art3/.

Robert B. Jackson, Ella R. Lowry, Amy Pickle, Mary Kang, Dominic DiGiulio, and Kaiguang Zhao. The Depths of Hydraulic Fracturing and Accompanying Water Use Across the United States. *Environmental Science & Technology*, 49 (15):8969–8976, August 2015. ISSN 0013-936X. doi: 10.1021/acs.est.5b01228. URL http://dx.doi.org/10.1021/acs.est.5b01228.

Mark Z. Jacobson, Mark A. Delucchi, Mary A. Cameron, and Bethany A. Frew. Low-cost solution to the grid reliability problem with 100% penetration of intermittent wind, water, and solar for all purposes. *Proceedings of the National Academy of Sciences*, 112(49):15060–15065, December 2015. ISSN 0027-8424, 1091-6490. doi: 10.1073/pnas.1510028112. URL http://www.pnas.org/content/112/49/15060.

Michael Jakob, Jan Christoph Steckel, Stephan Klasen, Jann Lay, Nicole Grunewald, Inmaculada Martínez-Zarzoso, Sebastian Renner, and Ottmar Edenhofer. Feasible mitigation actions in developing countries. *Nature Climate Change*, 4(11):961–968, November 2014. ISSN 1758-6798. doi: 10.1038/nclimate2370. URL https://www.nature.com/articles/nclimate2370.

Jenna R. Jambeck, Roland Geyer, Chris Wilcox, Theodore R. Siegler, Miriam Perryman, Anthony Andrady, Ramani Narayan, and Kara Lavender Law. Plastic waste inputs from land into the ocean. *Science*, 347(6223):768–771, February 2015. ISSN 0036-8075, 1095-9203. doi: 10.1126/science.1260352. URL http://www.sciencemag.org/content/347/6223/768.

Robin Jeffrey. *Politics, Women and Well-being: How Kerala Became "a Model"*. Macmillan Press Houndsmills, 1992. URL http://www.getcited.org/pub/103052083.

Eugenia Kalnay. *Atmospheric Modeling, Data Assimilation and Predictability*. Cambridge University Press, 1 edition, 2003. ISBN 0-521-79629-6.

Ji-Sun Kang, Eugenia Kalnay, Junjie Liu, Inez Fung, Takemasa Miyoshi, and Kayo Ide. "Variable localization" in an ensemble Kalman filter: Application to the carbon cycle data assimilation. *Journal of Geophysical Research: Atmospheres*, 116(D9):D09110, May 2011. ISSN 2156-2202. doi: 10.1029/2010JD014673. URL http://onlinelibrary.wiley.com/doi/10.1029/2010JD014673/abstract.

Ji-Sun Kang, Eugenia Kalnay, Takemasa Miyoshi, Junjie Liu, and Inez Fung. Estimation of surface carbon fluxes with an advanced data assimilation methodology. *Journal of Geophysical Research: Atmospheres*, 117(D24):D24101, December 2012. ISSN 2156-2202. doi: 10.1029/2012JD018259. URL http://onlinelibrary.wiley.com/doi/10.1029/2012JD018259/abstract.

Peter Kareiva, Sean Watts, Robert McDonald, and Tim Boucher. Domesticated Nature: Shaping Landscapes and Ecosystems for Human Welfare. *Science*, 316 (5833):1866–1869, June 2007. ISSN 0036-8075, 1095-9203. doi: 10.1126/science.1140170. URL http://science.sciencemag.org/content/316/5833/1866.

Peter Kareiva, Heather Tallis, Taylor H. Ricketts, Gretchen C. Daily, and Stephen Polasky. *Natural Capital: Theory and Practice of Mapping Ecosystem Services*. Oxford University Press, New York, NY, USA, April 2011. ISBN 978-0-19-162103-1.

David W. Keith, Joseph F. DeCarolis, David C. Denkenberger, Donald H. Lenschow, Sergey L. Malyshev, Stephen Pacala, and Philip J. Rasch. The influence of large-scale wind power on global climate. *Proceedings of the National Academy of Sciences*, 101(46):16115–16120, November 2004. ISSN 0027-8424, 1091-6490. doi: 10.1073/pnas.0406930101. URL http://www.pnas.org/content/101/46/16115.

Colin P. Kelley, Shahrzad Mohtadi, Mark A. Cane, Richard Seager, and Yochanan Kushnir. Climate change in the Fertile Crescent and implications of the recent Syrian drought. *Proceedings of the National Academy of Sciences*, 112(11):3241–3246, March 2015. ISSN 0027-8424, 1091-6490. doi: 10.1073/pnas.1421533112. URL http://www.pnas.org/content/112/11/3241.

Henry W. Kendall and David Pimentel. Constraints on the Expansion of the Global Food Supply. *Ambio*, 23(3):198–205, 1994. ISSN 0044-7447. URL http://www.jstor.org/stable/4314199.

Shahbaz Khan and Munir A. Hanjra. Footprints of water and energy inputs in food production – Global perspectives. *Food Policy*, 34(2):130–140, April 2009. doi: 10.1016/j.foodpol.2008.09.001. URL http://www.sciencedirect.com/science/article/pii/S0306919208000729.

Son H. Kim, Mohamad Hejazi, Lu Liu, Katherine Calvin, Leon Clarke, Jae Edmonds, Page Kyle, Pralit Patel, Marshall Wise, and Evan Davies. Balancing global water availability and use at basin scale in an integrated assessment model. *Climatic Change*, 136(2):217–231, May 2016. ISSN 1573-1480. doi: 10.1007/s10584-016-1604-6. URL https://doi.org/10.1007/s10584-016-1604-6.

Eli Kintisch. After Paris: The rocky road ahead. *Science*, 350(6264):1018–1019, November 2015. ISSN 0036-8075, 1095-9203. doi: 10.1126/science.350.6264.1018. URL http://www.sciencemag.org/content/350/6264/1018.

Elizabeth Kolbert. *The Sixth Extinction: An Unnatural History*. Henry Holt and Co., New York, first edition, February 2014. ISBN 978-0-8050-9299-8.

Leonard F. Konikow. Groundwater depletion in the United States (1900-2008). U.S. Geological Survey Scientific Investigations Report 2013-5079, US Department of the Interior, US Geological Survey, 2013. URL http://pubs.usgs.gov/sir/2013/5079/.

Randal D. Koster, Zhichang Guo, Rongqian Yang, Paul A. Dirmeyer, Kenneth Mitchell, and Michael J. Puma. On the Nature of Soil Moisture in Land Surface Models. *Journal of Climate*, 22(16):4322–4335, August 2009. ISSN 0894-8755. doi: 10.1175/2009JCLI2832.1. URL http://journals.ametsoc.org/doi/abs/10.1175/2009JCLI2832.1.

Fridolin Krausmann, Marina Fischer-Kowalski, Heinz Schandl, and Nina Eisenmenger. The Global Sociometabolic Transition. *Journal of Industrial Ecology*, 12(5-6):637–656, 2008a. ISSN 1530-9290. doi: 10.1111/j.1530-9290.2008.00065.x. URL http://onlinelibrary.wiley.com/doi/10.1111/j.1530-9290.2008.00065.x/abstract.

Fridolin Krausmann, Heinz Schandl, and Rolf Peter Sieferle. Socio-ecological regime transitions in Austria and the United Kingdom. *Ecological Economics*, 65(1):187–201, March 2008b. doi: 10.1016/j.ecolecon.2007.06.009. URL http://www.sciencedirect.com/science/article/pii/S0921800907003503.

Fridolin Krausmann, Simone Gingrich, Nina Eisenmenger, Karl-Heinz Erb, Helmut Haberl, and Marina Fischer-Kowalski. Growth in global materials use, GDP and population during the 20th century. *Ecological Economics*, 68(10):2696–2705, August 2009. ISSN 0921-8009. doi: 10.1016/j.ecolecon.2009.05.007. URL http://www.sciencedirect.com/science/article/pii/S0921800909002158.

Fridolin Krausmann, Karl-Heinz Erb, Simone Gingrich, Helmut Haberl, Alberte Bondeau, Veronika Gaube, Christian Lauk, Christoph Plutzar, and Timothy D. Searchinger. Global human appropriation of net primary production doubled in the 20th century. *Proceedings of the National Academy of Sciences*, 110(25):10324–10329, June 2013. ISSN 0027-8424, 1091-6490. doi: 10.1073/pnas.1211349110. URL http://www.pnas.org/content/110/25/10324.

N. A. Krotkov, C. A. McLinden, C. Li, L. N. Lamsal, E. A. Celarier, S. V. Marchenko, W. H. Swartz, E. J. Bucsela, J. Joiner, B. N. Duncan, K. F. Boersma, J. P. Veefkind, P. F. Levelt, V. E. Fioletov, R. R. Dickerson, H. He, Z. Lu, and D. G. Streets. Aura OMI observations of regional SO2 and NO2 pollution changes from 2005 to 2015. *Atmos. Chem. Phys.*, 16(7):4605–4629, April 2016.

ISSN 1680-7324. doi: 10.5194/acp-16-4605-2016. URL http://www.atmos-chem-phys.net/16/4605/2016/.

Fred Kucharski, Franco Molteni, Martin P. King, Riccardo Farneti, In-Sik Kang, and Laura Feudale. On the Need of Intermediate Complexity General Circulation Models: A “SPEEDY” Example. *Bulletin of the American Meteorological Society*, 94(1):25–30, August 2012. ISSN 0003-0007. doi: 10.1175/BAMS-D-11-00238.1. URL https://journals.ametsoc.org/doi/abs/10.1175/BAMS-D-11-00238.1.

Fred Kucharski, Ning Zeng, and Eugenia Kalnay. A further assessment of vegetation feedback on decadal Sahel rainfall variability. *Climate Dynamics*, 40(5):1453–1466, March 2013. ISSN 1432-0894. doi: 10.1007/s00382-012-1397-x. URL https://doi.org/10.1007/s00382-012-1397-x.

Anna Kuchment. Drilling for Earthquakes. *Scientific American*, March 2016. URL http://www.scientificamerican.com/article/drilling-for-earthquakes/.

Eliana La Ferrara, Alberto Chong, and Suzanne Duryea. Soap Operas and Fertility: Evidence from Brazil. *American Economic Journal: Applied Economics*, 4(4): 1–31, July 2012. ISSN 1945-7782. doi: 10.1257/app.4.4.1. URL https://www.aeaweb.org/articles?id=10.1257/app.4.4.1.

Sifeddine Labed. PV Large Scale Rural Electrification Programs and the Development of Desert Regions. In Frano Barbir and Sergio Ulgiati, editors, *Sustainable Energy Production and Consumption: Benefits, Strategies and Environmental Costing*, NATO Science for Peace and Security Series C: Environmental Security, pages 281–292. Springer Netherlands, 2008. ISBN 978-1-4020-8492-8. URL //www.springer.com/us/book/9781402084928.

A. S. Lafuite and M. Loreau. Time-delayed biodiversity feedbacks and the sustainability of social-ecological systems. *Ecological Modelling*, 351:96–108, May 2017. ISSN 0304-3800. doi: 10.1016/j.ecolmodel.2017.02.022. URL http://www.sciencedirect.com/science/article/pii/S0304380016307128.

A.-S. Lafuite, C. de Mazancourt, and M. Loreau. Delayed behavioural shifts undermine the sustainability of social–ecological systems. *Proc. R. Soc. B*, 284(1868): 20171192, December 2017. ISSN 0962-8452, 1471-2954. doi: 10.1098/rspb.2017.1192. URL http://rspb.royalsocietypublishing.org/content/284/1868/20171192.

A. S. Lafuite, G. Denise, and M. Loreau. Sustainable Land-use Management Under Biodiversity Lag Effects. *Ecological Economics*, 154:272–281, December 2018. ISSN 0921-8009. doi: 10.1016/j.ecolecon.2018.08.003. URL http://www.sciencedirect.com/science/article/pii/S0921800918305585.

Christian Lauk and Karl-Heinz Erb. Biomass consumed in anthropogenic vegetation fires: Global patterns and processes. *Ecological Economics*, 69(2):301–309, December 2009. ISSN 0921-8009. doi: 10.1016/j.ecolecon.2009.07.003. URL http://www.sciencedirect.com/science/article/pii/S0921800909002730.

William F. Laurance. Rapid Land-Use Change and its Impacts on Tropical Biodiversity. In Ruth S. Defries, Gregory P. Asner, and Richard A. Houghton, editors, *Ecosystems and Land Use Change*, pages 189–199. American Geophysical Union, 2004. ISBN 978-1-118-66598-5. URL http://onlinelibrary.wiley.com/doi/10.1029/153GM15/summary.

William F. Laurance, Susan G. Laurance, Leandro V. Ferreira, Judy M. Rankin-de Merona, Claude Gascon, and Thomas E. Lovejoy. Biomass Collapse in Amazonian Forest Fragments. *Science*, 278(5340):1117–1118, November 1997. ISSN 0036-8075, 1095-9203. doi: 10.1126/science.278.5340.1117. URL http://www.sciencemag.org/content/278/5340/1117.

William F. Laurance, Heraldo L. Vasconcelos, and Thomas E. Lovejoy. Forest loss and fragmentation in the Amazon: implications for wildlife conservation. *Oryx*, 34 (1):39–45, January 2000. ISSN 1365-3008. doi: 10.1046/j.1365-3008.2000.00094.x. URL http://onlinelibrary.wiley.com/doi/10.1046/j.1365-3008.2000.00094.x/abstract.

William F. Laurance, Thomas E. Lovejoy, Heraldo L. Vasconcelos, Emilio M. Bruna, Raphael K. Didham, Philip C. Stouffer, Claude Gascon, Richard O. Bierregaard, Susan G. Laurance, and Erica Sampaio. Ecosystem Decay of Amazonian Forest Fragments: a 22-Year Investigation. *Conservation Biology*, 16(3): 605–618, June 2002. ISSN 1523-1739. doi: 10.1046/j.1523-1739.2002.01025.x. URL http://onlinelibrary.wiley.com/doi/10.1046/j.1523-1739.2002.01025.x/abstract.

Scott Lawrence, Qin Liu, and Victor M. Yakovenko. Global Inequality in Energy Consumption from 1980 to 2010. *Entropy*, 15(12):5565–5579, 2013. ISSN 1099-4300. doi: 10.3390/e15125565. URL http://www.mdpi.com/1099-4300/15/12/5565.

C. Le Quéré, R. Moriarty, R. M. Andrew, G. P. Peters, P. Ciais, P. Friedlingstein, S. D. Jones, S. Sitch, P. Tans, A. Arneth, T. A. Boden, L. Bopp, Y. Bozec, J. G. Canadell, F. Chevallier, C. E. Cosca, I. Harris, M. Hoppema, R. A. Houghton, J. I. House, A. Jain, T. Johannessen, E. Kato, R. F. Keeling, V. Kitidis, K. Klein Goldewijk, C. Koven, C. S. Landa, P. Landschützer, A. Lenton, I. D. Lima, G. Marland, J. T. Mathis, N. Metzl, Y. Nojiri, A. Olsen, T. Ono, W. Peters, B. Pfeil, B. Poulter, M. R. Raupach, P. Regnier, C. Rödenbeck, S. Saito, J. E. Salisbury, U. Schuster, J. Schwinger, R. Séférian, J. Segschneider, T. Steinhoff, B. D. Stocker, A. J. Sutton, T. Takahashi, B. Tilbrook, G. R. van der Werf, N. Viovy, Y.-P. Wang, R. Wanninkhof, A. Wiltshire, and N. Zeng. Global carbon budget 2014. *Earth System Science Data Discussions*, 7(2):521–610, September 2014.

ISSN 1866-3591. doi: 10.5194/essdd-7-521-2014. URL http://www.earth-syst-sci-data-discuss.net/7/521/2014/essdd-7-521-2014.html.

Timothy M. Lenton, Hermann Held, Elmar Kriegler, Jim W. Hall, Wolfgang Lucht, Stefan Rahmstorf, and Hans Joachim Schellnhuber. Tipping elements in the Earth's climate system. *Proceedings of the National Academy of Sciences*, 105 (6):1786–1793, February 2008. ISSN 0027-8424, 1091-6490. doi: 10.1073/pnas.0705414105. URL http://www.pnas.org/content/105/6/1786.

M. Lenzen, D. Moran, K. Kanemoto, B. Foran, L. Lobefaro, and A. Geschke. International trade drives biodiversity threats in developing nations. *Nature*, 486(7401): 109–112, June 2012. ISSN 0028-0836. doi: 10.1038/nature11145. URL http://www.nature.com/nature/journal/v486/n7401/full/nature11145.html.

Ron Lesthaeghe. The Fertility Transition in Sub-Saharan Africa into the 21 st Century. Technical Report 14-823, Population Studies Center, University of Michigan, 2014. URL http://www.psc.isr.umich.edu/pubs/pdf/rr14-823.pdf.

Simon L. Lewis, David P. Edwards, and David Galbraith. Increasing human dominance of tropical forests. *Science*, 349(6250):827–832, August 2015. ISSN 0036-8075, 1095-9203. doi: 10.1126/science.aaa9932. URL http://www.sciencemag.org/content/349/6250/827.

Yan Li. Model simulation data for the climate impacts of large-scale wind and solar farms in the Sahara and the world's deserts, September 2018. URL https://figshare.com/articles/Model_simulation_data_for_the_climate_impacts_of_large-scale_wind_and_solar_farms_in_the_Sahara_and_the_world_s_deserts/6662963.

Yan Li, Maosheng Zhao, Safa Motesharrei, Qiaozhen Mu, Eugenia Kalnay, and Shuangcheng Li. Local cooling and warming effects of forests based on satellite observations. *Nature Communications*, 6:6603, March 2015. doi: 10.1038/ncomms7603. URL http://www.nature.com/ncomms/2015/150325/ncomms7603/full/ncomms7603.html.

Yan Li, Nathalie De Noblet-Ducoudré, Edouard L. Davin, Safa Motesharrei, Ning Zeng, Shuangcheng Li, and Eugenia Kalnay. The role of spatial scale and background climate in the latitudinal temperature response to deforestation. *Earth System Dynamics*, 7(1):167–181, March 2016a. ISSN 2190-4987. doi: 10.5194/esd-7-167-2016. URL http://www.earth-syst-dynam.net/7/167/2016/.

Yan Li, Maosheng Zhao, David J. Mildrexler, Safa Motesharrei, Qiaozhen Mu, Eugenia Kalnay, Fang Zhao, Shuangcheng Li, and Kaicun Wang. Potential and Actual impacts of deforestation and afforestation on land surface temperature. *Journal of Geophysical Research: Atmospheres*, 121(24):14,372–14,386, December 2016b. ISSN 2169-8996. doi: 10.1002/2016JD024969. URL http://onlinelibrary.wiley.com/doi/10.1002/2016JD024969/abstract.

Yan Li, Damien Sulla-Menashe, Safa Motesharrei, Xiao-Peng Song, Eugenia Kalnay, Qing Ying, Shuangcheng Li, and Zongwen Ma. Inconsistent estimates of forest cover change in China between 2000 and 2013 from multiple datasets: differences in parameters, spatial resolution, and definitions. *Scientific Reports*, 7(1):8748, August 2017. ISSN 2045-2322. doi: 10.1038/s41598-017-07732-5. URL https://www.nature.com/articles/s41598-017-07732-5.

Yan Li, Eugenia Kalnay, Safa Motesharrei, Jorge Rivas, Fred Kucharski, Daniel Kirk-Davidoff, Eviatar Bach, and Ning Zeng. Climate model shows large-scale wind and solar farms in the Sahara increase rain and vegetation. *Science*, 361 (6406):1019–1022, September 2018. ISSN 0036-8075, 1095-9203. doi: 10.1126/science.aar5629. URL http://science.sciencemag.org/content/361/6406/1019.

Zhe Li, Fergal Boyle, and Anthony Reynolds. Rainwater harvesting and greywater treatment systems for domestic application in Ireland. *Desalination*, 260(1):1–8, September 2010. ISSN 0011-9164. doi: 10.1016/j.desal.2010.05.035. URL http://www.sciencedirect.com/science/article/pii/S0011916410003504.

Erin K. Lipp, Anwar Huq, and Rita R. Colwell. Effects of Global Climate on Infectious Disease: the Cholera Model. *Clinical Microbiology Reviews*, 15(4):757–770, October 2002. ISSN 0893-8512, 1098-6618. doi: 10.1128/CMR.15.4.757-770.2002. URL http://cmr.asm.org/content/15/4/757.

Jianguo Liu, Thomas Dietz, Stephen R. Carpenter, Marina Alberti, Carl Folke, Emilio Moran, Alice N. Pell, Peter Deadman, Timothy Kratz, Jane Lubchenco, Elinor Ostrom, Zhiyun Ouyang, William Provencher, Charles L. Redman, Stephen H. Schneider, and William W. Taylor. Complexity of Coupled Human and Natural Systems. *Science*, 317(5844):1513–1516, September 2007. ISSN 0036-8075, 1095-9203. doi: 10.1126/science.1144004. URL http://science.sciencemag.org/content/317/5844/1513.

Y. Liu, Z. Liu, S. Zhang, R. Jacob, F. Lu, X. Rong, and S. Wu. Ensemble-Based Parameter Estimation in a Coupled General Circulation Model. *Journal of Climate*, 27(18):7151–7162, August 2014a. ISSN 0894-8755. doi: 10.1175/JCLI-D-13-00406.1. URL http://journals.ametsoc.org/doi/abs/10.1175/JCLI-D-13-00406.1.

Y. Liu, Z. Liu, S. Zhang, X. Rong, R. Jacob, S. Wu, and F. Lu. Ensemble-Based Parameter Estimation in a Coupled GCM Using the Adaptive Spatial Average Method. *Journal of Climate*, 27(11):4002–4014, February 2014b. ISSN 0894-8755. doi: 10.1175/JCLI-D-13-00091.1. URL http://journals.ametsoc.org/doi/abs/10.1175/JCLI-D-13-00091.1.

Ya Liu, Yan Li, Shuangcheng Li, and Safa Motesharrei. Spatial and Temporal Patterns of Global NDVI Trends: Correlations with Climate and Human Factors. *Remote Sensing*, 7(10):13233–13250, October 2015. doi: 10.3390/rs71013233. URL http://www.mdpi.com/2072-4292/7/10/13233.

J. T. Lizier and M. Prokopenko. Differentiating information transfer and causal effect. *The European Physical Journal B*, 73(4):605–615, 2010. ISSN 1434-6028. doi: 10.1140/epjb/e2010-00034-5. URL http://dx.doi.org/10.1140/epjb/e2010-00034-5.

Joseph T. Lizier, Mikhail Prokopenko, and Albert Y. Zomaya. Local information transfer as a spatiotemporal filter for complex systems. *Phys. Rev. E*, 77:026110, Feb 2008. doi: 10.1103/PhysRevE.77.026110. URL http://link.aps.org/doi/10.1103/PhysRevE.77.026110.

David B. Lobell and Christopher B. Field. Global scale climate–crop yield relationships and the impacts of recent warming. *Environmental Research Letters*, 2(1): 014002, March 2007. ISSN 1748-9326. doi: 10.1088/1748-9326/2/1/014002. URL http://iopscience.iop.org/1748-9326/2/1/014002.

David B. Lobell, Wolfram Schlenker, and Justin Costa-Roberts. Climate Trends and Global Crop Production Since 1980. *Science*, 333(6042):616–620, July 2011. ISSN 0036-8075, 1095-9203. doi: 10.1126/science.1204531. URL http://www.sciencemag.org/content/333/6042/616.

Brad Lobitz, Louisa Beck, Anwar Huq, Byron Wood, George Fuchs, A. S. G. Faruque, and Rita Colwell. Climate and infectious disease: Use of remote sensing for detection of Vibrio cholerae by indirect measurement. *Proceedings of the National Academy of Sciences*, 97(4):1438–1443, February 2000. ISSN 0027-8424, 1091-6490. doi: 10.1073/pnas.97.4.1438. URL http://www.pnas.org/content/97/4/1438.

Andrew C. Lorenc. The potential of the ensemble Kalman filter for NWP—a comparison with 4d-Var. *Quarterly Journal of the Royal Meteorological Society*, 129 (595):3183–3203, October 2003. ISSN 1477-870X. doi: 10.1256/qj.02.132. URL http://onlinelibrary.wiley.com/doi/10.1256/qj.02.132/abstract.

Edward N Lorenz. Deterministic nonperiodic flow. *Journal of the atmospheric sciences*, 20(2):130–141, 1963.

Xi Lu, Michael B. McElroy, and Juha Kiviluoma. Global potential for wind-generated electricity. *Proceedings of the National Academy of Sciences*, 106 (27):10933–10938, July 2009. ISSN 0027-8424, 1091-6490. doi: 10.1073/pnas.0904101106. URL http://www.pnas.org/content/106/27/10933.

Angela Luci-Greulich and Olivier Thévenon. The Impact of Family Policies on Fertility Trends in Developed Countries. *European Journal of Population / Revue européenne de Démographie*, 29(4):387–416, July 2013. ISSN 0168-6577, 1572-9885. doi: 10.1007/s10680-013-9295-4. URL http://link.springer.com/article/10.1007/s10680-013-9295-4.

Wolfgang Lutz and Samir Kc. Global Human Capital: Integrating Education and Population. *Science*, 333(6042):587–592, July 2011. ISSN 0036-8075, 1095-9203. doi: 10.1126/science.1206964. URL http://science.sciencemag.org/content/333/6042/587.

Wolfgang Lutz, Jesús Crespo Cuaresma, and Mohammad Jalal Abbasi-Shavazi. Demography, Education, and Democracy: Global Trends and the Case of Iran. *Population and Development Review*, 36(2):253–281, June 2010. ISSN 1728-4457. doi: 10.1111/j.1728-4457.2010.00329.x. URL http://onlinelibrary.wiley.com/doi/10.1111/j.1728-4457.2010.00329.x/abstract.

Wolfgang Lutz, William P. Butz, and Samir KC, editors. *World Population and Human Capital in the Twenty-First Century*. Oxford University Press, Oxford, UK, August 2014. ISBN 978-0-19-100822-1.

S. Kathleen Lyons, Felisa A. Smith, and James H. Brown. Of mice, mastodons and men: human-mediated extinctions on four continents. *Evolutionary Ecology Research*, 6(3):339–358, 2004. ISSN 1522-0613. URL http://www.evolutionary-ecology.com/abstracts/v06/1499.html.

Alexander E. MacDonald, Christopher T. M. Clack, Anneliese Alexander, Adam Dunbar, James Wilczak, and Yuanfu Xie. Future cost-competitive electricity systems and their impact on US CO_2 emissions. *Nature Climate Change*, 6(5): 526–531, May 2016. ISSN 1758-6798. doi: 10.1038/nclimate2921. URL https://www.nature.com/articles/nclimate2921.

G. M. Mace, H. Masundire, and J. Baillie. Biodiversity. In Rashid Hassan, Robert J. Scholes, and Neville Ash, editors, *Ecosystems and human well-being: Current state and trends, Volume 1*, volume 1 of *Millennium Ecosystem Assessment*, pages 77 – 122. Island Press, Washington, DC, 2005.

Angus Maddison. *The World economy: a millennial perspective*. Development Centre of the Organisation for Economic Co-operation and Development, [Paris], 2001. ISBN 92-64-18608-5 978-92-64-18608-8.

Syukuro Manabe and Richard T. Wetherald. Thermal Equilibrium of the Atmosphere with a Given Distribution of Relative Humidity. *Journal of the Atmospheric Sciences*, 24(3):241–259, May 1967. ISSN 0022-4928. doi: 10.1175/1520-0469(1967)024⟨0241:TEOTAW⟩2.0.CO;2. URL http://journals.ametsoc.org/doi/abs/10.1175/1520-0469(1967)024%3C0241%3ATEOTAW%3E2.0.CO%3B2.

Syukuro Manabe, Joseph Smagorinsky, and Robert F. Strickler. Simulated climatology of a general circulation model with a hydrologic cycle. *Monthly Weather Review*, 93(12):769–798, December 1965. ISSN 0027-0644. doi: 10.1175/1520-0493(1965)093⟨0769:SCOAGC⟩2.3.CO;2. URL http://journals.ametsoc.org/doi/abs/10.1175/1520-0493(1965)093%3C0769:SCOAGC%3E2.3.CO;2.

Daniele Marinazzo, Mario Pellicoro, and Sebastiano Stramaglia. Kernel method for nonlinear granger causality. *Phys. Rev. Lett.*, 100:144103, Apr 2008. doi: 10.1103/PhysRevLett.100.144103. URL http://link.aps.org/doi/10.1103/PhysRevLett.100.144103.

Gregg Marland, Tom A. Boden, and Robert J. Andres. Global, regional, and national fossil fuel CO2 emissions. Technical report, Carbon Dioxide Information Analysis Center, Oak Ridge National Laboratory, U.S. Department of Energy, Oak Ridge, Tenn., U.S.A., 2012.

Kate Marvel, Ben Kravitz, and Ken Caldeira. Geophysical limits to global wind power. *Nature Climate Change*, 3(2):118–121, February 2013. ISSN 1758-6798. doi: 10.1038/nclimate1683. URL https://www.nature.com/articles/nclimate1683.

William Henry Matthews, William W. Kellogg, and G. D. Robinson. *Man's impact on the climate*. MIT press, Cambridge, Mass., and London, England, 1971.

Christophe McGlade and Paul Ekins. The geographical distribution of fossil fuels unused when limiting global warming to 2 °C. *Nature*, 517(7533):187–190, January 2015. ISSN 1476-4687. doi: 10.1038/nature14016. URL https://www.nature.com/articles/nature14016.

Donella H. Meadows. *Thinking in Systems: A Primer*. Chelsea Green Publishing, White River Junction, VT, 2008. ISBN 978-1-60358-055-7.

Gerald A. Meehl and Claudia Tebaldi. More Intense, More Frequent, and Longer Lasting Heat Waves in the 21st Century. *Science*, 305(5686):994–997, August 2004. ISSN 0036-8075, 1095-9203. doi: 10.1126/science.1098704. URL http://science.sciencemag.org/content/305/5686/994.

Wei Mei and Shang-Ping Xie. Intensification of landfalling typhoons over the northwest Pacific since the late 1970s. *Nature Geoscience*, advance online publication, September 2016. ISSN 1752-0894. doi: 10.1038/ngeo2792. URL http://www.nature.com/ngeo/journal/vaop/ncurrent/full/ngeo2792.html.

M. M. Mekonnen and A. Y. Hoekstra. Four billion people facing severe water scarcity. *Science Advances*, 2(2):e1500323–e1500323, February 2016. ISSN 2375-2548. doi: 10.1126/sciadv.1500323. URL http://advances.sciencemag.org/cgi/doi/10.1126/sciadv.1500323.

Jerry M. Melillo, Terese (T. C.) Richmond, and Gary W. Yohe. *Climate Change Impacts in the United States: The Third National Climate Assessment*. U.S. Global Change Research Program, Washington, DC, 2014. URL doi:10.7930/J0Z31WJ2.

Frank Melzner, Jörn Thomsen, Wolfgang Koeve, Andreas Oschlies, Magdalena A. Gutowska, Hermann W. Bange, Hans Peter Hansen, and Arne Körtzinger. Future ocean acidification will be amplified by hypoxia in coastal habitats. *Marine Biology*, 160(8):1875–1888, May 2012. ISSN 0025-3162, 1432-1793. doi: 10.1007/s00227-012-1954-1. URL http://link.springer.com/article/10.1007/s00227-012-1954-1.

Michel Meybeck. Global analysis of river systems: from Earth system controls to Anthropocene syndromes. *Philosophical Transactions of the Royal Society of London B: Biological Sciences*, 358(1440):1935–1955, December 2003. ISSN 0962-8436, 1471-2970. doi: 10.1098/rstb.2003.1379. URL http://rstb.royalsocietypublishing.org/content/358/1440/1935.

Richard J. Millar, Jan S. Fuglestvedt, Pierre Friedlingstein, Joeri Rogelj, Michael J. Grubb, H. Damon Matthews, Ragnhild B. Skeie, Piers M. Forster, David J. Frame, and Myles R. Allen. Emission budgets and pathways consistent with limiting warming to 1.5 °C. *Nature Geoscience*, 10(10):741–747, October 2017. ISSN 1752-0908. doi: 10.1038/ngeo3031. URL https://www.nature.com/articles/ngeo3031.

James R. Miller, Gary L. Russell, and Guilherme Caliri. Continental-Scale River Flow in Climate Models. *Journal of Climate*, 7(6):914–928, June 1994. ISSN 0894-8755. doi: 10.1175/1520-0442(1994)007⟨0914:CSRFIC⟩2.0.CO;2. URL https://journals.ametsoc.org/doi/abs/10.1175/1520-0442(1994)007%3C0914%3ACSRFIC%3E2.0.CO%3B2.

L. M. Miller, F. Gans, and A. Kleidon. Estimating maximum global land surface wind power extractability and associated climatic consequences. *Earth Syst. Dynam.*, 2(1):1–12, February 2011. ISSN 2190-4987. doi: 10.5194/esd-2-1-2011. URL https://www.earth-syst-dynam.net/2/1/2011/.

Lee M. Miller, Nathaniel A. Brunsell, David B. Mechem, Fabian Gans, Andrew J. Monaghan, Robert Vautard, David W. Keith, and Axel Kleidon. Two methods for estimating limits to large-scale wind power generation. *Proceedings of the National Academy of Sciences*, 112(36):11169–11174, September 2015. ISSN 0027-8424, 1091-6490. doi: 10.1073/pnas.1408251112. URL http://www.pnas.org/content/112/36/11169.

Ronald E. Miller and Peter D. Blair. *Input-Output Analysis: Foundations and Extensions*. Cambridge University Press, New York, NY, July 2009. ISBN 978-1-139-47759-8.

Dev Millstein and Surabi Menon. Regional climate consequences of large-scale cool roof and photovoltaic array deployment. *Environmental Research Letters*, 6(3):034001, 2011. ISSN 1748-9326. doi: 10.1088/1748-9326/6/3/034001. URL http://stacks.iop.org/1748-9326/6/i=3/a=034001.

David Molden. *Water for Food, Water for Life: A Comprehensive Assessment of Water Management in Agriculture*. Earthscan, London, UK; Sterling, VA, USA, 2007. ISBN 978-1-84407-397-9.

François Molle, Philippus Wester, and Philip Hirsch. River basin closure: Processes, implications and responses. *Agricultural Water Management*, 97(4):569–577, April 2010. doi: 10.1016/j.agwat.2009.01.004. URL http://www.sciencedirect.com/science/article/pii/S037837740900016X.

F. Molteni. Atmospheric simulations using a GCM with simplified physical parametrizations. I: model climatology and variability in multi-decadal experiments. *Climate Dynamics*, 20(2):175–191, January 2003. ISSN 1432-0894. doi: 10.1007/s00382-002-0268-2. URL https://doi.org/10.1007/s00382-002-0268-2.

Eric Monnin, Andreas Indermhle, Andr Dllenbach, Jacqueline Flckiger, Bernhard Stauffer, Thomas F. Stocker, Dominique Raynaud, and Jean-Marc Barnola. Atmospheric co2 concentrations over the last glacial termination. *Science*, 291 (5501):112–114, 2001. doi: 10.1126/science.291.5501.112. URL http://www.sciencemag.org/content/291/5501/112.abstract.

Frances C. Moore and David B. Lobell. The fingerprint of climate trends on European crop yields. *Proceedings of the National Academy of Sciences*, 112(9):2670–2675, March 2015. ISSN 0027-8424, 1091-6490. doi: 10.1073/pnas.1409606112. URL http://www.pnas.org/content/112/9/2670.

Safa Motesharrei. *Minimal Models of Human–Nature Interaction*. PhD Dissertation, University of Maryland, College Park, MD, USA, 2014.

Safa Motesharrei, Jorge Rivas, and Eugenia Kalnay. Human and nature dynamics (HANDY): Modeling inequality and use of resources in the collapse or sustainability of societies. *Ecological Economics*, 101:90–102, May 2014. ISSN 0921-8009. doi: 10.1016/j.ecolecon.2014.02.014. URL http://www.sciencedirect.com/science/article/pii/S0921800914000615.

Safa Motesharrei, Jorge Rivas, Eugenia Kalnay, Ghassem R. Asrar, Antonio J. Busalacchi, Robert F. Cahalan, Mark A. Cane, Rita R. Colwell, Kuishuang Feng, Rachel S. Franklin, Klaus Hubacek, Fernando Miralles-Wilhelm, Takemasa Miyoshi, Matthias Ruth, Roald Sagdeev, Adel Shirmohammadi, Jagadish Shukla, Jelena Srebric, Victor M. Yakovenko, and Ning Zeng. Modeling sustainability: population, inequality, consumption, and bidirectional coupling of the Earth and Human Systems. *National Science Review*, 3 (4):470–494, December 2016. ISSN 2095-5138. doi: 10.1093/nsr/nww081. URL https://academic.oup.com/nsr/article/3/4/470/2669331/Modeling-sustainability-population-inequality.

Safa Motesharrei, Cortney Gustafson, Jorge Rivas, Fang Zhao, Huan Wu, Fernando Miralles-Wilhelm, Ning Zeng, Klaus Hubacek, and Eugenia Kalnay. COWA: a

Two-way Coupled Human–Climate–Water Model to explore water management options. 2019.

Pablo Muñoz, Stefan Giljum, and Jordi Roca. The Raw Material Equivalents of International Trade. *Journal of Industrial Ecology*, 13(6):881–897, December 2009. ISSN 1530-9290. doi: 10.1111/j.1530-9290.2009.00154.x. URL http://onlinelibrary.wiley.com/doi/10.1111/j.1530-9290.2009.00154.x/abstract.

Joy Murray and Richard Wood. *The Sustainability Practitioner's Guide to Input-output Analysis*. Common Ground Pub., Champaign, IL, 2010. ISBN 978-1-86335-747-0.

Norman Myers. Environmental refugees: a growing phenomenon of the 21st century. *Philosophical Transactions of the Royal Society of London B: Biological Sciences*, 357(1420):609–613, April 2002. ISSN 0962-8436, 1471-2970. doi: 10.1098/rstb.2001.0953. URL http://rstb.royalsocietypublishing.org/content/357/1420/609.

Samuel S. Myers, Lynne Gaffikin, Christopher D. Golden, Richard S. Ostfeld, Kent H. Redford, Taylor H. Ricketts, Will R. Turner, and Steven A. Osofsky. Human health impacts of ecosystem alteration. *Proceedings of the National Academy of Sciences*, 110(47):18753–18760, November 2013. ISSN 0027-8424, 1091-6490. doi: 10.1073/pnas.1218656110. URL http://www.pnas.org/content/110/47/18753.

Nebosja Nakicenovic and Keywan Riahi. Model runs with MESSAGE in the Context of the Further Development of the Kyoto-Protocol. FINAL REPORT submitted to the Secretariat of the German Advisory Council on Global Change Contract Nr. WBGU II/2003; IIASA Contract No. 03-116, International Institute for Applied Systems Analysis (IIASA), Laxenburg, Austria, 2003. URL http://www.wbgu.de/fileadmin/templates/dateien/veroeffentlichungen/sondergutachten/sn2003/wbgu_sn2003_ex03.pdf.

NAS. *The Growth of World Population: Analysis of the Problems and Recommendations for Research and Training*. National Academy of Sciences, Committee on Science and Public Policy. National Academies Press, Washington, D.C., January 1963. ISBN 978-0-309-59363-2. URL http://www.nap.edu/catalog/9543.

NAS. *Rapid Population Growth: Consequences and Policy Implications*. National Academy of Sciences, Office of the Foreign Secretary. The Johns Hopkins University Press, for the National Academy of Sciences, Baltimore, August 1971. ISBN 978-0-8018-1264-4.

NAS. *Population Growth and Economic Development: Policy Questions*. National Academies of Sciences, Engineering, and Medicine, Committee on Population, Division of Behavioral and Social Sciences and Education, National Research

Council. National Academies Press, Washington, D.C., January 1986. ISBN 978-0-309-03641-2. URL http://www.nap.edu/catalog/620.

NAS. *Population and Land Use in Developing Countries: Report of a Workshop*. National Academy of Sciences, Committee on Population, Division of Behavioral and Social Sciences and Education, National Research Council. National Academies Press, Washington, D.C., January 1993. ISBN 978-0-309-04838-5. URL http://www.nap.edu/catalog/2211.

NAS. *Critical Perspectives on Schooling and Fertility in the Developing World*. National Academy of Sciences, Committee on Population, Division of Behavioral and Social Sciences and Education, National Research Council. National Academies Press, Washington, D.C., December 1999. ISBN 978-0-309-06191-9. URL http://www.nap.edu/catalog/6272.

NAS. *The Determinants of Recent Trends in Fertility in Sub-Saharan Africa: A Workshop Summary*. National Academies of Sciences, Engineering, and Medicine, Committee on Population, Division of Behavioral and Social Sciences and Education. National Academies Press, Washington, D.C., 2016. ISBN 978-0-309-38119-2. URL http://www.nap.edu/catalog/21857.

NAS and Royal Society. The Royal Society and the National Academy of Sciences on Population Growth and Sustainability: Population Growth, Resource Consumption, and a Sustainable World. *Population and Development Review*, 18(2):375–378, 1992. ISSN 0098-7921. doi: 10.2307/1973696. URL http://www.jstor.org/stable/1973696.

NASA. *Earth System Science: A Closer View*. National Aeronautics and Space Administration, Washington, DC, 1988.

National Research Council. *Can Earth's and Society's Systems Meet the Needs of 10 Billion People? Summary of a Workshop*. The National Academies Press, Washington, DC, August 2014. ISBN 978-0-309-30634-8. URL https://doi.org/10.17226/18817. Board on Environmental Change and Society and Committee on Population, Division of Behavioral and Social Sciences and Education. Board on Life Sciences, Division on Earth and Life Studies.

Andrés Navarro, Raúl Moreno, Alfonso Jiménez-Alcázar, and Francisco J. Tapiador. Coupling population dynamics with earth system models: the POPEM model. *Environmental Science and Pollution Research*, September 2017. ISSN 1614-7499. doi: 10.1007/s11356-017-0127-7. URL https://doi.org/10.1007/s11356-017-0127-7.

Andrés Navarro, Raúl Moreno, and Francisco J. Tapiador. Improving the representation of anthropogenic CO_2 emissions in climate models: impact of a new parameterization for the Community Earth System Model (CESM). *Earth System Dynamics*, 9(3):1045–1062, August 2018. ISSN 2190-4979. doi: https://

doi.org/10.5194/esd-9-1045-2018. URL https://www.earth-syst-dynam.net/9/1045/2018/.

Carlos Nobre, Guy P. Brasseur, Melvyn A. Shapiro, Myanna Lahsen, Gilbert Brunet, Antonio J. Busalacchi, Kathy Hibbard, Sybil Seitzinger, Kevin Noone, and Jean P. Ometto. Addressing the Complexity of the Earth System. *Bulletin of the American Meteorological Society*, 91(10):1389–1396, August 2010. ISSN 0003-0007. doi: 10.1175/2010BAMS3012.1. URL http://journals.ametsoc.org/doi/abs/10.1175/2010BAMS3012.1.

Carlos Afonso Nobre and Laura De Simone Borma. 'Tipping points' for the Amazon forest. *Current Opinion in Environmental Sustainability*, 1(1):28–36, October 2009. doi: 10.1016/j.cosust.2009.07.003. URL http://www.sciencedirect.com/science/article/pii/S1877343509000062.

G. Nolte, A. Ziehe, V. Nikulin, A. Schlögl, N. Krämer, T. Brismar, and K.-R. Müller. Robustly Estimating the Flow Direction of Information in Complex Physical Systems. *Physical Review Letters*, 100:234101, June 2008. URL http://doc.ml.tu-berlin.de/causality.

William D. Nordhaus, Hendrik Houthakker, and Robert Solow. The Allocation of Energy Resources. *Brookings Papers on Economic Activity*, 1973(3):529–576, 1973. ISSN 0007-2303. doi: 10.2307/2534202. URL http://www.jstor.org/stable/2534202.

Dirk Notz and Julienne Stroeve. Observed Arctic sea-ice loss directly follows anthropogenic CO2 emission. *Science*, page aag2345, November 2016. ISSN 0036-8075, 1095-9203. doi: 10.1126/science.aag2345. URL http://science.sciencemag.org/content/early/2016/11/02/science.aag2345.

OECD. *OECD Factbook 2014*. Organisation for Economic Co-operation and Development, Paris, May 2014. ISBN 978-92-64-20415-7. URL http://www.oecd-ilibrary.org/content/book/factbook-2014-en.

Taikan Oki and Y. C. Sud. Design of Total Runoff Integrating Pathways (TRIP)—A Global River Channel Network. *Earth Interactions*, 2(1):1–37, January 1998. ISSN 1087-3562. doi: 10.1175/1087-3562(1998)002⟨0001:DOTRIP⟩2.3.CO;2. URL https://journals.ametsoc.org/doi/abs/10.1175/1087-3562%281998%29002%3C0001%3ADOTRIP%3E2.3.CO%3B2.

Brian C. O'Neill, Michael Dalton, Regina Fuchs, Leiwen Jiang, Shonali Pachauri, and Katarina Zigova. Global demographic trends and future carbon emissions. *Proceedings of the National Academy of Sciences*, 107(41):17521–17526, October 2010. ISSN 0027-8424, 1091-6490. doi: 10.1073/pnas.1004581107. URL http://www.pnas.org/content/107/41/17521.

J M Pacyna and E G Pacyna. An assessment of global and regional emissions of trace metals to the atmosphere from anthropogenic sources worldwide. *Environmental*

Reviews, 9(4):269–298, December 2001. ISSN 1181-8700. doi: 10.1139/a01-012. URL http://www.nrcresearchpress.com/doi/abs/10.1139/a01-012.

M. A. Palmer, E. S. Bernhardt, W. H. Schlesinger, K. N. Eshleman, E. Foufoula-Georgiou, M. S. Hendryx, A. D. Lemly, G. E. Likens, O. L. Loucks, M. E. Power, P. S. White, and P. R. Wilcock. Mountaintop Mining Consequences. *Science*, 327 (5962):148–149, January 2010. ISSN 0036-8075, 1095-9203. doi: 10.1126/science.1180543. URL http://www.sciencemag.org/content/327/5962/148.

Mercedes Pascual, Xavier Rodó, Stephen P. Ellner, Rita Colwell, and Menno J. Bouma. Cholera Dynamics and El Niño-Southern Oscillation. *Science*, 289(5485): 1766–1769, September 2000. ISSN 0036-8075, 1095-9203. doi: 10.1126/science.289.5485.1766. URL http://www.sciencemag.org/content/289/5485/1766.

Judea Pearl. *Causality: models, reasoning and inference*, volume 29. Cambridge Univ Press, 2000.

Louis M Pecora, Thomas L Carroll, Gregg A Johnson, Douglas J Mar, and James F Heagy. Fundamentals of synchronization in chaotic systems, concepts, and applications. *Chaos: An Interdisciplinary Journal of Nonlinear Science*, 7(4):520–543, 1997.

M. Peña and E. Kalnay. Separating fast and slow modes in coupled chaotic systems. *Nonlinear Processes in Geophysics*, 11(3):319–327, July 2004. URL https://hal.archives-ouvertes.fr/hal-00302339.

Shaobing Peng, Jianliang Huang, John E. Sheehy, Rebecca C. Laza, Romeo M. Visperas, Xuhua Zhong, Grace S. Centeno, Gurdev S. Khush, and Kenneth G. Cassman. Rice yields decline with higher night temperature from global warming. *Proceedings of the National Academy of Sciences of the United States of America*, 101(27):9971–9975, July 2004. ISSN 0027-8424, 1091-6490. doi: 10.1073/pnas.0403720101. URL http://www.pnas.org/content/101/27/9971.

G. P. Peters, S. J. Davis, and R. Andrew. A synthesis of carbon in international trade. *Biogeosciences*, 9(8):3247–3276, August 2012. ISSN 1726-4189. doi: 10.5194/bg-9-3247-2012. URL http://escholarship.org/uc/item/5h6341jg.

Glen P. Peters. From production-based to consumption-based national emission inventories. *Ecological Economics*, 65(1):13–23, March 2008. ISSN 0921-8009. doi: 10.1016/j.ecolecon.2007.10.014. URL http://www.sciencedirect.com/science/article/pii/S0921800907005162.

Glen P. Peters, Jan C. Minx, Christopher L. Weber, and Ottmar Edenhofer. Growth in emission transfers via international trade from 1990 to 2008. *Proceedings of the National Academy of Sciences*, 108(21):8903–8908, May 2011. ISSN 0027-8424, 1091-6490. doi: 10.1073/pnas.1006388108. URL http://www.pnas.org/content/108/21/8903.

John M. Polimeni, Kozo Mayumi, Mario Giampietro, and Blake Alcott. *The Jevons Paradox and the Myth of Resource Efficiency Improvements*. Earthscan, 2008.

Malcolm Potts. Sex and the Birth Rate: Human Biology, Demographic Change, and Access to Fertility-Regulation Methods. *Population and Development Review*, 23 (1):1–39, 1997. ISSN 0098-7921. doi: 10.2307/2137459. URL http://www.jstor.org/stable/2137459.

Malcolm Potts. Getting family planning and population back on track. *Global Health, Science and Practice*, 2(2):145–151, May 2014. ISSN 2169-575X. doi: 10.9745/GHSP-D-14-00012. URL http://www.ncbi.nlm.nih.gov/pmc/articles/PMC4168624/.

Malcolm Potts and Leah Marsh. The Population Factor: How Does it Relate to Climate Change. *Climate Adaptation*, 2010. URL http://bixby.berkeley.edu/wp-content/uploads/2011/10/THE-POPULATION-FACTOR-How-does-it-relate-to-climate-change1.pdf.

Malcolm Potts, Virginia Gidi, Martha Campbell, and Sarah Zureick. Niger: Too Little, Too Late. *International Perspectives on Sexual and Reproductive Health*, 37(2):95–101, 2011. ISSN 1944-0391. URL http://www.jstor.org/stable/41229000.

Luke L. Powell, Gustavo Zurita, Jared D. Wolfe, Erik I. Johnson, and Philip C Stouffer. Changes in Habitat Use at Rain Forest Edges Through Succession: a Case Study of Understory Birds in the Brazilian Amazon. *Biotropica*, 47(6): 723–732, November 2015. ISSN 1744-7429. doi: 10.1111/btp.12253. URL http://onlinelibrary.wiley.com/doi/10.1111/btp.12253/abstract.

PRB. World Population Data Sheet. Technical report, Population Reference Bureau, Washington, DC, 2014. URL http://www.prb.org/DataFinder/Topic/Rankings.aspx?ind=17.

R. Prinn, H. Jacoby, A. Sokolov, C. Wang, X. Xiao, Z. Yang, R. Eckhaus, P. Stone, D. Ellerman, J. Melillo, J. Fitzmaurice, D. Kicklighter, G. Holian, and Y. Liu. Integrated Global System Model for Climate Policy Assessment: Feedbacks and Sensitivity Studies. *Climatic Change*, 41(3-4):469–546, 1999. ISSN 0165-0009, 1573-1480. doi: 10.1023/A:1005326126726. URL http://link.springer.com/article/10.1023/A:1005326126726.

Lant H. Pritchett. Desired Fertility and the Impact of Population Policies. *Population and Development Review*, 20(1):1–55, 1994. ISSN 0098-7921. doi: 10.2307/2137629. URL http://www.jstor.org/stable/2137629.

S. S. Rabotyagov, C. L. Kling, P. W. Gassman, N. N. Rabalais, and R. E. Turner. The Economics of Dead Zones: Causes, Impacts, Policy Challenges, and a Model of the Gulf of Mexico Hypoxic Zone. *Review of Environmental Economics and*

Policy, 8(1):58–79, January 2014. ISSN 1750-6816, 1750-6824. doi: 10.1093/reep/ret024. URL http://reep.oxfordjournals.org/content/8/1/58.

Navin Ramankutty, Jonathan A. Foley, and Nicholas J. Olejniczak. People on the Land: Changes in Global Population and Croplands during the 20th Century. *AMBIO: A Journal of the Human Environment*, 31(3):251–257, May 2002. ISSN 0044-7447. doi: 10.1579/0044-7447-31.3.251. URL http://www.bioone.org/doi/abs/10.1579/0044-7447-31.3.251.

David A. Randall, Richard A. Wood, Sandrine Bony, Robert Colman, Thierry Fichefet, John Fyfe, Vladimir Kattsov, Andrew Pitman, Jagadish Shukla, and Jayaraman Srinivasan. Climate models and their evaluation. In *Climate change 2007: The physical science basis. Contribution of Working Group I to the Fourth Assessment Report of the IPCC (FAR)*, pages 589–662. Cambridge University Press, Cambridge, United Kingdom and New York, NY, USA, 2007.

Michael R. Raupach, Steven J. Davis, Glen P. Peters, Robbie M. Andrew, Josep G. Canadell, Philippe Ciais, Pierre Friedlingstein, Frank Jotzo, Detlef P. van Vuuren, and Corinne Le Quéré. Sharing a quota on cumulative carbon emissions. *Nature Climate Change*, 4(10):873–879, October 2014. ISSN 1758-678X. doi: 10.1038/nclimate2384. URL http://www.nature.com/nclimate/journal/v4/n10/full/nclimate2384.html.

William E. Rees. Revisiting carrying capacity: Area-based indicators of sustainability. *Population and Environment*, 17(3):195–215, 1996. ISSN 0199-0039, 1573-7810. doi: 10.1007/BF02208489. URL http://link.springer.com/article/10.1007/BF02208489.

Helen M. Regan, Richard Lupia, Andrew N. Drinnan, and Mark A. Burgman. The Currency and Tempo of Extinction. *The American Naturalist*, 157(1):1–10, 2001. ISSN 0003-0147. doi: 10.1086/317005. URL http://www.jstor.org/stable/10.1086/317005.

Horst Rinne. *The Weibull distribution: a handbook*. CRC Press, 2008.

Johan Rockström, W. Steffen, Kevin Noone, Åsa Persson, F. Chapin, Eric Lambin, Timothy Lenton, Marten Scheffer, Carl Folke, Hans Schellnhuber, Björn Nykvist, Cynthia de Wit, Terry Hughes, Sander van der Leeuw, Henning Rodhe, Sverker Sörlin, Peter Snyder, Robert Costanza, Uno Svedin, Malin Falkenmark, Louise Karlberg, Robert Corell, Victoria Fabry, James Hansen, Brian Walker, Diana Liverman, Katherine Richardson, Paul Crutzen, and Jonathan Foley. Planetary Boundaries: Exploring the Safe Operating Space for Humanity. *Ecology and Society*, 14(2):32, January 2009. URL http://www.ecologyandsociety.org/vol14/iss2/art32/.

M. Rodell, J. S. Famiglietti, D. N. Wiese, J. T. Reager, H. K. Beaudoing, F. W. Landerer, and M.-H. Lo. Emerging trends in global freshwater availability. *Nature*, 557(7707):651–659, May 2018. ISSN 1476-4687. doi: 10.1038/s41586-018-0123-1. URL https://www.nature.com/articles/s41586-018-0123-1.

Matthew Rodell, Isabella Velicogna, and James S. Famiglietti. Satellite-based estimates of groundwater depletion in India. *Nature*, 460(7258):999–1002, August 2009. ISSN 0028-0836. doi: 10.1038/nature08238. URL http://www.nature.com/nature/journal/v460/n7258/abs/nature08238.html.

Stuart Rojstaczer, Shannon M. Sterling, and Nathan J. Moore. Human Appropriation of Photosynthesis Products. *Science*, 294(5551):2549–2552, December 2001. ISSN 0036-8075, 1095-9203. doi: 10.1126/science.1064375. URL http://science.sciencemag.org/content/294/5551/2549.

Crystal Romeo Upperman, Jennifer Parker, Chengsheng Jiang, Xin He, Raghuram Murtugudde, and Amir Sapkota. Frequency of Extreme Heat Event as a Surrogate Exposure Metric for Examining the Human Health Effects of Climate Change. *PLOS ONE*, 10(12):e0144202, December 2015. ISSN 1932-6203. doi: 10.1371/journal.pone.0144202. URL http://journals.plos.org/plosone/article?id=10.1371/journal.pone.0144202.

Cynthia Rosenzweig, Ana Iglesias, X. B. Yang, Paul R. Epstein, and Eric Chivian. Climate Change and Extreme Weather Events; Implications for Food Production, Plant Diseases, and Pests. *Global Change and Human Health*, 2(2):90–104, 2001. ISSN 1389-5702, 1573-7314. doi: 10.1023/A:1015086831467. URL http://link.springer.com/article/10.1023/A:1015086831467.

Farzaneh Roudi-Fahimi. *Iran's family planning program: responding to a nation's needs*. Population Reference Bureau, Washington, DC, 2002. URL http://rezvanhealth.com/fa_IR/wp-content/uploads/2014/04/FH-4B.pdf.

S. Baidya Roy, S. W. Pacala, and R. L. Walko. Can large wind farms affect local meteorology? *Journal of Geophysical Research: Atmospheres*, 109(D19), October 2004. ISSN 2156-2202. doi: 10.1029/2004JD004763. URL https://agupubs.onlinelibrary.wiley.com/doi/abs/10.1029/2004JD004763.

Somnath Baidya Roy and Justin J. Traiteur. Impacts of wind farms on surface air temperatures. *Proceedings of the National Academy of Sciences*, 107(42):17899–17904, October 2010. ISSN 0027-8424, 1091-6490. doi: 10.1073/pnas.1000493107. URL http://www.pnas.org/content/107/42/17899.

Gregory M. Ruiz, Tonya K. Rawlings, Fred C. Dobbs, Lisa A. Drake, Timothy Mullady, Anwarul Huq, and Rita R. Colwell. Global spread of microorganisms by ships. *Nature*, 408(6808):49–50, November 2000. ISSN 0028-0836. doi: 10.1038/35040695. URL http://www.nature.com/nature/journal/v408/n6808/abs/408049a0.html.

Juan Jose Ruiz, Manuel Pulido, and Takemasa Miyoshi. Estimating Model Parameters with Ensemble-Based Data Assimilation: A Review. *Journal of the Meteorological Society of Japan. Ser. II*, 91(2):79–99, 2013. doi: 10.2151/jmsj.2013-201.

Alfredo Ruiz-Barradas, Eugenia Kalnay, Malaquías Peña, Amir E. BozorgMagham, and Safa Motesharrei. Finding the driver of local ocean–atmosphere coupling in reanalyses and CMIP5 climate models. *Climate Dynamics*, 48(7):2153–2172, April 2017. ISSN 1432-0894. doi: 10.1007/s00382-016-3197-1. URL https://doi.org/10.1007/s00382-016-3197-1.

Matthias Ruth. *Integrating Economics, Ecology and Thermodynamics*, volume 3 of *Ecology, Economy & Environment*. Springer, 1993. ISBN 978-94-017-1899-8. URL http://link.springer.com/chapter/10.1007/978-94-017-1899-8_8.

Matthias Ruth. Information, order and knowledge in economic and ecological systems: implications for material and energy use. *Ecological Economics*, 13(2): 99–114, May 1995a. doi: 10.1016/0921-8009(94)00064-3. URL http://www.sciencedirect.com/science/article/pii/0921800994000643.

Matthias Ruth. Thermodynamic constraints on optimal depletion of copper and aluminum in the United States: a dynamic model of substitution and technical change. *Ecological Economics*, 15(3):197–213, December 1995b. doi: 10.1016/0921-8009(95)00053-4. URL http://www.sciencedirect.com/science/article/pii/0921800995000534.

Matthias Ruth. A quest for the economics of sustainability and the sustainability of economics. *Ecological Economics*, 56(3):332–342, March 2006. ISSN 0921-8009. doi: 10.1016/j.ecolecon.2005.09.012. URL http://www.sciencedirect.com/science/article/pii/S0921800905004258.

Matthias Ruth. The Nature of the Beast and the Beast in Nature: Broadening the Perspective of Technology. *Bulletin of Science, Technology & Society*, 29(5):374–382, October 2009. ISSN 0270-4676, 1552-4183. doi: 10.1177/0270467609342863. URL http://bst.sagepub.com/content/29/5/374.

Matthias Ruth. Economic and Social Benefits of Climate Information: Assessing the Cost of Inaction. *Procedia Environmental Sciences*, 1:387–394, 2010. ISSN 1878-0296. doi: 10.1016/j.proenv.2010.09.026. URL http://www.sciencedirect.com/science/article/pii/S1878029610000277.

Matthias Ruth and Brynhildur Davidsdottir. *Changing Stocks, Flows and Behaviors in Industrial Ecosystems*. Edward Elgar Publishing, Cheltenham, UK; Northampton, MA, USA, January 2009. ISBN 978-1-84844-513-0.

Matthias Ruth and Bruce Hannon. *Modeling Dynamic Economic Systems*. Springer, New York, 2nd edition, February 2012. ISBN 978-1-4614-2208-2.

Matthias Ruth and María Eugenia Ibarrarán. *Distributional Impacts of Climate Change and Disasters: Concepts and Cases*. Edward Elgar Publishing, Cheltenham, UK; Northampton, MA, USA, January 2009. ISBN 978-1-84980-233-8.

Matthias Ruth, Eugenia Kalnay, Ning Zeng, Rachel S. Franklin, Jorge Rivas, and Fernando Miralles-Wilhelm. Sustainable prosperity and societal transitions: Long-term modeling for anticipatory management. *Environmental Innovation and Societal Transitions*, 1(1):160–165, June 2011. ISSN 2210-4224. doi: 10.1016/j.eist.2011.03.004. URL http://www.sciencedirect.com/science/article/pii/S2210422411000104.

Roald Z. Sagdeev and Susan Eisenhower. The Global Warming Problem: A Vital Concern for Global Security. In Terrell J. Minger, editor, *Greenhouse Glasnost: The Crisis of Global Warming*, pages 261–268. Ecco Press, New York, NY; Salt Lake City, UT, 1st edition edition, September 1990. ISBN 978-0-88001-258-4.

L. Sala and M. Serra. Towards sustainability in water recycling. *Water Science and Technology*, 50(2):1–7, July 2004. ISSN 0273-1223. doi: 10.2166/wst.2004.0074. URL /wst/article/50/2/1/9254/Towards-sustainability-in-water-recycling.

Jayant Sathaye, O. Lucon, A. Rahman, J. Christensen, F. Denton, J. Fujino, G. Heath, S. Kadner, M. Mirza, H. Rudnick, and others. Renewable energy in the context of sustainable development. Technical Report IPCC special report on renewable energy sources and climate change mitigation, 2011.

Tim Sauer, JamesA. Yorke, and Martin Casdagli. Embedology. *Journal of Statistical Physics*, 65(3-4):579–616, 1991. ISSN 0022-4715. doi: 10.1007/BF01053745. URL http://dx.doi.org/10.1007/BF01053745.

A. A. Scaife, F. Kucharski, C. K. Folland, J. Kinter, S. Brönnimann, D. Fereday, A. M. Fischer, S. Grainger, E. K. Jin, I. S. Kang, J. R. Knight, S. Kusunoki, N. C. Lau, M. J. Nath, T. Nakaegawa, P. Pegion, S. Schubert, P. Sporyshev, J. Syktus, J. H. Yoon, N. Zeng, and T. Zhou. The CLIVAR C20c project: selected twentieth century climate events. *Climate Dynamics*, 33(5):603–614, October 2009. ISSN 1432-0894. doi: 10.1007/s00382-008-0451-1. URL https://doi.org/10.1007/s00382-008-0451-1.

Bridget R. Scanlon, Kelley E. Keese, Alan L. Flint, Lorraine E. Flint, Cheikh B. Gaye, W. Michael Edmunds, and Ian Simmers. Global synthesis of groundwater recharge in semiarid and arid regions. *Hydrological Processes*, 20(15):3335–3370, October 2006. ISSN 1099-1085. doi: 10.1002/hyp.6335. URL http://onlinelibrary.wiley.com/doi/10.1002/hyp.6335/abstract.

Bridget R. Scanlon, Claudia C. Faunt, Laurent Longuevergne, Robert C. Reedy, William M. Alley, Virginia L. McGuire, and Peter B. McMahon. Groundwater depletion and sustainability of irrigation in the US High Plains and Central Valley.

Proceedings of the National Academy of Sciences, 109(24):9320–9325, June 2012. ISSN 0027-8424, 1091-6490. doi: 10.1073/pnas.1200311109. URL http://www.pnas.org/content/109/24/9320.

Anke Schaffartzik, Andreas Mayer, Simone Gingrich, Nina Eisenmenger, Christian Loy, and Fridolin Krausmann. The global metabolic transition: Regional patterns and trends of global material flows, 1950–2010. *Global Environmental Change*, 26: 87–97, May 2014. ISSN 0959-3780. doi: 10.1016/j.gloenvcha.2014.03.013. URL http://www.sciencedirect.com/science/article/pii/S095937801400065X.

Marten Scheffer and Stephen R. Carpenter. Catastrophic regime shifts in ecosystems: linking theory to observation. *Trends in Ecology & Evolution*, 18(12): 648–656, December 2003. doi: 10.1016/j.tree.2003.09.002. URL http://www.sciencedirect.com/science/article/pii/S0169534703002787.

Marten Scheffer, Steve Carpenter, Jonathan A. Foley, Carl Folke, and Brian Walker. Catastrophic shifts in ecosystems. *Nature*, 413(6856):591–596, October 2001. ISSN 0028-0836. doi: 10.1038/35098000. URL http://www.nature.com/nature/journal/v413/n6856/full/413591a0.html.

Hans Joachim Schellnhuber. Tipping elements in the Earth System. *Proceedings of the National Academy of Sciences*, 106(49):20561–20563, December 2009. ISSN 0027-8424, 1091-6490. doi: 10.1073/pnas.0911106106. URL http://www.pnas.org/content/106/49/20561.

Wolfram Schlenker and David B. Lobell. Robust negative impacts of climate change on African agriculture. *Environmental Research Letters*, 5(1):014010, January 2010. ISSN 1748-9326. doi: 10.1088/1748-9326/5/1/014010. URL http://iopscience.iop.org/1748-9326/5/1/014010.

Wolfram Schlenker and Michael J. Roberts. Nonlinear temperature effects indicate severe damages to U.S. crop yields under climate change. *Proceedings of the National Academy of Sciences*, 106(37):15594–15598, September 2009. ISSN 0027-8424, 1091-6490. doi: 10.1073/pnas.0906865106. URL http://www.pnas.org/content/106/37/15594.

Mary C. Scholes and Robert J. Scholes. Dust Unto Dust. *Science*, 342(6158):565–566, November 2013. ISSN 0036-8075, 1095-9203. doi: 10.1126/science.1244579. URL http://science.sciencemag.org/content/342/6158/565.

Thomas Schreiber. Measuring information transfer. *Phys. Rev. Lett.*, 85:461–464, Jul 2000. doi: 10.1103/PhysRevLett.85.461. URL http://link.aps.org/doi/10.1103/PhysRevLett.85.461.

Sonia I. Seneviratne, Markus G. Donat, Andy J. Pitman, Reto Knutti, and Robert L. Wilby. Allowable CO_2 emissions based on regional and impact-related climate targets. *Nature*, 529(7587):477–483, January 2016. ISSN 1476-4687. doi: 10.1038/nature16542. URL https://www.nature.com/articles/nature16542.

Ralf Seppelt, Ameur M. Manceur, Jianguo Liu, Eli P. Fenichel, and Stefan Klotz. Synchronized peak-rate years of global resources use. *Ecology and Society*, 19(4):50, 2014. doi: 10.5751/ES-07039-190450. URL http://www.ecologyandsociety.org/vol19/iss4/art50/.

Jeremy D Shakun, Peter U Clark, Feng He, Shaun A Marcott, Alan C Mix, Zhengyu Liu, Bette Otto-Bliesner, Andreas Schmittner, and Edouard Bard. Global warming preceded by increasing carbon dioxide concentrations during the last deglaciation. *Nature*, 484(7392):49–54, 2012.

Justin Sheffield, Gopi Goteti, and Eric F. Wood. Development of a 50-Year High-Resolution Global Dataset of Meteorological Forcings for Land Surface Modeling. *Journal of Climate*, 19(13):3088–3111, July 2006. ISSN 0894-8755. doi: 10.1175/JCLI3790.1. URL https://journals.ametsoc.org/doi/abs/10.1175/JCLI3790.1.

Stephen Shennan, Sean S. Downey, Adrian Timpson, Kevan Edinborough, Sue Colledge, Tim Kerig, Katie Manning, and Mark G. Thomas. Regional population collapse followed initial agriculture booms in mid-Holocene Europe. *Nature Communications*, 4:2486, October 2013. doi: 10.1038/ncomms3486. URL http://www.nature.com/ncomms/2013/131001/ncomms3486/full/ncomms3486.html.

Drew T. Shindell, Yunha Lee, and Greg Faluvegi. Climate and health impacts of US emissions reductions consistent with 2 °C. *Nature Climate Change*, 6(5):503–507, May 2016. ISSN 1758-6798. doi: 10.1038/nclimate2935. URL https://www.nature.com/articles/nclimate2935.

Manoochehr Shirzaei, William L. Ellsworth, Kristy F. Tiampo, Pablo J. González, and Michael Manga. Surface uplift and time-dependent seismic hazard due to fluid injection in eastern Texas. *Science*, 353(6306):1416–1419, September 2016. ISSN 0036-8075, 1095-9203. doi: 10.1126/science.aag0262. URL http://science.sciencemag.org/content/353/6306/1416.

Julian L. Simon. *The Ultimate Resource*. Princeton University Press, Princeton, NJ, 1981.

Prerna Singh. We-ness and Welfare: A Longitudinal Analysis of Social Development in Kerala, India. *World Development*, 39(2):282–293, February 2011. doi: 10.1016/j.worlddev.2009.11.025. URL http://www.sciencedirect.com/science/article/pii/S0305750X1000197X.

Vaclav Smil. Detonator of the population explosion. *Nature*, 400(6743):415–415, July 1999. ISSN 0028-0836. doi: 10.1038/22672. URL http://www.nature.com/nature/journal/v400/n6743/full/400415a0.html.

Vaclav Smil. *Enriching the Earth: Fritz Haber, Carl Bosch, and the transformation of world food production*. MIT press, Cambridge, Mass., and London, England, 2004.

Vaclav Smil. Long-range energy forecasts are no more than fairy tales. *Nature*, 453(7192):154–154, May 2008. ISSN 0028-0836. doi: 10.1038/453154a. URL http://www.nature.com/nature/journal/v453/n7192/full/453154a.html.

Andrei P. Sokolov, C. Adam Schlosser, Stephanie Dutkiewicz, Sergey Paltsev, David W. Kicklighter, Henry D. Jacoby, Ronald G. Prinn, Chris Eliot Forest, John M. Reilly, and Chien Wang. MIT integrated global system model (IGSM) version 2: model description and baseline evaluation. Technical report, MIT Joint Program on the Science and Policy of Global Change, 2005. URL http://18.7.29.232/handle/1721.1/29789.

Robert M. Solow. The Economics of Resources or the Resources of Economics. *The American Economic Review*, 64(2):1–14, 1974. ISSN 0002-8282. URL http://www.jstor.org/stable/1816009.

Jelena Srebric, Mohammad Heidarinejad, and Jiying Liu. Building neighborhood emerging properties and their impacts on multi-scale modeling of building energy and airflows. *Building and Environment*, 91:246–262, September 2015. ISSN 0360-1323. doi: 10.1016/j.buildenv.2015.02.031. URL http://www.sciencedirect.com/science/article/pii/S0360132315000888.

Elizabeth A. Stanton. Development without Carbon: Climate and the Global Economy through the 21st Century. Technical report, Stockholm Environment Institute-U.S. Center, 2011. URL http://www.sei-international.org/publications?pid=1982.

Jennifer Steffen, Mark Jensen, Christine A. Pomeroy, and Steven J. Burian. Water Supply and Stormwater Management Benefits of Residential Rainwater Harvesting in U.S. Cities. *JAWRA Journal of the American Water Resources Association*, 49(4):810–824, August 2013. ISSN 1752-1688. doi: 10.1111/jawr.12038. URL https://onlinelibrary.wiley.com/doi/abs/10.1111/jawr.12038.

Will Steffen, Regina Angelina Sanderson, Peter D. Tyson, Jill Jäger, Pamela A. Matson, Berrien Moore III, Frank Oldfield, Katherine Richardson, Hans Joachim Schellnhuber, Billie L. Turner, and Robert J. Wasson. *Global Change and the Earth System: A Planet Under Pressure*. Springer-Verlag, Berlin; Heidelberg; New York, January 2006. ISBN 978-3-540-26607-5.

Will Steffen, Wendy Broadgate, Lisa Deutsch, Owen Gaffney, and Cornelia Ludwig. The trajectory of the Anthropocene: The Great Acceleration. *The Anthropocene Review*, January 2015. ISSN 2053-0196, 2053-020X. doi: 10.1177/2053019614564785. URL http://anr.sagepub.com/content/early/2015/01/08/2053019614564785.

John Sterman, Thomas Fiddaman, Travis Franck, Andrew Jones, Stephanie McCauley, Philip Rice, Elizabeth Sawin, and Lori Siegel. Climate interactive: the C-ROADS climate policy model. *System Dynamics Review*, 28(3):295–305, 2012.

ISSN 1099-1727. doi: 10.1002/sdr.1474. URL http://onlinelibrary.wiley.com/doi/10.1002/sdr.1474/abstract.

Nicholas Stern. *The Economics of Climate Change: The Stern Review*. Cambridge University Press, New York, NY, January 2007. ISBN 978-0-521-70080-1.

Y. C. Sud and W. E. Smith. The influence of surface roughness of deserts on the July circulation. *Boundary-Layer Meteorology*, 33(1):15–49, September 1985. ISSN 1573-1472. doi: 10.1007/BF00137034. URL https://doi.org/10.1007/BF00137034.

George Sugihara, Robert May, Hao Ye, Chih-hao Hsieh, Ethan Deyle, Michael Fogarty, and Stephan Munch. Detecting causality in complex ecosystems. *Science*, 338(6106):496–500, 2012. doi: 10.1126/science.1227079. URL http://www.sciencemag.org/content/338/6106/496.abstract.

John Sulston, Patrick Bateson, Nigel Biggar, Fang Cai, Suzana Cavenaghi, John Cleland, Joel Cohen, Pratha Dasgupta, Parfait M. Eloundou-Enyegue, Alastair Fitter, Demissie Habte, Sarah Harper, Tim Jackson, Georgina Mace, Susan Owens, Jonathan Porritt, Malcolm Potts, Jules Pretty, Faujdar Ram, Roger Short, Sarah Spencer, Xiaoying Zheng, and Eliya Zulu. People and the Planet. Technical Report 01/12, The Royal Society Science Policy Centre, London, UK, April 2012. URL https://royalsociety.org/topics-policy/projects/people-planet/report/.

A. Sathiya Susuman, Siaka Lougue, and Madhusudana Battala. Female Literacy, Fertility Decline and Life Expectancy in Kerala, India: An Analysis from Census of India 2011. *Journal of Asian and African Studies*, 51(1):32–42, February 2016. ISSN 0021-9096, 1745-2538. doi: 10.1177/0021909614541087. URL http://jas.sagepub.com/content/51/1/32. Published online before print on July 14, 2014.

Haider Taha. The potential for air-temperature impact from large-scale deployment of solar photovoltaic arrays in urban areas. *Solar Energy*, 91:358–367, May 2013. ISSN 0038-092X. doi: 10.1016/j.solener.2012.09.014. URL http://www.sciencedirect.com/science/article/pii/S0038092X12003386.

Floris Takens. Detecting strange attractors in turbulence. In *Dynamical systems and turbulence, Warwick 1980*, pages 366–381. Springer, 1981.

John Talberth, Clifford Cobb, and Noah Slattery. The Genuine Progress Indicator 2006. Technical report, Redefining Progress, Oakland, CA, 2007. URL http://ase.tufts.edu/gdae/CS/GPI.pdf.

David Tilman, Joseph Fargione, Brian Wolff, Carla D'Antonio, Andrew Dobson, Robert Howarth, David Schindler, William H. Schlesinger, Daniel Simberloff, and Deborah Swackhamer. Forecasting Agriculturally Driven Global Environmental Change. *Science*, 292(5515):281–284, April 2001. ISSN 0036-8075, 1095-9203. doi: 10.1126/science.1057544. URL http://science.sciencemag.org/content/292/5515/281.

David Tilman, Kenneth G. Cassman, Pamela A. Matson, Rosamond Naylor, and Stephen Polasky. Agricultural sustainability and intensive production practices. *Nature*, 418(6898):671–677, August 2002. ISSN 0028-0836. doi: 10.1038/nature01014. URL http://www.nature.com/nature/journal/v418/n6898/abs/nature01014.html.

David Tilman, Christian Balzer, Jason Hill, and Belinda L. Befort. Global food demand and the sustainable intensification of agriculture. *Proceedings of the National Academy of Sciences*, 108(50):20260–20264, December 2011. ISSN 0027-8424, 1091-6490. doi: 10.1073/pnas.1116437108. URL http://www.pnas.org/content/108/50/20260.

Zoltan Toth and Eugenia Kalnay. Ensemble Forecasting at NMC: The Generation of Perturbations. *Bulletin of the American Meteorological Society*, 74(12):2317–2330, December 1993. ISSN 0003-0007. doi: 10.1175/1520-0477(1993)074⟨2317:EFANTG⟩2.0.CO;2. URL http://journals.ametsoc.org/doi/abs/10.1175/1520-0477(1993)074%3C2317:EFANTG%3E2.0.CO;2.

Simon Toze. Reuse of effluent water—benefits and risks. *Agricultural Water Management*, 80(1):147–159, February 2006. ISSN 0378-3774. doi: 10.1016/j.agwat.2005.07.010. URL http://www.sciencedirect.com/science/article/pii/S0378377405002957.

M. Steven Tracton and Eugenia Kalnay. Operational Ensemble Prediction at the National Meteorological Center: Practical Aspects. *Weather and Forecasting*, 8(3):379–398, September 1993. ISSN 0882-8156. doi: 10.1175/1520-0434(1993)008⟨0379:OEPATN⟩2.0.CO;2. URL http://journals.ametsoc.org/doi/abs/10.1175/1520-0434(1993)008%3C0379:OEPATN%3E2.0.CO;2.

Aradhna K. Tripati, Christopher D. Roberts, and Robert A. Eagle. Coupling of CO2 and Ice Sheet Stability Over Major Climate Transitions of the Last 20 Million Years. *Science*, 326(5958):1394–1397, December 2009. ISSN 0036-8075, 1095-9203. doi: 10.1126/science.1178296. URL http://www.sciencemag.org/content/326/5958/1394.

Adair Turner. Population priorities: the challenge of continued rapid population growth. *Philosophical Transactions of the Royal Society B: Biological Sciences*, 364(1532):2977–2984, October 2009. ISSN 0962-8436, 1471-2970. doi: 10.1098/rstb.2009.0183. URL http://rstb.royalsocietypublishing.org/content/364/1532/2977.

Hugh Turral, Mark Svendsen, and Jean Marc Faures. Investing in irrigation: Reviewing the past and looking to the future. *Agricultural Water Management*, 97(4):551–560, April 2010. doi: 10.1016/j.agwat.2009.07.012. URL http://www.sciencedirect.com/science/article/pii/S0378377409002042.

Bradley Udall and Jonathan Overpeck. The twenty-first century Colorado River hot drought and implications for the future. *Water Resources Research*, 53(3):

2404–2418, March 2017. ISSN 1944-7973. doi: 10.1002/2016WR019638. URL http://onlinelibrary.wiley.com/doi/10.1002/2016WR019638/abstract.

UNEP. The UN Water - Status Report on the Application of Integrated Approaches to Water Resource Management. Technical Report DEP/1532/NA, United Nation Environmental Programme, 2012. URL http://www.un.org/waterforlifedecade/pdf/un_water_status_report_2012.pdf.

UNHCR. Global Trends: Forced Displacement in 2015. Technical report, United Nations High Commissioner for Refugees, Geneva, Switzerland, June 2016. URL https://s3.amazonaws.com/unhcrsharedmedia/2016/2016-06-20-global-trends/2016-06-14-Global-Trends-2015.pdf.

United Nations. The Dublin Statement on Water and Sustainable Development, 1992. URL http://un-documents.net/h2o-dub.htm.

United Nations. The World at Six Billion. Working Paper ESA/P/WP.154, United Nations, Department of Economic and Social Affairs, Population Division, October 1999.

United Nations. Toward Global Water Security, 2003. URL https://issuu.com/atlanticcouncil/docs/global_water_security_web_0823.

United Nations. World Population to 2300. Working Paper ST/ESA/SER.A/236, United Nations, Department of Economic and Social Affairs, Population Division, 2004. URL http://www.un.org/esa/population/publications/longrange2/WorldPop2300final.pdf.

United Nations. Guidance on Water and Adaptation to Climate Change, 2009. URL https://issuu.com/unpublications/docs/9789210543422.

United Nations. The Millennium Development Goals Report 2013, 2013a. URL https://issuu.com/unpublications/docs/13i9isbn9789210562010.

United Nations. World Population Prospects: The 2012 Revision, Highlights and Advance Tables. Working Paper ESA/P/WP.228, United Nations, Department of Economic and Social Affairs, Population Division, 2013b. URL http://esa.un.org/unpd/wpp/Publications/Files/WPP2012_HIGHLIGHTS.pdf.

United Nations. World Population Prospects: The 2012 Revision, DVD Edition. Working Paper ESA/P/WP.228, United Nations, Department of Economic and Social Affairs, Population Division, 2013c.

United Nations. The United Nations World Water Development Report 2015: Water for a Sustainable World, 2015a. URL https://issuu.com/undp/docs/wwdr-report-2015.

United Nations. The World Population Prospects: 2015 Revision, Key Findings and Advance Tables. Working Paper ESA/P/WP.241, United Nations, Department of Economic and Social Affairs, Population Division, 2015b. URL https://www.un.org/development/desa/publications/world-population-prospects-2015-revision.html.

United Nations. World Population Prospects: The 2017 Revision, Key Findings and Advance Tables. Technical Report Working Paper No. ESA/P/WP/248, United Nations, Department of Economic and Social Affairs, Population Division, 2017. URL https://esa.un.org/unpd/wpp/publications/files/wpp2017_keyfindings.pdf.

US EIA. Assessing HVDC Transmission for Impacts of Non-Dispatchable Generation. Technical report, US Energy Information Agency, Department of Energy, Washington, DC, USA, June 2018a. URL https://www.eia.gov/analysis/studies/electricity/hvdctransmission/.

US EIA. Electric Power Monthly with data for April 2018. Technical report, US Energy Information Agency, Department of Energy, Washington, DC, USA, April 2018b.

USCB. Maricopa County Added Over 222 People Per Day in 2016. Press Release CB17-44, United Staes Census Bureau, March 2017. URL https://www.census.gov/newsroom/press-releases/2017/cb17-44.html.

Farnaz Vahidnia. Case study: fertility decline in Iran. *Population and Environment*, 28(4-5):259–266, April 2007. ISSN 0199-0039, 1573-7810. doi: 10.1007/s11111-007-0050-9. URL http://link.springer.com/article/10.1007/s11111-007-0050-9.

Gayathri Vaidyanathan. Fracking Can Contaminate Drinking Water. *Scientific American*, April 2016. URL http://www.scientificamerican.com/article/fracking-can-contaminate-drinking-water/.

Geurt Van de Kerk and Arthur R. Manuel. A comprehensive index for a sustainable society: The SSI — the Sustainable Society Index. *Ecological Economics*, 66 (2–3):228–242, June 2008. doi: 10.1016/j.ecolecon.2008.01.029. URL http://www.sciencedirect.com/science/article/pii/S0921800908000438.

Martin K. van Ittersum, Lenny G. J. van Bussel, Joost Wolf, Patricio Grassini, Justin van Wart, Nicolas Guilpart, Lieven Claessens, Hugo de Groot, Keith Wiebe, Daniel Mason-D'Croz, Haishun Yang, Hendrik Boogaard, Pepijn A. J. van Oort, Marloes P. van Loon, Kazuki Saito, Ochieng Adimo, Samuel Adjei-Nsiah, Alhassane Agali, Abdullahi Bala, Regis Chikowo, Kayuki Kaizzi, Mamoutou Kouressy, Joachim H. J. R. Makoi, Korodjouma Ouattara, Kindie

Tesfaye, and Kenneth G. Cassman. Can sub-Saharan Africa feed itself? *Proceedings of the National Academy of Sciences*, 113(52):14964–14969, December 2016. ISSN 0027-8424, 1091-6490. doi: 10.1073/pnas.1610359113. URL http://www.pnas.org/content/113/52/14964.

Egbert H van Nes, Marten Scheffer, Victor Brovkin, Timothy M Lenton, Hao Ye, Ethan Deyle, and George Sugihara. Causal feedbacks in climate change. *Nature Climate Change*, 2015.

Raquel Vaquer-Sunyer and Carlos M. Duarte. Thresholds of hypoxia for marine biodiversity. *Proceedings of the National Academy of Sciences*, 105(40):15452–15457, October 2008. ISSN 0027-8424, 1091-6490. doi: 10.1073/pnas.0803833105. URL http://www.pnas.org/content/105/40/15452.

Robert Vautard, Françoise Thais, Isabelle Tobin, François-Marie Bréon, Jean-Guy Devezeaux de Lavergne, Augustin Colette, Pascal Yiou, and Paolo Michele Ruti. Regional climate model simulations indicate limited climatic impacts by operational and planned European wind farms. *Nature Communications*, 5:3196, February 2014. ISSN 2041-1723. doi: 10.1038/ncomms4196. URL https://www.nature.com/articles/ncomms4196.

Raul Vicente, Michael Wibral, Michael Lindner, and Gordon Pipa. Transfer entropya model-free measure of effective connectivity for the neurosciences. *Journal of Computational Neuroscience*, 30(1):45–67, 2011. ISSN 0929-5313. doi: 10.1007/s10827-010-0262-3. URL http://dx.doi.org/10.1007/s10827-010-0262-3.

P. M. Vitousek, J. D. Aber, R. W. Howarth, G. E. Likens, P. A. Matson, D. W. Schindler, W. H. Schlesinger, and D. Tilman. Human alteration of the global nitrogen cycle: Sources and consequences. *Ecological Applications*, 7(3):737–750, August 1997a. ISSN 1051-0761. doi: 10.2307/2269431. URL http://onlinelibrary.wiley.com/doi/10.1890/1051-0761(1997)007%5B0737:HAOTGN%5D2.0.CO;2/full. WOS:A1997XQ08100002.

Peter M. Vitousek, Harold A. Mooney, Jane Lubchenco, and Jerry M. Melillo. Human Domination of Earth's Ecosystems. *Science*, 277(5325):494–499, July 1997b. ISSN 0036-8075, 1095-9203. doi: 10.1126/science.277.5325.494. URL http://science.sciencemag.org/content/277/5325/494.

Charles J. Vörösmarty, Pamela Green, Joseph Salisbury, and Richard B. Lammers. Global Water Resources: Vulnerability from Climate Change and Population Growth. *Science*, 289(5477):284–288, July 2000. ISSN 0036-8075, 1095-9203. doi: 10.1126/science.289.5477.284. URL http://science.sciencemag.org/content/289/5477/284.

Katalyn A. Voss, James S. Famiglietti, MinHui Lo, Caroline de Linage, Matthew Rodell, and Sean C. Swenson. Groundwater depletion in the Middle East from GRACE with implications for transboundary water management in the Tigris-Euphrates-Western Iran region. *Water Resources Research*, 49(2):904–914, February 2013. ISSN 1944-7973. doi: 10.1002/wrcr.20078. URL http://onlinelibrary.wiley.com/doi/10.1002/wrcr.20078/abstract.

Thorsten Wagener, Murugesu Sivapalan, Peter A. Troch, Brian L. McGlynn, Ciaran J. Harman, Hoshin V. Gupta, Praveen Kumar, P. Suresh C. Rao, Nandita B. Basu, and Jennifer S. Wilson. The future of hydrology: An evolving science for a changing world. *Water Resources Research*, 46(5):W05301, May 2010. ISSN 1944-7973. doi: 10.1029/2009WR008906. URL http://onlinelibrary.wiley.com/doi/10.1029/2009WR008906/abstract.

C. Wang and R. G. Prinn. Potential climatic impacts and reliability of very large-scale wind farms. *Atmospheric Chemistry and Physics*, 10(4):2053–2061, February 2010. ISSN 1680-7316. doi: https://doi.org/10.5194/acp-10-2053-2010. URL https://www.atmos-chem-phys.net/10/2053/2010/.

Guiling Wang and Elfatih A. B. Eltahir. Ecosystem dynamics and the Sahel Drought. *Geophysical Research Letters*, 27(6):795–798, March 2000a. ISSN 1944-8007. doi: 10.1029/1999GL011089. URL https://agupubs.onlinelibrary.wiley.com/doi/abs/10.1029/1999GL011089.

Guiling Wang and Elfatih A. B. Eltahir. Role of vegetation dynamics in enhancing the low-frequency variability of the Sahel rainfall. *Water Resources Research*, 36(4):1013–1021, April 2000b. ISSN 1944-7973. doi: 10.1029/1999WR900361. URL https://agupubs.onlinelibrary.wiley.com/doi/abs/10.1029/1999WR900361.

Stephen G. Warren. Can human populations be stabilized? *Earth's Future*, 3(2):2014EF000275, February 2015. ISSN 2328-4277. doi: 10.1002/2014EF000275. URL http://onlinelibrary.wiley.com/doi/10.1002/2014EF000275/abstract.

Western Water. Choosing Water-Efficient Appliances. Fact Sheet, Western Water, August 2009.

Dominic Waughray. *Water Security: The Water-Food-Energy-Climate Nexus*. Island Press, January 2011. ISBN 978-1-59726-736-6.

Christopher L. Weber, Glen P. Peters, Dabo Guan, and Klaus Hubacek. The contribution of Chinese exports to climate change. *Energy Policy*, 36(9):3572–3577, September 2008. ISSN 0301-4215. doi: 10.1016/j.enpol.2008.06.009. URL http://www.sciencedirect.com/science/article/pii/S0301421508002905.

Jan Weinzettel, Edgar G. Hertwich, Glen P. Peters, Kjartan Steen-Olsen, and Alessandro Galli. Affluence drives the global displacement of land use. *Global Environmental Change*, 23(2):433–438, April 2013. doi: 10.1016/j.gloenvcha.

2012.12.010. URL http://www.sciencedirect.com/science/article/pii/S0959378012001501.

Jeffrey S. Whitaker and Thomas M. Hamill. Ensemble Data Assimilation without Perturbed Observations. *Monthly Weather Review*, 130(7):1913–1924, July 2002. ISSN 0027-0644. doi: 10.1175/1520-0493(2002)130⟨1913:EDAWPO⟩2.0.CO;2. URL http://journals.ametsoc.org/doi/abs/10.1175/1520-0493(2002)130%3C1913:EDAWPO%3E2.0.CO%3B2.

Michael Wibral, Nicolae Pampu, Viola Priesemann, Felix Siebenhhner, Hannes Seiwert, Michael Lindner, Joseph T. Lizier, and Raul Vicente. Measuring information-transfer delays. *PLoS ONE*, 8(2):e55809, 02 2013. doi: 10.1371/journal.pone.0055809. URL http://dx.doi.org/10.1371%2Fjournal.pone.0055809.

Thomas O. Wiedmann, Heinz Schandl, Manfred Lenzen, Daniel Moran, Sangwon Suh, James West, and Keiichiro Kanemoto. The material footprint of nations. *Proceedings of the National Academy of Sciences*, 112(20):6271–6276, May 2015. ISSN 0027-8424, 1091-6490. doi: 10.1073/pnas.1220362110. URL http://www.pnas.org/content/112/20/6271.

Norbert Wiener. The theory of prediction. *Modern mathematics for engineers*, 1: 125–139, 1956.

Dean N. Williams, Bryan N. Lawrence, Michael Lautenschlager, Don Middleton, and V. Balaji. The Earth System Grid Federation: Delivering globally accessible petascale data for CMIP5. *Proceedings of the Asia-Pacific Advanced Network*, 32 (0):121–130–130, December 2011. ISSN 2227-3026. doi: 10.7125/APAN.32.15. URL http://journals.sfu.ca/apan/index.php/apan/article/view/50.

Thomas Wire. Fewer Emitters, Lower Emissions, Less Cost: Reducing Future Carbon Emissions By Investing In Family Planning. Technical report, London School of Economics, 2009. URL http://bocs.hu/0-ujdoc/LSE%20Report.doc.

World Bank. Global Monitoring Report 2008 : MDGs and the Environment, Agenda for Inclusive and Sustainable Development, 2008a. URL https://openknowledge.worldbank.org/handle/10986/6518.

World Bank. Sink or Swim – Towards Water Security for All, 2008b. URL https://openknowledge.worldbank.org/handle/10986/11759.

Grace C. Wu, Ranjit Deshmukh, Kudakwashe Ndhlukula, Tijana Radojicic, Jessica Reilly-Moman, Amol Phadke, Daniel M. Kammen, and Duncan S. Callaway. Strategic siting and regional grid interconnections key to low-carbon futures in African countries. *Proceedings of the National Academy of Sciences*, 114(15):E3004–E3012, April 2017. ISSN 0027-8424, 1091-6490. doi: 10.1073/pnas.1611845114. URL http://www.pnas.org/content/114/15/E3004.

Huan Wu, John S. Kimball, Nate Mantua, and Jack Stanford. Automated upscaling of river networks for macroscale hydrological modeling. *Water Resources Research*, 47(3), March 2011. ISSN 1944-7973. doi: 10.1029/2009WR008871. URL https://agupubs.onlinelibrary.wiley.com/doi/abs/10.1029/2009WR008871.

Huan Wu, John S. Kimball, Hongyi Li, Maoyi Huang, L. Ruby Leung, and Robert F. Adler. A new global river network database for macroscale hydrologic modeling. *Water Resources Research*, 48(9), September 2012. ISSN 1944-7973. doi: 10.1029/2012WR012313. URL https://agupubs.onlinelibrary.wiley.com/doi/abs/10.1029/2012WR012313.

Donald Wuebbles, Gerald Meehl, Katharine Hayhoe, Thomas R. Karl, Kenneth Kunkel, Benjamin Santer, Michael Wehner, Brian Colle, Erich M. Fischer, Rong Fu, Alex Goodman, Emily Janssen, Viatcheslav Kharin, Huikyo Lee, Wenhong Li, Lindsey N. Long, Seth C. Olsen, Zaitao Pan, Anji Seth, Justin Sheffield, and Liqiang Sun. CMIP5 Climate Model Analyses: Climate Extremes in the United States. *Bulletin of the American Meteorological Society*, 95(4):571–583, July 2013. ISSN 0003-0007. doi: 10.1175/BAMS-D-12-00172.1. URL http://journals.ametsoc.org/doi/abs/10.1175/BAMS-D-12-00172.1.

Laura Würtenberger, Thomas Koellner, and Claudia R. Binder. Virtual land use and agricultural trade: Estimating environmental and socio-economic impacts. *Ecological Economics*, 57(4):679–697, June 2006. ISSN 0921-8009. doi: 10.1016/j.ecolecon.2005.06.004. URL http://www.sciencedirect.com/science/article/pii/S0921800905002673.

WWF. *Living Planet Report 2016. Risk and resilience in a new era.* World Wildlife Fund International, Gland, Switzerland, 2016. ISBN 978-2-940529-40-7. URL http://assets.worldwildlife.org/publications/964/files/original/lpr_living_planet_report_2016.pdf.

Yongkang Xue, Fernando De Sales, William K.-M. Lau, Aaron Boone, Kyu-Myong Kim, Carlos R. Mechoso, Guiling Wang, Fred Kucharski, Kathleen Schiro, Masahiro Hosaka, Suosuo Li, Leonard M. Druyan, Ibrah Seidou Sanda, Wassila Thiaw, Ning Zeng, Ruth E. Comer, Young-Kwon Lim, Sarith Mahanama, Guoqiong Song, Yu Gu, Samson M. Hagos, Mian Chin, Siegfried Schubert, Paul Dirmeyer, L. Ruby Leung, Eugenia Kalnay, Akio Kitoh, Cheng-Hsuan Lu, Natalie M. Mahowald, and Zhengqiu Zhang. West African monsoon decadal variability and surface-related forcings: second West African Monsoon Modeling and Evaluation Project Experiment (WAMME II). *Climate Dynamics*, 47(11):3517–3545, December 2016. ISSN 1432-0894. doi: 10.1007/s00382-016-3224-2. URL https://doi.org/10.1007/s00382-016-3224-2.

Shu-Chih Yang, Debra Baker, Hong Li, Katy Cordes, Morgan Huff, Geetika Nagpal, Ena Okereke, Josue Villafañe, Eugenia Kalnay, and Gregory S Duane. Data assimilation as synchronization of truth and model: Experiments with the three-variable lorenz system. *Journal of the atmospheric sciences*, 63(9):2340–2354, 2006.

Yang Yu, Kuishuang Feng, and Klaus Hubacek. Tele-connecting local consumption to global land use. *Global Environmental Change*, 23(5):1178–1186, October 2013. ISSN 0959-3780. doi: 10.1016/j.gloenvcha.2013.04.006. URL http://www.sciencedirect.com/science/article/pii/S0959378013000721.

Stephen E. Zebiak and Mark A. Cane. A Model El Niño-Southern Oscillation. *Monthly Weather Review*, 115(10):2262–2278, October 1987. ISSN 0027-0644. doi: 10.1175/1520-0493(1987)115⟨2262:AMENO⟩2.0.CO;2. URL http://journals.ametsoc.org/doi/abs/10.1175/1520-0493(1987)115%3C2262:AMENO%3E2.0.CO;2.

N. Zeng, A. Mariotti, and P. Wetzel. Terrestrial mechanisms of interannual CO2 variability. *Global Biogeochemical Cycles*, 19(1), March 2005. ISSN 1944-9224. doi: 10.1029/2004GB002273. URL https://agupubs.onlinelibrary.wiley.com/doi/abs/10.1029/2004GB002273.

Ning Zeng. Glacial-interglacial atmospheric CO2 change —The glacial burial hypothesis. *Advances in Atmospheric Sciences*, 20(5):677–693, September 2003. ISSN 1861-9533. doi: 10.1007/BF02915395. URL https://doi.org/10.1007/BF02915395.

Ning Zeng and Jinho Yoon. Expansion of the world's deserts due to vegetation-albedo feedback under global warming. *Geophysical Research Letters*, 36(17), September 2009. ISSN 1944-8007. doi: 10.1029/2009GL039699. URL https://agupubs.onlinelibrary.wiley.com/doi/abs/10.1029/2009GL039699.

Ning Zeng, J. David Neelin, K.-M. Lau, and Compton J. Tucker. Enhancement of Interdecadal Climate Variability in the Sahel by Vegetation Interaction. *Science*, 286(5444):1537–1540, November 1999. ISSN 0036-8075, 1095-9203. doi: 10.1126/science.286.5444.1537. URL http://science.sciencemag.org/content/286/5444/1537.

Ning Zeng, J. David Neelin, and Chia Chou. A Quasi-Equilibrium Tropical Circulation Model—Implementation and Simulation. *Journal of the Atmospheric Sciences*, 57(11):1767–1796, June 2000. ISSN 0022-4928. doi: 10.1175/1520-0469(2000)057⟨1767:AQETCM⟩2.0.CO;2. URL https://journals.ametsoc.org/doi/abs/10.1175/1520-0469%282000%29057%3C1767%3AAQETCM%3E2.0.CO%3B2.

Ning Zeng, Fang Zhao, George J. Collatz, Eugenia Kalnay, Ross J. Salawitch, Tristram O. West, and Luis Guanter. Agricultural Green Revolution as a driver of increasing atmospheric CO2 seasonal amplitude. *Nature*, 515(7527):394–397, November 2014. ISSN 0028-0836. doi: 10.1038/nature13893. URL http://www.nature.com/nature/journal/v515/n7527/full/nature13893.html.

Liming Zhou, Yuhong Tian, Somnath Baidya Roy, Chris Thorncroft, Lance F. Bosart, and Yuanlong Hu. Impacts of wind farms on land surface temperature. *Nature Climate Change*, 2(7):539–543, July 2012. ISSN 1758-6798. doi: 10.1038/nclimate1505. URL https://www.nature.com/articles/nclimate1505.